GAS TURBINE MODELS FOR COMPENSATION OF TRANSIENT FUEL FLOW SCHEDULES

By

Larbi Merahi

Thesis presented for the degree of Master of science to the Faculty of Engineering

Department of Mechanical Engineering
Glasgow University

November, 1988

CONTENTS OF PROJECT

ACKNOWLEDGEMENTS

I would like to thank Dr. N.R.L. Maccallum for his invaluable help, support and guidance throughout this work. My thanks are extended to all staff of the department of Mechanical Engineering for their assisstance. I am also indebted to the computing staff for their help. I would like to express my gratitude to the Algerian Ministry of High Education for their financial support throughout the period of study. I also wish to thank Miss Maureen Monaghan and my parents for their continuous support.

SUMMARY

In the present work, mathematical models have been devised to enable the prediction of the gas turbine engine performance during transient operations. The method used is based upon the engine component characteristics where an adequate information for a typical two-spool turbofan engine with mixed exhaust was available. Basically, this thesis deals with the effects of heat transfer on the engine performance and behaviour, especially during transient operations. Also methods of improving the engine response and performance are of great concern in this work. Therefore, the scope of this project lies on the following points:

1) Pedigree of gas turbine with general background needed, together, with a brief exposure of the problem involved, are illustrated in chapter one.

2) In chapter two, an insight into aircraft gas turbine engine investigations previously carried out is given. Different methods permitting the simulation of any gas turbine engine configuration, are proposed and the reasons for the method used in the present work are given.

3) Chapter three deals with adiabatic simulation of engine during both steady-state operation and transient at both sea-level and altitude conditions.

4) All heat transfer effects which might affect the engine behaviour during transient operation are then modelled and included in the programme. A standard

fuel schedule is used during all transients considered. The results obtained are directly compared to the adiabatic predictions. To this end, chapter four is devoted.

5) The results obtained in chapter four for acceleration of 'hot' engines show different acceleration rates and different usages of surge margins as compared with predicted accelerations of 'cold' engines. This leads to the proposal to "compensate" the fuel schedule to give more consistent acceleration behaviours.
Chapter five deals with the fuel flow schedule compensation during both 'cold' and 'Bodie' transient at both sea-level and altitude operations. Different methods based on different models have been investigated and in each case the resulting engine response is compared with that resulting from use of an uncompensated fuel schedule.

6) General discussion of all compensated results obtained from different simulations, at different conditions, different assumptions and different transients is given in chapter six. Chapter seven gives a brief conclusion drawn from all investigations carried out along suggestions for further investigations, which time had not allowed to be carried out.

NOMENCLATURE

Symbols

A	cross sectional area
a	index of compensation
b	index of compensation
C_p	specific heat at constant pressure
$C_1,\ldots,C_n$	constants
D	diameter
E	Young' modulus
e	cooling effectiveness
e^*	deflection(* : design conditions)
F	ratio of work transfer to heat transfer
F_{cp}	factor of compensation
$\dot{f}$	fuel flow
Gr	Grashof number
g	staggered gap between blades
H	height
h	heat transfer coefficient
i	angle of incidence of flow
k	proportionality coefficient
L	axial length
l	thickness of diaphragm
M	mass
Ma	Mach number
m	mass flow
$\dot{m}$	mass flow rate
N	rotational speed
Nu	Nusselt number
n	index of expansion or compression
p	pressure
PR	pressure ratio
Pr	Prandtl number
Q	rate of heat transfer
R	gas constant/ radius
Re	Reynolds number
r	pressure ratio
T	temperature
t	time
U	tangential velocity
V	fluid velocity

v	volume
W	work transfer
X	thrust
α	air angle
β	blade angle
γ	ratio of specific heat
δ	air deviation from blade angle or clearance
η	efficiency
λ	non-dimensional clearance (C/Hb)
μ	by-pass ratio
ω	angular acceleration
σ	poisson's ratio
ϕ	flow coefficient (Va/U)
ρ	density
τ	time constant
ψ	blade loading ($2C_p \Delta T/U^2$)
Δ	variation / difference/ increment

Subscripts

ad	air flow on disc/ adiabatic
ah	air on the hub
air	air
AIRD	disc air flow
AVD	disc averaged
b	blade
bp	by-pass
bt	blade tip
c	compressor / air cooling
cg	core gas
chc	characteristics
cl	calculated
D	disc / delayed
e	exit
g	gas
h	hub
hm	hub metal
ht	with heat transfer
H.P.	high pressure
i	inner / inlet/ increment
L.P.	low pressure

m	mean / metal
ma	mean air...
C.V.	calorific value
o	outer
p	pressure / platform
Ref	reference
sh	shroud
s	stabilised
T	turbine
t	at time
th	thermal

INTRODUCTION

The later stages of the work of Holzwarth and other engineers coincided with the first stirrings of a great surge of new ideas from which the gas turbine was to receive the main impetus of its development. The development of the gas turbine began by the second world war with the shaft power in mind, but attention was later on transferred to the turbojet engine for aircraft propulsion. Several reasons for which gas turbine was first developed as an aircraft power plant. One of these reasons is the fear of war which made available large funds for aeronautical research. Another reason is that the gas turbine is essentially an aerodynamic machine which is peculiarly suited to aircraft in that its performance improves with increase in altitude and forward speed.

The requirement of current aircraft companies is that the engine must be capable of accelerating from a lower thrust (filght idle) to about 95% rated take-off power in not more than 8 seconds. Also it is desirable for an engine to have a faster response rate with a minimum acceleration time needed, but limits to the acceleration rate are determined by the compressor surge and turbine over-temperature considerations. Therefore, an accurate and reliable prediction of gas turbine performance during transients is of great importance. During transients, gas turbine performance is affected by heat release caused by the thermal effects of non-adiabatic flow and when experiencing a change of state, gas turbine engine materials will exchange heat with the working fluid because of the temperature changes. To accelerate an engine, the use

of a fuel controller is necessary to ensure that the engine operates safely, thereby, no compressor surge or excessively high gas temperature at the turbine inlet are predicted.

Good dynamic response requires transient operation at temperatures greater than the design values, resulting in transient operating lines (acceleration and deceleration trajectories) close to the compressor surge line. Both turbine inlet temperature and surge margin are difficult to measure during rapid and severe transients, because attempts taken by altering the acceleration and deceleration fuel schedules results in lots of test bed running which might result in a damage to the engine or an acceleration rate power higher than could be obtained. Instead, simulation of the dynamic behaviour can greatly improve the safety and determines the limits within the engine can operate by providing detailed information on surge margin, transient temperatures or any other variables of interest for different acceleration schedules. It is obviously desirable for an engine to have a faster response rate when necessary. For this reason, efforts should be made to establish the minimum acceleration time commemsurate with engine safety. Limits to the acceleration rate are determined by compressor surge and turbine over-temperature considerations. During a rapid acceleration, the gas temperatures will lag because of the thermal capacity of the blade material. The acceleration of the rotor and hence the thrust will be dependent on the over-fuelling during the transient. At low speeds the permissible over-fuelling will be restricted by surge rather than temperature considerations. Whereas at higher speeds, the

maximum allowable temperature will be reached before surge is encountered. Therefore, the fuel flow will be limited by temperature considerations.

With today's high cost of fuel, more than 50% of the direct operating costs of a civil aircraft is due to fuel charges. However, fuel prices in the long-term can be expected to continue to escalate and for this reason high fuel efficiency and improved performance must be the dominant factors governing the design of modern aero-engines. In other words, less fuel has to be used during engine operation to reach the very high possible thrust and power within the limits of the engine safety.

To accelerate an engine, it was realised (Ref.6) that the use of the same fuel schedule without regard to the engine immediately preceding history for the acceleration of the hot and cold engine results in differing rates of engine response and different usage of surge margins. So, some adjustement might be applied to the fuel schedule in order to allow for a greater utilisation of the surge margin. To this object, efforts have been made throughout this work and for the purpose of carrying theoretical investigation, mathematical models have been devised and incorporated in the simulation programme.

CHAPTER I

GENERAL GAS TURBINE BACKGROUND

1.1 INTRODUCTION

Gas turbine is one of the various means of producing mechanical power (Fig.1). It was realised that it is the most satisfactory for aircraft propulsion and also in many countries for electrical power generation. The gas turbine has found its niche in aircraft and naval ship propulsion, many oil industry applications, intermittent electricity generation and total energy systems.

The main attraction for the development of a gas turbine for aircraft is its high power per unit of machinery weight, and it is becoming more widely used in both industrial and naval applications.

With the desire to increase the power and efficiency, gas turbines became more complex to design. Therefore, there is a necessity to predict their performance in both steady-state and transient conditions. Mathematical models have been devised for this purpose.

1.2. AIRCRAFT GAS TURBINE ENGINE

Aircraft gas turbine cycles differ from shaft power cycles in that the useful power output of the former is produced wholly or in part as a result of expansion in a propelling nozzle. A second distinguishing feature is the need to consider the effect of forward speed and altitude on the performance of aircraft engines. Current turbo-jets

employ the constant-pressure cycle and it has been common practice to design for sea-level static conditions (zero forward speed). Turbo-jets required to fly at high forward speeds or give extreme economy may be designed for other conditions than 'sea-level static'. To calculate the performance of the turbo-jet at the design point, we follow the thermodynamic cycle of the working gases according to the data given.(Fig.2)

For several reasons, not least the availability of suitable information and the existence of personal contacts with an aircraft engine manufacturer, jet engines are the main subject of the present work and from this point onwards, gas turbines for aircraft propulsion, are the ones considered.

1.2.1 General background

In order to provide thrust for an aircraft, the engine has to give an increase in momentum to the air which is flowing past the aircraft. The net thrust developed by the engine, is given by :

$$X_n = \dot{m} (V_j - V_o) \qquad (1.1)$$

Fuel prices in the long term can be expected to continue to escalate and for this reason high fuel efficiency must be the dominant factor in the design of future aero-engines. For aircraft engines, the overall efficiency is the product of the thermal and propulsive efficiencies. The thermal efficiency can be shown to be :

$$\eta_{th} = \frac{m\ (V_j^2 - V_0^2)}{2\ f\ (C.V)} \qquad (1.2)$$

and the propulsive efficiency by :

$$\eta_p = \frac{2}{\left(1 + \frac{V_j}{V_0}\right)} \qquad (1.3)$$

The overall efficiency is given by the following relation :

$$\eta_{ov} = \eta_p . \eta_{th} \qquad (1.4)$$

1.2.2 Turbojet engine development

As it is already known, the thermal efficiency of a gas turbine will improve with increased engine pressure ratio (Fig.7). Therefore, the necessity of developing higher pressure ratio engines is apparent. Attempts have been made in designing one-spool engines with higher pressure ratio but mechanical and aerodynamical difficulties arose in the compression process. At low speeds, stalling was likely to occur at the front end stages of the compressor, whereas at high speeds, this occured at the rear stages. This problem was solved by designing the turbojet engine with two compressors and two turbines mechanically independent (Figs.3; 4 and 5). This gave birth to the twin-spool engine, which can easily achieve a pressure ratio up to twenty or even thirty.

It is also to be noted that the use of by-pass engines

raises the propulsive efficiency η_p.

1.3. TRANSIENT BEHAVIOUR OF GAS TURBINE

Although transients represent only a few seconds of the engine operating cycle, it is very important to predict engine response and performance during rapid accelerations and decelerations within limits of engine safety. However, transient acceleration and deceleration of aircraft engines with high pressure ratio cycles as mentioned in previous section, if not carefully controlled, can cause surge in a compressor or excessive turbine entry temperatures. Therefore, a suitable controller has to be devised to avoid the above danger. Today, modern aircraft engines are fitted with very sophisticated forms of controllers to suitably constrain the minimum and maximum fuel flows during transients.

To develop a suitable control system, an accurate and reliable transient prediction program is invaluable and programs have been proved successful. Good predictions are also essential if engines are to be sold while still at the design stage.

In gas turbine engines, the limiting control is sometimes referred to as the fuel flow schedule. However, it has been found that a single standard fuel schedule for a given flight condition, may not always be satisfactory. For example 'hot' engines are the most endangered by surge compared to 'cold' engines. Test pilots have experienced this and it has recently been confirmed experimentally in a test bed programme by Burwell and Crawford (1985). This problem has also been investigated theoretically by Maccallum and Pilidis

(1985). The latter study indicated that lower surge margin and faster acceleration response resulted when 'hot' acceleration of a two-spool by-pass engine was compared with a 'cold' acceleration. This observation led to the proposal to compensate the fuel flow shedule, as illustrated in an ASME paper of Maccallum and Pilidis (1986).

The work in this thesis is an investigation of this proposal with the aim of developing accurate models describing fuel schedule compensation, capable of giving consistent surge margins and fast acceleration rates. A theoretical method is used because of the difficulties and costs of an experimental study.

1.4. ENGINE SIMULATION AS A THEORETICAL INVESTIGATION

Transient behaviour of the engine is of the utmost importance. Therefore, experimental and theoretical investigations of the engine transient operation are necessary. Before it can be used and with the complexity of current engines, however, control problems as stated in previous section must be examined early at the design stage.

1.4.1. Choice of the theoretical investigation

Unfortunately experimental investigation cannot take place until late in the development programme. However, simulation, if proved successful, gives valuable information about the performance and behaviour of the engine. Further, the methodology could also be applied to any other configuration of aero-engine gas turbine.

1.4.2. Purpose of the simulation

The purpose of the simulation is to give valuable information about the engine transient operation. Based on mathematical models it permits the investigation of the engine as early as the design stage. Additionally, for the design of an optimum jet engine it is of a prime requirement to predict the transient operation a long time before the first development engine can run on the test bed.

1.4.3. Contemporary investigations being carried out

In parallel with the present work, other investigations concerning gas turbine performance improvement, in terms of the increase of efficiency and engine response have been carried out at Glasgow University. The first investigation deals with heat absorption in the combustion chamber and the lag in the combustion process. To incorporate these effects, a three-zone mathematical model of transient heat transfer effects within combustion chamber has been developed. The second investigation was focussed on the use of alternative models for representing the fan and intermediate compressor sections, originating from different fan treatments and flow distributions after the fan.

1.5 HEAT TRANSFER PROBLEMS IN AERO-ENGINES

1.5.1 Analysis of problem

Since aircraft engine performance and behaviour change with the change of component characteristics and working fluid properties caused by heat transfer effects during transients, the exchange of heat in the engine material components is a very important aspect of an aero-engine

transient operation which has to be considered at the early stages of the engine design. During early investigations of performance of turbo-jet engines, heat transfer effects which are known to be more serious during transient operations were ignored. However, today's investigators have deeply considered the non-adiabatic flow effects on the engine components behaviour and efforts have been made towards a better understanding of what really occurs inside a turbomachine, such as gas turbine. The parts of the engine which are usually prone to heat transfer are those exposed to the hot stream of gas and air.

When the air or gas temperatures change in turbomachinery as in a gas turbine when it changes speed, transient heat transfer takes place between the air (or gas) and the engine materials until the engine materials reach their new equilibrium temperatures. The heat transfer rate which can have important influences on the behaviour of the machine depends on the heat transfer coefficients and material geometry during and following a transient. However, many uncertainties still remain in attempting to predict precisely the distribution of heat transfer to gas turbine blading and other parts. These are due mainly to the ignorance of the details of flow existing in the engine and how these flows can be simulated in theoretical and experimental investigations to provide the data required. Flows in aero-engines are rarely steady and there is doubt about which parameters are the most critical in determining the true convective heat transfer rate to blade and oher surfaces.

1.5.2 Quantification of transient effects

There are three important effects which have to be

considered in an improved method for transient performance investigation of an aero-engine gas turbine. The most important effect is the exchange of heat between the gas stream in the engine and the material of the component. Usually when heat is released for example from a working fluid at a temperature T_2 to an engine component material, such as a blade at a temperature T_1, the rate of heat exchanged by convection is given by equation (1.5) where h is the heat transfer coefficient, A being the surface of the area exposed to heat transfer.

$$Q = h\ A\ (T_2 - T_1) \qquad (1.5)$$

The second factor is the change in tip and seal clearance movements due to the thermal and mechanical growth.

The third effect concerns the changes in the boundary layers developments and component characteristics.

Another factor which is not a heat transfer figure is the so-called packing lag for the filling up of volumes in the engine whenever the pressure and temperature change.

1.6. CONFIGURATION INVESTIGATED IN THIS WORK

A typical two-spool turbofan engine with mixed exhausts and medium by-pass has been used to illustrate heat transfer effects on overall engine performance and it has been used also for exploration of transient fuel scheduling with compensation for thermal effects. A schematic representation of this configuration is shown in Fig.8b.

CHAPTER II

PREVIOUS WORK IN AIRCRAFT GAS TURBINE AND CHOICE OF THE METHOD USED

2.1 INTRODUCTION

During the early days of development of gas turbines, the need to evaluate the performance of these engines in both steady state and transient aspects became apparent. At the beginning, little attention had been paid to the prediction of the transient behaviour of gas turbines and the response rate of an engine was established empirically during the development testing.

Another procedure adopted was to predict the performance of the various components and once this had been completed the next step was to forecast the steady state engine performance from the predicted characteristics of the components. These predictions of the steady-state performance could be compared with test bed results, if available. Then, the prediction of engine performance during the transient phase could be investigated. Because of the lack of computing facilities at that period, engine transient performance was estimated using hand but very lengthy calculations.

Recently, the evaluation of engine performance has been carried out by means of a digital computer. The current techniques recognise the importance of using the steady state component characteristics and all off-design calculations depend on satisfying the essential conditions of the

compatibility of the mass flow, work and rotational speed between the various components. Two distinct methods based on these characteristics are employed. These will be discussed in section 2.4.

2.2 EARLY DESIGN AND PERFORMANCE OF AIRCRAFT GAS TURBINE

When gas turbines were being designed in the mid and late forties, the first interest was to predict the performance of the various components and once this has been established, the next move was to evaluate the steady state performance of the whole engine. For prediction of component performance, reference was made to work with the experimental cascade information and aerofoil theory. From this information the component performance was predicted. Once the task of predicting the performance of the components had been completed, the next step was to obtain the steady state engine performance from the predicted characteristics of the components. The results were produced in charts where all the necessary parameters are shown. Analytical and experimental investigations of the dynamic behaviour of gas turbines began around the early 1950s. Much of this work was pioneered by NACA. Otto and Taylor (1950) were probably the first to show that a single spool gas turbine could be approximated by a first order system.

Consideration was given to treating the gas turbine engine as a non linear system, rather than a linear system. This can be done by applying the matching conditions with the knowledge of the compressors and turbine characteristics. This approach was first analysed by Dugan and Fillipi (1956), who studied the acceleration of a twin spool turbo-jet engine following a large step change in the fuel flow. A

range of operating points was found for which the flow compatibility was satisfied. From the resulting torque imbalances, the rotor acceleration rates and the engine speed response were determined.

2.3 PRESENT DESIGN AND ASSESSMENT OF ENGINE PERFORMANCE

In recent years, the development cost of modern gas turbines has increased greatly and the need for accurate information on engine behaviour at the design stage has become critical. It is becoming common for customers to demand guarantees on response rate at the proposal stage and this requires a detailed insight into the transient behaviour of the engine. The development of a suitable control system also requires a full understanding of the transient response. A good insight into the dynamic behaviour of an engine can be obtained by use of the mathematical modelling methods, the development of which has been introduced in section 2.2 above. The judicious use of simulation techniques can be expected to yield a saving in both development time and cost.

Saravanamuttoo and Fawke (1971) compared the relative merits of the analog and the digital simulation. They showed that the analog was useful in preliminary studies, whereas the digital computer thanks to its accuracy and speed was much superior for detailed analysis. Consequently today the digital computer is almost universally used for off-design and transient predictions.

In today's procedures, a programme is designed to read the component characteristics and perform off-design point calculations. The next logical development from these

investigations is the prediction of engine performance during the transient phase. In this work, the transient or dynamic phase is defined as being that during controlled acceleration and deceleration of the engine.

2.4 METHODS USED IN DETERMINING STEADY STATE AND TRANSIENT TRAJECTORIES

As discussed previously, the first attempts to establish the transient behaviour of an engine were of an empirical nature and they were based on the test bed analysis of the machines.

Current techniques recognise the importance of using steady state component characteristics. Two distinct methods based on these characteristics are employed. These being the method of continuity of mass flow and the method of intercomponent volumes. These are now discussed.

2.4.1 The method of continuity of the mass flow

This assumes that mass continuity at all times and locations in which the engine operates has to be satisfied. The intercomponent volumes are usually ignored and the calculation procedure at each time step is iterative until continuity of mass flow is achieved. The inlet parameters of a component and its rotational speed are known or have been assumed (Fig.10). From these conditions and the component's characteristics, the outlet thermodynamic variables can be evaluated. This is carried out for all components in the engine and the mass flows are noted. In general the mass flows will not satisfy the principle of continuity. To satisfy this principle, initial parameters of some components are modified and the process is repeated until the mass flows

are compatible. The work produced or absorbed by each component is then calculated and acceleration or deceleration rates are evaluated for the shafts. The process is repeated for the next time interval until a specific limiting time is reached. Difficulty may arise in obtaining convergence of the computation. In some circumstances, the difficulty could be overcome by using a shorter time interval.

As an illustration of a simulation based on this method, the calculation procedure for engine configuration being investigated in this work is fully described in chapter III.

2.4.2 The method of intercomponent volumes (I.C.V.)

In this method, mass flow imbalances are allowed to occur. Volumes are introduced between the various components and all flow imbalances are assumed to occur in these volumes. The mass flow through each individual component is assumed to be instantaneously constant. These mass flow imbalances are used to evaluate the rate of pressure increase within the engine. The pressures rise or fall and from the new pressures at the end of the time interval, new mass flows in the components are then determined. Once all the components have been analysed in this manner, the power delivered or absorbed by the components is evaluated and subsequently the rotor torques and accelerations are determined. The process is repeated for the next time interval until a specified limiting time is reached. This procedure requires short time intervals and considerable computing time.

The method of the intercomponent volumes was used for a previous simulation of a typical turbofan engine (Ref.6). In this work, it was assumed that the size of an intercomponent

volume is the volume of the space between two components plus one half of each adjacent volume. For the calculation in addition to knowing the flight conditions and shaft speed, an initial guess of the pressures within the volumes must be made. From the known starting parameters, the compressor inlet temperature and pressure are determined. By calculation procedure the compressor mass flow rate and exit temperature can be found (Fig.11). An identical calculation to that of continuity of mass flow method can be used for the combustion chamber. Turbine inlet temperature and pressure and shaft speed are known. These can be used to calculate the mass flow rate through the turbine as well as the exit temperature. Turbine exit parameters, together, with the ambient pressure are used to calculate the mass flow rate through the final nozzle. Then, the mass flow mismatches are used to determine the new pressures in the volumes after the specified incremental time step has elapsed.

For a particular volume :

$$M_0 = \frac{PV}{RT} \qquad (2.1)$$

and

$$M_f = M_0 + \Delta M . \Delta t \qquad (2.2)$$

where $$\Delta M = \dot{m}_{in} - \dot{m}_{ou} \qquad (2.3)$$

so the new pressure :

$$P_n = \frac{M_f RT}{V} \qquad (2.4)$$

Similar to continuity of mass flow method, work imbalance between turbine and compressor can be used to calculate the shaft acceleration. Hence the new shaft speed for the next pass through component calculations at the next time step. The new values of pressure and shaft speed are substituted for the original values. The process is repeated until both mass flow mismatches and work imbalances disappear.

2.5 CHOICE OF METHOD USED IN THE PRESENT WORK

2.5.1. Introduction

A very simple method can be used for the modelling of the gas turbine engines when only small changes from one or several operating points are taking place. This can be done by assuming a linear system to represent the engine (this had been the approach used by early investigators such as Otto and Taylor (1950)). The above method is neither useful for a large scale transient nor for the determination of the operating line and is therefore of no assistance in the present work. Another possible method based on the first principles can be used for the engine's modelling. In this case, the performance of each component has to be determined from the component's geometry, which leads to lengthy calculations giving an inaccurate evaluation.

In the present work, the predicted characteristics are used in a computational method, as discussed below in section 2.5.2, for the calculation of the complete engine's steady state and transient performance. As the model development

proceeds and experimentally observed performance of the components becomes available, only the component performance maps need to be modified for continuing the investigation.

An approach has been introduced in the development programme for the scaling of the component characteristics. This has been used for two reasons. Firstly, in order to suit the engine configuration being investigated, it is necessary to factor up or down the performance of other engines. The second reason for scaling is that the observed steady running performance of the component in the engine is not necessarily the same as the one observed in the component rig, due to the intercomponent effects occuring during the matching of the components which modify the engine performance.

Turning now to the thermodynamic procedure for describing the engine during the transient, two methods have been studied by previous investigators. These are method of mass flow continuity and method of intercomponent volumes, these have been described in sections 2.4.1 and 2.4.2 above. Two sets of comparison of the prediction of these methods have been made. In Fawke and Saravanamuttoo (1971) study, they found that the methods gave similar prediction except for the first two time intervals of the transient when the intercomponent volumes method gave more realistic predictions. They also found that simulation of very complex configurations based on the continuity of mass flow method (itterative method) ended by difficulty in convergence.

More recently, Stoddart (1987) found for the case of two-spool medium by-pass turbofan engine that continuity of mass flow and intercomponent volumes methods were in good agreement for steady-running predictions. Considering predicted transient behaviour, acceleration and deceleration

trajectories of the I.P.Compressor predicted by the two methods were found the same, whereas those of the H.P.Compressor differ slightly in the high speed range. With comparison to continuity of mass flow method, acceleration and deceleration trajectories predicted by intercomponent volumes method were closer to the steady-running line. In the above investigation, it was realised that the computing time required by the I.C.V. method was of the order of thousands of seconds and with the inclusion of thermal effects or any other effects, the running time will be considerably greater. Therefore, the method of continuity of mass flow was adopted in the present work for the following reasons:

1) The computing time required for the simulation is much smaller compared to the I.C.V. method.

2) Sufficient information for this method was available.

3) Failure in convergence was realised when complex engines were simulated using the I.C.V. method.

2.5.2. Computational method

The engine on which the investigation has been based is a two-spool turbofan engine with mixed exhausts (Fig.8b). Typical characteristics have been used for the components. The resulting engine develops a maximum thrust at sea-level of about 12400 Lbf. As already stated earlier, the computational procedure for this two-spool engine which is shown diagramatically in Fig.10 is described in section 3.3. The simulation programme is written in Fortran 77. This was run on a digital computer mainframe system ICL2988 available in Glasgow University Computer Centre (G.U.C.C) and on

ICL3980 during the late stages of the work.

2.5.3 Choice of means of computation

An extensive amount of numerical handling and storing results from the mathematical modelling of the gas turbine engines. To obtain the results quickly and to allow the models to be used efficiently, the use of a computer is indispensable. Simulation of the engine dynamic behaviour can be carried out by means of analog, digital or hybrid computers. Each of these computers has its advantages and disadvantages and have been used successfully. (Ref.7)

Due to the accuracy, availability and information in Glasgow University Computing Centre, the digital computer was selected for simulation during all investigations in this work. Additionally the component characteristics and engine data such as fuel schedules could be stored and readily updated as the programme developed.

2.5.4. Handling of fan characteristics

In the present work, the fan has been treated as two separate components of the engine and so, the characteristics were supplied as two separate representations. These are the inner and the outer sections of the fan. The former delivers air to the by-pass duct, while the latter delivers the core air. A parameter GEOM to the value 0.25 was assumed. It represents the fraction of the total frontal flow area allocated to the inner section in order to make allowance for the interchange of flow. When we treat the fan as two separated components this might, however, be too rigid for the transient behaviour of the engine. Another parameter FCSP called the 'fraction of split' was initially set to the value

of 1. This represents the fraction of the GEOM area which feeds the inner section of the fan (core) - see Maccallum's Report to Rolls-Royce (1984) for a fuller explanation of the fraction of split.

CHAPTER III

ADIABATIC SIMULATION OF THE ENGINE

3.1 INTRODUCTION

Any simulation which has to predict the transient behaviour of an engine should take into account effects of heat transfer. In order to assess the significance of the heat transfer effects, predictions should first be made using a simulation which takes no account of thermal effects - this is called an " adiabatic simulation ". The simulation which incorporates models of the heat transfer effects is then used for a new set of engine predictions. Comparison between the two sets of engine predictions show the significance of the heat transfer effects. In this chapter, the adiabatic simulation is described. The steady-running predictions, which are an extension of adiabatic simulation are also given. For the modelling of the gas turbine engine, the method of continuity of mass flow has been used for both steady-running and transient predictions of the engine behaviour as stated in the previous chapter.

First, the simulation was carried out at sea-level conditions, Mach number 0.2 for both steady state and transient operations. The Mach number of 0.2 was used for a moving engine approaching the runway. The simulation was then extended to high altitudes of flight, assuming the engine operation at 41,000 ft and 50,000ft respectively, at Mach number 0.8.

Some assumptions have been used in the simulation in

order to exclude heat transfer effects. These are the following :

- The flow in the compressors and turbines was adiabatic.

- The characteristics of the compressors and turbines during the transients were the same as those recorded under steady-running conditions.

- The small air-flows controlled by seal clearances, which are drawn from the compressor to cool various hot sections remain the same fractions of the total air-flow.

3.2 COMPUTATIONAL METHOD OF SIMULATION

The computational procedure which is based on the method of "continuity of mass flow", has already been introduced in section 2.5.2 (chapter 2). Some further details are now given.

The method based upon the characteristics of each of the engine components represents the 'simulation method', which allows a greater insight into the dynamic behaviour of a gas turbine engine. The relationship between the engine components is determined by the engine configuration and by the thermodynamic behaviour of each component. Therefore, if all the component characteristics and the engine configuration are known, the gas turbine is defined and its dynamic behaviour can be expressed mathematically. The method is flexible in that more complex component representations are possible. Once the engine dynamics have been expressed mathematically the resulting equations may be programmed for the solution. This can be done with the aid of a digital

computer.

The first requirement to start a digital simulation of a gas turbine engine is the selection of the initial shaft speeds. These speeds, together with the externally applied conditions of the fuel flow, ambient temperature, pressure and flight Mach number, enable the operating point for each engine component to be determined as summarised below.

To predict the engine behaviour during a transient, the calculation procedure is as follows:

First, the L.P. and H.P.shaft speeds, together, with flight conditions of ambient temperature, pressure and Mach Number at the intake (fan inlet) are the known starting parameters. An initial guess for the factor of split (FCSP=1, explained in chapter II) at the start of the simulation is made. From the intake conditions, the I.P.Compressor inlet temperature and pressure can be determined. An initial guess of fan inlet mass flow rate is made. Then mass flow rate at the inlet of the I.P.Compressor is obtained (Fig.10). FCSP and GEOM permit the calculation of the mass flow rate at the exit of the outer section of the fan (to the by-pass duct). For the H.P.Compressor, an initial guess of pressure ratio is made. The compressor inlet temperature and pressure can be determined. At this stage, non-dimensional mass flow at the exit of the H.P.Compressor obtained from the characteristics is compared to that calculated (TEST A) and in case of disagreement between the two mass flows, either a revised guess of the H.P.Compressor pressure ratio has to be made or the value of the mass flow rate of the core engine at the entry of the inner section of the fan has to be revised until the two mass flows match together (see Fig.10). For the combustion chamber, the fuel flow rate is known from the

selected transient fuel schedule and with an energy balance equation, the combustion chamber outlet temperature can be determined. By applying a pressure loss factor to the inlet pressure, the outlet pressure can be determined. Once the combustion chamber exit parameters are found, the actual non-dimensional mass flow at the entry to the H.P.Turbine will be compared (TEST B) to that given by the characteristics. In case of mismatch, either H.P.Compressor pressure ratio or mass flow rate at the inlet of the inner fan section have to be revised. For the L.P.Turbine, however, the inlet parameters are known from the turbine characteristics. By using the work done factor, the turbine exit temperature can be determined. L.P.Turbine pressure ratio being known permits the calculation of the outlet pressure. A comparison between the calculated non-dimensional mass flow and the one obtained from the characteristics is made (TEST C) and if the two mass flows differ, H.P.Turbine work done factor has to be modified until agreement is achieved. At the mixer, the gas and air static pressures at the exit are compared (TEST D) and in this case, work done factor of the L.P.Turbine has to be revised if the two pressures are different. To test compatibility of mass flow continuity, the nozzle area required to discharge the flow at the exit and the area obtained from the characteristics are compared (TEST E). If the two areas differ, it is the factor of split FCSP initially guessed which has to be revised until these areas are the same to the required degree of accuracy. Once this compatibility is achieved, the work imbalance is used to calculate the net torque on the rotors. From the given values of the rotor inertia, the rotor accelerations will be determined.

Once the acceleration is determined the rotational speed at the end of the next time interval can be obtained from this parameter. Several techniques of varying complexity can be used for this purpose. The simplest one which has already been used previously by Pilidis in 1983 (Ref.8) was applied to the present work. This is known as the 'Euler's method' shown by equation (3.1). In this method the acceleration is assumed to remain constant during the time interval for which it has been calculated.

$$\omega_{t+dt} = \omega_t + \left(\frac{d\omega}{dt} \right)_t \Delta t \qquad (3.1)$$

The time increment has to be small for the Euler method to be reasonably accurate. Also, it was found that if the time increment was not sufficiently small, convergence of the iterative procedure described above became impossible. Thus it was desirable to use a short time interval, typically of 0.05 second or less. However if the time interval selected was too short, computing times became excessive. So finally a time of 0.05 second was selected, with the modification of shortening to 0.025 second for the first second of a deceleration (to overcome difficulties in convergence).

Several fuel flow schedules are possible; the fuel flow can be scheduled as a function of the rotational speed of either the L.P. or H.P.Shafts as shown by equation (3.2)

$$\dot{f} = f(N) \qquad (3.2)$$

This fuel schedule is not non-dimensional and can be used only for one specified altitude and Mach number. As the desired transient simulation of the engine should be valid at

any level, fuel flow scheduled on shaft rotational speed was left out of use. For this reason, a non-dimensional fuel flow schedule was used where all the parameters are related to the H.P.Shaft. This is shown by the following formula :

$$\left(\frac{\dot{f}}{N\ P}\right)_{HP} = f(PR_C) \qquad (3.3)$$

This fuel schedule can essentially be used at any engine altitude simulation and for any value of the flight Mach Number at this particular altitude.

The steady-running of the engine is predicted by holding the fuel flow at a fixed value within the time limit given and when this is reached, a steady state operating point is then determined. The steady-running goes through many iterations along the time intervals. Once an operating point is determined the incremented fuel flow value will be held constant during the next interval, until the next operating point is found. The calculation proceeds so on until the last operating point is reached. A range of steady state operating points will be determined to form what is called ' the working line ' or 'steady state operating line'.

The programme incorporates allowances for Reynolds numbers effects on component efficiencies and mass flow rate. Very simple and empirical coefficients supplied by Rolls-Royce have been used.

3.3 ENGINE PREDICTION PROCEDURE AND RESULTS

3.3.1 Steady-running operation

The steady-running line was plotted on the engine component characteristics. The operation was carried out at

sea-level and also altitude . The fuel flow is held constant at a specified value, allowing the engine to stabilise itself. Only the logic of the programme has to be changed when transient accelerations and decelerations are required. Initial values of shafts speed are given together with the starting fuel flow as data input. These will be adjusted as the programme converges. The steady-running conditions predicted by the present programme are compared to those predicted by Rolls-Royce programme in order to find out the probable discrepancies between the two programmes. At sea-level conditions where the ambient temperature and pressure are 288K and 101.3kN/m^2 respectively and with a flight Mach Number of 0.2. A maximum and a minimum fuel flow limits of 0.84kg/s and 0.08kg/s, respectively, have been used as the terminating conditions. The positions of the working lines in the various component map characteristics were examined during steady state adiabatic operation. It was found that the inner fan which represents the engine component through which the core mass flow passes before reaching the first stages of the I.P.Compressor presented flat map characteristics. The fan pressure ratio P_{24}/P_1 was plotted versus the non-dimensional mass flow. The steady-running points predicted by the present programme, deviated apparently from those given by Rolls-Royce programme (Fig.21a). The reason for this deviation may be attributed to the different logics of the two programmes and the different ways of handling the characteristics of the two sections of the fan.

The engine component through which most of the air mass flow passes is the outer section of the fan. In this section, the pressure ratio is greater and the map characteristics are

markedly different from those of the inner section. Also at high speeds, the constant speed-lines become vertical. This is the onset point of the choking process. As shown in Fig.21b, the steady running points deviate, but only slightly from the prediction of the Rolls-Royce programme. The reason for this deviation could be as already discussed for the inner section. The I.P.Compressor is an engine component which is directly coupled mechanically to the L.P.Turbine and thermodynamically to the H.P.Compressor. Some of the air mass flow coming from the outlet of the fan (the by-pass air) flows into the by-pass duct to meet the hot gases in the final nozzle (in the mixer) to be exhausted into the atmosphere whereas, the remainder of the flow (the core air) passes through the three stages of the I.P.Compressor before reaching the first stages of the H.P.Compressor. As can be seen from Fig.22b, the steady-running points in the I.P.Compressor present a slight discrepancy at the higher values of speed, compared to those predicted by Rolls-Royce. In fact, the working line deviates slightly towards surge at high speeds in the present programme whereas, at the low values of speed a good agreement between the two programmes is apparent. However, the discrepancy is probably caused by the differing fan treatments.

Considering the H.P.Compressor, the constant speed-lines are almost vertical at high speeds and the corresponding mass flow is that given by the choking conditions. In this component, the steady running line nearly coincides with that given by Rolls-Royce's programme, as clearly shown in Fig.22a.

Engine adiabatic prediction has also been simulated at 41,000ft altitude of flight. At this altitude the

corresponding ambient conditions of temperature and pressure are 216.5 K and 17.87 kN/m^2 respectively. A Mach Number of 0.8 was assumed. Maximum and minimum fuel flow limits of 0.19kg/s and 0.06kg/s were used as terminating conditions. In this case, the steady-running line deviated from that predicted at sea-level conditions on the inner fan maps characteristics. Considering the outer section of the fan, the position of the working line predicted at 41,000 ft and the one predicted at sea-level conditions deviate and this noticeable deviation reduces as the speed approaches the high values. Results are clearly shown in Figs.23. The reason for these movements in the fans is due to the choking of the final nozzle caused by the higher value of the Mach number (0.8). For the I.P.Compressor, as shown in Fig.24b, the working line is slightly raised from its sea-level position. This movement is much less in magnitude than those of the inner and outer fan sections. The steady-running operating points for the H.P.Compressor almost coincide with those predicted at sea-level. The increase of flight Mach number with the increase in altitude causes little change to the H.P.Compressor behaviour during steady-running conditions (Fig.24a). This is because the H.P.Shaft is operating with a choked H.P.Turbine. The only influence is that caused by development of boundary layers as a result of reduction of Reynolds Numbers due to the decrease in the density.

At 50,000ft altitude, the working lines were predicted to be very similar to those predicted at 41,000ft. At this very high altitude, the corresponding values for the ambient conditions of temperature and pressure are 216.5k and 11.59 kN/m^2 respectively. A maximum and a minimum fuel flow limits of 0.13 kg/s and 0.05 kg/s were used with a flight Mach

number of 0.8.

3.3.2 Engine transient acceleration

An adiabatic transient acceleration simulation was carried out at both sea-level Mach Number 0.2 conditions and altitude Mach 0.8. The heat transfer and thermal effects which are likely to occur during the transients are not taken into account at this stage. The initial values of the L.P. and H.P. Shaft speeds are specified at the start, together, with the fuel flow. This is fed into the combustion chamber by the fuel schedule used during this acceleration (Fig.99). The nature of the fuel schedule used depends on whether the transient is experienced at sea-level or at altitude conditions of flight. Two alternative forms of logic can be used; This depends on the value given to the parameter NLOGIC (1 or 2) used in the computer programme. For both acceleration and deceleration, logic 1 could be used. However, for more rapid acceleration schedules the procedure followed with NLOGIC 1 enters a loop resulting in a failure to converge. The explanation for that is as follows: under NLOGIC 1, if the mass flow rate obtained from the characteristics of th H.P.Compressor is greater than the actual mass flow rate at TEST A (Fig. 10) then the mass flow rate at the intake of the inner fan has to be increased. This causes the pressure ratio across the I.P.Compressor P_{26}/P_{24} to drop during an acceleration. This dropping during a rapid acceleration is too much resulting in an increase in the mass flow rate at the inlet of the H.P.Compressor while the pressure P_{26} decreases. The temperature T_{26} at the exit of the H.P.Compressor rises as moving into low efficiency region of the I.P.Compressor characteristics. As a result of this, the

non-dimensional speed line of the H.P.Compressor characteristics $N_H/(T_{26})^{0.5}$ decreases and so does the mass flow rate on the characteristics. Thus the convergence becomes too rapid and correction overshoots. Similar overshoot on return occurs and thereby convergence may never be achieved. A solution to overcome this problem was to use NLOGIC 2 in which case P_3/P_{26} is increased if the characteristics mass flow at TEST A is greater than the actual figure. Under NLOGIC 2, the inlet mass flow at the inner fan is revised following TEST B at the H.P.Turbine. A multiplying factor of 0.90 was used during this acceleration to scale down the acceleration schedule given by CASC-211 thereby, avoiding surge of the H.P.Compressor due to excessive acceleration rates. At altitude operation the scaling factor of 0.90 was still not convenient. To avoid surge, this factor was reduced to 0.83. At sea-level conditions where a flight Mach Number of 0.2 was assumed, the starting speeds for this transient acceleration were 1805 r.p.m. and 6030 r.p.m. for the L.P. and H.P.Shafts, respectively. A maximum fuel flow limit of 0.82 kg/s, was used as the terminating condition for the acceleration.

Examining the movement of the transient trajectories on the components characteristics, as shown in Fig21, the operating points predicted during the acceleration on the inner and outer fan sections characteristics coincide with those of the steady-state operation. Therefore, no additional problems should be experienced during acceleration. For the I.P.Compressor the transient acceleration operating line departs significantly from the steady-running line (Fig.22b). At the beginning of the low speeds, the two lines coincide, but from the medium values of the speed and up to the high

values, a deviation of the operating points was noticed. The pressure ratio is lowered down towards unity. The reason for this is that after a few seconds of the transient, the air demand of the H.P.Compressor increases more quickly than that available from the I.P.Compressor outlet. This results in the reduction of the I.P.Compressor presure ratio provided to the value of about unity, which in turn allows the H.P.Compressor to meet the non-dimensional air mass-flow required. This effect is most noticeable when the I.G.V's of the H.P.Compressor begin to open.

From idling to maximum speed the transient acceleration working line for the H.P.Compressor is raised from the steady-state towards surge. Hence, this causes an usage of the surge margin. Approximately 80% of this margin was already used after which the trajectory moved away from the surge line, at the high values of speed. Also noticeable from Fig.22a is a considerable overshoot in the non-dimensional speed before stabilisation of the engine. This is primarily due to an overshoot in the H.P.Shaft speed.

At 41,000 ft, the starting speeds for the acceleration were 4012 r.p.m. for the L.P.Shaft and 9296 r.p.m. for the H.P.Shaft. The maximum terminating condition fuel flow used was 0.19 kg/s. From Fig.23, it can be seen on the inner and outer sections of the fan characteristics that the steady-running operating line and transient acceleration trajectories coincide. With the I.P.Compressor, the transient operating points depart significantly from the steady-state points and at the low values of speed, the former moves away towards the low values of the compressor pressure ratio during the first second of the speed transient (Fig.24b). The magnitude of the deviation is almost the same as that

experienced at sea-level conditions. For the H.P.Compressor, unlike the other engine components, the acceleration is critically rapid. The transient operating line was predicted to approach and coincide with the surge line, thus all surge margin was used. This is clearly shown in Fig.24a.

Engine transient acceleration was also simulated at 50,000 ft. The starting speeds used on the L.P.Shaft and H.P.Shafts were 4200 and 9100 r.p.m. ,respectively, and a maximum fuel flow limit of 0.13 kg/s was used as the terminating condition of the transient. The movements of the trajectories on the various engine components were similar to those predicted at 41,000ft.

3.3.3 Transient deceleration

Transient deceleration was also predicted at sea-level conditions and altitude. The deceleration process was allowed for in using the alternative logic. This can be done by setting the parameter NLOGIC to the value of 1. The starting speeds for this deceleration predicted at sea-level conditions were 8630 r.p.m. and 12164 r.p.m. for the L.P. and H.P.Shafts respectively. A limiting fuel flow limit of 0.08 kg/s has been used as a terminating condition for the deceleration.

The transient deceleration operating points for the inner and outer section of the fan coincide with the steady running point, and hence with those of the acceleration, as shown in Fig.21. Regarding the I.P.Compressor characteristics, shown in Fig.22b a very significant displacement of the transient deceleration trajectory is apparent. Transient trajectory is predicted to approach surge immediately after the beginning of deceleration during the first quarter of the first second

of the speed transient. The process is, therefore consistent with that occuring during the acceleration where this was predicted to be far from surge. Unlike the I.P.Compressor, the H.P.Compressor transient deceleration operating points shown in Fig.22a are lower than those of the steady-state. The two trajectories move closer and closer as the speed reduces.

At the altitude of 41,000 ft, starting speeds set for deceleration were 7700 r.p.m. for the L.P.Shaft and 10940 r.p.m. for the H.P.Shaft. The minimum fuel flow limit used as the terminating condition for this prediction was 0.04 kg/s. A scaling factor of 0.90 was used to scale down the deceleration schedule, as a transient test during deceleration process. Fig.23 shows the respective movements of the working trajectory in the inner and outer sections of the fan . As can be seen from this figure, no deviation of the transient operating points from those of the steady-state is noticeable for the inner fan section. Whereas, for the outer fan, a slight movement of the transient trajectory at the medium values of the speed was noticed. For the I.P.Compressor, the relatively modest deceleration schedule gives a transient trajectory which was predicted to cross the revised surge line. This event occured at the first half of the first second of the speed during deceleration and at this time all the margin was used. The surge margin recovers at the end of the speed transient (the deceleration trajectory moves closer to the steady running line) as is clearly shown in Fig.24b. At altitude of 41,000 ft, the H.P.Compressor performance behaves in a different manner to that predicted at sea-level. In fact, acceleration (non-dimensionally) takes place after the overshoot in the non-dimensional speed,

following the decceleration. The deceleration schedule was such that the engine cannot drop to a fuel flow of less than about 0.04kg/s.

The adiabatic prediction for the transient deceleration, was also simulated at 50,000 ft. For this, the starting speeds of 7700 and 10940 r.p.m. for the L.P. and H.P.Shafts, respectively, were used. Terminating condition for this altitude deceleration was controlled by a minimum fuel flow limit of 0.06 kg/s. As can be seen from Fig.26b, a similar event to that of 41,000ft occured at an altitude of 50,000 ft during transient deceleration of the I.P.Compressor. The transient deceleration trajectory crosses the revised surge line (Fig.26b) and as a result all the surge margin available was used in less than one second from the start of the speed transient. By examining transient trajectories of the H.P.Compressor, the movements of the transient deceleration working line are more pronounced (Fig.26a).

CHAPTER IV

PREDICTION OF NON ADIABATIC ENGINE PERFORMANCE WITH UNCOMPENSATED FUEL FLOW SCHEDULE

(WITH HEAT TRANSFER EFFECTS INCLUDED)

4.1 INTRODUCTION

During transients, gas turbine performance is influenced by some effects. These are due to the thermal effects of non adiabatic flow, altered boundary layer development and changes in tip and seal clearances. During the early stages of the development of gas turbine, modelling was carried out assuming adiabatic conditions or using unrealistic models to simulate the engine. It was only very recently that it was realised that heat transfer effects have an important influence on the transient performance.

When a gas turbine experiences a change of state, the engine materials will exchange heat with the working fluid because of the temperature changes of the latter. These heat exchanges influence the performance of the engine in an important manner. Thermal effects which are considered in transients are :

- Non adiabatic flows in compressors and turbines.
- Changes in boundary layer development on blade aerofoils in compressors.
- Changes in the boundary layer development on end-walls in compressors.
- Tip clearance changes, controlled by disc, casing and blade responses.

- Seal clearance changes,controlled by disc,casing and ring responses.

All these effects influence the performance of the components and hence the engine as a whole system, leading to revised transient trajectories in the compressors and to important changes in predicted performance.

Also in steady-running, heat transfer is very important. The efficiency of aircraft gas turbine engines is strongly affected by the maximum allowable turbine inlet temperature. The performance improvements that can be achieved by increases in this parameter are substantial. Such increases are limited by heat transfer considerations. For this reason, many contemporary research efforts are directed at obtaining a better understanding of cooling schemes which can be incorporated into component designs in order to permit higher gas temperature operation. In addition to the design of the cooling systems of the hot parts of the engine such as the combustion chamber and the turbine, the evaluation and assessement of the thermal behaviour of other parts such as the fan, compressors, seals etc., are indispensable. This is the result of the trend in modern aero-engines towards higher cycle pressures and temperatures, increased reliability together with reduced engine weight and ever tighter clearances to improve performance and thus achieve a further reduction in fuel consumption.

4.2 DEVELOPMENTS REQUIRED IN MODERN AERO-ENGINES DESIGN

Modern aero-engines are characterised by their extremely high power and low specific fuel consumption leading to a relatively low weight and small size. To illustrate this trend, two fighter engines with different thrusts are shown

in Fig.9. These are the RB-199 and the JT7D. For civil engines, engine overall efficiency is of paramount importance. It is well known that two of the main factors contributing towards this achievement are the high pressure ratio and the high turbine entry gas temperature wich provide high thermal efficiency in the thermodynamic cycle. Today's aero-engines have a turbine entry temperature of 1600K to 1700K and above. Therefore, an intensive cooling of turbine blades is necessary.

4.3 HEAT TRANSFER PROBLEMS IN THE MAJOR ENGINE COMPONENTS

Gas turbine engine components are subjected to various heat transfer problems. These are considerable during transient conditions where components behaviour and hence engine operation becomes more severe. Some of these problems which are related to each of the engine components (Fig.12) are discussed below.

Intake and fan

In certain altitude, flight and atmospheric conditions, the engine inlet and fan may be subjected to severe icing problems. Therefore, it is very necessary to design appropriate means to prevent the build up of harmful ice.

Compressor

The present trends in compressor design are towards higher overal pressure ratio (up to 30) resulting in high exit temperature (800K to 900K), increased rotor speed and higher aerodynamic efficiency and loading. For this reason, a much more detailed analytical design including thermal analysis and heat transfer effects is necessary to predict

accurately the transient temperature distribution of the compressor disc and casing during the whole engine operation. In addition to the stresses resulting from the centrifugal forces, the thermal stresses resulting from heat transfer effects are considerable, especially during transient conditions. These affect the compressor discs and casing life. The disc rim which is close to the main stream follows a change in power much faster than the hub section which is removed from the main stream. An example of a typical compressor disc is shown in Fig.14. The resulting radial deflection of the rotor during transient conditions is relatively slow. In contrast, the radial movement of the casing is usually much faster because the temperature of the thin casing, which is exposed to the main stream follows a change in power very rapidly.

For modern engines to achieve a more favorable transient thermal behaviour, a careful and accurate design of the components is needed. With the compressor, the aim is to speed up the temperature response of the rotor and to slow down that of the casing. For the rotor this can be achieved by venting the cavities between the discs with a small amount of air taken from the main stream (Ref.9). To slow down the casing one may simply add mass which is not exactly desirable in aero-engines. It is clear that very advanced computational methods and accurate knowledge of convective heat transfer are required to achieve the optimum life and clearance variation throughout the engine operation.

Combustion chamber

The design of complex configuration for the combustion chamber calls for very sophisticated computational methods

with good models for flame radiation, heat transfer coefficients at the inner and outer flame tube surfaces and hot gas temperature effective for the gas side convection. Another heat transfer problem in the combustion chamber involves vaporisation of the fuel droplets. The speed of this process is one of the factors controlling subsequent combustion. Therefore, detailed knowledge of the heat and mass transfer during the vaporisation of clouds of droplets is required. In the light of today's highly-loaded combustors and increasing cycle pressures, the current methods are not sufficiently accurate and a considerable amount of research effort is still required.

The turbine

Similar to the combustion chamber, the first turbine stages of modern aero-engines operate in an environment where the gas temperatures are well above the allowable metal temperature. Therefore, an efficient cooling is necessary. High temperature parts are prone to failure, therefore in aero-engines, turbine cooling is a particularly important subject.

The tendency to increase the turbine entry temperature more quickly than the allowable material temperature, generally means higher heat flow into the turbine blade. Since this heat is energy taken out of the main gas stream, it is lost for the performance of work at that particular turbine stage, which may be expressed as a loss of turbine efficiency. Besides the task of cooling the various turbine parts, such as blades, discs, etc., careful design for optimum clearances is required if the high efficiencies are to be achieved. A procedure similar to that with the

compressor is necessary.

4.4 MODELS FOR HEAT TRANSFER EFFECTS

4.4.1. Effects happening during transients

Usually in a turbomachine, heat transfer has not only an effect on the energy balance of the thermodynamic cycle but can considerably change the performance of the components. The heat exchanges influence the performance of the engine and thermal effects which are considered to be relevant in transients are described in the previous section. One of these effects to influence the performance of a turbomachine is the change of clearances within a compressor or turbine during transient operation. First, the changes of clearances with gas temperatures and time has to be determined. once this has been accomplished, the influence of these changes on the engine performance has to be predicted. the important change is usually in efficiency.

4.4.1.1 Clearances

Gas turbines are subjected to thermal and mechanical loading which produce small changes in both the radial and axial dimensions of the components. These changes of dimension occur during transient operation and they result in relative movements between rotating and stationary components; thus causing varying tip clearances and non-design mass-flows. In the present work, only radial clearances are considered and further investigation is required for the prediction of the axial clearances. One of the reasons for which clearance changes occur during transients is the thermal growth of the components. During transients, the components of an engine expand at different

rates because some sections absorb heat faster than others. For this reason, a convenient partition of the disc was suggested by Pilidis and Maccallum in 1984 (Ref.11) where the disc is treated as three sections, each of uniform temperature - a thick hub section, thin diaphragm and an outer rim (Fig.17). Single subdivisions are possible for the blade and the casing. The clearance opening is also affected by another factor which is the centrifugal expansion. This requires the same subdivision of a stage, as used for the calculation of thermal growths in order to obtain centrifugal growths.

Tip clearance changes can be regarded as an indirect effect of heat transfer, during engine transient operation. Another indirect effect of heat transfer lies in the response of seals which control cooling air flows. It is, therefore, very desirable to develop models for representing both tip and seal clearance changes and to use these models to predict the effect of these clearance changes during transients, on the performance of the various components and hence of the engine. A development of this nature has been carried out by Pilidis and Maccallum (Ref.11).

The influence of the non adiabatic flow (a direct heat transfer effect) has been studied for a typical two-spool by-pass turbofan engine. The transient programme has been extended to include these models so as to enable the calculation of the desired effects on engine transient response. In this work, a single equivalent stage was assumed for calculation of tip clearance movements, with averaged stage dimensions of either the compressor or turbine. The mechanical and thermal loadings of the components vary

producing small changes in the dimensions (in both the radial and axial directions). A tip clearance of a turbo-jet engine depends on the following factors:

- Thermal extension of the casing (radial).
- Thermal extension of the blades.
- Thermal extension of the discs.
- Extension of the blades and disc due to centrifugal forces.

4.4.1.1.1 Thermal effects

a) Blade tip movement

The movement of the blade tip depends on the responses of the disc and blade. For the disc some faces rotate adjacent to stationary faces, while other faces form walls of what are effectively rotating chambers. With regard to faces adjacent to stationary walls, several investigations have been carried out to examine the heat transfer coefficient (Ref.8). A correlation has been obtained for the mean Nusselt number in terms of axial Reynolds number and rotational Grashof number (Ref.11). An adequate general correlation which has been used in the previous investigation (Ref.8) is suggested for the local Nusselt number for the present work. This is given by equat(4.1).

$$Nu_r = 0.0253(Re_r)^{0.8} \qquad (4.1)$$

For the rotating faces which form the rotating chambers or cavities, heat transfer mechanism is a naturel convection in a high gravity field. In this case, Nusselt number is given by equation(4.2).

$$Nu_r = 0.12\ (Gr)^{0.33}\ (Pr)^{0.33} \qquad (4.2)$$

For heat transfer to turbine blades, where initially uncooled blades are to be considered, a suitable correlation is given by Halls (Ref.12):

$$Nu = 0.235\ (Re_b)^{0.64} \qquad (4.3)$$

For compressor blades, one approach that has been used is to adopt a weighted average between laminar and turbulent boundary layers developing on flat plates. The results of this method have been found to be within 5% of the results obtained by applying Halls`s turbine correlation to compressor blades. Therefore, Hall`s correlation has been used for all blades.

b) Casing movement

The casing has a complex structure with inner and outer surfaces subjected to gases or air at differing temperatures and pressures moving with differing velocities. In order to estimate heat transfer coefficient at the internal surface of the casing the approach used was to regard the casing as a cylinder in which a smaller cylindrical shape is rotating. The heat transfer coefficient is given by (Ref.8):

$$Nu_{ic} = 0.015\left[1+2.3\ \frac{(D_0+D_i)}{L}\right]\left(\frac{D_0}{D_i}\right)^{0.45}\ (Re)^{0.8}\ (Pr)^{0.33} \qquad (4.4)$$

where

$$Re = \left(V_{am}^2 + \frac{V_t^2}{2}\right)\frac{D_0 - D_i}{2} \qquad (4.5)$$

For the outer surface of the casing, the expression

used was for a developing turbulent boundary layer on a flat plate. It is also important to note that the casing expansion is larger than that of the disc, which brings the clearance to the equilibrium value (Disc is cooled much more effectively than the casing).

4.4.1.1.2 Mechanical effects

When a gas turbine changes state, the modified rotational speed results in changes of the stresses experienced by the components. These mechanical effects cause centrifugal growth, due to changes in the angular velocity of the rotor, change in the "pull" of the blades and of the disc sections. For the calculation of mechanical effects, the same subdivision of the rotor was used as for the calculation of thermal effects. Also each disc is assumed to be represented by the same three rings used for the thermal model (Fig.17).

a) Disc

To simplify developing the model, the disc could be represented by the same three rings as in the thermal model and a multiplying factor of 1.3 was necessarily applied to the predictions in order to bring them into agreement with those given by a finite element analysis.

b) Blades

The blades are subjected to "pulling" due to the very high rotational speed. These were assumed to be rods of a uniform cross sectional area, with or without a shroud at the blade tip.

c) Casing

The only relevant mechanical loading considered was the pressure change during the transient and its effect was found (Ref.8) to be very small (about 1% of the total movement of the rotor due to mechanical effects).

4.4.1.1.3 Disc averaged temperature method

The use of single 'equivalent' stages instead of complete components would be highly desirable. A single equivalent stage, can give satisfactory heat transfer rates (Ref.20). A single equivalent stage has, therefore, been developed based on averaged dimensions of the 12 stages and using averaged properties of specific heat, thermal expansion coefficient. The subdivision of the equivalent disc is retained for the calculation of thermal effects. The various rotor sections are assumed individually to have infinite thermal conductivity and material properties are assumed to be constant throughout the relevant temperature range. The process, ensuring continuity of the radial dimension of the disc section interfaces is, however, eliminated and replaced by an average disc temperature given by equation (4.6) and hence thermal expansion of the disc is obtained.

$$T_{av} = \frac{\Sigma T_i V_i}{\Sigma V_i} \qquad (4.6)$$

The method of calculation is retained for the thermal growths of the blades and casing. The centrifugal growth is simplified for this model by calculating the expansion of a disc of the same inner and outer radii and of a uniform

thickness equals to the minimum diaghragm thickness. To check the validity of this simplification, growths were compared with those obtained from finite element analysis and it was found (Ref.11) that the introduction of the same factor of 1.3, gave satisfactory congruency. The resulting expression for centrifugal growth of the disc is given by equation (4.7)

$$\Delta_{Rd} = 1.3\ R_0\ \omega^2 \left[\frac{\Sigma M_b}{L\left(R_0^2 + \frac{R_i^2}{R_0^2} - R_i^2\right)} + \rho_d\left[R_i^2(3+\sigma) + R_0^2(1-\sigma)\right]\right] \qquad (4.7)$$

In (Ref.11), pressure effects were found to be very small and so they are neglected in this simplified analysis. The centrifugal growth of the blades is calculated as described in the previous sections and is given by equation (4.8).

$$\Delta_{Hb} = \left[\frac{R_{bt}^3}{3} + \frac{R_h^3}{6} - \frac{R_{bt}^2\ R_h}{2}\right]\rho_b \frac{\omega^2}{E_b} \qquad (4.8)$$

When effects of the blade shroud are included, the elongation due to the mass of the shroud must be taken into account and the equation becomes :

$$\Delta_{Hb} = \left[\left(\frac{R_{bt}^3}{3} + \frac{R_h^3}{6} - \frac{R_{bt}^2\ R_h}{2}\right)\rho_b + R_{bt}\frac{(R_{bt} - R_h)}{A_b}\right]\frac{\omega^2}{E_b} \qquad (4.9)$$

4.4.1.1.4 Efficiency loss calculation

The most important effect of non-design blade tip

clearance, is that of efficiency changes of the compressors and turbines. The component being considered is simplified to a single-stage equivalent compressor or turbine. The tip clearance is estimated as indicated previously and the efficiency reduction relative to zero tip clearance is given by the correlation suggested by Lakshsminarayana (Ref.10), which is illustrated by equation (4.10)

$$\Delta\eta = \frac{0.7\ \psi\lambda}{\cos\beta m}\ (1 + 10\sqrt{\frac{\lambda\phi A}{\psi\cos\beta m}}\ ) \qquad (\ 4.10\ )$$

The efficiency loss compared to the stabilised value of clearance at that particular speed and inlet conditions can be calculated. The stabilised clearances at the desired conditions are evaluated using the same methods, and hence stabilised values of efficiency loss due to clearance openings are obtained. The difference in efficiency is calculated by subtracting the transient efficiency loss from the stabilised efficiency loss and thus the transient efficiency of the component can then be determined.

4.4.1.2 Procedure of estimation of seal clearances.

The methods and models used for tip clearance movements can be adapted and applied to estimate the seal clearance movements during transients. The seal clearance controls the amount of fluid leaking through it. Two seals are placed at different positions in the engine to allow controlled amount of air to reach and cool the hot sections of the engine. The clearance of these seals controls the flow escaping from the core and if these clearances are not as designed, the incorrect amount of flow will escape. In the two-spool

turbofan engine investigated, there are two important seals, the H.P.compressor 12th stage outer seal and the H.P.cooling air seal on the H.P.1 turbine disc. These seals are influential in delaying the attainment of the final state of the engine.

a) H.P.compressor 12th stage outer seal

This seal is placed on a small disc at the upstream end of the H.P.compressor and controls the flow that escapes to the by-pass duct from the H.P.compressor delivery.

b) H.P.cooling air seal on H.P.1 turbine disc

This seal is mounted on the H.P.1 turbine disc, as illustrated in Fig.18. The seal is formed between the tips of fins which are integral with the turbine disc (first stage of the high pressure turbine) and a stationary ring mounted on the partition wall, A. High pressure cooling air, taken from the delivery of the high pressure compressor, is supplied to the left side of the seal. The purpose of this seal is to allow a small controlled flow of this cooling air to pass through zone B, cooling the face of the turbine disc. The flow then passes through the gap between the downstream edge of the platforms of the first set of high pressure nozzle guide vanes and the front edge of the platforms of the first set of high pressure blades.

4.4.1.3 Heat capacity of the components

Engine materials and the working fluid exchange heat. Because of this heat exchange, the index of compression n_c or expansion n_t of the working fluid changes too. Thus, the

performance of the various engine components will be altered. These effects have been investigated by several authors. Pilidis and Maccallum (Ref.19) have proposed the following model, which has been elaborated from the first principles described earlier by the second of these authors.

for compressors:

$$\frac{(n_{ht} - 1)}{n_{ht}} = \frac{1 - F}{n_{po}} \cdot \frac{(\gamma - 1)}{\gamma} \qquad (4.11)$$

for turbines:

$$\frac{(n_{ht} - 1)}{n_{ht}} = (1 - F)\, n_{p0}\, \frac{(\gamma - 1)}{\gamma} \qquad (4.12)$$

4.4.1.4 Changes in compressor characteristics

During transients of axial flow gas turbines, the heat exchange occuring between engine materials and working fluid produces changes in the component characteristics. These changes are due to the density changes of the fluid affecting the axial velocity and changes in the aerofoil performance, which in turn produces changes in the magnitude of the deflection of the fluid. When heat transfer is present, the blades will not deflect the flow as they do under adiabatic conditions. The result will be a modification of the performance of the component in question. Three reasons have been suggested (Ref.14) for the modification of the characteristics during a transient :

- Fluid density changes.

- Alterations in the aerofoil boundary layer.
- Tip clearance changes.

i) Effect of fluid density changes

When a cold engine is accelerated, heat is transfered from the air to the blades and casing. This will increase the density of the air giving it a lower axial component of velocity at a particular stage of the compressor. As a result, the loading on that particular stage is altered and thus changes the stage pressure rise. Consequently, the overall pressure rise is altered and hence, alters the working points of the stages.

Previous investigation has been carried out by Maccallum (Ref.15) in order to predict modification of the non-dimensional speed line due to heat transfer effects. The calculation proceeds normally for the next blade pair but with a reduced inlet temperature (during an acceleration) because some heat has been removed after the exit from the previous blade pair. The amount of heat removed is the heat transfered to the material. This loss of heat alters the density of the fluid. As a result, the velocities will change.

The premise adopted in this work is to assume that only heat transfer to or from the aerofoils of the blades alters the density as compared to adiabatic running. This is because it was found in Ref.15 that heat transfers to or from platforms and casing had little influence on the temperature and hence, density of the air at the pitch-line. After heat transfer effects were incorporated into the pitch-line prediction method, Maccallum (Ref.15) found that for a given inlet non-dimensional speed a new pressure ratio to non-

dimensional mass flow characteristics was obtained. To quantify this change, it is possible to retain the adiabatic characteristics and use a modified 'effective' speed. Also, the surge pressure ratio at a particular non-dimensional mass flow can be changed. For these small changes the following expressions have been suggested (Ref.15)

- For change in effective speed :

$$\frac{\Delta N}{N} = C_1 . \frac{Q}{m\ C_p\ T_m} \qquad (4.13)$$

- For changes in surge pressure ratio at a given mass flow:

$$\frac{PR_{ht\ -\ 1}}{PR_{ad\ -1}} = 1 + C_2\ F \qquad (4.14)$$

The values of the constant coefficients, C_1 and C_2, are valid for several transients in various situations, but for only one compressor. Additionally, blade with its aerofoil and platform combination, can be treated as two components, comprising firstly the aerofoil and secondly a finned platform (Ref.16). The effectiveness of the finning depends on the instantaneous aerofoil temperature.

ii) Boundary layer development

Heat transfer from a wall to a boundary layer increases the rate at which the layer develops by the influence of local density reduction on the momentum integral equation. The effect is increased by the presence of an adverse pressure gradient. It was shown in Ref.22 that the separation

from a convex surface in an adverse pressure gradient can occur earlier if the surface is hotter than the flowing air. Transition from laminar to turbulent flow in the boundary layer is also influenced by heating, causing the transition region to move upstream and reduce in length. It has also been shown (Ref.21) that in cases where the boundary layer separates, heat transfer generally accelerates the process and results in an increase in the displacement thickness of the boundary layer on the suction side of the blade. This effect will result in an incorrect deflection of the working fluid, in an increase of the profile drag of the blade and in a wider wake at the trailing edge. The changed deflection will produce changes in profile drag and blade performance. This change in deflection was found to be given by equation (4.15)

$$\frac{\Delta\alpha}{e^*} = \Delta T \left[0.0005 + 0.00084\frac{(i - i^*)}{e^*}\right] \qquad (4.15)$$

ii1) Boundary layer development on blade aerofoil

It has been shown that the resulting movements in effective speed and surge pressure ratio are given by the following equations (Refs.14 and 20):

- For effective speed :

$$\frac{\Delta N}{N} = C_3 . \frac{T_b - T_{air}}{T_{air}} \qquad (4.16)$$

- For surge pressure ratio :

$$\frac{PR_{ht} - 1}{PR_{ad} - 1} = 1 + C_4 \, F \qquad (4.17)$$

ii2) Boundary layer development on end-walls

An approximation has been used, which assumed (Ref.15) that the effect of heat transfer is similar to the effect on thickness of turbulent boundary layers on flat plates (Refs.14 and 15).

$$\frac{\delta_{ht}}{\delta} = \left(\frac{\nu_w}{\nu_f}\right)^{0.2} \qquad (4.18)$$

and

$$\frac{\Delta N}{N} = C_5 . \frac{T_w - T_{air}}{T_{air}} \qquad (4.19)$$

and

$$\frac{PR_{ht} - 1}{PR_{ad} - 1} = 1 + C_6 \, F \qquad (4.20)$$

ii3) Tip clearance changes

Blade tip clearances during transients do not exhibit their equilibrium openings. Their effect on the characteristics can be determined using the correlation presented by Koch (Ref.59) between the limiting pressure rise of a stage and the non-dimensional tip clearance. This method has been included in the programme and applied to the H.P.compressor of the engine investigated in the present work. The change in effective speed is given (Ref.14) by equation (4.21)

$$\frac{\Delta N}{N} = -0.3 \frac{\Delta(\delta)}{g} \qquad (4.21)$$

The change in surge pressure ratio is also given by the following equation (Ref.14):

$$\frac{PR_{cl} - 1}{PR_{Ref} - 1} = 1 - 1.1 \frac{\Delta(\delta)}{g} \qquad (4.22)$$

4.4.2 Overal effect of heat transfer

An overall effect of heat transfer on the compressor characteristics can be approximated by the following expression (Ref.14):

$$\frac{\Delta N}{N} = C_1 . \frac{T_b - T_{air}}{T_{air}} + C_2 . \frac{Q}{m\, C_p\, T_m} + C_3 . \frac{\Delta(\delta)}{g} \qquad (4.23)$$

A similar expression will indicate the movements of the surge pressure ratio. This is given by equation (4.24)

$$\frac{PR_{ht} - 1}{PR_{ad} - 1} = 1 + C_4\, F + C_5 \frac{\Delta(\delta)}{g} \qquad (4.24)$$

The coefficients C_1 and C_2, C_4 and C_3, C_5, represent the respective changes due to the movements of the aerofoil boundary layer, changes in the fluid density and changes in the blade tip clearances. The mean values adopted for the H.P.compressor are respectively , -0.1, -0.1, 0.36, -0.3 and -1.10

In the paragraphs given above in this section 4.4, models have been described which quantify the thermal effects and

their influences on the predicted transient performance of an engine. These models were not available at the time of many previous investigations and predictions of the transient performance of engines. However, the existence of these effects was known and empirical adjustments were used in the prediction programme. In one such procedure, the polar moments of inertia of the two-spools (L.P. and H.P. shafts) were scaled up by a multiplying factor of 1.3 to make the adiabatic prediction more in line with how the real engine will respond. The factor derives from experience - Maccallum's report to Rolls-Royce (1984).

4.5. DEVELOPMENTS INCORPORATED INTO THE SIMULATION PROGRAMME

4.5.1 Turbine blades not cooled

After being proved to give satisfactory results and expected predictions, the programme required further developments in order to improve the capacity of the prediction giving additional information about the engine's behaviour. For this reason, some developments were incorporated into the programme. One such development was a modification of the logic to take into account not only components heat absorption for heat transfer effects but also the changes in effective speed which resulted.

In the present development of the programme, the author introduced an automatic procedure for initialisation of the metal temperatures. For this reason, a negative starting time transient was used with corresponding shaft speeds and initial fuel flow. This enables the metal temperatures of the engine component to be stabilised before the real starting time of the transient operation.

Inclusion of a model to take into account the thermal

capacity of the combustion chamber has been incorporated into the programme.

A further development concerns the rate of change of the fuel flow. During the early predictions of this work, the fuel flow was assumed to change instantaneously from the steady-running value to the value given by the fuel schedule used. Studies undertaken during the real engine testing showed that the fuel flow change occurs over a period of 0.4 to 0.5 seconds but not instantaneously (Ref.23). For this reason, a ramped fuel flow procedure was adopted and clearly illustrated in appendix.1.

4.5.2 H.P.Turbine blades cooled

Modern aero-engines are required to operate better in three basic respects: to give more thrust (Fig.19), to have less weight and to require less fuel. The efforts to reach these demands have led to the development of gas turbines operating at higher and higher turbine entry temperatures. The breakthrough which accelerated the rate of progress above that dictated by the development of materials is the introduction of H.P.Turbine cooling. Problems of high temperature operation affect all the components in the hot part of the engine. However, the life limiting component is usually the high pressure turbine blade and its failure is associated with thermal fatigue. If a blade temperature is reduced by the internal circulation of a cooling fluid within it, then heat is transferred to the blade by forced convection.

The purpose of cooling is to allow the gas temperatures to be raised whilst the blade metal temperature remains at a value low enough to preserve the desired metal properties

(Fig.13). This has become established as an important aspect of turbine engine design.

The simplest way to cool airfoils is by convection. In this process the air is brought in at the root of the airfoil and then discharged at the tip. This method of cooling which is quite efficient and satisfactory for present-day aero-engine performance has been used for the cooling of the H.P.Turbine blades of the configuration simulated in this work. To consider the cooling of the H.P.Turbine blades, a typical value of 0.6 was used for the cooling effectiveness, e (see appendix.2). A simple expression which incorporates the cooling arrangement of the turbine blades was incorporated into the thermal model (equat.4.28) in the engine programme.

$$T_m = T_g - e(T_g - T_c) \qquad (4.28)$$

This equation shows that the temperature which drives the heat transfer is smaller than Tg when turbine blade cooling is taken into account.

For the cases of other engine components which are not cooled e.g. compressor blades and seals, the relevant cooling factors were set to zero.

4.6 RESULTS AND DISCUSSION

In the present work, an already established adiabatic simulation for a two-spool turbofan engine was extended by the author to incorporate the heat transfer effects described in the previous sections. The program was then used to give predictions for a range of steady-running and transient conditions. The transient predictions which, now account for heat transfer, are compared with the predictions given by the adiabatic simulation (chapter III). These results for the cases of flight at sea-level, Mach Number 0.2 and altitude, Mach Number 0.8, are now presented and discussed.

4.6.1 Performance of the components

4.6.1.1 Steady-state operation

Before transient operations were investigated, the steady-running engine operation was predicted in order to find out if there are any effects of heat transfer during the steady-running operation. At sea-level, the fuel flow schedules operate between a maximum of 0.84kg/s and a minimum of 0.08kg/s. A time limit of 300 seconds was used in order to allow for the stabilisation of the engine metal temperatures. Two altitude cases were also considered, 41,000ft and 50,000ft. Minimum fuel flows of 0.06kg/s for the former and 0.05kg/s for the latter have been used. Maximum fuel flows of 0.19kg/s and 0.13kg/s respectively were used as the terminating conditions.

The behaviour of the various components during steady-running conditions is illustrated in Figs.33 to 38. These operations are simulated at sea-level, Mach Number 0.2 conditions (Figs.33 and 34), 41,000ft (Figs.35 and 36) and 50,000ft (Figs.37 and 38). The predicted positions of the

sea-level working lines for the inner and outer sections of the fan when heat transfer effects are included, do not deviate from those of the adiabatic case. At altitudes and as shown in Figs.35 and 37, the predicted positions of the working lines are slightly lowered. At 50,000ft, the steady-state heat transfer line is very slightly lowered from that of the adiabatic. The explanation for these not coinciding is that the heat transfer procedure includes a recalculation of seal clearances. At conditions lower than the design speed, these clearances and hence the escaping airflows, tend to be greater than the nominal values which had been used in the adiabatic program.

The predictions for the I.P.Compressor are shown in Figs.34b;36b and 38b at sea level and altitudes, respectively. At sea-level, the adiabatic operating line and that of the heat transfer effects coincide (Fig.34b) from idling to maximum speed. However, at 41,000ft and as shown in Fig.36b the latter is slightly raised. The resulting deviation is too small to be illustrated. This deviation can be seen in Fig.38b to be similar to that predicted at 50,000ft. At This altitude, the non-adiabatic operating line is apparently raised from the adiabatic. Again the slight deviations are due to the recalculated seal clearances, as explained above.

The H.P.Compressor results are given in Fig.34a for sea-level operation prediction. At these conditions, working lines are seen to be very similar over the operating range of the speed. Whereas, at altitudes as shown in Figs.36a and 38a, a very slight deviation can be predicted. These very slight deviations, at altitude, of the steady-running (with heat transfer) are due to the allowances for the seal opening, explained above.

4.6.1.2 Transient acceleration

The first transient illustrated is an acceleration carried out at both sea-level and altitude conditions. For this acceleration, the starting speeds were 1805r.p.m. and 6030r.p.m. at sea-level, 4012r.p.m. and 9296r.p.m. at 41,000ft and 4200r.p.m. and 9100r.p.m. at 50,000ft for the L.P. and H.P.Shaft speeds respectively. Maximum fuel flow limits of 0.82kg/s, 0.19kg/s and 0.13kg/s were used as the terminating conditions at sea-level, 41,000ft and 51,000ft, respectively. Important movements of the working trajectories can be observed on the various components from Fig.33 to 38.

The effects on the inner and outer sections of the fan, due to heat transfer are shown in Figs.33;35 and 37. As can be seen from Fig.33, the sea-level acceleration trajectories (with heat transfer) are predicted to move closely alongside the adiabatic trajectory. These trajectories are seen to be very similar and follow closely the steady-running line. The transient trajectories are slightly displaced from the steady-state operating line. The predictions of the equivalent acceleration predicted at 41,000ft and 50,000ft are given in Figs.35 and 37. As can be seen from these figures, the adiabatic and the non-adiabatic trajectories coincide as had been the case at sea-level.

Upon examination of the trajectories for the I.P.Compressor, the results are shown in Fig.34b for sea-level conditions, Fig.36b for 41,000ft and Fig.38b for 50,000ft. At sea-level the transient acceleration trajectory is significantly lower than the steady-state operating line. With thermal effects included, this would be lowered still further (Fig.34b). This is due to the

enhanced air demand of the H.P.Compressor, causing the pressure ratio across the I.P.Compressor to drop. At 41,000ft with thermal effects included, the transient trajectory is also lower than the adiabatic but not to the same extent as the sea-level case. At 50,000ft the magnitude of the deviation is identical to that at 41,000ft (Figs.36b and 38b).

The H.P.Compressor trajectories are given in Fig.34a. The transient trajectory at sea-level conditions is significantly lower (surge margin usage about 60%) relative to the adiabatic case (surge margin usage about 95%) over most of the speed range. This is in agreement with earlier predictions (Ref.1) for a two-spool by-pass engine. The explanation is due to heat absorption in the H.P.Compressor and the resulting changes in the H.P.Compressor characteristics. It can also be noted that the overshoot in non-dimensional speed is considerably greater with the predictions including heat transfer effects. This is primarily due to the heat absorption in the I.P.Compressor cooling the air so that the temperature of the air entering the H.P.Compressor is reduced, thus $(N_H/T_{26}^{0.5})$ value is increased. The corresponding movements at altitudes can be seen in Figs.36a and 38a. The predicted trajectories with heat transfer are generally slightly lower than the adiabatic predictions, but again there is a greater overshoot at high speed. It can be seen that as altitude increases the trajectories move closer to, and then cross, the surge line. This is due to the deterioration in the performance of the compressors due to the increasing Reynolds Number effects, and the lower accelerating powers available, caused by the reducing air density.

4.6.1.3 Transient deceleration

Similar to the transient acceleration, an investigation of heat transfer effects affecting the various engine components was carried out during deceleration at both sea-level and altitudes. The starting speeds for this transient deceleration were 8630r.p.m. and 12164r.p.m. at sea-level, 7700r.p.m. and 10940r.p.m. at both 41,000ft and 50,000ft altitudes for the L.P. and H.P.Shaft speeds, respectively. A minimum fuel flow limit of 0.08kg/s, 0.04kg/s and 0.06kg/s were used as the terminating conditions.

The predicted results for this deceleration for the inner and the outer sections of the fan are given in Figs.39 to 44. As can be seen from these figures, there is little departure from the steady-running line of the adiabatic trajectory. With thermal effects taken into account, only a minor influence on the predicted transients was noticed. It is also shown that no noticeable effects have been predicted at altitude operation on the engine components (Figs.41 and 43).

For the I.P.Compressor, the adiabatic trajectory at sea-level can be seen in Fig.40b to approach the revised surge line. The predicted results given in Fig.40b show that when heat transfer effects are considered, the transient trajectory was found to move more closely to surge even during the early stages of deceleration. Compared to the original surge line both trajectories are still far away. At altitudes, the effects are more severe. The transient trajectory with thermal effects is raised significantly and crosses over the revised surge line from the beginning of the transient (Figs.42b and 44b). At 50,000 ft it is predicted to approach considerably the original surge line. This greater proximity to surge at

altitude conditions is at least partly due to the altitude steady-running line being at a higher pressure ratio, for a non-dimensional mass flow, than the sea-level steady-running line.

The results during transient deceleration for H.P.Compressor are shown in Fig.40a At sea-level conditions. The transient trajectory was predicted to move closely below the steady-running line (see figure) when thermal effects are taken into account. This is also seen almost to cross it in about half way from the start of the deceleration. The reason for the apparent crossing of the steady-running line midway through the deceleration is due to the movements in effective H.P.Compressor characteristics due to heat transfer - this being most pronounced in this part of the deceleration. At 41,000ft, Fig.42a shows that similar events occur. It is to be noted that after two thirds of this transient, both adiabatic and non-adiabatic trajectories are seen to change their direction towards acceleration slightly above the steady-running points. This is principally due to the less rapid speed reduction of the L.P.shaft, when compared with the H.P.shaft which causes the temperature at inlet to the H.P.Compressor to continue dropping in the latter part of the transient, whereas the H.P.shaft speed has almost stabilised - thus the non-dimensional speed of the H.P.Compressor ($N_H/T_{26}^{0.5}$) rises. This effect is more noticeable in the predictions where heat transfer is accounted for.

4.6.1.4 Bodie transient

Engine simulation with heat transfer effects accounted for was investigated during a 'Bodie' transient. In this transient, an 8 second deceleration (for this example) is

followed by acceleration while engine component materials are still hot. During engine reacceleration, the starting speeds were forced to exactly the same speeds as used at the start of the cold acceleration. In the 'Bodie' transient carried out at sea-level conditions, Fig.47 shows that inclusion of thermal effects leads to a thrust response which is about 2 seconds more rapid than for the adiabatic prediction, but the surge margin usage in the H.P.Compressor is about 90% as compared to 95% in the adiabatic prediction (Fig.45) and 60% for the predicted acceleration of the cold engine, when accounting for heat transfer. Therefore, there is a more rapid acceleration with a greater surge margin usage than for the acceleration of the cold engine (Figs.34 and 49).

The 'Bodie' transient was also investigated during altitude operation. Fig.46 shows that reacceleration of the hot engine was predicted to surge the H.P.Compressor. All surge margin available was used and thermal effects were found to cause surge problems when reacceleration of the engine at altitude was desired. The reason for H.P.Compressor surge at altitude during a 'Bodie' transient is that while the metal masses are the same, the air-mass flows are lower compared to those at sea-level and because of that, effects of heat transfer are more significant i.e. the temperature difference (T_{3HT}-T_{3AD}) is larger.

Prediction of the proximity of H.P.compressor working trajectory to the surge line during a'Bodie' transient at sea-level and real surge at altitude has lead to the investigation of fuel schedule compensation, to be introduced and described in chapter V. This aims to slow down engine reacceleration in this transient, thus avoiding surge as will be illustrated.

4.6.2 Engine performance

Acceleration

Inclusion of all thermal effects results in a slight delay in the predicted acceleration rate of the 'cold' engine relative to the adiabatic case.

During cold acceleration at sea level conditions, when thermal effects are accounted for, the time to reach 50% of maximum thrust takes about 7.5 seconds, as compared with a time of 7.0 seconds when thermal effects are ignored (see Fig.49).

At altitudes of 41,000ft and 50,000ft, the thrust with thermal effects considered is delayed by about 0.25 seconds compared to the adiabatic case (thrust with heat transfer effects included takes about 2.0 seconds to reach 85% of maximum value, whereas the adiabatic figure takes only 1.75 seconds as shown in Figs.51a and 53a). Comparison of speed transient has been at 85% Of maximum thrust rather than 50% as had been the case at sea-level because at altitude the idle thrust is higher compared to sea-level and at 50% of maximum thrust, there is no difference between thrust with thermal effects accounted for and thrust with adiabatic assumptions.

It can be seen from Figs.49a, 51a and 53a that at sea-level, maximum value of thrust is achieved in about 9 seconds whereas at altitude, the corresponding levels of thrust are achieved in only about 6 seconds. This reduction in the time required for the speed transients at altitude is due to the starting speeds being higher.

Deceleration

Investigations carried out during decelerations have revealed that when analysed with heat transfer effects accounted for, the engine is predicted to take longer to slow down. The reason is because of the heat release from engine material to the working fluid.

At sea-level conditions (Fig.55a), the engine response is slower by about 0.5 seconds compared to the adiabatic case (thrust with thermal effects considered takes 2.5 seconds to reach 11% of maximum value, whereas thrust with adiabatic assumptions takes only 2 seconds).

At altitude and as shown in Figs.57 to 60, heat transfers have greater effect in delaying engine response during deceleration. As shown in Fig.57a, engine response is slower by about 2 seconds compared to the adiabatic case (thrust with heat transfer effects considered takes 6.5 seconds to reach 25% of maximum value, whereas that with adiabatic assumptions takes only 4.5 seconds).

On comparison of predicted decelerations including allowance for heat transfer effects at different altitudes, it is noted that at sea-level conditions, the deceleration rate is faster due to the higher air mass-flows compared to the altitude case.

4.6.3 Effects of clearance movements in transients

The programme incorporating heat transfer effects which was used to give the predictions described in the previous sub-sections (4.6.1.1 to 4 inclusive) included modelling of the movements of the components which control blade tip clearances. It is interesting to look more closely at these predicted clearance movements.

4.6.3.1 Blade tip clearances

As has already been stated earlier, for calculation of tip clearance movements, an "equivalent-stage" procedure was used where dimensions and fluid properties of the stages of the compressor being considered were averaged to a single-equivalent stage. A similar procedure is used for turbines (see Fig.20).

Cold acceleration

The changes in tip clearances for the high pressure compressor during cold acceleration at sea-level conditions are shown in Fig.61. From this figure, it can be seen that the clearance is tighter during transient and significantly deviates from the stabilised value. Looking at the clearance paths at the beginning of the transient, there is a sharp decrease in tip clearance due to centrifugal strain and the fast thermal growth of the blades (time constant of blade response at 50% of maximum thrust is about 1 second). The thermal response of the casing is slower than that of the blades (time constant of casing at 50% of maximum thrust is about 13 seconds). Much of the casing response takes place after the speed transient is completed, producing an increase in tip clearance. The slowest expansion is that of the disc (averaged time constant of the H.P.Compressor disc at 50% of maximum thrust is about 50 seconds) which at the end of the transient reduces the clearance.

At altitude and as shown in Fig.63 the clearance is much tighter and remains constant throughout the transient, except at the beginning of the transient where a slight decrease is noticed due to centrifugal growths.
For the H.P.Turbine, the clearances are initially open and

then tighten as a result of centrifugal growths at the start of the acceleration (Fig.62). As the casing expansion takes place (time constant at 50% of max. thrust is 5.2 seconds) the clearance starts increasing slightly but the fast expansion of the blades (time constant at 50% of max. thrust is 2.8 seconds) results in a decrease in tip clearance. Additionally, the later expansion of the disc (time constant at 50% of max. thrust is 46 seconds) tends to close the clearance at the end of the transient.

Since the I.P.Compressor and L.P.Turbine undergo less severe temperature changes, no analysis of their clearances has been made in the present work.

Deceleration

During deceleration at sea-level, the opposite processes occur. A sudden increase in the H.P.Compressor tip clearance (Fig.65) is due to the contraction of the rotor components resulting from the reduced centrifugal stressing. This is followed by the fast contraction of the casing (time constant at 50% of speed transient is 47.9 seconds) compared to the disc slowest contraction (time constant is 192 seconds) which results in the closing of the clearance. The slower response of the disc (contraction) causes a final slow increase in the tip clearance.

At altitude only a slight increase in clearance is experienced due to the reduced centrifugal stressing (Fig.67).

For the H.P.Turbine, movements of tip clearance during deceleration at sea-level are given in Fig.66. From this figure, it can be seen that the reduction in mechanical growths (as a result of reduction in shaft speeds) is responsible for the opening of the clearance at the start

of the deceleration.

At altitude, the clearance in the later stages (after 6 seconds) is tighter, due mainly to casing contraction.

'Bodie' transient

During the 'Bodie' transient, movements of tip clearance differ from those obtained during a cold acceleration. As shown in Figs.69 and 70, at sea-level, tip clearance of both the H.P.Compressor and H.P.Turbine at the beginning of the reacceleration part of the 'Bodie' are widely opened, due to the reduction in centrifugal growths at the end of deceleration (reduction of speed) and due also to the thermal contraction of blades (and to a lesser extent of casing and disc). As reacceleration takes place, clearances of both H.P.Compressor and H.P.Turbine start decreasing because of the centrifugal growths and fast expansion of the blades.

At altitude, compressor and turbine tip clearance are tighter during most of the transient compared to the cold engine.

The discontinuities of speed transient observed during the 'Bodie' in the movements of H.P.Compressor and H.P.Turbine clerances are due to the fact that the starting speeds for the reacceleration part of the 'Bodie' were forced to exactly the same starting speeds as for the cold engine for compensation reasons (see chapters V and VI).

4.6.3.2 Seal clearances

The seal opening is designed so that a small predetermined amount of air will be removed from the core flow. This can have a considerable effect on the engine performance.

The H.P.Compressor seal is designed so that a small amount of air escapes to the by-pass duct. The the H.P.Turbine seal controls approximately one quarter of the cooling flow extracted from the compressor delivery. This particular flow is required for cooling the turbine. Both seals have during transients clearance openings that exceed their design values.

Cold acceleration

At sea-level conditions typical results for the H.P.Compressor and H.P.Turbine seal movements during cold acceleration are given in Figs.73 and 74. The seal openings are seen to depart significantly from the design values, due to the incomplete expansion of the discs at the end of the speed transient.

Among the two seals mentioned above, it is the H.P.Turbine seal which has the largest opening during an acceleration with comparison to the stabilised seal clearance. This is mainly because the turbine seal has a design opening value which is half that of the compressor seal.

At altitude, seal openings of both compressor and turbine are not as pronounced as those recorded under sea-level conditions, due to the higher minimum H.P.shaft speed and also to reduced heat transfer coefficients.

Deceleration

During deceleration, lower values of heat transfer coefficients resulting from reduced mass flow and rotational speed at the end of the deceleration, together with reduced rotational shaft speeds, cause a much longer 'heat soak' period. Contraction of the discs result in a

large opening of seal clearances as shown in Figs.77 and 78.

'Bodie' transient

Predicted seal responses during a 'Bodie' transient at sea-level conditions are shown in Figs.81 and 82. It can be seen from these figures that H.P.Compressor and H.P.Turbine seals behave in a very similar manner to those predicted during acceleration of the 'cold' engine. Similar results at altitude are shown in Figs.83 and 84. The reason for the speed discontinuities noticed during the 'Bodie' transient is as already discussed above.

CHAPTER V

COMPENSATION OF TRANSIENT FUEL FLOW SCHEDULES

5.1 INTRODUCTION

For aircraft gas turbine engine, the fuel schedule controller constrains the maximum or the minimum fuel flow used during the engine operation. These restrictions ensure the stable operation of the compressor clear of surge, and avoid high gas temperatures at the turbine inlet and hence give safety to the whole engine. The fuel schedule which has been used during heat transfer effects investigations, illustrated in the previous chapter is the standard fuel schedule where a non-dimensional fuel flow is expressed as a function of the H.P.Compressor pressure ratio. It was found in chapter four that the use of the same fuel schedule without regard to the engine immediately preceding history, for the acceleration of a 'hot' and a 'cold' engine results in differing rates of the engine response and different usage of surge margins. Therefore, what is intended from the compensation scheme is to have a faster engine response during 'cold' acceleration, in the same time to slow down the engine response during 'hot' acceleration, making possible engine reacceleration within safety. These results suggest that some adjustment might be applied to the fuel schedule in order to allow for a better utilisation of the surge margin, especially during the 'hot' acceleration of the engine. One possible way of doing this is to compensate the fuel flow

schedule used previously by making some allowance for the previous thermal history of the engine. For this purpose, two methods of compensating the fuel flow schedule were used for the investigation in this work. These are compensation by temperature response of a characteristic component and compensation by 'delayed' shaft speed signal.

5.2 STABLE OPERATION OF THE COMPRESSION SYSTEM

Safe operation of the compression system of an aircraft gas turbine engine is essential for an acceptable engine performance and behaviour. In the engine configuration considered in this work, I.P.Compressor and H.P.Compressor are the most important part responsible for the compression process. Therefore, their stability during engine operation has to be ensured. For this reason, movement of the transient operating trajectory in relation to the surge line should be predicted at each time during engine operation.

When transient deceleration is experienced, it is the I.P.Compressor which is prone to surge if care is not taken, whereas the H.P.Compressor is most likely to surge during acceleration of the engine. Heat transfer effects on the I.P.Compressor are still not well understood and since severe transient deceleration of the engine is only very rarely experienced, much attention has been focused on the H.P.Compresor behaviour during the acceleration.

A modern high pressure ratio compressor produces a large temperature rise corresponding to the operating pressure ratio. Therefore, a large amount of thermal energy transfer exists between the compressor blading and the gas stream during transient acceleration. The increase in total temperature which occurs across the high pressure compressor

results from work addition to raise total pressure and from heat transfer gas to metal. The effect of transient heat transfer on compressor stable operation is most significant during the 'Bodie' transient, due to the thermal energy previously stored in the compressor material, which can be released to the gas stream. This internal release of energy is responsible for the movement of the transient operating trajectory towards the surge line. In the same time, the compressor blades heat transfer boundary layer interaction lowers the surge line toward the operating trajectory. Transient effects, such as transient clearance changes and stored volume discharge, are seen to alter the compressor performance. Heat transfer effects have thus been recognised as major contributors to compressor surge margin reduction.

5.3 TRANSIENTS CONSIDERED IN THE COMPENSATION

Cold and hot accelerations are the transient operations which are mainly considered during compensation. An engine is experiencing a 'cold' acceleration when it has been stabilised at the idling speed before accelerating. Contrarily, a 'hot' acceleration, also called 'Bodie' transient is a reacceleration following a rapid deceleration (in this case of 8 seconds duration, for example). Prior to the deceleration, the engine was at maximum speed.

A 'Bodie' transient is a standard stability test for aircraft gas turbine engines, because it represents real flight events and requirement associated, especially, during combat (military aircraft) and formation flying. In addition, instabilities usually occur when the engine is reaccelerated and the transient operating line is moved towards the surge line. For this reason, engine performance and behaviour are

investigated during both the 'cold' and 'hot' accelerations as these represent extreme operations during severe transients.

5.4 ILLUSTRATION OF NON-DIMENSIONAL STANDARD FUEL SCHEDULE

When compensation is not accounted for, the fuel schedule which has been used for the engine configuration investigated in the present work is a function of the pressure ratio across the H.P.Compressor. This is represented by the standard fuel flow schedule given in equation (5.1). Typical schedules for acceleration and deceleration of the configuration being studied are shown in Fig.99.

$$\frac{\dot{f}}{N_H \; P_2} = f\left(\frac{P_3}{P_2}\right) \qquad (5.1)$$

With fuel compensation considered, a compensating factor F_{cp} has to be multiplied to the standard fuel schedule and the expression of the compensated fuel flow schedule is illustrated in equation (5.2).

$$\frac{\dot{f}}{N_H \; P_2} = F_{cp} \; f\left(\frac{P_3}{P_2}\right) \qquad (5.2)$$

where F_{cp} being the fuel compensating factor. From equations (5.1) and (5.2), the new compensated fuel schedule to be used when compensation is taking place is given by equation (5.3)

$$\dot{f} = F_{cp} \; F_{fs} \; f\left(\frac{P_3}{P_2}\right) \; N_H \; P_{2i} \qquad (5.3)$$

where F_{fs} is the factor of fuel schedule (0.9 in this case) N_H is the H.P.Shaft speed, P_2 and P_3 are the H.P.Compressor inlet and exit pressure, respectively.

5.5 METHODS OF TRANSIENT FUEL SCHEDULE COMPENSATION

In the last chapter, it has been found that the departures from the adiabatic performance are due mainly to heat capacity of the components, changes in compressor characteristics and the non-design seal clearances arising from the transient temperature distribution of the materials within the engine. In this chapter, the immediately preceding engine history has been considered for compensating the fuel schedule which has been used previously. The two main methods mentioned in the first section of this chapter have been extended in the present work. These will be discussed in more detail in the following sub-sections.

5.5.1 Compensation by temperature response of a characteristic component

A compensation scheme based on the temperature response of a characteristic component uses the main air or gas temperature flowing over the component material being discussed as the temperature driving that of the characteristic component. The selection of the characteristic component to be used for compensating the fuel flow schedule depends on the rate of the temperature response of the component and consequently on the time constant of the characteristic component. Therefore, the mean air or gas temperature and the temperature of the component are selected to form the factor F_{cp} to be used in compensating the fuel

flow schedule. This factor is given by the following equation:

$$F_{cp} = \left(\frac{T_{ma}}{T_{chc}} \right)^{a} \qquad (5.4)$$

T_{ma} and T_{chc} are the mean air and characteristic component temperatures, respectively. 'a', being the index of compensation selected to give a suitable value of F_{cp}.

In this work, the components which have been used during the investigation are the H.P.Compressor and H.P.Turbine of a two-spool turbofan engine and the characteristic component could be either the blade or the disc. Both characteristics of the two mentioned components have been investigated.

5.5.1.1 H.P.Compressor blade temperature compensation

In this procedure, the H.P.Compressor blade temperature is selected to be used for the compensation process. The fuel schedule compensating factor obtained thereby is illustrated in Equation (5.5). T_i and T_e being the gas temperatures at the inlet and at the exit of the compressor, respectively. T_{ce} represents the compressor blade aerofoil temperature.

$$F_{cp} = \left[\frac{\frac{T_i + T_e}{2}}{T_{ce}} \right]^{a} \qquad (5.5)$$

The arithmetic mean value of T_i and T_e represents the temperature driving the compressor blade temperature. A range of values between 0.5 and 2.0 for the index 'a' of

compensation has been examined and typical results are illustrated and discussed in the next chapter.

5.5.1.2 H.P.Turbine blade temperature compensation

The H.P.Turbine blade aerofoil temperature can be used as a mean for compensating the fuel flow schedule during the engine transient operation. This method might be worth comparing with the previous method because of the longer time constant of turbine blades. Fuel schedule compensating factor resulting from this method is illustrated in equation (5.6). T_{tg} and T_{tb} are the gas temperature and turbine blade aerofoil temperature, respectively.

$$F_{cp} = \left[\frac{T_{tg}}{T_{tb}} \right]^{a} \qquad (5.6)$$

T_{tg} is the temperature which drives the blade aerofoil temperature T_{tb}. To take into account blade cooling in the H.P.Turbine, the expression of T_{tg} which has been used in the above equation is shown by equation (5.7) where T_{cd} is the H.P.Compressor delivery temperature.

$$T_{tb} = \left(\frac{T_{ti} + T_{te}}{2} \right) - e \left(\frac{T_{ti} + T_{te}}{2} - T_{cd} \right) \qquad (5.7)$$

e, is the cooling effectiveness given a value of 0.6 in the present work.

Several values ranging from 0.1 to 0.5 were examined for the index 'a' of compensation. Results for typical values 0.1; 0.3 and 0.5 for the index 'a' are illustrated and discussed in chapter 5.

5.5.1.3 H.P.Turbine disc temperature compensation

It is well recognised that there is additional thermal storage in the more massive compressor and turbine parts outside the gas path. These parts such as discs and frames transmit thermal energy by conduction to the blades. It was found that the time constant of the temperature response of the aerofoil of the characteristic blade in the H.P.Turbine is too short which results in a too rapid temperature response of the aerofoil. Unlike the thin blades, the time constant for the thermal transients of the massive parts of the disc is of the order of a minute or more. A more reasonable solution is therefore to use as a correcting parameter the temperature of a more massive section of the H.P.Compresor or turbine discs, such as the hub. Both H.P.Compressor and H.P.Turbine can be used for the compensation scheme of the fuel schedule, but attention has been focussed on the H.P.Turbine disc temperature compensation as this is subjected to higher gas and air temperatures compared to the compressor.

The approach which has been used in the present work is to investigate compensation of the fuel flow schedule based on the temperature response of each of the three sections of the disc: hub; diaphragm and platform (or disc rim). The reason for this subdivision is to find out which part of the disc will to give the desired compensation schemes, thereby improving the engine response during transients. Once this has been accomplished, another method based on an averaged disc temperature is considered taking into account the three sections of the disc. Although compensation by averaged disc temperature response is difficult to implement on an engine,

due to practical difficulties involved, it will be demonstrated that compensation of fuel flow schedule based on this method gives the intended results, in contrast to the blade temperature compensation introduced previously.

a) Hub temperature compensation

The hub represents the more massive part of the disc and because of this, it is characterised by a slow temperature response during transient operation of the engine, due to the longer time constant compared to the other parts. The fuel schedule compensating factor resulting from the hub temperature compensation is illustrated in equation(5.8)

$$F_{cp} = \left(\frac{T_{ah}}{T_{hm}}\right)^{a} \qquad (5.8)$$

T_{hm} and T_{ah} being the hub metal temperature and mean temperature of the air flowing on the disc faces which is equal to the H.P.compressor air delivery temperature.

Engine performance and component behaviour have been investigated during both 'cold' and 'hot' accelerations at sea level conditions and a flight Mach number of 0.2. Different values starting from 0.1 to 0.5 were investigated for the index of compensation 'a'. Typical results for the selected values of 0.20; 0.25 and 0.30 are fully discussed in the following chapter.

b) Diaphragm temperature compensation

Investigation concerning fuel schedule compensation has also been extended to the thin section of the turbine disc,

called the 'diaphragm'. The fuel schedule used for the case of the diaphragm is expressed in the following equation:

$$F_{cp} = \left(\frac{T_{adp}}{T_{dpm}} \right)^{a} \qquad (5.9)$$

T_{adp} is the mean air temperature driving the metal temperature T_{dpm}. The same values of the index 'a' which were used for the hub temperature compensation have been examined for the diaphragm and results obtained will be discussed.

c) Platform temperature compensation

For the platform, also called 'rim of the disc', the expression of the temperature which drives the metal temperature is difficult to define. From Fig.17, it can be seen that the platform is attached to the turbine blade and it is therefore subjected to different flows with different densities, different velocities and different temperatures. The main temperature of the air flowing on the disc side, T_{ai}, is given by the following equation:

$$T_{ai} = \frac{T_a + T_{cool}}{2} \qquad (5.10)$$

where T_a is the temperature of the air flowing on the disc and T_{cool} is the temperature of the cooling air passing through the platform to cool the blades. In practice, both these temperatures are taken as the temperature of the air at delivery from the H.P.Compressor.

The cooling of the turbine blades by air taken from the H.P.Compressor delivery is via the platform. It is clear that

the platform is exposed to three different flows with different temperatures. Knowledge of the heat transfer coefficients (see appendix.4) on the disc side and on the gas side permits the calculation of the air/gas temperature driving the platform metal temperature which is expressed by equation(5.11).

$$T_{map} = \frac{h_0 T_{mao} + h_i T_{ai}}{h_0 + h_i} \qquad (5.11)$$

h_i and h_o being heat transfer coefficients inside and outside the platform, respectively. T_{mao} is the mean gas temperature outside the disc. The fuel schedule compensating factor with platform temperature response is illustrated in equation (5.12) where T_{mp} is the platform metal temperature.

$$F_{cp} = \left(\frac{T_{map}}{T_{mp}}\right)^{a} \qquad (5.12)$$

A range of values has been examined for the index 'a' of compensation, and results for three selected values of 0.10; 0.15 and 0.20 are illustrated and discussed in the next chapter.

d) Compensation by disc average temperature

Compensation using the temperature response of a characteristic component has been examined where an H.P.Turbine disc averaged temperature was used. Average temperature of the disc was estimated using equation (5.13).

$$T_{AVD} = \frac{\Sigma V_i \; T_m(i)}{\Sigma V_i} \qquad (5.13)$$

and the mean air temperature driving the disc temperature, T_{AIRD}, is given by equation (5.14)

$$T_{AIRD} = \frac{\Sigma V_i \; T_{ms}(i)}{\Sigma V_i} \qquad (5.14)$$

The resulting expression of the fuel schedule compensating factor is shown by the following equation:

$$F_{cp} = \left(\frac{T_{AIRD}}{T_{AVD}} \right)^{a} \qquad (5.15)$$

To illustrate fuel schdedule compensation based on the average temperature response of the turbine disc, three values were selected and investigated for the index of compensation 'a'. These are 0.15; 0.25 and 0.35. Predicted corresponding results will be discussed in the following chapter.

5.5.2. Compensation by 'delayed' shaft speed signal

An alternative way for compensating the fuel flow schedule of an aircraft engine gas turbine during transient operations is the method based on a 'delayed' shaft speed signal. In this approach, the shaft speed which is delayed by a known time constant chosen arbitrarily will be compared with the actual shaft speed at that instant. Both, L.P. and H.P. shaft speeds could be used for the compensation scheme. The H.P.shaft speed was selected for investigation in the present work due to the instabilities which are most likely to occur in the high pressure shaft components, such as the

H.P.Compressor. The factor of compensation obtained on the basis of this method is illustrated in equation (5.16) where N_H is the actual shaft speed at a particular instant.

$$F_{cp} = \left(\frac{N_H}{N_{HD}}\right)^b \qquad (5.16)$$

N_{HD}, which is the shaft speed delayed by a time constant 'τ', is given by the following expression:

$$N_{HD}(t) = N_{HD}(t-\Delta t_i) + (N_H - N_{HD}) \frac{\Delta t_i}{\tau} \qquad (5.17)$$

Δt_i being the interval time increment, taken as 0.05 second in this work.

A range of values has been examined for the index 'b' as has been for the time constant 'τ' during both 'cold' and 'hot' acceleration of the engine and results for typical combinations of the time constant and the index of compensation '*b*' are presented and discussed in chapter V.

5.5.3. Compensation at altitude operation

As the performance of an engine is different at altitude from that at sea-level, fuel schedule compensation has been also investigated at altitude of 41,000 ft. At this altitude, flight conditions are 216.50 ^{0}K and 17.87 kN/m^2 for ambient temperature and pressure respectively, with a flight Mach number of 0.8.

To illustrate fuel flow schedule compensation at altitude

operation, two compensation methods, one based on the temperature response of the hub section of the H.P.Turbine disc and the other using a 'delayed' speed signal of the H.P.shaft, have been investigated during 'cold' and 'hot' acceleration of the engine. For each case, results are presented and discussed in the following chapter.

CHAPTER VI

DISCUSSION OF THE COMPENSATED RESULTS

6.1. INTRODUCTION

This chapter gives the discussion of the predictions that were obtained when compensation of the fuel schedule was used with the two-spool turbofan engine already described. The conditions under which the predictions were obtained have been given in the previous chapter.

6.2. DISCUSSION OF RESULTS

After heat transfer effects on the performance and behaviour of the engine components were investigated, the next step was to retain the models allowing for heat transfer effects previously used and to these models, those describing fuel flow schedule compensation are added. Compensation predictions based on different methods and different models which were investigated in this work, are presented below and discussed.

H.P.Compressor blade temperature

Investigation of the fuel flow schedule compensation based on the temperature response of the H.P.Compressor blade has been examined for a range of values between 0.5 and 2.0 for the index 'a' of compensation and predictions for three typical values of the index 'a' (0.5; 1.0 and 2.0 - in Equat. 5.5), were illustrated and discussed.

Fig.100 shows the movement of the transient trajectories

on the H.P.Compressor characteristics at sea level conditions during 20 seconds of a 'cold' acceleration. The starting speeds for this transient were 1805 r.p.m. and 6030 r.p.m. for the L.P. and H.P.shaft speeds respectively with a starting fuel flow of 0.08kg/s. The predictions referred to in Fig.100, used an acceleration fuel schedule line which is 5 percent lower than the schedule line used in the results described in chapter four (Fig.45). It can be seen that better performance is predicted when the fuel flow schedule compensation uses a value of 1.0 for the index 'a' (Fig.100b) and approximately 90% of the surge margin was used compared to about 50% with a standard uncompensated fuel flow schedule. This is due to the increase in the pressure ratio caused by the increased acceleration rate of the engine resulting from the increase in the fuel flow (factor of compensation greater than unity). However, decreasing the value of the index of compensation below unity is seen to give a less enhanced engine acceleration rate (Fig.100a) and for a very low value, the effect of compensation seems to disappear. On the other hand, increasing the index over unity creates another problem, illustrated by the case of 'a' equals to 2.0 shown in Fig.100c. The transient operating trajectory was predicted to cross the surge line. This is due to the rapid increase in the fuel flow rate as a result of the increase of the index, resulting in a very rapid engine acceleration and hence, the pressure ratio across the H.P.Compressor rises excessively.

Considering the values of thrust response, compensation illustrated by the case with a=1.0, gives a more rapid response compared with the uncompensated results. The 50% of maximum thrust level was obtained in 7.2 seconds as against 8.2 seconds (the predicted time for the adiabatic engine is

8.0 seconds). Therefore a considerable improvment can be achieved in that a faster thrust response was predicted, together, with an increased usage of surge margin.

For acceleration of the 'Bodie' which is an 8 second deceleration at sea level with starting speeds of 8630 and 12164 r.p.m. for the L.P. and H.P.shaft respectively followed by an acceleration with exactly the same starting speeds as for 'cold' acceleration, the resulting predicted engine response is given in Fig.102. For the case of index a=0.5, it can be observed that the engine reaccelerates slightly faster than the uncompensated case. There is still, however, a considerable unused part of the surge margin. Therefore, reacceleration of the engine (with a value of 0.5 for the index 'a') is possible and safe. With an index greater than 1.0 the engine accelerates rapidly and the 'Bodie' transient operating trajectory with an index of 2.0 was predicted to move very close to surge. Consequently, it is apparently accelerating the engine very rapidly instead of slowing down the response due to the increase in the fuel flow resulting from the high values of the factor of compensation at the start of the reacceleration (greater than unity). The reason for this result which is opposite to that intended from the compensation, may be attributed to the fact that the temperature response of the H.P.Compresor blade aerofoil is too rapid due to the time constant (see appendix.1) which is too short at the start of the acceleration (0.2 second) and instead of reducing the fuel flow with a high index of compensation, the fuel flow schedule compensating parameter is increasing it as is shown in Fig.104 where the variation of the compensating factor is illustrated.

The corresponding predicted engine performance is

illustrated in Fig.103. The thrust response is faster, relative to the uncompensated case by about one second at 50% of maximum thrust (with a=0.5 and a=1.0). Overall engine pressure ratio and shaft speeds are also shown alongside.

The unsatisfactory nature of this method of compensation, due to the excessively short time constant of the compressor aerofoil blades, leads to the investigation of the temperature response of the H.P.Turbine blade aerofoil.

H.P.Turbine blade temperature

For compensation based on H.P.Turbine blade temperature response, several values ranging from 0.1 to 0.5 were examined for the index 'a' of compensation and results for only typical values of the index 'a' (0.1; 0.3 and 0.5) are illustrated.

Refering to this method, resulting predicted engine responses during 'cold' acceleration at sea-level are given in Fig.105. As can be seen from this figure, the best way to compensate the fuel flow schedule using this method was predicted with an index 'a' of 0.1 and 0.3. The engine accelerates rapidly and about 80% of the surge margin was used (a=0.1). Prediction with an index of 0.3 showed that almost all the surge margin was used (Fig.105b). However, it is very important to notice that increasing the index up to 0.50 causes the transient operating trajectory to cross into surge. The reason is as discussed earlier due to the rapid engine response as a result of the increase in the fuel flow (with a higher index). Consequently, the pressure ratio across the H.P.Compressor rises. Typical results for index 0.5 are shown in Fig.105c.

The engine performance parameters associated are given in

Fig.106. The thrust response is faster, relative to the uncompensated case, by about 0.8 second with 'a' equals to 0.10 (at 50% of maximum thrust).

During 'Bodie' transient Fig.107c shows that the transient operating trajectory with an index of 0.5 is predicted to move very closely to the surge line. That is a result which is not desired from fuel compensation during acceleration of the hot engine. Similar result but smaller in magnitude has been predicted when an index of 0.30 was used (Fig.107b). However an acceptable prediction has been achieved with an index of 0.10. The surge margin usage was apparently increased by about 10% compared to the uncompensated case (Fig.107a). Therefore in most cases, unsatisfactory 'Bodie' transient performance was predicted by this method (Fig.107).

Fig.108 shows that during a 'hot' acceleration ('Bodie'), the thrust response is faster by about 0.9 second with an index of 0.10 (at 50% of maximum thrust) and increasing the value of index of compensation up to 0.5 results in a faster response by 2 to 3 seconds compared to the uncompensated thrust response (at 50% of max. thrust).

As can be seen from Fig.109, the compensating parameter being applied to the fuel schedule during acceleration of the 'cold' engine is increasing the fuel flow. At the start of the transient and as shown in the above mentioned figure, the values of this parameter are well above unity which is consistent with the expected predictions. From the same figure, however, compensating factor during the reacceleration part of the 'Bodie' transient is apparently increasing the fuel flow with all values of the index 'a', instead of decreasing it (factor of compensation is greater than 1.0, except for the first quarter of a second). The worst case is

obviously with an index of 0.50 (Fig 109b). The explanation for the compensating factor being greater than unity in the reacceleration part of the 'Bodie' is that, in order to achieve the reacceleration, the fuel flow rises and the turbine gas temperature jumps rapidly to well above the previous blade temperatures.

Because of the unsatisfactory results predicted during acceleration of the 'hot' engine, consideration was given to selecting the temperature response of a more massive part of the engine, such as, compressor or turbine disc because of the very long time constant and the very slow response of these parts. Also, these parts are not exposed to the fluctuations of the turbine entry gas temperature. For this reason, compensation based on the temperature response of the H.P.Turbine disc was next investigated. To illustrate predictions based on this method, predicted results for each section of the H.P.Turbine disc are presented below and discussed separetly.

H.P.Turbine disc (Hub) temperature response

For the hub section of the H.P.Turbine disc, different values starting from 0.1 to 0.5 were examined for the index of compensation 'a' and typical results for three values (0.20; 0.25 and 0.30) are illustrated.

Predicted engine behaviour during engine 'cold' acceleration is shown in Fig.110. From this figure it can be seen that a good engine response can be achieved by using temperature response of the hub section of the disc as a means for compensating the fuel flow schedule. Referring to the same figure, a value of 0.30 for the index 'a' is seen to raise the transient operating line to surge (Fig.110c) due to the

excessive acceleration rate resulting in an increase in the pressure ratio. However, decreasing the index to 0.25 was found to remove the operating trajectory from the surge line, thereby increasing the surge margin (Fig.110b). Using an index of 0.20, however, gives a transient trajectory which is as intended from the compensation scheme and approximately 70% of the surge margin is predicted to be used (Fig.110a).

Engine performance is shown in Fig.111 and typical results are also shown for the three values of the index 'a' of compensation. The thrust response is faster by about one second in comparison to the thrust obtained without compensation of the fuel schedule at 50% of maximum thrust (with a=0.20). Increasing the value of 'a' from 0.20 to 0.30 results in a speeding up of the thrust response by about 0.2 second (compared to that predicted with a=0.20). L.P. and H.P.shaft speeds are shown alongside for each of the values of the index 'a'.

When considering the 'Bodie' transient, satisfactory results were predicted for all the three selected values of the index 'a'. Good compensation was predicted with 0.25 and 0.30 (Fig.112). With an index of 0.30, the surge margin in the transient is increased by about 60% compared to the uncompensated case (Fig.112c). However, with an index of 0.20, the compensated trajectory has been lowered only very slightly.

Examining engine performance during 'hot' acceleration, Fig.113 shows that the thrust for all three values is slower and a delay of 1.2 seconds of the thrust response was predicted with an index of 0.30 (at 50% of maximum thrust). The reason for the slow acceleration response is due to the very long time constant of the hub metal resulting in a slow

temperature response because of the quantity of mass contained in the hub. With a higher value of the index 'a', the factor of compensation is lower and hence the fuel flow obtained is lower, thus causing a slower acceleration rate.

To summarise this examination of fuel schedule compensation based on the hub temperature response, the studies carried out at sea-level conditions have revealed that the use of a value of 0.25 for the index of compensation 'a', was found to give the intended predictions during both 'cold' and 'hot' acceleration of the engine. The trajectory in the H.P.Compressor is lowered, and the transient surge margin increases by about 50% and therefore engine reacceleration is possible.

H.P.Turbine disc (Diaphragm) temperature response

For the diaphragm, fuel flow schedule compensation based on the diaphragm temperature response was also predicted to give satisfactory results during both 'cold' and 'hot' acceleration of the engine, when the same values of the index 'a' as for the case of the hub were examined. This is because of the slow response of the diaphragm due to the time constant which is relatively long (30 seconds), compared to the thin blades (2.8 seconds). Similar results to those of the hub were predicted during acceleration of the 'cold' and 'hot' engine. These are illustrated in Figs.115 to 119.

H.P.Turbine disc (Platform) temperature response

Investigations of fuel schedule compensation based on the platform temperature response have revealed that the use of 0.20 for the index 'a' of compensation gave good performance prediction during acceleration of the 'cold' engine. Using an

index smaller than 0.20 (a=0.15) was predicted to give an only slightly enhanced engine response (Fig.120b) due to the decrease of the resulted fuel flow caused by a lower compensating factor (with a smaller index). However, decreasing the index still further is seen from Fig.120a to show no effect compared to the uncompensated case.

Fuel compensation during a 'Bodie' transient was unsatisfactory (Fig.122). This can be seen from the values of the fuel compensating factor (over unity for all values of index a) shown in Fig.124b. This parameter is shown to increase the fuel flow rather than decreasing it. The reason is that the platform is partially cooled and at the end of a deceleration the metal temperature is lower, while the gas temperatures driving the metal temperatures become high for the reacceleration, thus resulting in an increased compensating fuel flow factor and hence the fuel flow rate. As a result, the engine accelerates rapidly and the pressure ratio rises. This is the same difficulty as had been discussed earlier in this section when considering compensation by H.P.Turbine blade aerofoil temperature.

H.P.Turbine disc averaged temperature

To illustrate fuel schdedule compensation based on the average temperature response of the H.P.Turbine disc, three values were examined for the index of compensation 'a'. These are 0.15; 0.25 and 0.35. Predicted corresponding results are discussed below.

Fig.125 shows the movement of the trajectories on the H.P.Compressor characteristics for each of the indexes during engine 'cold' aceleration. As can be seen from this figure,

good response of the engine has been obtained with an index of 0.15 (Fig.125a). However, with an index of 0.25 the engine accelerates faster and the resulting trajectory is raised further but still far from surge (Fig.125b). This behaviour is as usually expected for cold accelerations of the engine. However increasing 'a' beyond 0.25 causes the compressor to surge, due to the rapid increase in the pressure ratio caused by rapid engine acceleration rate. Typical results for a value of 0.35 can be seen from Fig.125c.

Resulting predicted engine performance is shown in Fig.126 during 20 seconds of transient acceleration. The thrust response is advanced by about 1.2 second with a = 0.25, and about 0.7 seconds at 50% of maximum thrust with a = 0.15.

Engine response during 'hot' acceleration is illustrated in Fig.127 and Fig.128. As can be seen from Fig.127, unsatisfactory results were predicted with an index of 0.15 (Fig.127a) - this giving insufficient lowering of the trajectory in the H.P.Compressor. However, a value of 0.25 for the index 'a' gave good performance prediction in slowing the engine response and easing the trajectory (Fig.127b). It can be clearly seen that engine acceleration response is slowed down even further with 0.35 and the surge margin in the transient is increased by about 50% compared to the uncompensated case. The resulting trajectory is exactly as was expected and intended from compensation during a 'Bodie' transient (Fig.127c). Good prediction obtained on the basis of this method is due to the hub contribution because of its longer time constant (47 seconds) compared to the other sections of the disc.

Fig.128 shows engine performance during this transient. With 0.25 the thrust response is delayed by about 0.6 second

(at 50% Of maximum thrust) which is not excessive compared to the gain achieved in increasing the surge margin available. To get an idea about the variation of the fuel flow schedule and engine acceleration rate during 'cold' and 'hot' accelerations, values of the fuel compensating factor plotted versus time are shown in Fig.129 for both transients. From this figure, it can be clearly seen that during 'hot' acceleration of the engine the fuel compensating parameter at the start of the transient is well under unity up to 6 seconds. Thus, it is clearly reducing the fuel flow as it is intended.

'Delayed' H.P.shaft speed signal

As for fuel schedule compensation based on a 'Delayed' shaft speed signal of the H.P.Shaft, a range of values has been examined for the index 'b' (shown in Equation 5.16 in the previous chapter and reviewed below in Equation 6.1) and also a range of values for the time constant 'τ' (shown in Equation 5.17 in chapter V). Both 'cold' and 'hot' accelerations have been investigated.

$$F_{cp} = \left(\frac{N_H}{N_{HD}}\right)^b \qquad (6.1)$$

A value of 1.0 was first selected for the index 'b', together, with a short time constant 'τ' of 6.0 seconds. The combination of these two values was predicted to give good behaviour of the 'cold' engine (Fig.130). The surge margin used was approximately 60% compared to 50% with the uncompensated fuel schedule (Fig.130a).

Considering the thrust response, Fig.131 shows that the response is faster by about 1.3 seconds (at 50% of maximum thrust) compared to that given with an uncompensated fuel flow schedule.

During the 'Bodie' transient, predicted engine behaviour was unsatisfactory (compensated fuel schedule gives a greater surge margin usage than in the uncompensated case). As a result of this, the compensating factor is less than unity for only the first 0.25 second of the reacceleration. Thereafter, compensating factor serves to increase the fuel flow and hence increases the pressure ratio and acceleration rate.

To improve engine behaviour during a 'Bodie' transient, a much longer time constant of 40 seconds has been used for obtaining the 'Delayed' H.P.shaft speed. When coupled with an index 'b' of a value of 0.13 gave a good engine performance prediction during cold acceleration.

The thrust response resulted from the combination of these two values is faster by about 1.0 second compared to the uncompensated case (at 50% of maximum thrust).

During the 'Bodie' transient ,however, only a minor improvement in the engine behaviour was predicted (engine acceleration rate was slowed but only very slightly) as shown in Fig.132.

An even longer time constant of 60 seconds has therefore been adopted with a value of 0.30 for the index 'b' of compensation. The predictions, presented in Figs.130b and 132b, show that this combination gives a very good engine behaviourn during 'cold acceleration. The surge margin usage was increased from 50% (uncompensated case) to about 90% (Fig.130c).

For acceleration of the 'cold' engine, the thrust response is faster by about 2.7 seconds (at 50% of maximum thrust) compared to the case with an uncompensated fuel schedule.

For the 'Bodie' transient also, this combination of the time constant of 60 seconds when coupled with an index of compensation 'b' of 0.30 gave a very satisfactory prediction. The surge margin usage was reduced from 80% (uncompensated case) to about 60%.

The thrust response resulted during the 'Bodie' is delayed by about 0.8 seconds at 50% of maximum thrust (compared to that obtained with uncompensated fuel schedule).

Compensation at altitude

Fuel flow schedule compensation based on the temperature response of the H.P.Turbine disc (hub) was also investigated at 41,000 ft and predicted results are discussed below.

Fig.135 shows the resulting predicted trajectories on the H.P.Compressor characteristics during 'cold' acceleration of the engine for three selected values of the index of compensation 'a' already used at sea-level conditions. This figure shows that for the same values used previously, fuel schedule compensation at altitude affects the engine behaviour to a much lesser extent than it does at sea-level. With an index 'a' of 0.10 and 0.15 fuel flow compensation has little noticeable effect, whereas, with 0.30 the engine accelerates slightly more rapidly during only a few seconds of the transient. The predicted performance is shown in Fig.136. From this figure, it can be seen that only very slight improvement in the thrust response was predicted.

The resulting predicted trajectories for the 'Bodie' transient are shown in Fig.137 . From this figure, it can be

seen that a very good behaviour was predicted using an index of 0.30, whereas, 0.10 and 0.15 are seen to give only an acceptable behaviours during 'hot' acceleration of the engine.

With an index of 0.30, the acceleration of the engine was slowed down slightly but not as that predicted at sea-level conditions. The thrust response is delayed by about 0.2 second (at 50% of max. thrust) compared to that predicted with the standard fuel schedule, uncompensated (Fig.138).

The values adopted for the index 'a' of compensation at sea-level have been proved to be inadequate for altitude compensation. Therefore, attention has been given to increase the value of the index 'a' above 0.30 and a range of values between 0.30 and 1.0 have been examined. The results for the cold acceleration are illustrated in Figs.140 and 142 for two typical values of the index 'a' (0.5 and 1.0). As can be seen from Fig.140 satisfactory results were obtained with values of 0.5 and 1.0 for the index. However, with index value of 1.0, the trajectory is predicted to approach closely to the surge line. The surge margin usage is increased by approximately 50% with comparison to that of the uncompensated case and the thrust response is faster by about 0.2 second at 50% of maximum thrust (Fig.141).

The predicted trajectories during the 'Bodie' transient are shown in Fig.142 for the two values of the index 'a'. This figure shows that an index of unity gave a very good prediction in slowing down engine response, thereby, reducing the surge margin usage by about 50%. A satisfactory prediction was also achieved with an index of 0.5. The thrust response is seen from Fig.143 to be delayed by about one second with index value of 1.0 and about half of a second with 0.5 (at 50% of maximum thrust).

Fuel schedule compensation based on the H.P.Shaft 'Delayed' speed signal was also investigated at 41,000ft and corresponding predictions are illustrated from Fig.144 to 148.

For acceleration of the 'cold' engine, it can be seen from Fig.144 that a good engine behaviour is predicted with a time constant of 60 seconds when coupled with an index of 0.30. An acceptable prediction is seen from the same figure to be also given by a time constant of 40 seconds (with an index of 0.13). However predicted behaviour with a short time constant of 6 seconds is hardly noticeable. The poor engine behaviour predicted with the same parameters as had been at sea-level is due to the time constants being too short for altitude conditions.

Because of the reduced heat transfer coefficients at altitude operation, a longer time constant of 100 seconds in combination with an index of 0.30 was adopted. The combination of these two values gave a good prediction during cold acceleration. This is due to heat transfer coefficient which is reduced at altitude (compared to that at sea-level conditions), resulting in a longer time constant.

Predictions during the 'Bodie' transient are shown in Fig.146. From this figure it can be seen that with this very long time constant, a very satisfactory prediction was achieved.

For a better illustration of predicted results obtained on the basis of different methods and different models, at both sea-level and altitude operations, fuel flow schedule compensation schemes investigated in this work are summarised in a table shown in Fig.150.

H.P.Turbine entry temperature (T.E.T)

Beside compressor surge caused by excessively rapid transient movements, a very high value of T.E.T if reached could cause serious damage to turbine blades. An engine control system if judiciously devised could not only protect compression system against surge problems but also could avoid turbine entry over-temperatures. For this reason, values of T.E.T were predicted against time for transient operations using the fuel controller discussed previously. The predictions incorporating allowance for thermal effects are described below.

During engine cold acceleration at sea-level conditions, Fig.15 shows that during the first ten seconds of the transient, with thermal efects considered, T.E.T. exceeds the adiabatic figure by about 25K (up to 1350K). This is due to the transient inefficiencies of the engine components particularly the excessive opening of the turbine and compressor air seals. With the fuel schedule compensated, the temperature response is faster by about 2 seconds (at 70% of maximum value) compared to that with uncompensated fuel schedule.

During the reacceleration in the 'Bodie' transient, the response is slowed by about 5 seconds at 70% of maximum thrust value (compared to the uncompensated case). The maximum T.E.T. value reached exceeds slightly the uncompensated case, then drops very closely below the uncompensated values.

From Fig.15 it can be seen that both T.E.Ts, with and without fuel schedule compensation are the same after completing the speed transient, from about 2 seconds, due to the fuel flow being fixed at a maximum value.

At altitude and as shown in Fig.16, the turbine entry

temperature increases rapidly during the first few seconds of cold acceleration. With thermal effects considered, values of T.E.T. are relatively lower compared to that obtained from the adiabatic assumptions. Maximum value does not exceed 1250K for all cases. From Fig. , it can be seen that a slightly faster response of T.E.T. is predicted when fuel schedule is compensated (about 0.1 second at about 75% of maximum value).

During 'Bodie', the response is slowed by 1.2 seconds at 70% of maximum temperature. As already noticed at sea-level, both temperatures with and without fuel compensation are the same from about 6 seconds of the reacceleration. the reason is as discussed above.

CHAPTER VII

CONCLUSION AND SUGGESTIONS FOR FURTHER WORK

7.1. GENERAL CONCLUSION

Work on the prediction of the performance of a two-spool turbofan aircraft engine during steady-state and transient operation was available. Procedures which have already been used for the estimation of heat transfer effects in earlier engines were modified, improved and then incorporated into the computer programme. The transient performance programme which has been developed uses the continuity of mass flow method based on the achievement of flow balances at any time and at any engine location. Changes of component characteristics, fluid density changes and component heat capacities are the factors which are responsible for alteration of the overall engine performance from that of the steady-state operation. Additionally, modification of engine performance is mainly due to the movement of tip and seal clearances.

As stated above, the non-adiabatic prediction of a gas turbine engine was investigated and illustrated for a typical two-spool turbofan engine with a medium by-pass of which more information was available. This engine was simulated during six transients. These are a 'cold' acceleration, a transient deceleration and a 'Bodie' transient at both sea-level conditions and altitude. Results obtained were directly compared to the adiabatic assumptions.

The heat transfer effects taken into account were-

(a) heat absorption in the materials of the compressors and turbines.

(b) heat absorption in combustion chamber material.

(c) changes in compressor characteristics, due to the heat absorption and boundary layer changes.

(d) changes in tip clearances (H.P.Compressor and H.P.Turbine) from steady-running values.

(e) changes in seal clearances from design values (the two seals considered to be critical were H.P.Compressor 12^{th} stage seal and H.P.1 Turbine disc front face seal.)

The most significant of the above effects was the movement of the tip clearance in the H.P.Turbine. The changes in the seal openings also showed significant effects.

The results showed that, when these heat transfer effects were taken into account, the predicted transient responses were slowed down when compared with the adiabatic prediction. This was more pronounced at altitude condition.

'Bodie' transient was found to be the most critical engine test where a major part of the surge margin available in the H.P.Compressor was already used before reacceleration of the engine. The effects are more severe at altitude.

Reasons have been presented for introducing a modifying factor which will adjust the transient fuel schedule to compensate for the immediately preceding temperature history of the engine. When accelerating a 'cold' engine, this factor should enhance the acceleration rate with greater resulting margin usage. The opposite should occur when reaccelerating a

'hot' engine. Two compensation method have been illustrated based on different models, one uses the temperature response of a characteristic component and the other considers a 'delayed' shaft speed signal. H.P.Turbine disc temperature response was proved to be convenient for fuel schedule compensation during both 'cold' and 'hot' acceleration of the engine, especially when the temperature response of a massive part, such as, the hub was adopted, due to the longer time constant. However, the blade aerofoil temperature response induced the desired effects only during acceleration of the 'cold' engine (blade aerfoil temperature response was found to be too fast for acceleration of a 'Bodie' transient due to the very short time constant at the start of the reacceleration).

The second method was satisfactory during both transients if a judicious selection of the engine parameters was made (time constant and index of compensation). At altitude, fuel schedule compensation differs from that predicted at sea-level conditions when the same parameters were used and only minor improvement in the engine response was achieved when a very long time constant was adopted (second method at altitude)

For Rolls-royce engines up to RB 211, hydromechanical systems were used as engine limit controls during transient operations. The simulation programme used in this work permits engine control if information could be stored in what is called "Block control" as the case of the FADEC for example (Full Authority Digital Electronic Control). By alteration of engine parameters (such as fuel flow in this work) judicious control of engine operation could be possible and invaluable.

7.2. RECOMMENDATION FOR FURTHER INVESTIGATIONS

Due to the incorporation of models describing heat transfer effects in a gas turbine engine, where heat exchange occurs between the working fluid and engine material, computing time was increased considerably compared to the simulation with adiabatic assumptions. Therefore, the development of more simple , reasonable but accurate models is required for reduction in the computing time needed.

Fuel flow schedule compensation based on the temperature response of the H.P.Turbine disc (hub or disc averaged temperature) when investigated at altitude condition showed that the values of the index (or the time constant τ) used at sea-level cases, were not adequate. Therefore, a study of indexes which give a suitable compensation scheme at altitude condition is required. Also very important to investigate is fuel compensation when H.P.Compressor disc temperature response is used. It is also desirable to investigate compensation based on the 'delayed' speed of the L.P.shaft.

Heat transfer effects in the I.P.Compressor are still not very well understood. However, an investigation into fuel compensation during a transient deceleration would be valuable, as the I.P.Compressor is prone to surge only during deceleration.

REFERENCES

1. N.R.L. Maccallum & P. Pilidis,
" Gas turbine transient fuel scheduling with compensation for thermal effects."
A.S.M.E. paper 86GT208, 1986.

2. H.W. Bennett,
" Aero-engine development for the future."
Paper proceedings I.Mech.E, 197 paper 48, 1983.

3. H. Cohen G.F.C. Rogers & H.I.H. Saravanamuttoo,
" Gas turbine theory."
2nd edition (Longman), London 1972.

4. Rolls-Royce Limited,
" The jet engine."
Report T.S.D. 1302; 3rd edition July 1969.

5. A.J. Fawke & H.I.H. Saravanamuttoo,
" Digital computer methods for prediction of gas turbine dynamic response."
S.A.E. paper 710550, June 1971.

6. R. Stoddart,
" Prediction of the transient performance of the Rolls-Royce Tay engine using the method of 'Intercomponent volumes'."
Final year project for B.Eng Glasgow university,
May 1987.

7. A.J. Fawke & H.I.H. Saravanamuttoo,
" Experimental investigation of methods for improving the dynamic response of a twin-spool turbojet engine."
A.S.M.E. paper 71GT14, 1971.

8. P. Pilidis,
" Digital simulation of gas turbine performance."
PhD thesis; Glasgow University, November 1983.

9. David M. Evans & Boris Glezer,
" Critical gas turbine blade tip clearance; heat transfer analysis and experiment."
Hemisphere Publishing Corporation Washington 1984
pages 485-497.

10. A. Pandya & B. Lakshminarayana,
" Investigation of the tip clearance flow inside and at the exit of a compressor rotor passage."
Part I : Mean velocity field.
Journal of Enginneering for Power,
Vol. 105, January 1983, pages 1-12

11. P. Pilidis & N.R.L. Maccallum,
" A study of the prediction of tip and seal clearances and their effects in gas turbine transients."
A.S.M.E. paper 84GT245, 1984.

12. G.A. Halls,
" Air cooling of turbine blades and vanes."
Rolls-Royce Limited Derby, paper presented to AGARD,
May 1967.

13. J.M. Owen & H.S. Onur,
" Convective heat transfer in a rotating cylindrical cavity."
Journal of Engineering for Power
Vol. 105, April 1983, pages 265-271.

14. N.R.L. Maccallum & P. Pilidis,
" The prediction of surge margins during gas turbine transients."
A.S.M.E. paper 85GT208, 1985.

15. N.R.L. Maccallum,
" The axial compressor characteristics during transients."
Paper from conference proceedings 324,
AGARD 'Engine handling' October 1982.

16. N.R.L. Maccallum,
" Models for the representation of turbomachine blades during temperature transients."
A.S.M.E. paper 76GT23, 1976.

17. P. Pilidis & N.R.L. Maccallum,
" A general programme for the prediction of the transient performance of gas turbines."
A.S.M.E. paper 85GT209, 1985.

18. C.M.Haynes & J.M. Owen,
" Heat transfer from a shrouded disc system with a radial outflow of coolant."
Transactions of the A.S.M.E. paper.
Journal of Engineering for Power
January 1975, pages 28-36

19. P. Pilidis & N.R.L. Maccallum,
" The effect of heat transfer on gas turbine transients."
A.S.M.E. paper 86GT275, 1986.

20. N.R.L. Maccallum,
" Thermal influences in gas turbine transients - effects of changes in compressor characteristics."
A.S.M.E. paper 79GT143, 1979.

21. N.R.L. Maccallum & A.D. Grant,
" The effect of boundary layer changes due to transient heat transfer on the performance of an axial-flow air compressor."
S.A.E. paper 770284, March 1977.

22. N.R.L. Maccallum,
" Proposed studies to improve the transient prediction procedures for Rolls-Royce Tay engine."
Report, Glasgow university, August 1987.

23. Darryl E. Metzger & Naim H. Afgan,
" Heat and mass transfer in rotating machinery."
Hemisphere Publishing Corporation
Washington, 1984.

24. M. Glyn,
" Gas turbine a successful developing technology."
23rd annual international gas turbine conference,
London april 1978.

25. R.T.C. Harman,
" Gas turbine engineering."
London 1981.

26. A.W. Morley,
" Aircraft propulsion (theory and performance)."
Longman, London 1953.

27. Gordon C. Oates & J.S. Prezemieniecki,
" Aerothermodynamics of aircraft engine components."
A.I.A.A. education series.
New York 1985, page 275 to 330.

28. M.F. Blair,
" An experimental study of heat transfer and film cooling on large-scale turbine end-walls."
A.S.M.E. paper 74GT38, 1974.

29. H.I.H. Saravanamuttoo & A.J. Fawke,
" Simulation of gas turbine dynamic performance."
A.S.M.E. paper 70GT23, 1970.

30. H. Pfeil & R. Herbst & T. Schroder,
" Investigation of the laminar-turbulent transition of boundary layers disturbed by wakes."
Journal of Engineering for Power
Transactions of the A.S.M.E. paper
January 1983, pages 130-137

31. E.l. Houghton & N.B. Carruthers,
" Aerodynamics for engineering students."
Arnold, 3rd edition, London 1982.

32. W.J. Duncan & A.S. Thom & A.D. Young,
" Mechanics of fluids."
Arnold, second edition, London 1970.

33. D.M. Evans,
" Calculation of the temperature distribution in multistage axial gas turbine assemblies when blades are uncooled."
Journal of Engineering for Power,
Vol. 95, October 1973, pages 309-318

34. P.J. Ashmole,
" Introducing the Rolls-Royce Tay."
AIAA paper 83-1377, Rolls-royce 1983.

35. R.W. Stuart Mitchell & V.A. Ogale,
" Gas turbine blade cooling-Retrospect and prospect."
A.S.M.E. paper 67-WA/GT-9, 1968.

36. N.R.L. Maccallum,
" Transient expansion of the components of an air seal on a gas turbine disc."
S.A.E. paper 770974, November 1977.

37. Dietmar K. Hennecke,
" Heat transfer problems in aero-engines."
Hemisphere Publishing Corporation.
London 1984.

38. T.F. Balsa & G.L. Mellor,
" The simulation of axial compressor performance using an annulus wall boundary layer theory."
Paper from Journal of engineering for power,
Vol. 97, July 1975, pages 305-318.

39. N.R.L. Maccallum
" Further studies of the influence of thermal effects on the predicted acceleration of gas turbines."
A.S.M.E. paper 81-GT-21, 1981.

40. David A. Anderton,
" The addition of heat transfer effects to an adiabatic simulation programme for the Rolls-Royce turbofan."
Final year project for B.Eng Glasgow University,

May 1987.

41. J.M. Owen,
" Fluid flow and heat transfer in rotating disc systems"
Hemisphere Publishing Corporation.
London 1984, pages 81-103.

42. P. Pilidis & N.R.L. Maccallum,
" Models for predicting tip clearance changes in gas turbines."
AGARD paper from Conference Proceedings No.324

43. M. Kato & A. Sakai & T. Inui,
" Gas turbine combined desalination plant offers greater flexibility and improved efficiency."
Based on a paper presented at the General Electric International Gas turbine State of the Art Congress paper HITACHI, May 1976, Dubrovnik, Yugoslavia..

44. Wong H.Y.,
" Heat transfer for engineers."
Longman, first edition, London 1977.

45. Enrico Fermi,
" Thermodynamics."
Dover, first edition, London 1938.

46. W.J. Priddy & F.J. Bayley,
" Heat transfer to turbine blading."
Hemisphere Publishing Corporation.
Washington 1984.

47. J.H. Horlock,
" Some recent research in turbomachinery - Thermodynamics and fluid mechanics group."
Proceedings of I.Mech.E. paper.
Vol. 64E, October 1970.

48. George K. Serovy,
" Compressor and turbine performance prediction-system development: lessons from thirty years of

history."
Paper presented in 1976.

49. Constant Hayne,
" Gas turbines and their problems."
London Todd Publishing Group, London 1953.

50. H. Marsh,
" A digital computer program for the through-flow fluid mechanics in an arbitrary turbomachine using a 'Matrix method'."
Report No.282 A.R.C. 28246, London July 1966.

51. N.R.L. Maccallum,
" Computational models for the transient performance of RB183-02 (Spey) and RB183-03 (Tay) engines."
Report RR/1 Glasgow university, August 1984.

52. Janusz W. Polkowski,
" Turbulent flow between a rotating disc and a stationary wall with heat transfer."
Hemisphere Publishing Corporation.
London 1984, pages 105-116.

53. W. Kuhl & U. Stocker,
" Temperature measurement techniques and their application on gas turbine rotor heat transfer research."
Hemisphere Publishing Corp[oration.
London 1984, pages 337-350.

54. Rogers G.F.C. & Mayhew Y.R.,
" Engineering thermodynamics work and heat transfer."
Longman, 3rd edition, London 1980.

55. J. Hodge,
" Gas turbine: Cycles and prformance estimation."
Andover, London 1955.

56. G. Geoffrey Smith,
" Gas turbines and jet propulsion."
Iliffe Phylosophy Library, 6th edition
Sheffield 1955.

57. D.G. Shepherd,
" Introduction to the gas turbine."
Constable, 2nd edition, 1960.

58. Roger A. Crawford, & Alan E. Burwell,
" Quantitative evaluation of transient heat transfer on axial flow compressor stability."
Paper from AIAA-85-1352 Propulsion conference, Monterey California, july 1985.

59. Koch C. C.,
" Stalling pressure rise capability of axial flow compressor stages."
Journal of Engineering for power, Vol. 103, pages 645-656, 1981.

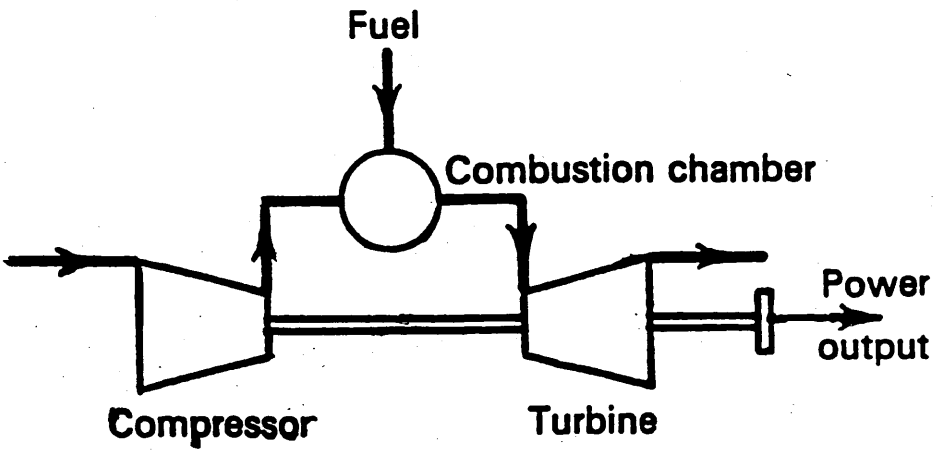

Fig. 1 SIMPLE GAS TURBINE SYSTEM.

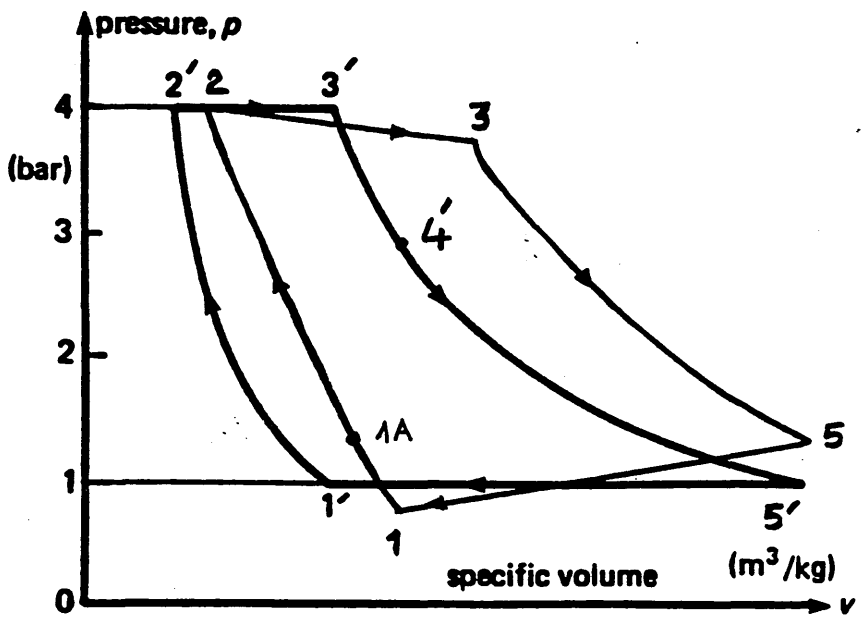

Fig. 2 PRESSURE-VOLUME CYCLE FOR AN AIRCRAFT ENGINE.

Fig.3 **SINGLE-SPOOL**

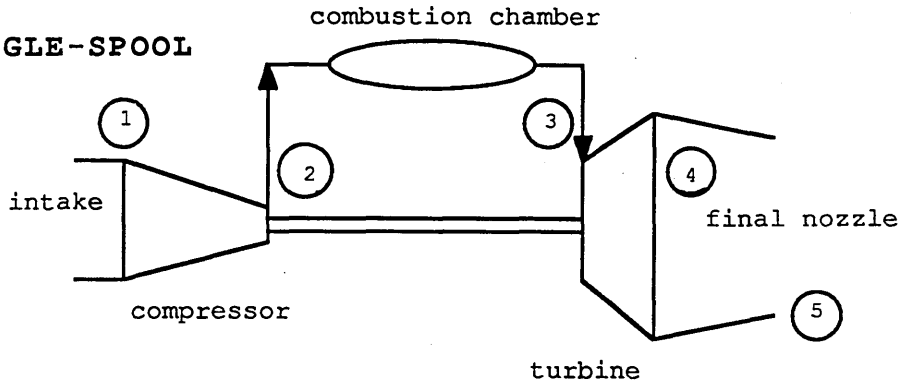

Fig.4 **TWO-SPOOL**

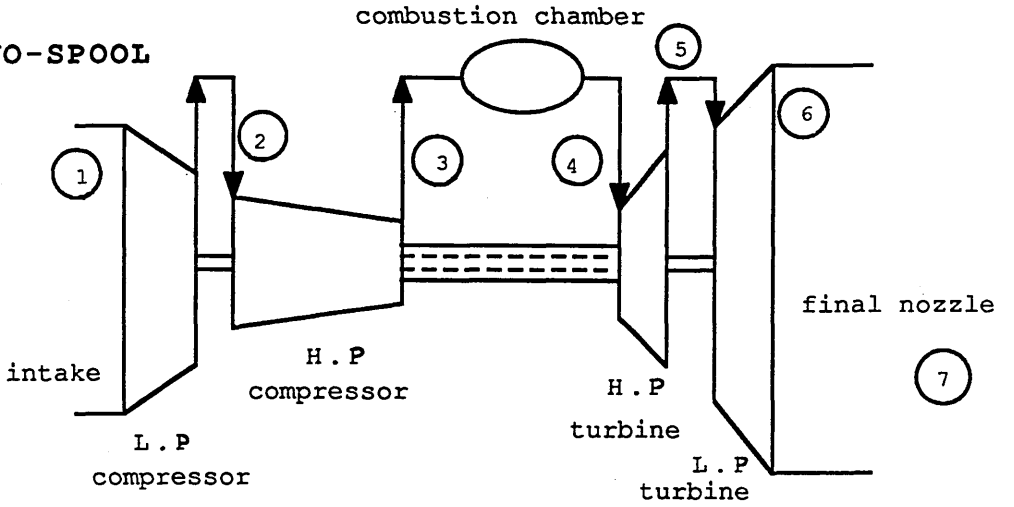

Fig.5 **THREE-SPOOL**

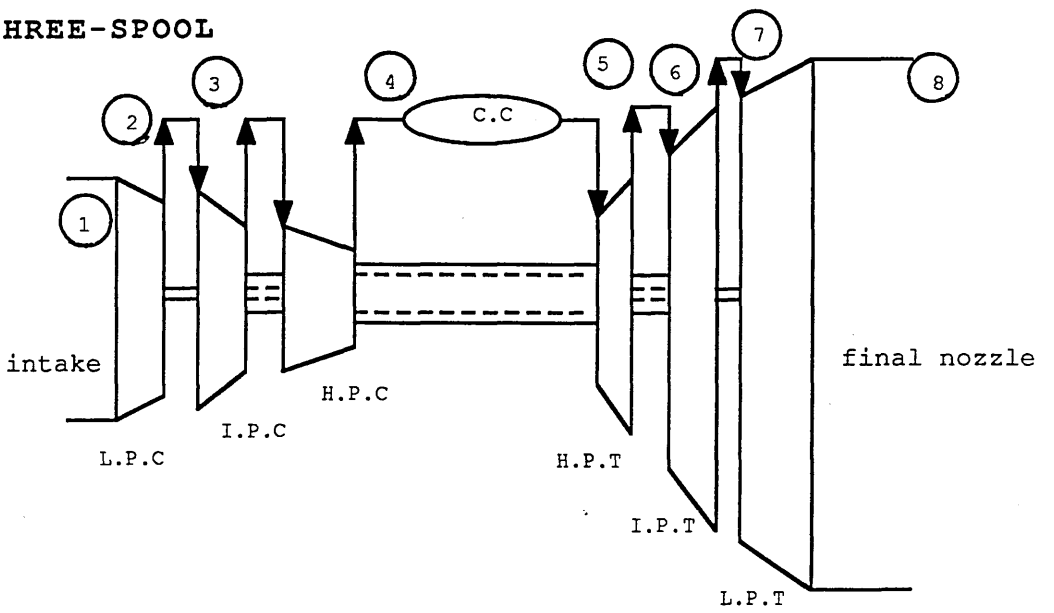

DIFFERENT CONFIGURATIONS OF AIRCRAFT
GAS TURBINE ENGINES.

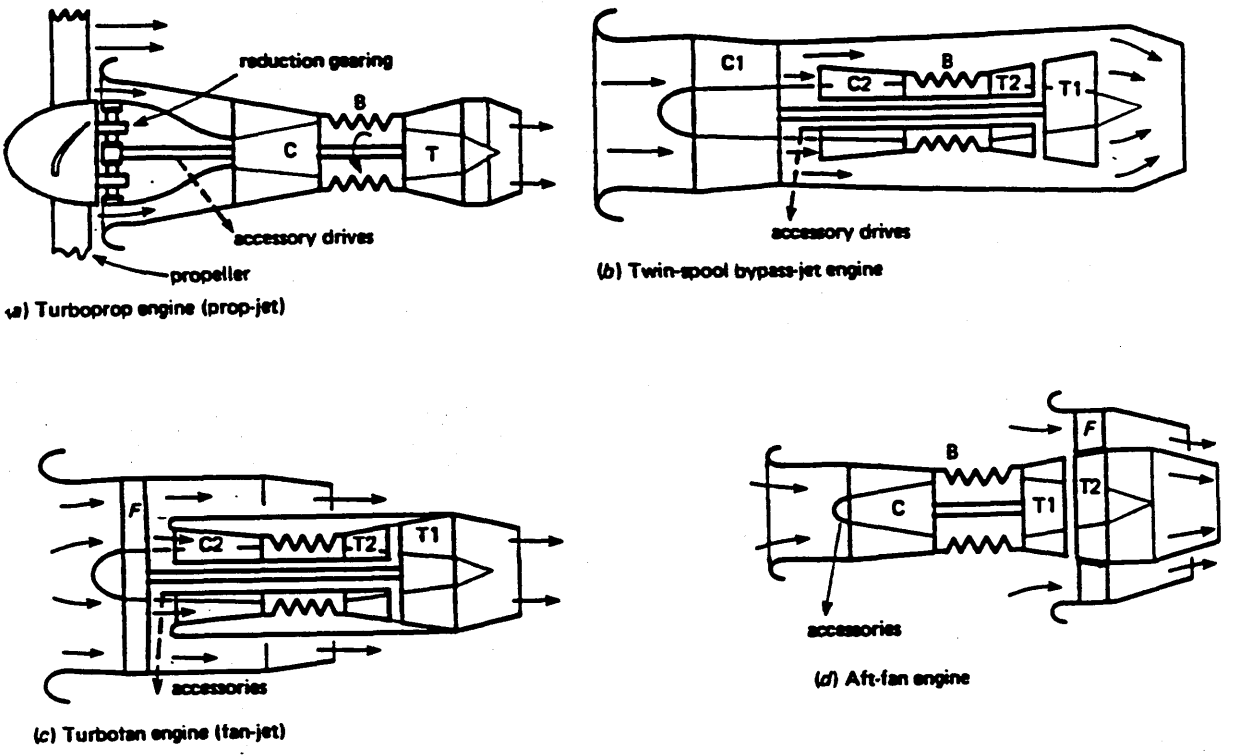

Fig 6 *Various aircraft engine configurations*

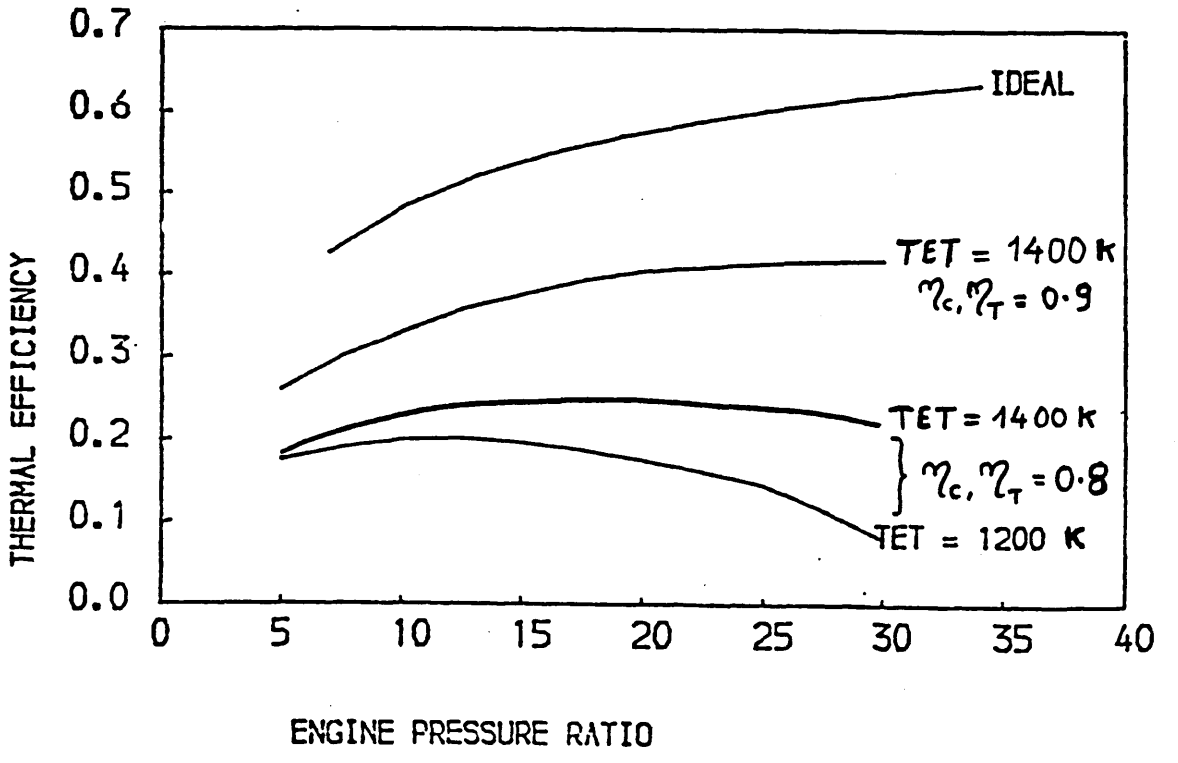

Fig. 7 EFFECT OF PRESSURE RATIO AND TURBINE INLET TEMPERATURE ON THERMAL EFFICIENCY

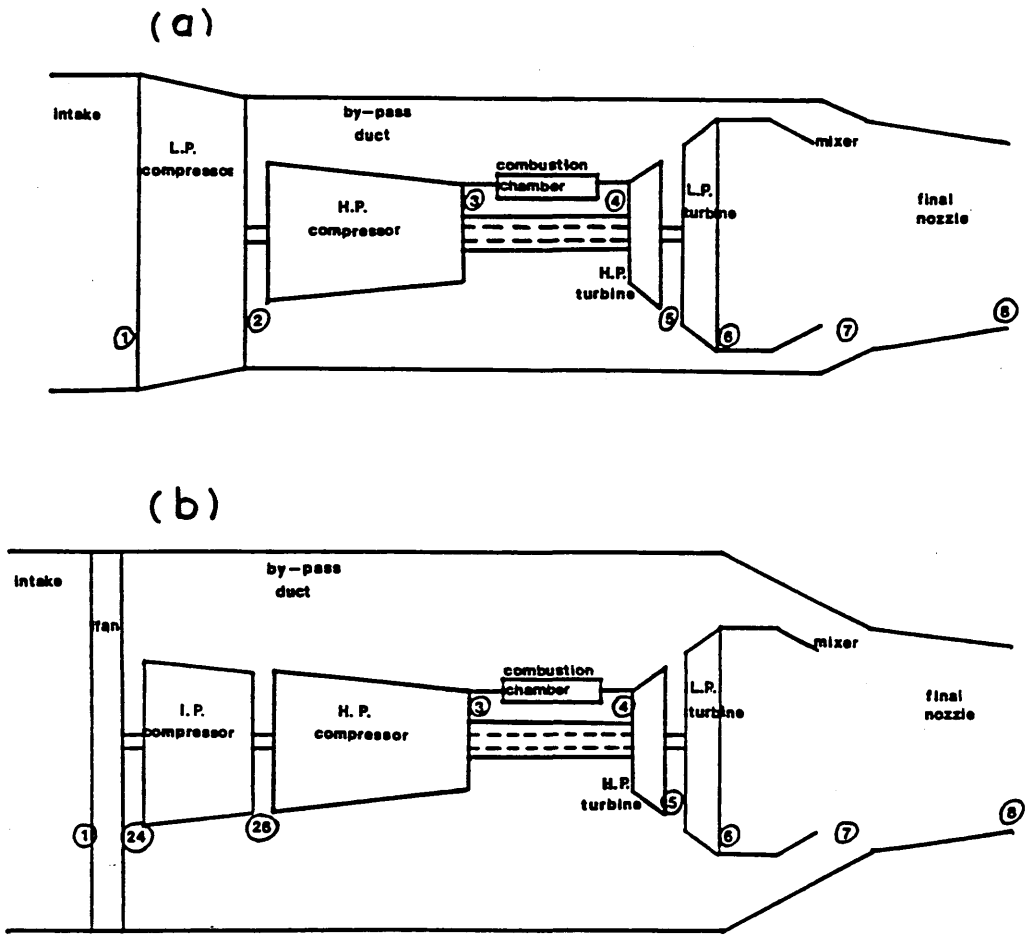

Fig. 8 SCHEMATIC CONFIGURATIONS OF ROLLS-ROYCE ENGINES.

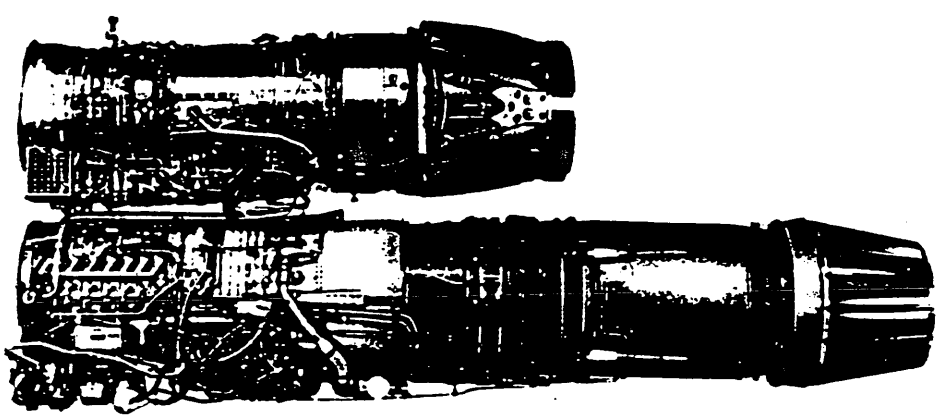

Fig. 9 Progress in aero-engine design
Top: RB 199 engine; bottom: J79 engine

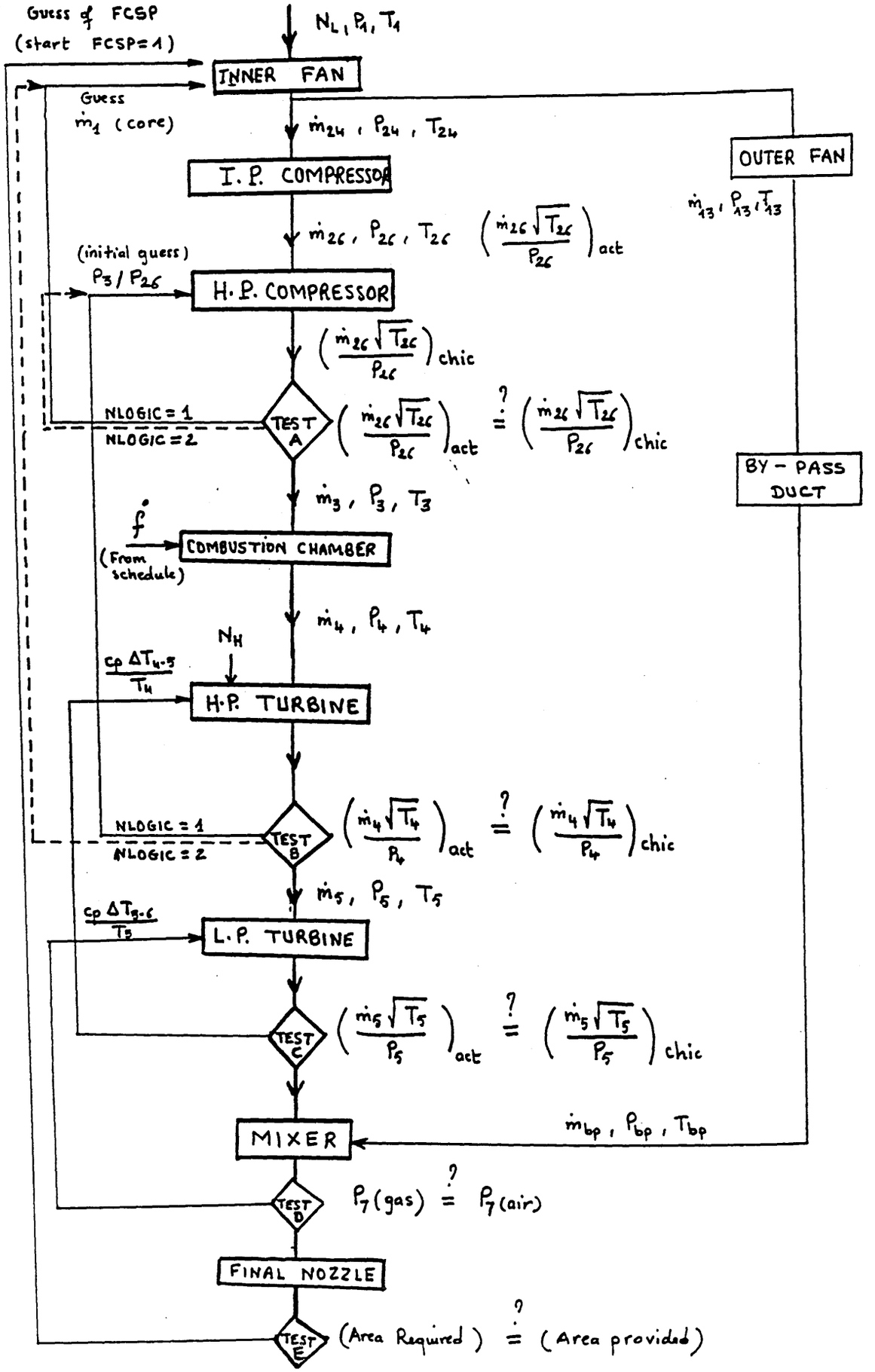

Fig. 10

FLOW CHART OF A TYPICAL TWO-SPOOL BY-PASS ENGINE
CONTINUITY OF MASS FLOW LOGIC.
station numbering as defined in Fig.8b

Fig. 11 LOGIC FOR TAY ENGINE (I.C.V. METHOD)

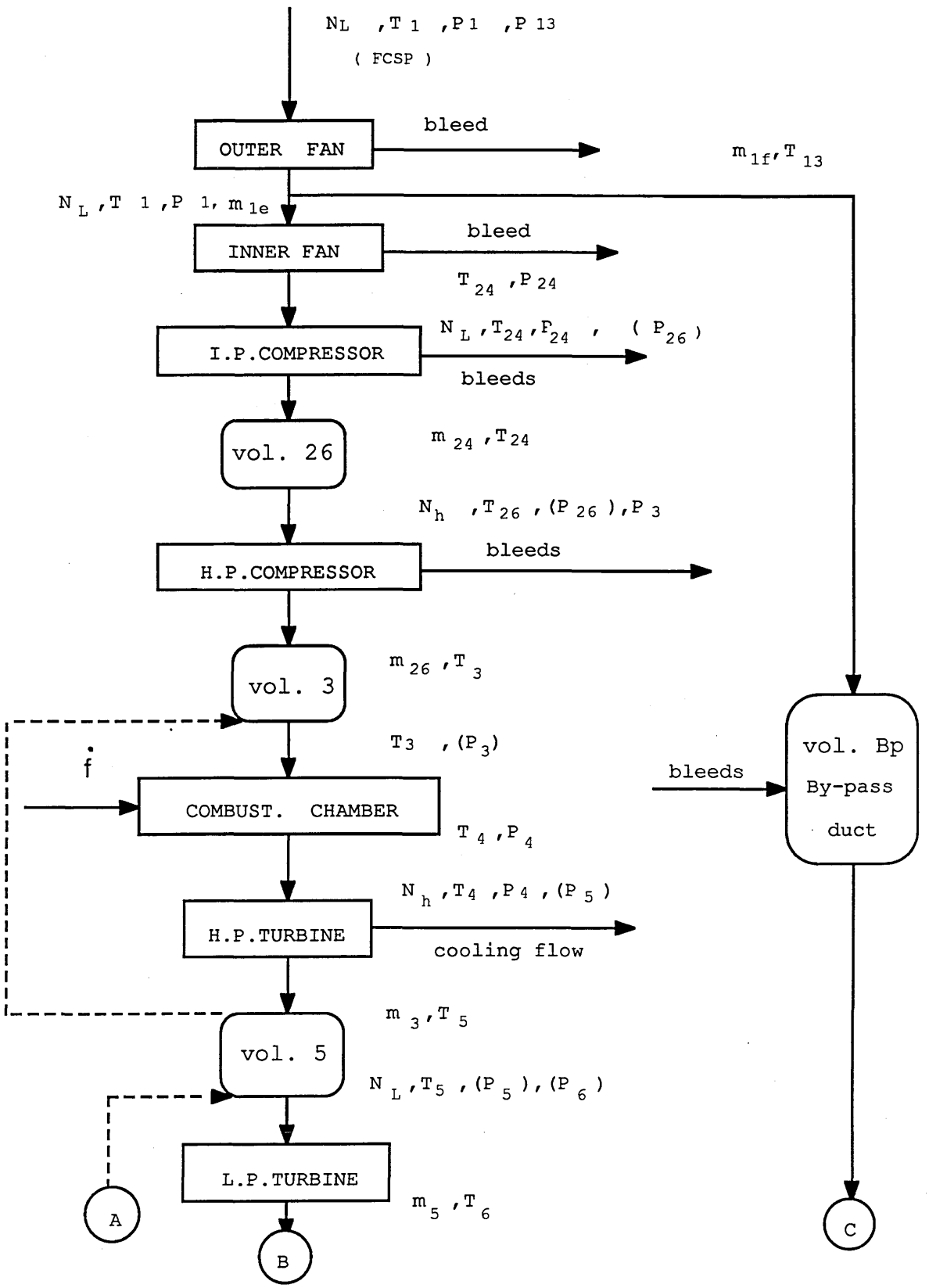

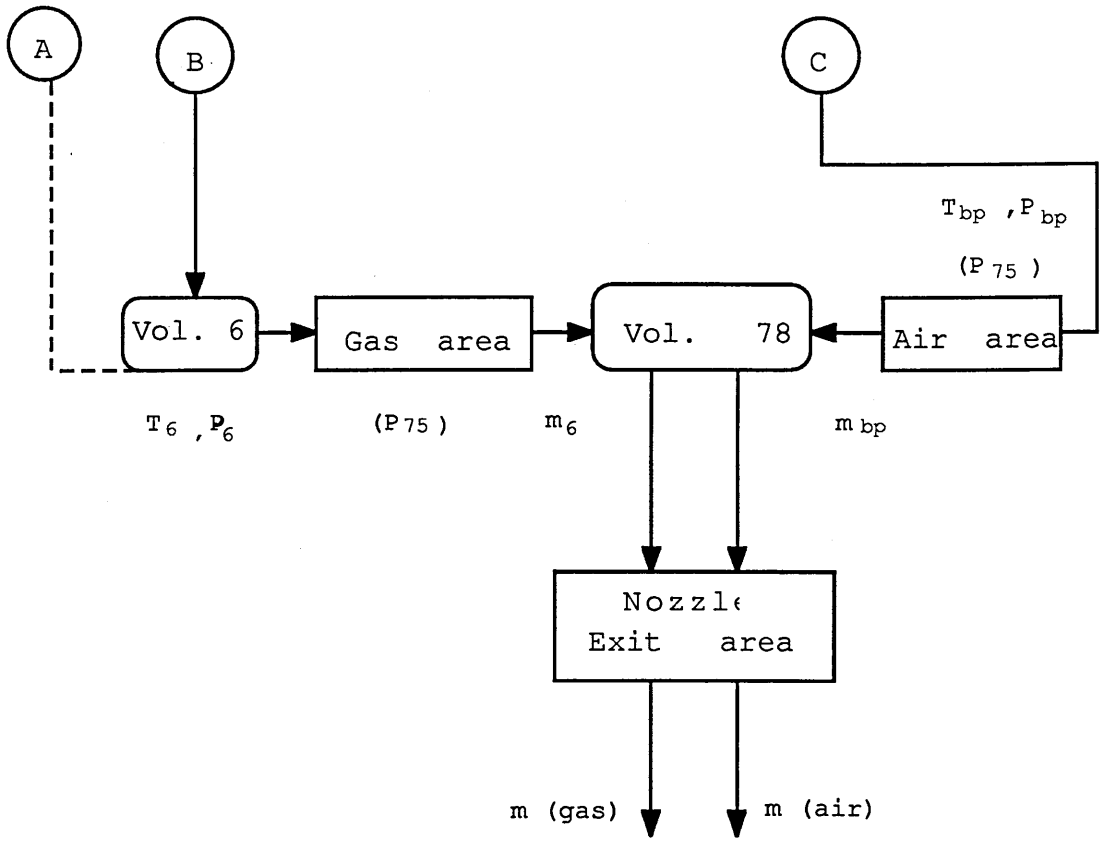

+ calculate new pressures and accelerations.

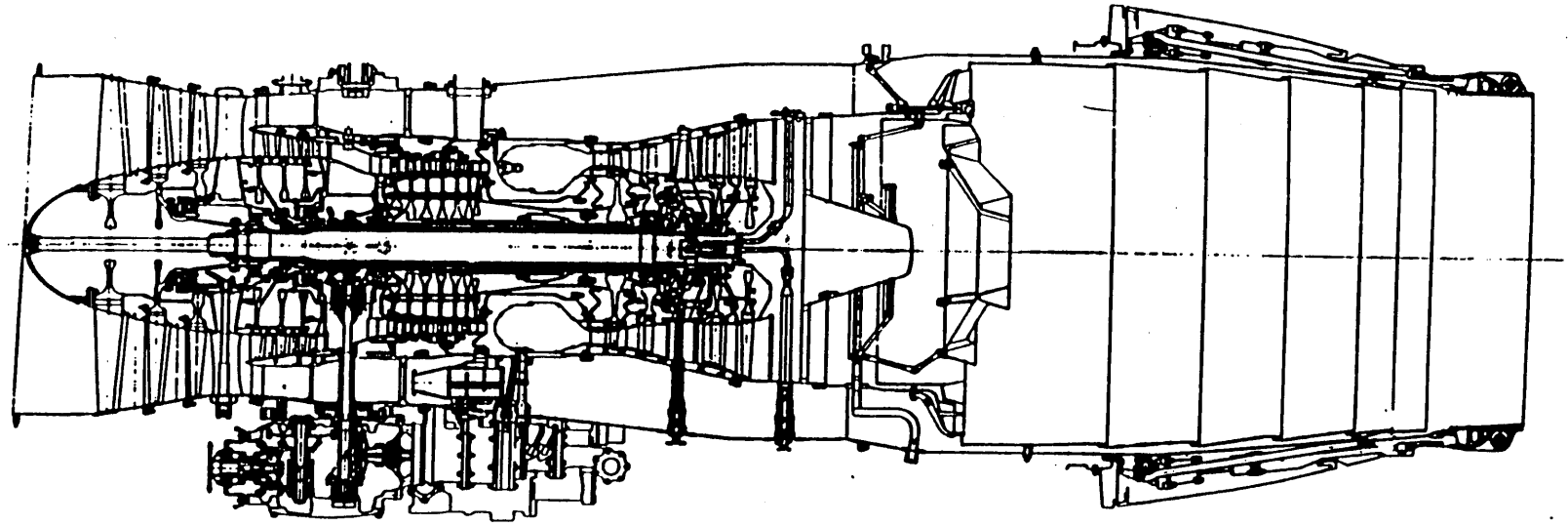

O Inlet, Fan, Compressor	O Combustor	O Turbine	O Afterburner, Nozzle
- inlet de-icing	- flame tube cooling	- blade cooling	- liner cooling
- disk temperatures	- fuel evapor.	- platform cooling	- gutter cooling
- casing temperatures	- flame radiation	- liner/casing cool.	- flame radiation
- active clearance control		- disk cooling	
		- act.clear.contr.	

Further areas

O Labyrinth Seals

O Bearings

O Heat Exchangers

O Heat Rejection of the Engine

Fig. 12 Heat transfer problems in aero-engines

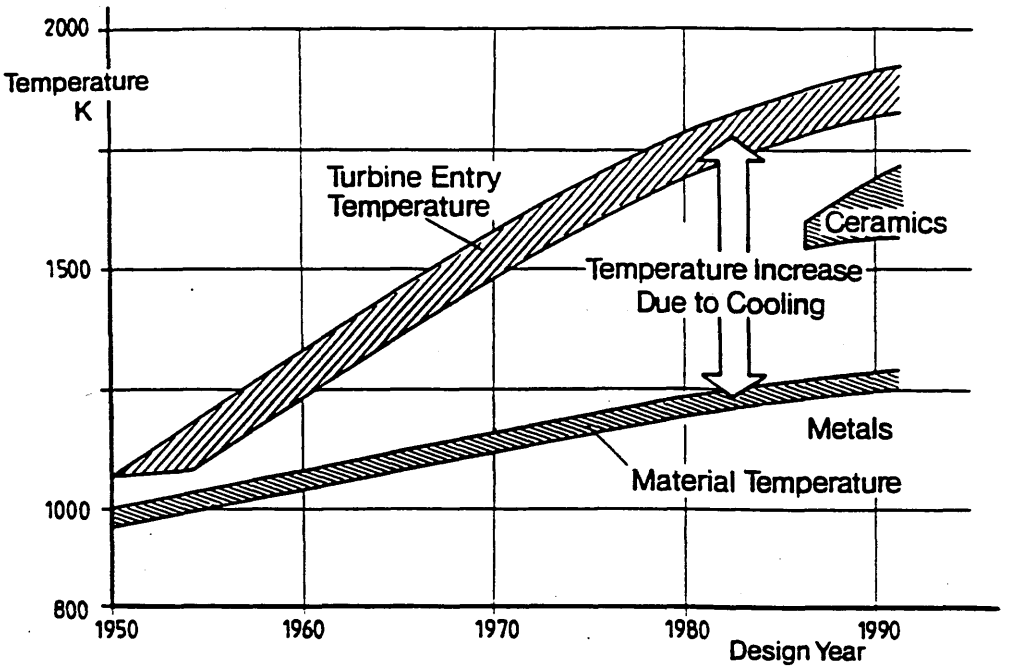

Fig. 13 Development of turbine entry temperature

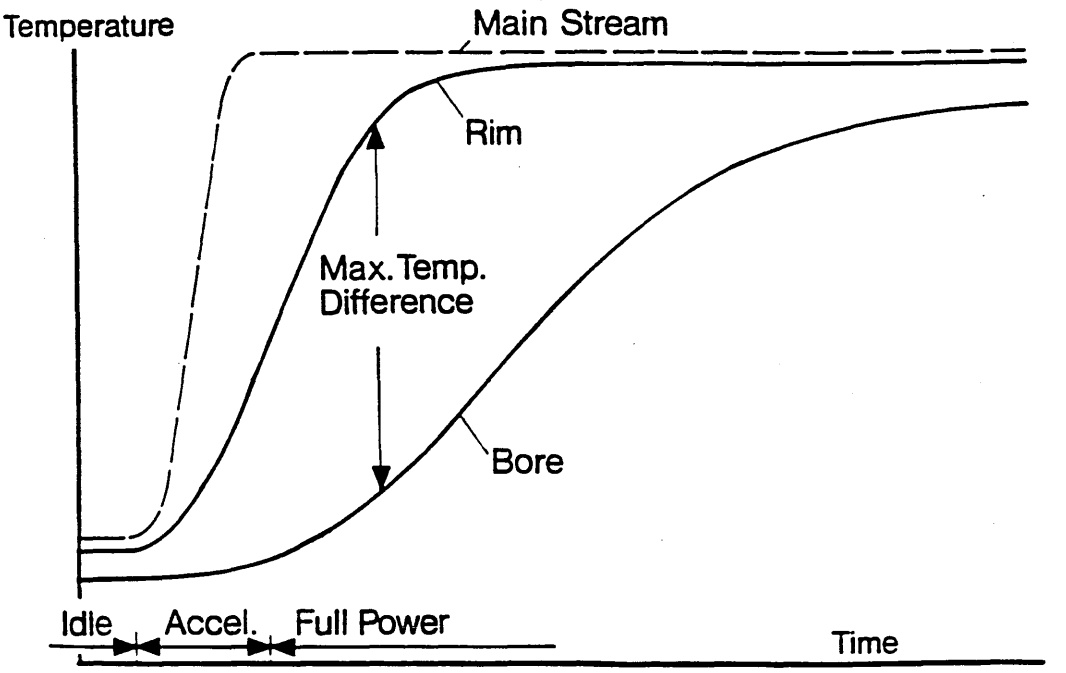

Fig. 14 Temperature response of a typical compressor disk during acceleration

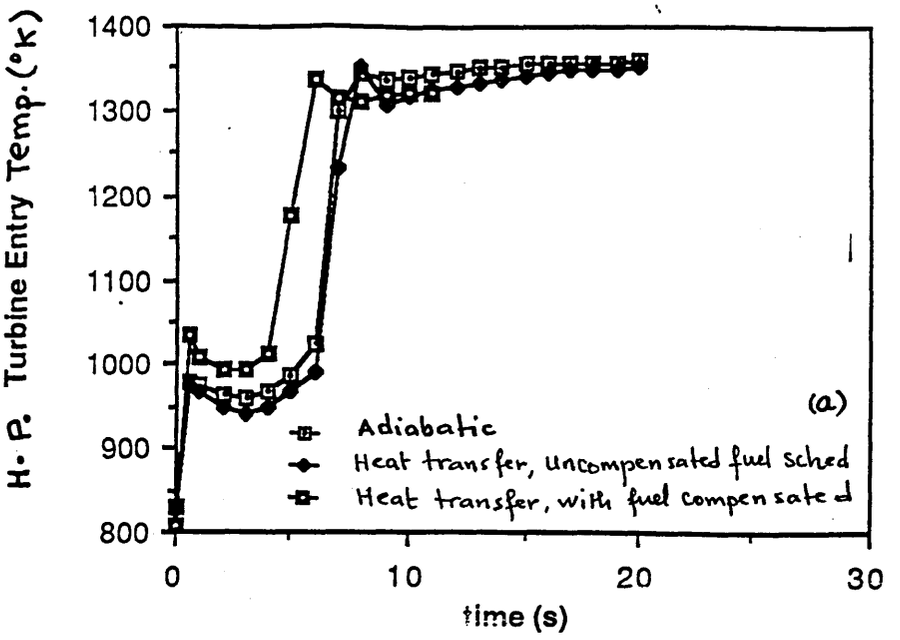

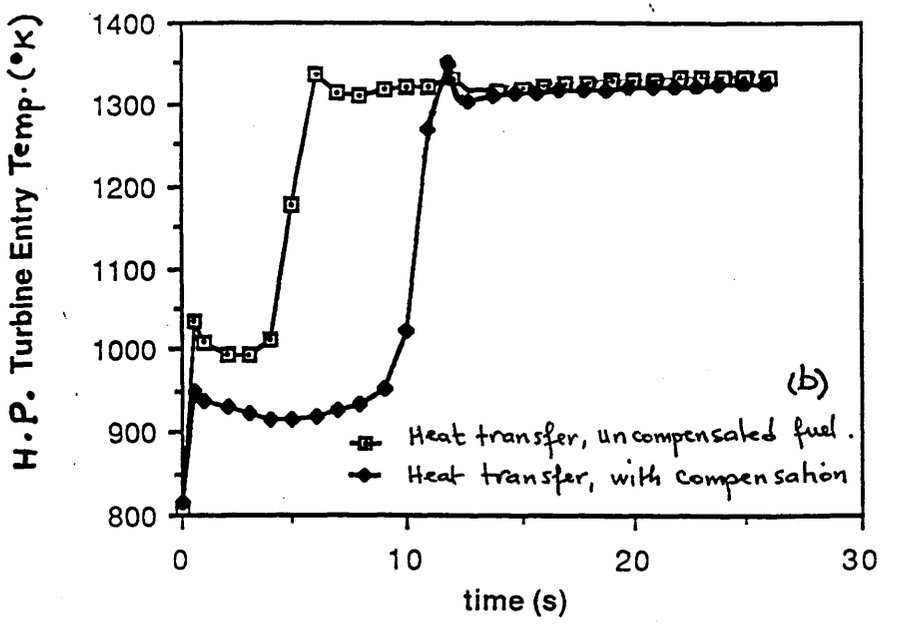

Fig.15 EFFECTS OF HEAT TRANSFER ON THE H.P.TURBINE ENTRY TEMPERATURE (T.E.T.) DURING ACCELERATION AT SEA-LEVEL, MACH 0.2

(a) COLD ACCELERATION

(b) HOT ACCELERATION

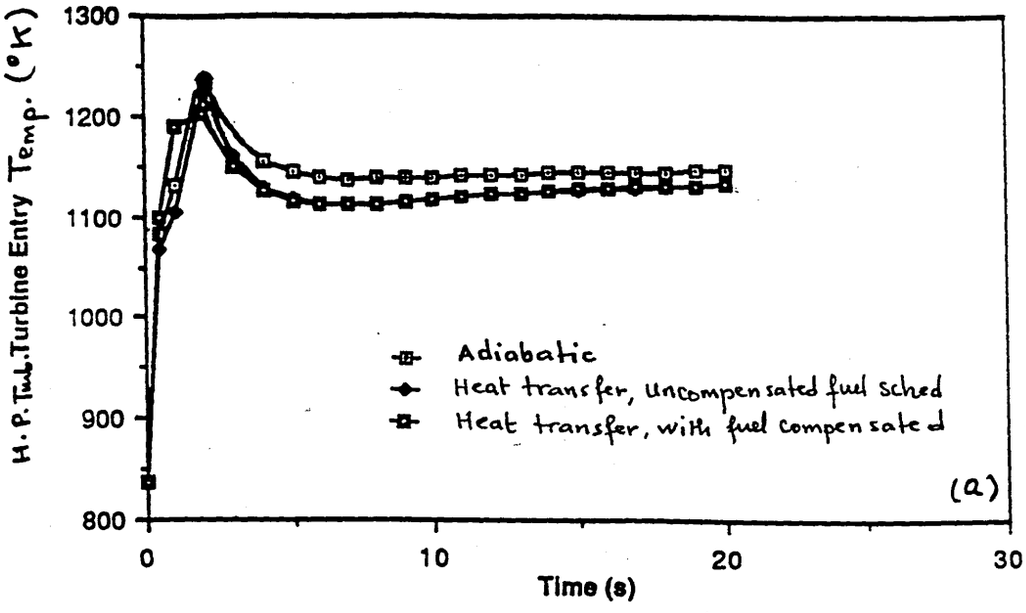

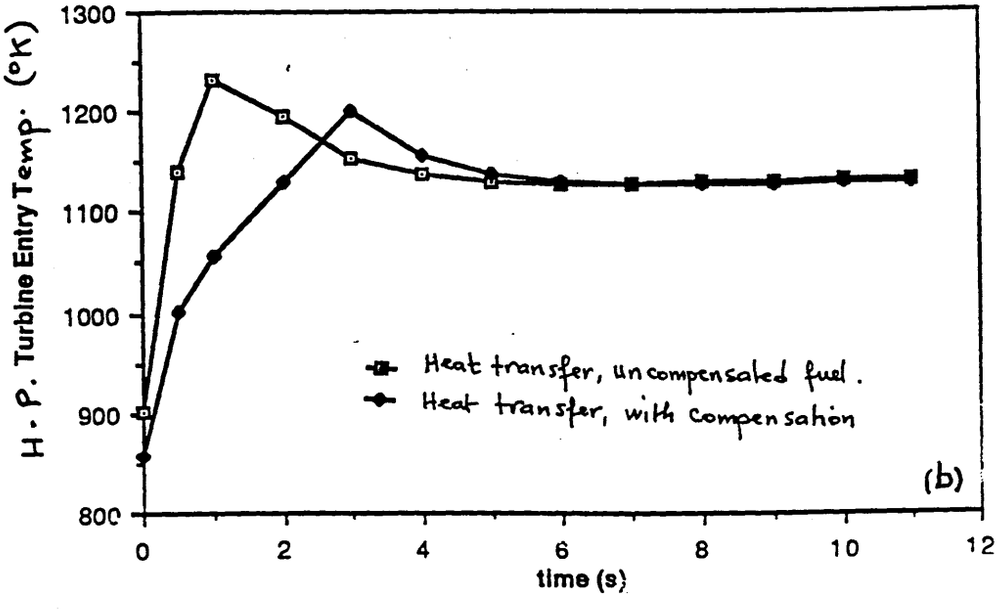

Fig.16 EFFECTS OF HEAT TRANSFER ON THE H.P.TURBINE ENTRY TEMPERATURE (T.E.T.) DURING ACCELERATION AT 41,000 FT ; MACH 0.8

(a) COLD ACCELERATION

(b) HOT ACCELERATION

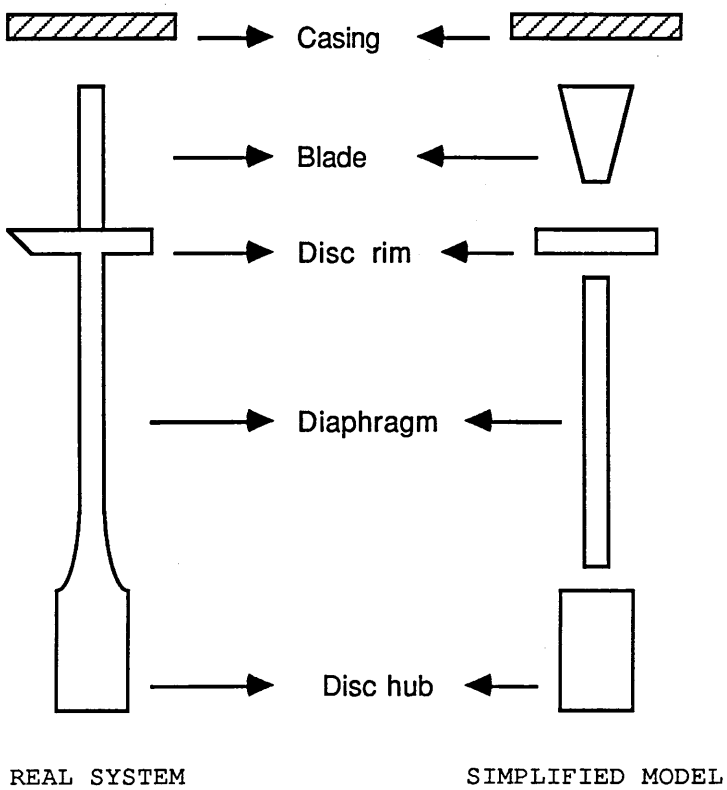

Fig. 17

SCHEMATIC OF MODEL REPRESENTING A TYPICAL STAGE.

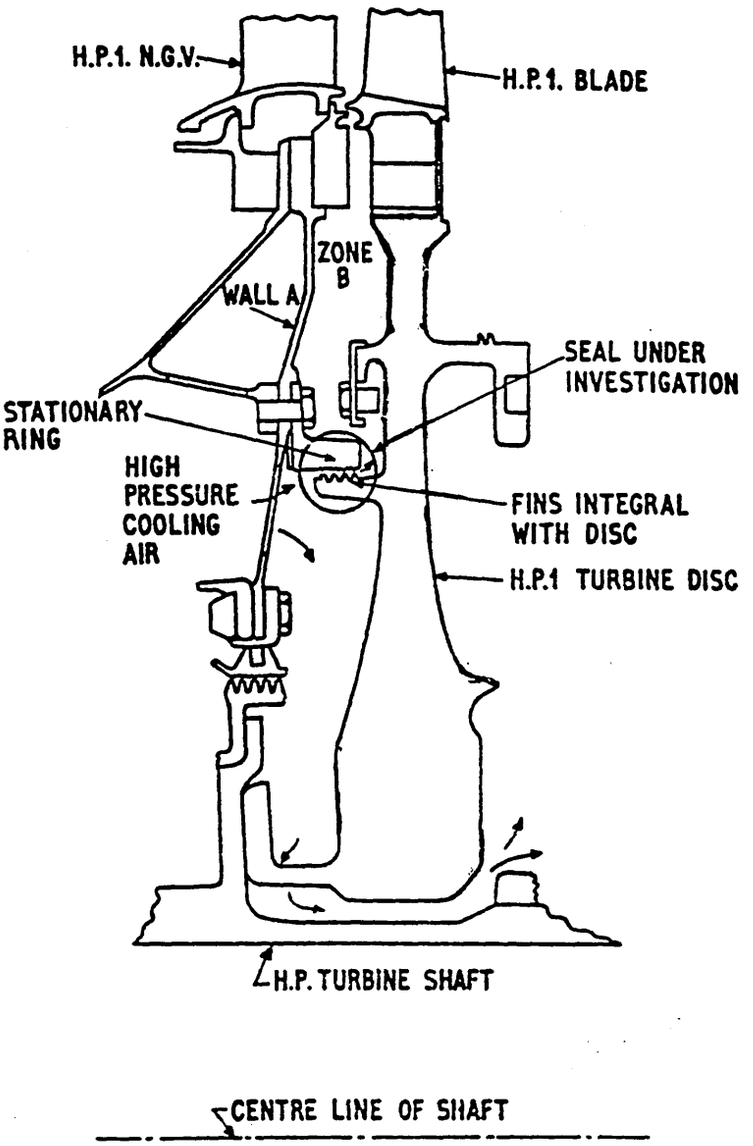

Fig. 18 Seal on H.P.1 turbine disc

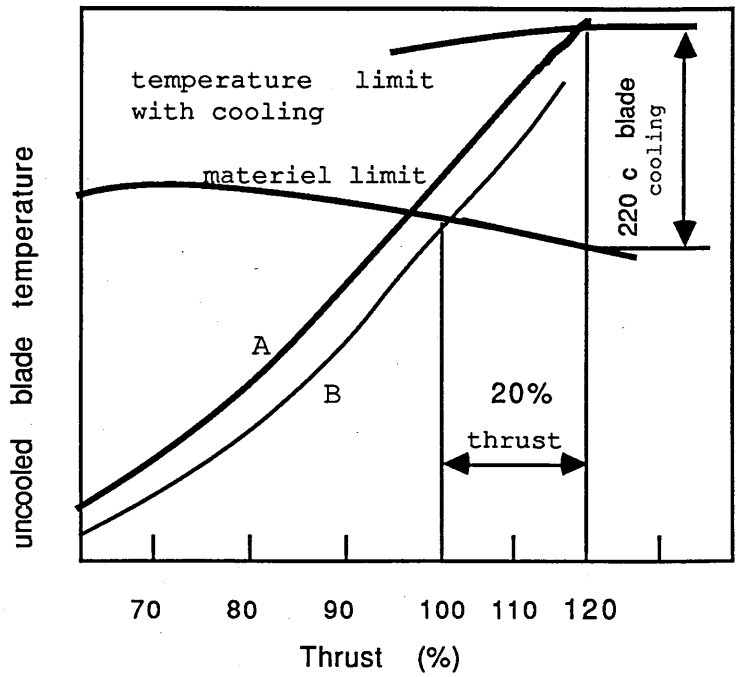

Fig. 19

EFFECT OF TURBINE BLADE COOLING
ON THRUST (TWO-SPOOL ENGINE)

A : with 2% cooling
air to blades.

B : wthout blade cooling.

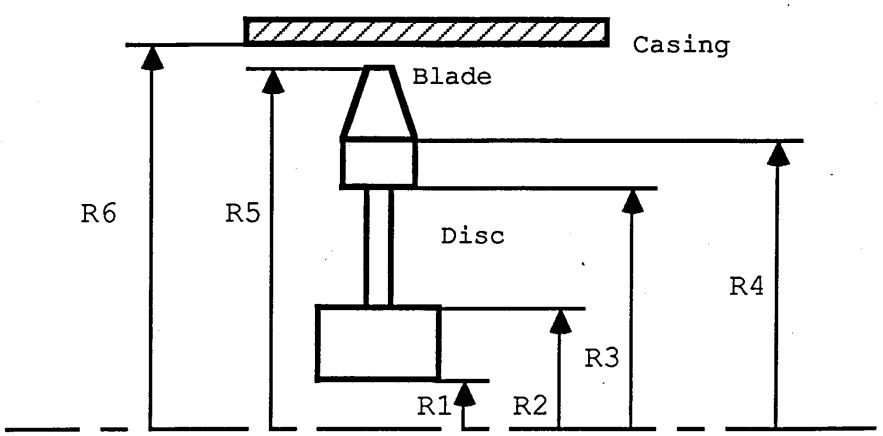

Fig. 20

RADIAL DIMENSIONS OF A TYPICAL TURBINE STAGE.

Fig. 21 PREDICTED ADIABATIC PATHS OF THE FAN SECTIONS DURING TRANSIENTS AT SEA LEVEL, MACH NUM=0.2

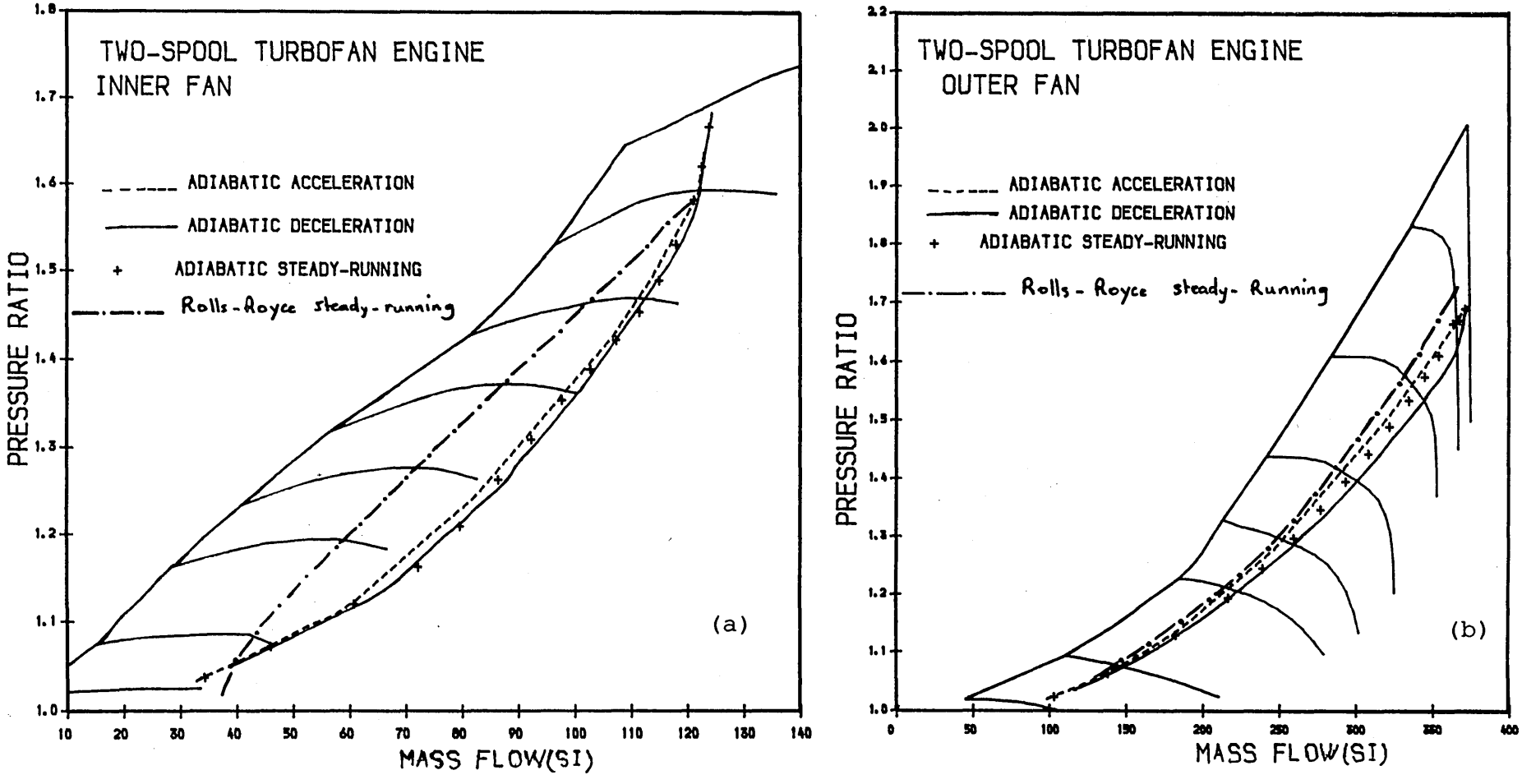

Fig. 22 PREDICTED ADIABATIC TRANSIENTS AT SEA LEVEL, MACH NUM=0.2

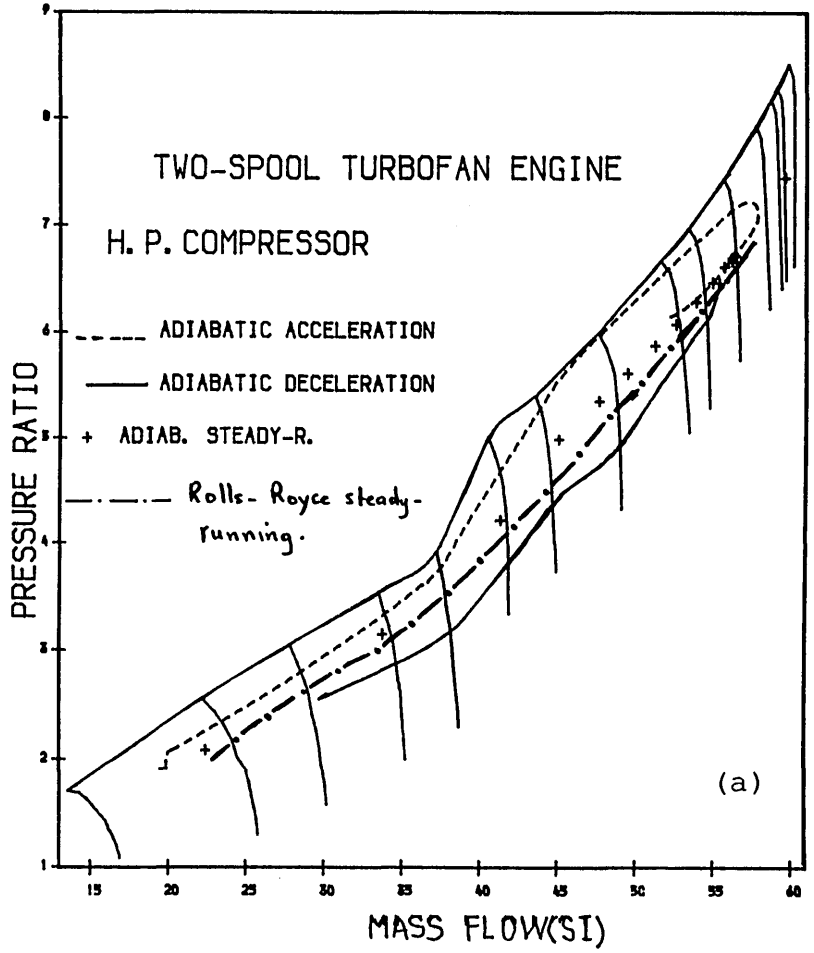

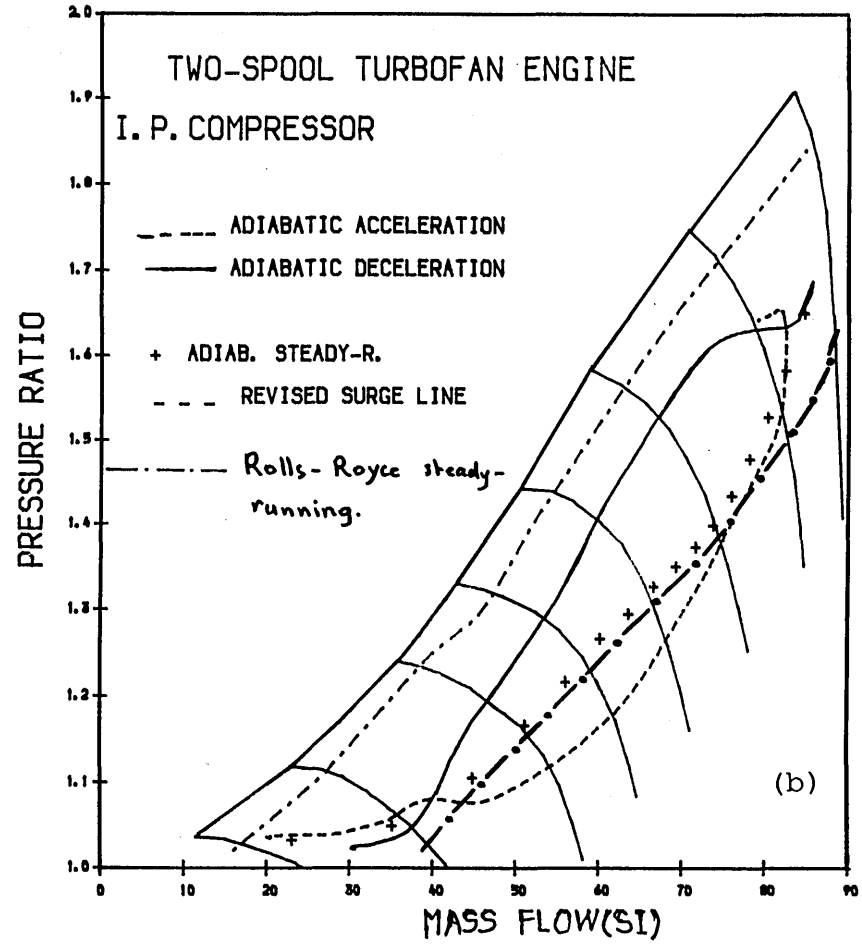

Fig. 23 PREDICTED ADIABATIC PATHS OF THE FAN SECTIONS DURING TRANSIENTS AT 41,000 FT, MACH NUM=0.8

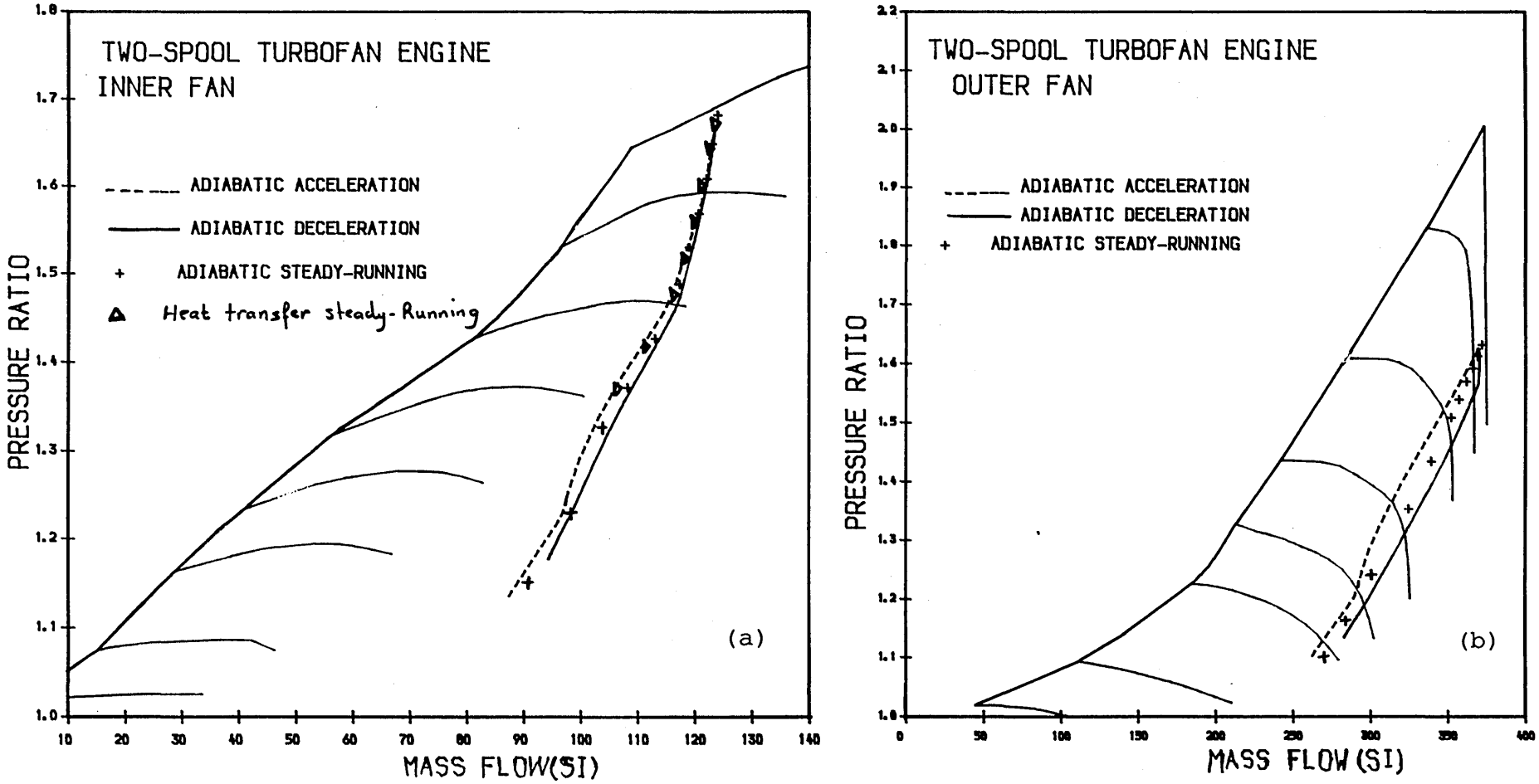

Fig. 24 PREDICTED ADIABATIC TRANSIENTS AT 41,000 FT, MACH NUM=0.8

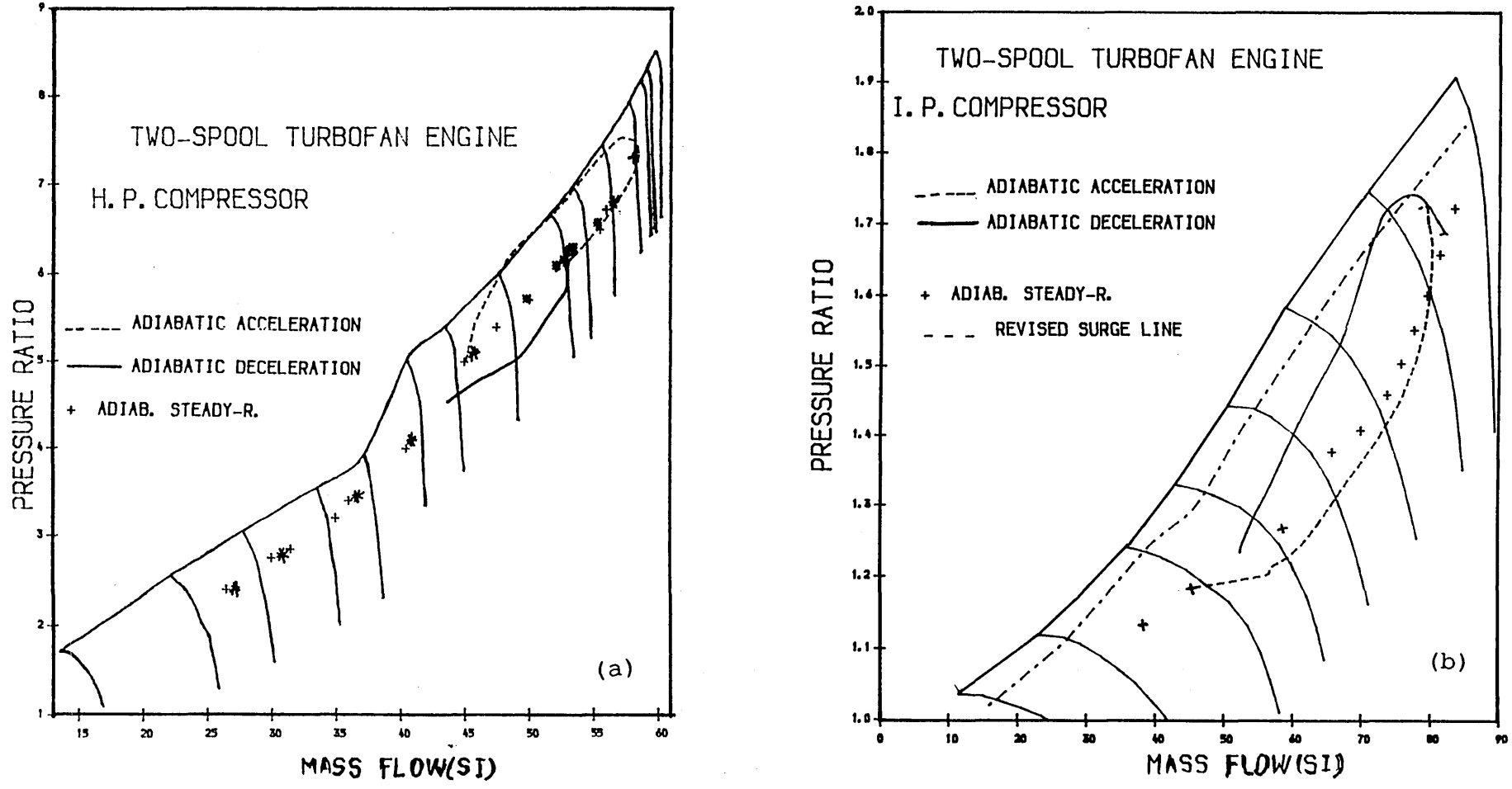

Fig. 25 PREDICTED ADIABATIC PATHS OF THE FAN SECTIONS DURING TRANSIENTS AT 50,000 FT, MACH NUM=0.8

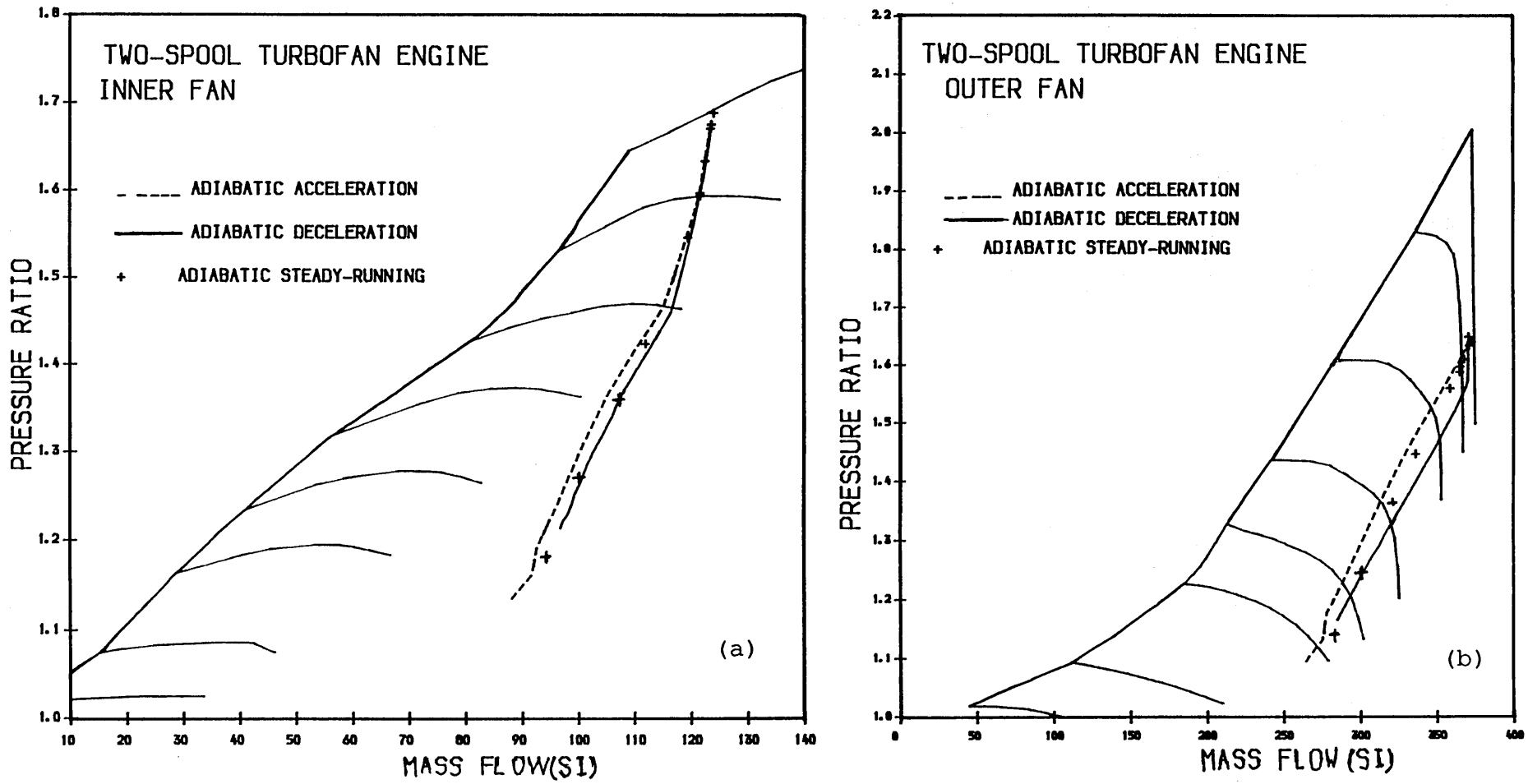

Fig. 26 PREDICTED ADIABATIC TRANSIENTS AT
50,000 FT, MACH NUM=0.8

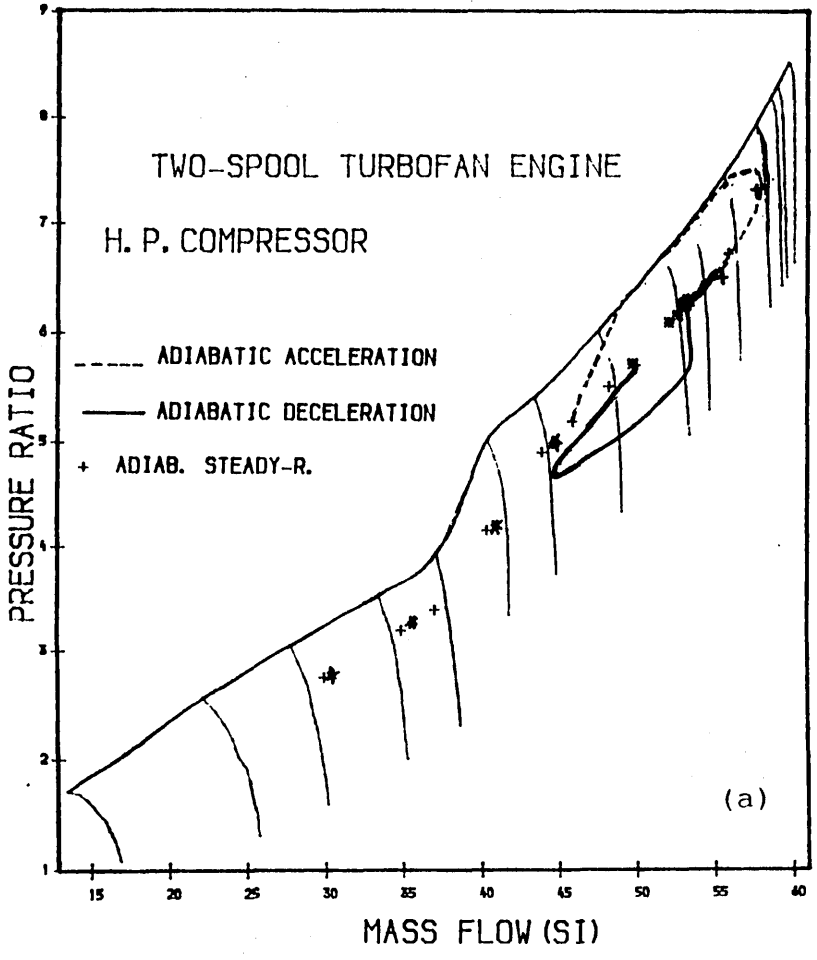

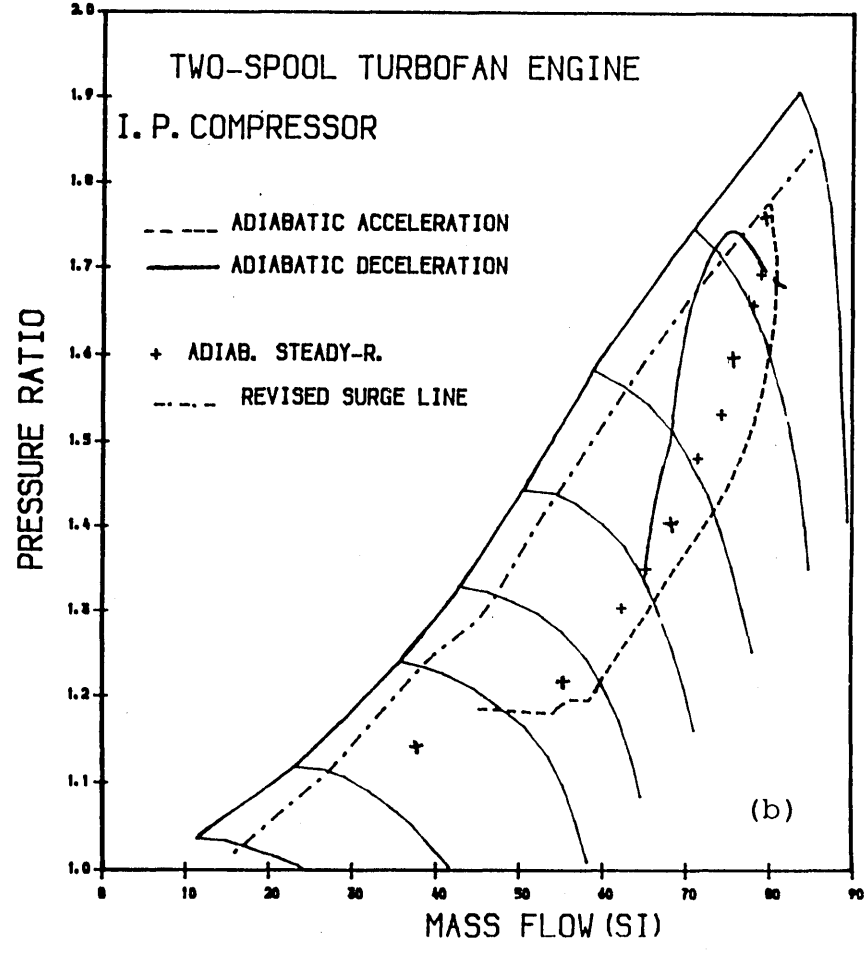

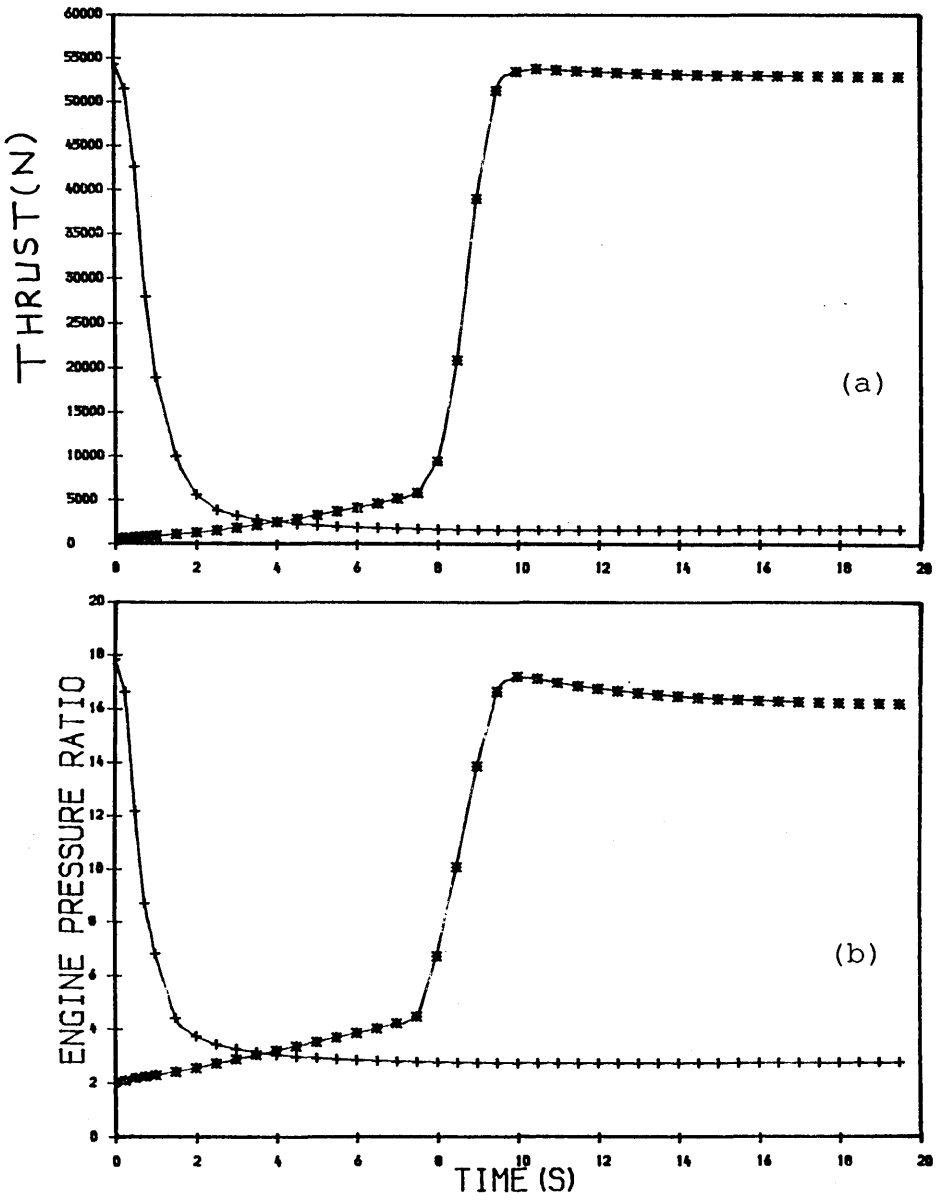

Fig. 27 PREDICTED ADIABATIC TRANSIENTS AT SEA LEVEL, MACH NUM=0.2

* ADIABATIC ACCELERATION

+ ADIABATIC DECELERATION

Fig. 28 PREDICTED ADIABATIC TRANSIENTS AT SEA LEVEL, MACH NUM=0.2

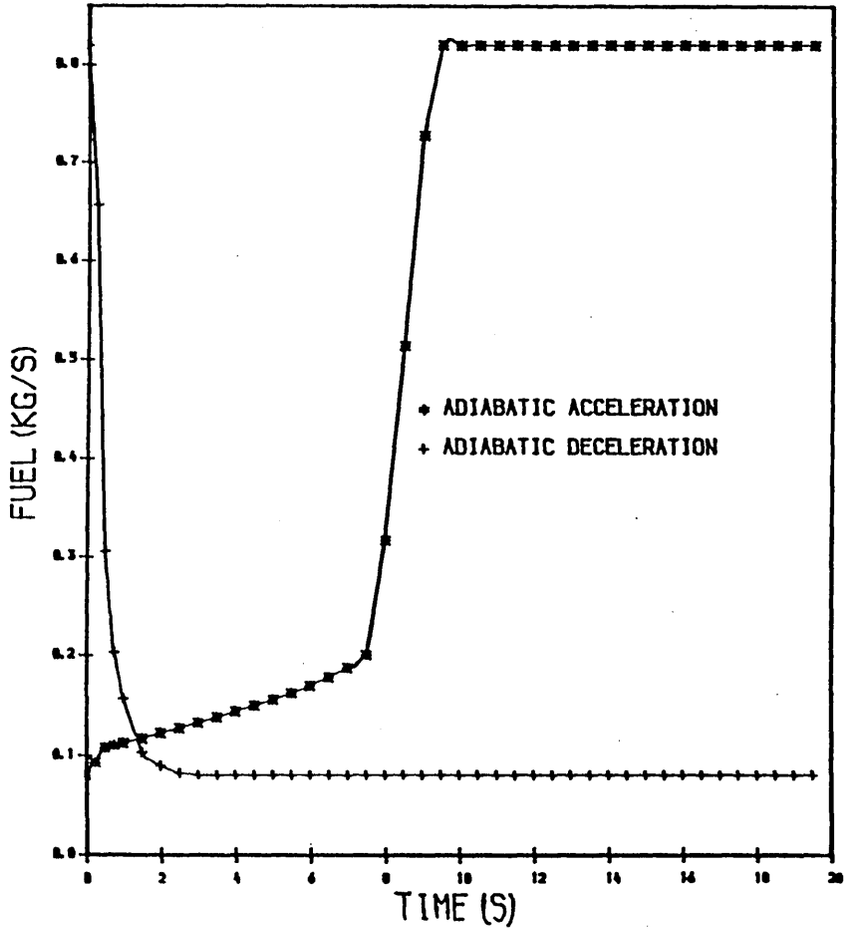

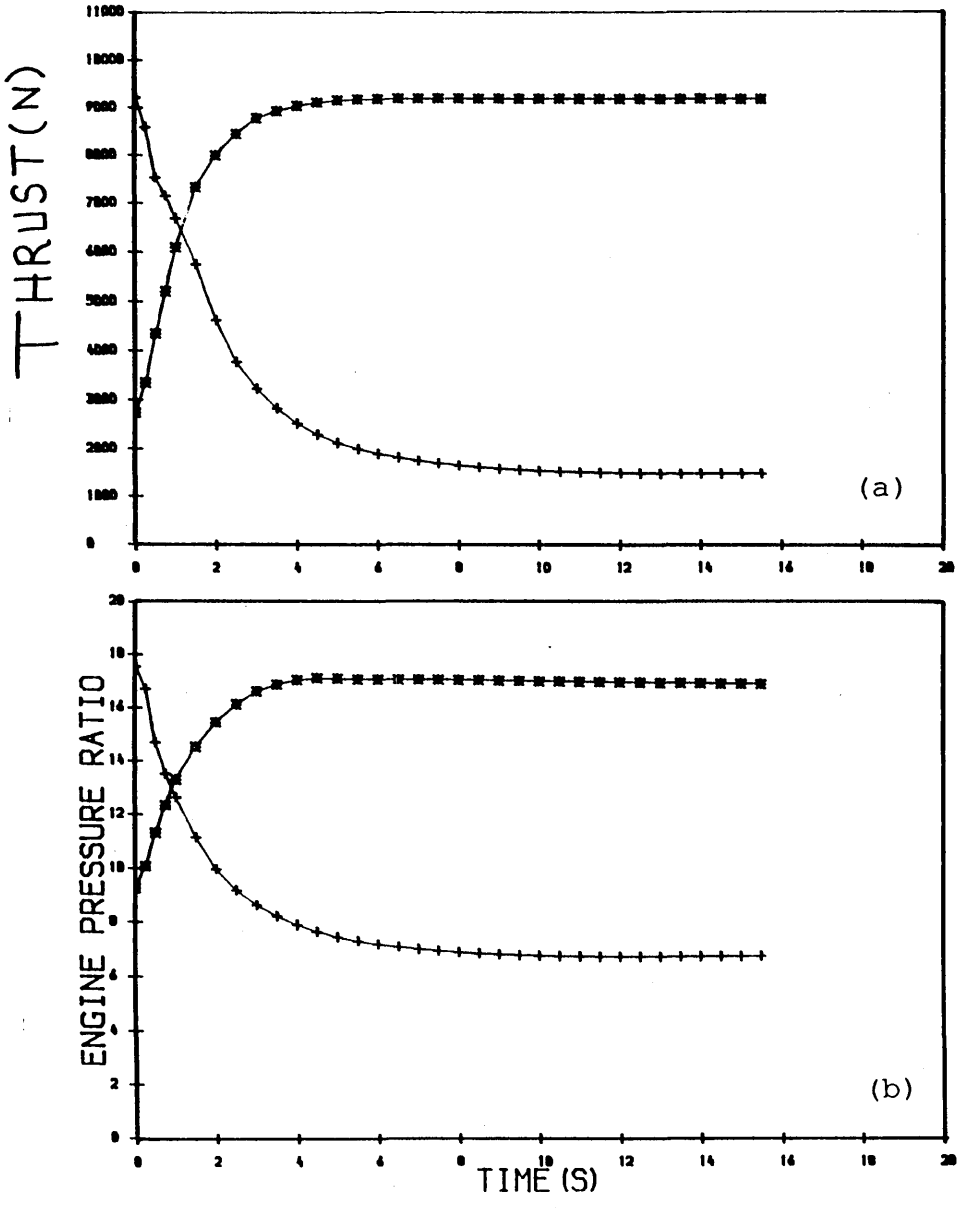

Fig. 29 PREDICTED ADIABATIC TRANSIENTS AT 41,000 FT, MACH NUM=0.8

* ADIABATIC ACCELERATION
+ ADIABATIC DECELERATION

Fig. 30 PREDICTED ADIABATIC TRANSIENTS AT 41,000 FT, MACH NUM=0.8

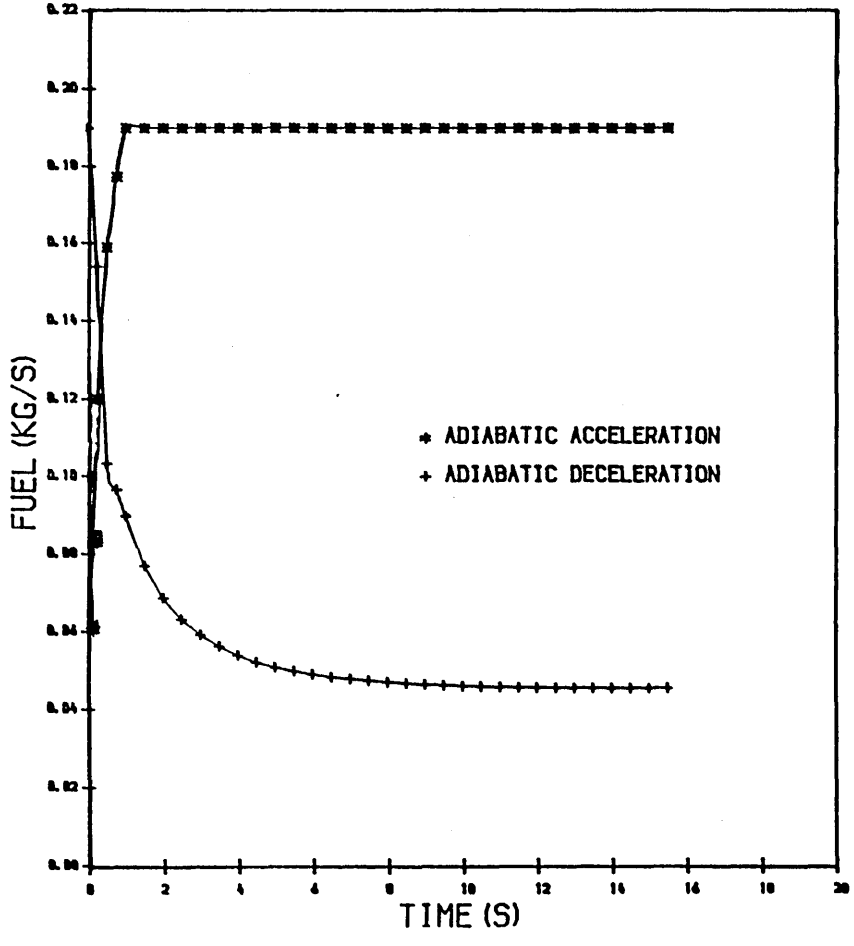

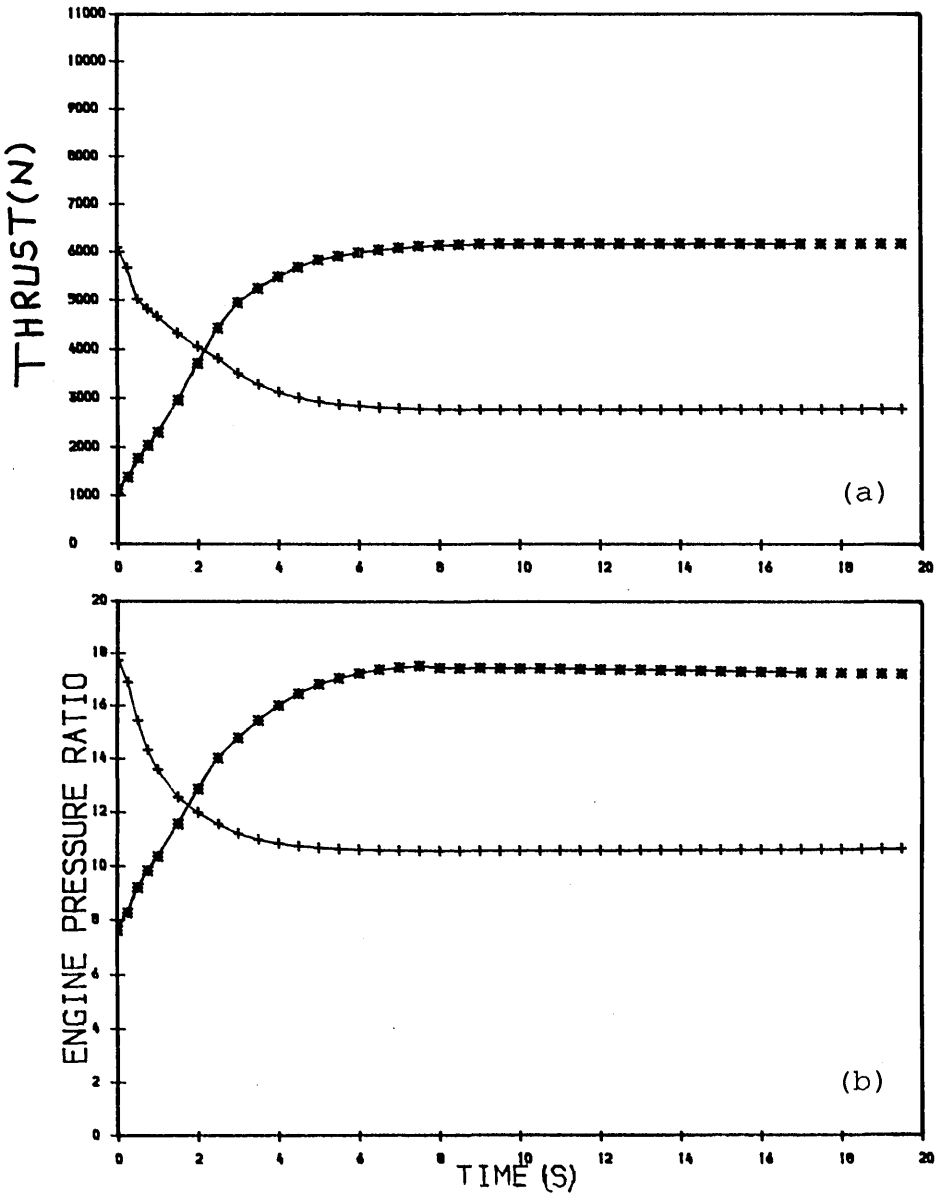

Fig. 31 PREDICTED ADIABATIC TRANSIENTS AT 50,000 FT, MACH NUM=0.8

* ADIABATIC ACCELERATION
+ ADIABATIC DECELERATION

Fig. 32 PREDICTED ADIABATIC TRANSIENTS AT 50,000 FT, MACH NUM=0.8

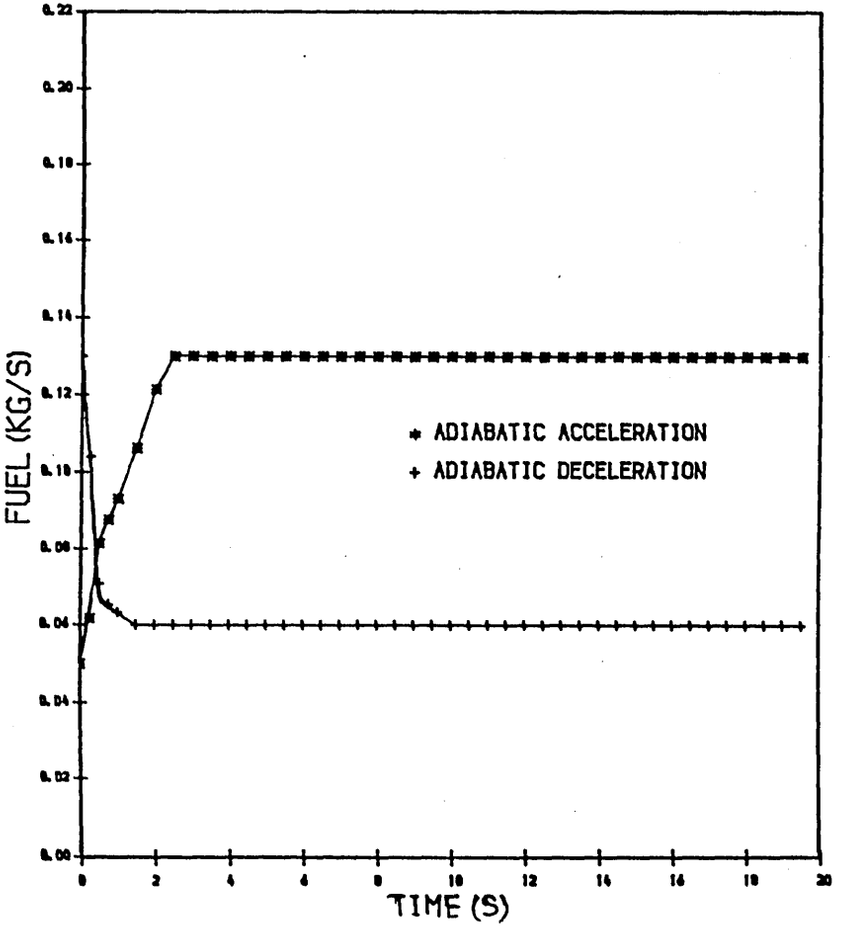

Fig. 33 PREDICTED PATHS OF THE FAN SECTIONS
DURING TRANSIENT ACCEL. AT SEA LEVEL
MACH NUM=0.2

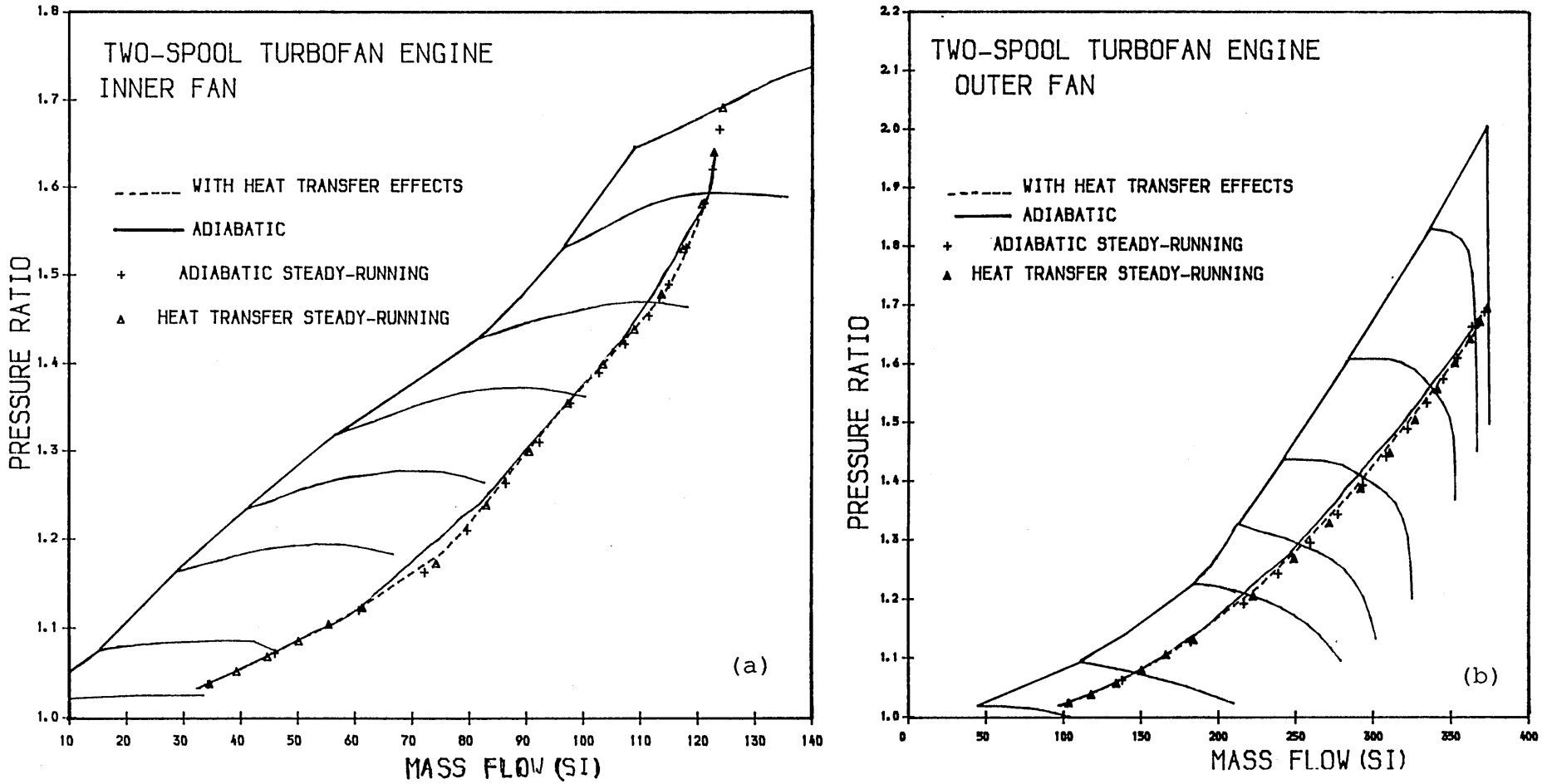

Fig. 34 PREDICTED ACC. AT SEA LEVEL
MACH NUM=0.2.

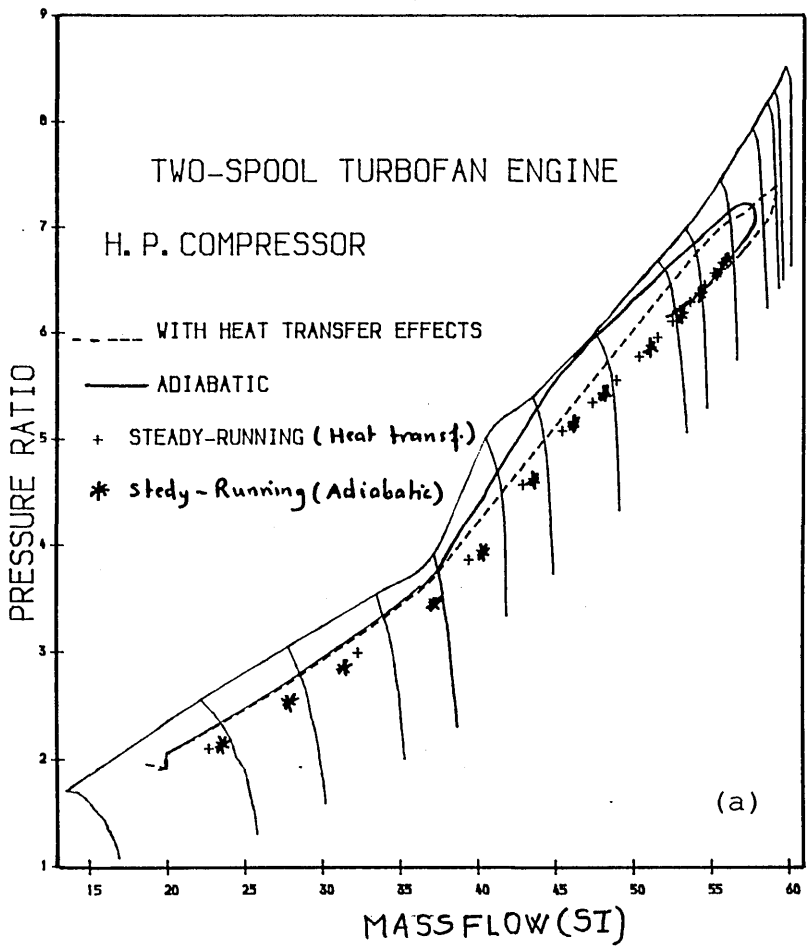

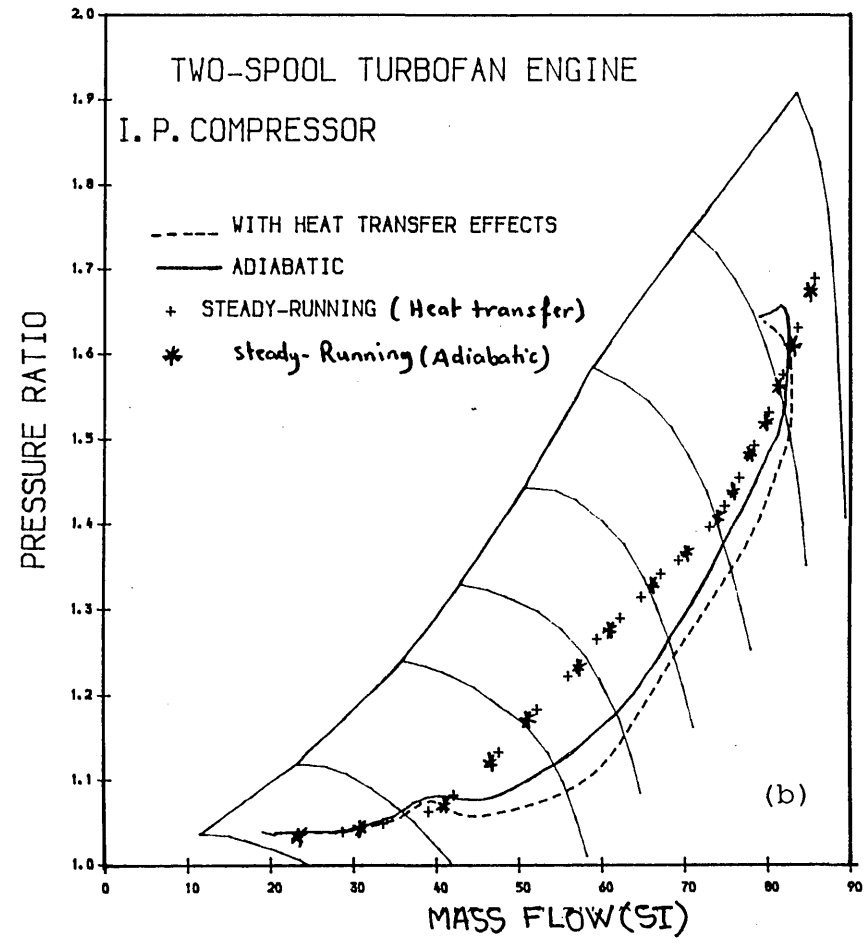

Fig. 35 PREDICTED PATHS OF THE FAN SECTIONS
DURING TRANSIENT ACCEL. AT 41,000 ft
MACH NUM=0.8

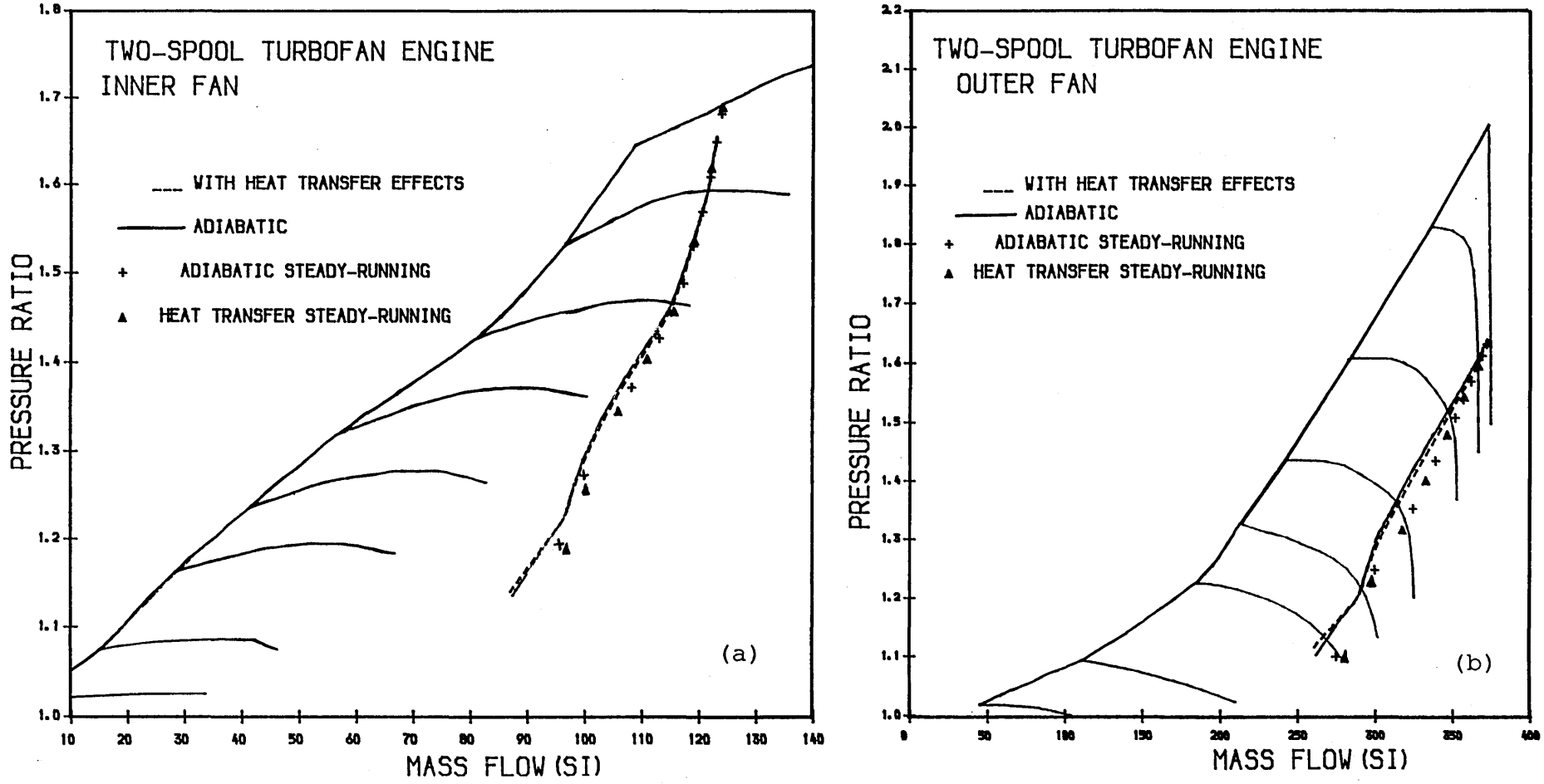

Fig. 36 PREDICTED ACCELERATION AT 41,000 FT
MACH NUM=0.8

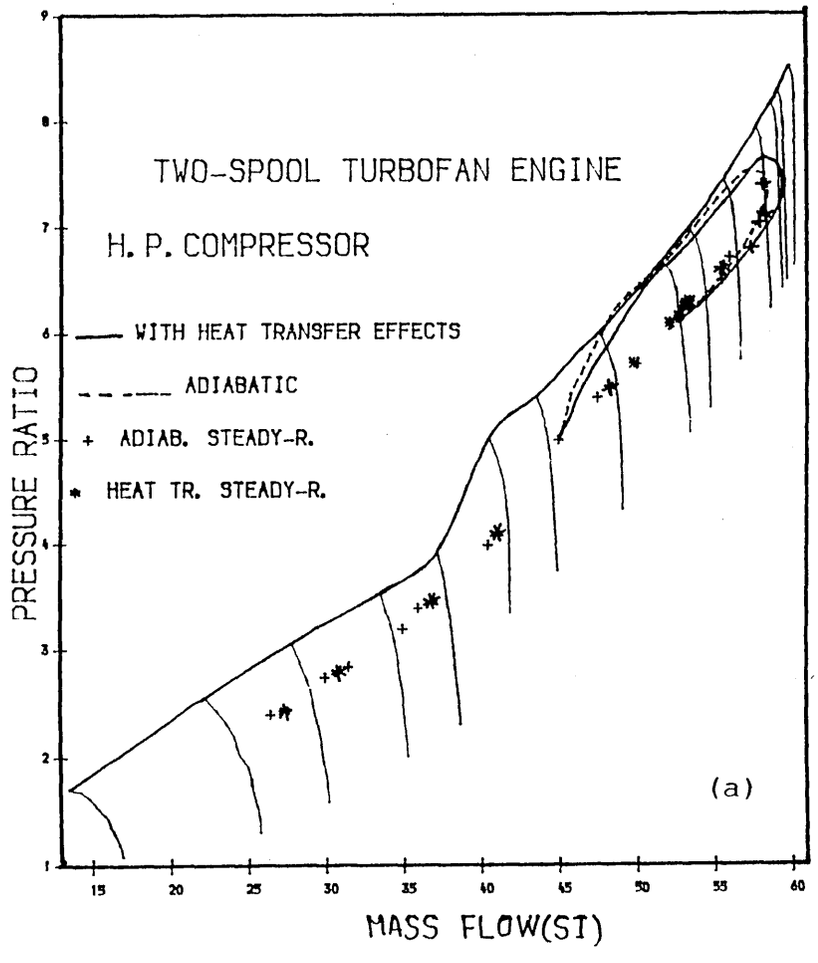

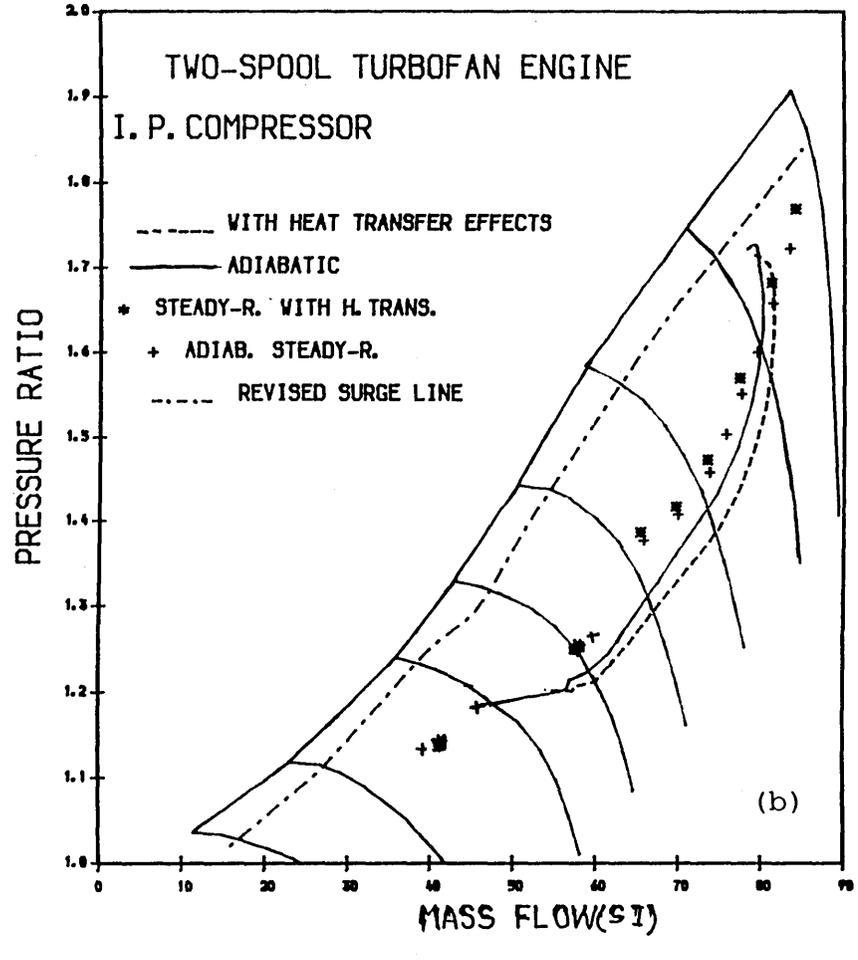

Fig. 37 PREDICTED PATHS OF THE FAN SECTIONS
DURING TRANSIENT ACCEL. AT 50,000 ft
MACH NUM=0.8

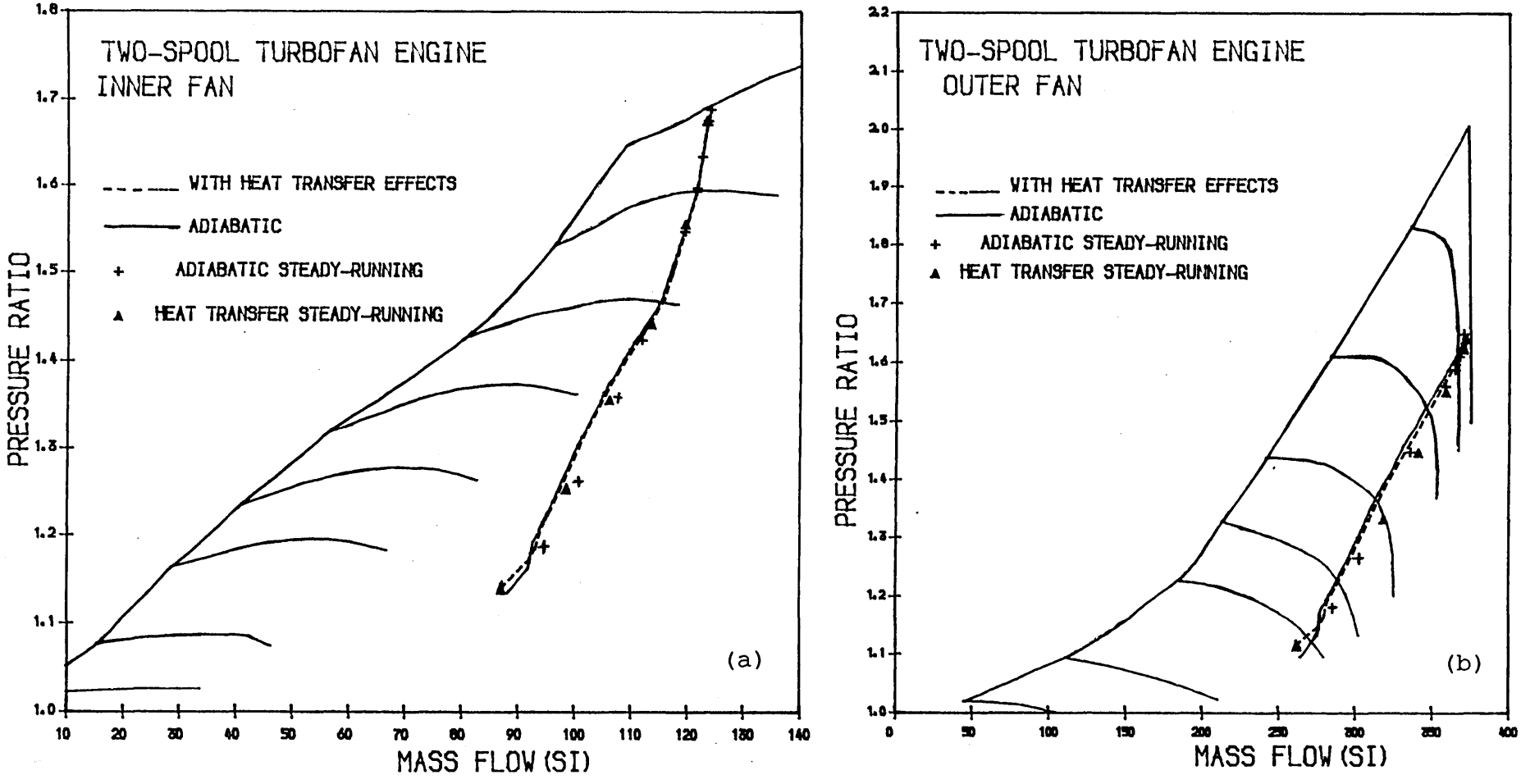

Fig. 38 PREDICTED ACCELERATION AT 50,000 FT
MACH NUM=0.8

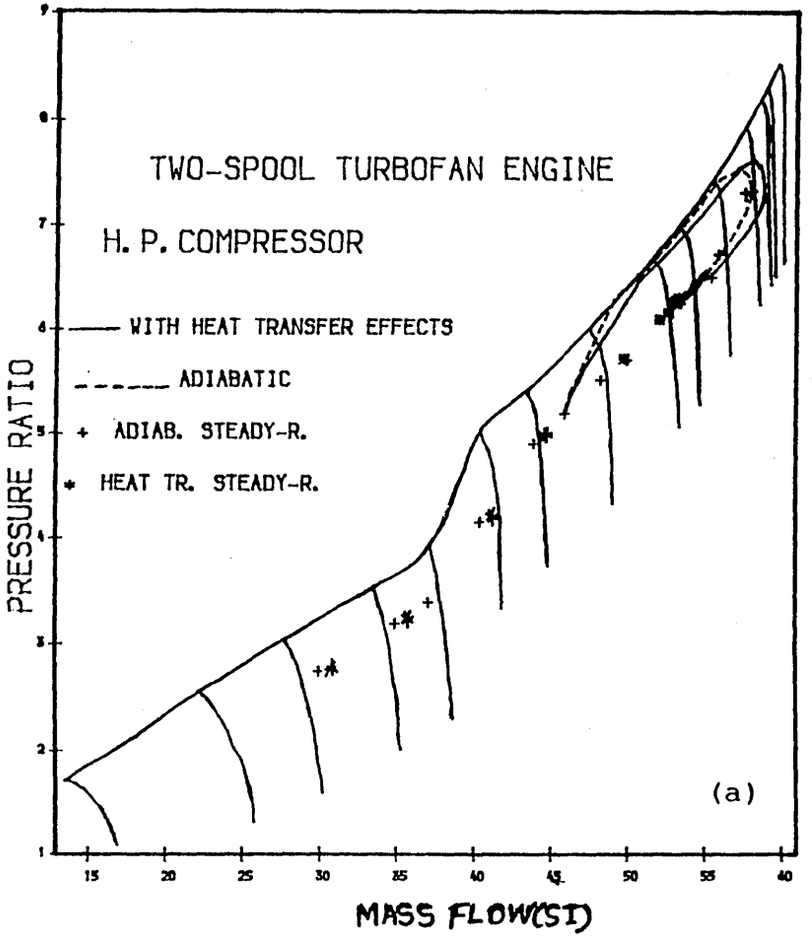

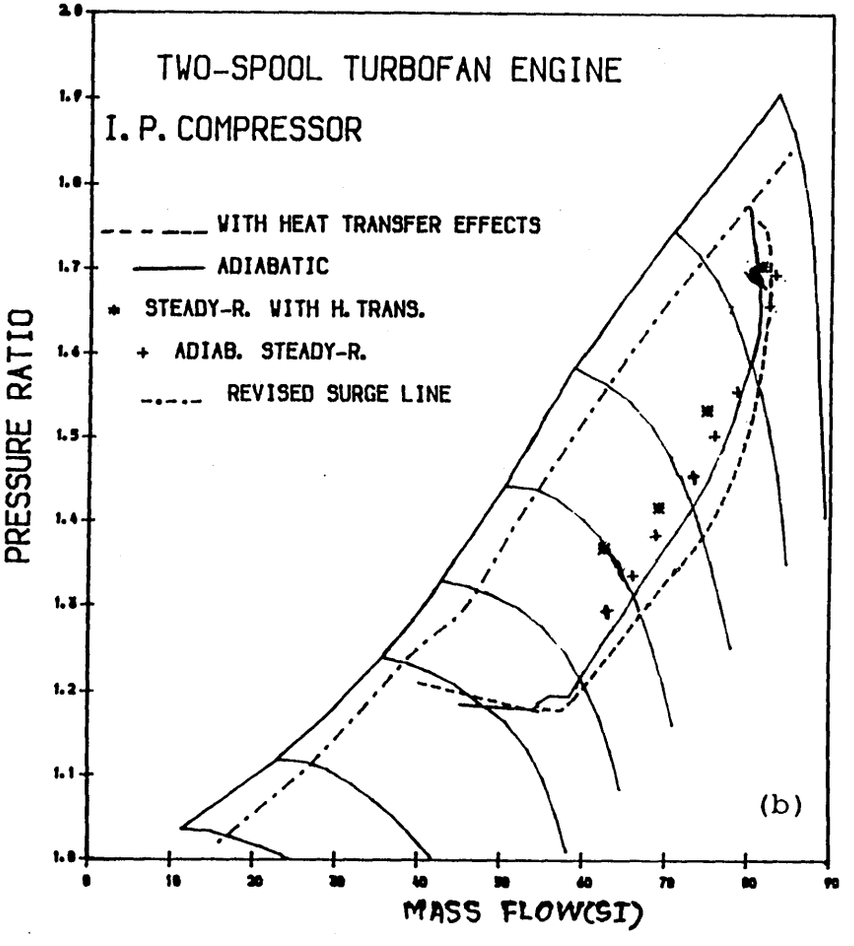

Fig. 39 PREDICTED PATHS OF THE FAN SECTIONS
DURING TRANSIENT DECE. AT SEA LEVEL
MACH NUM=0.2

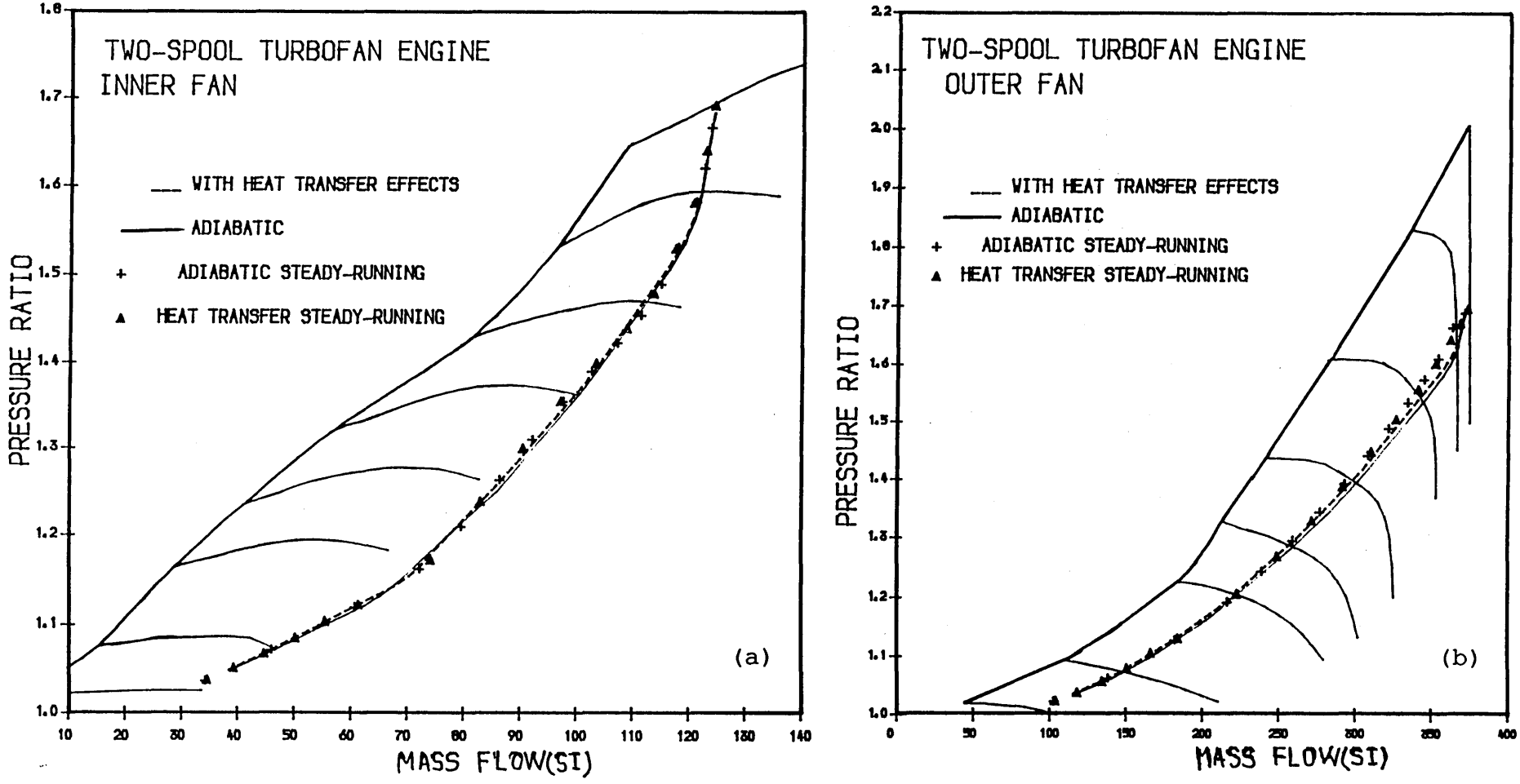

Fig. 40 PREDICTED DECELERATION AT SEA LEVEL
MACH NUM=0.2.

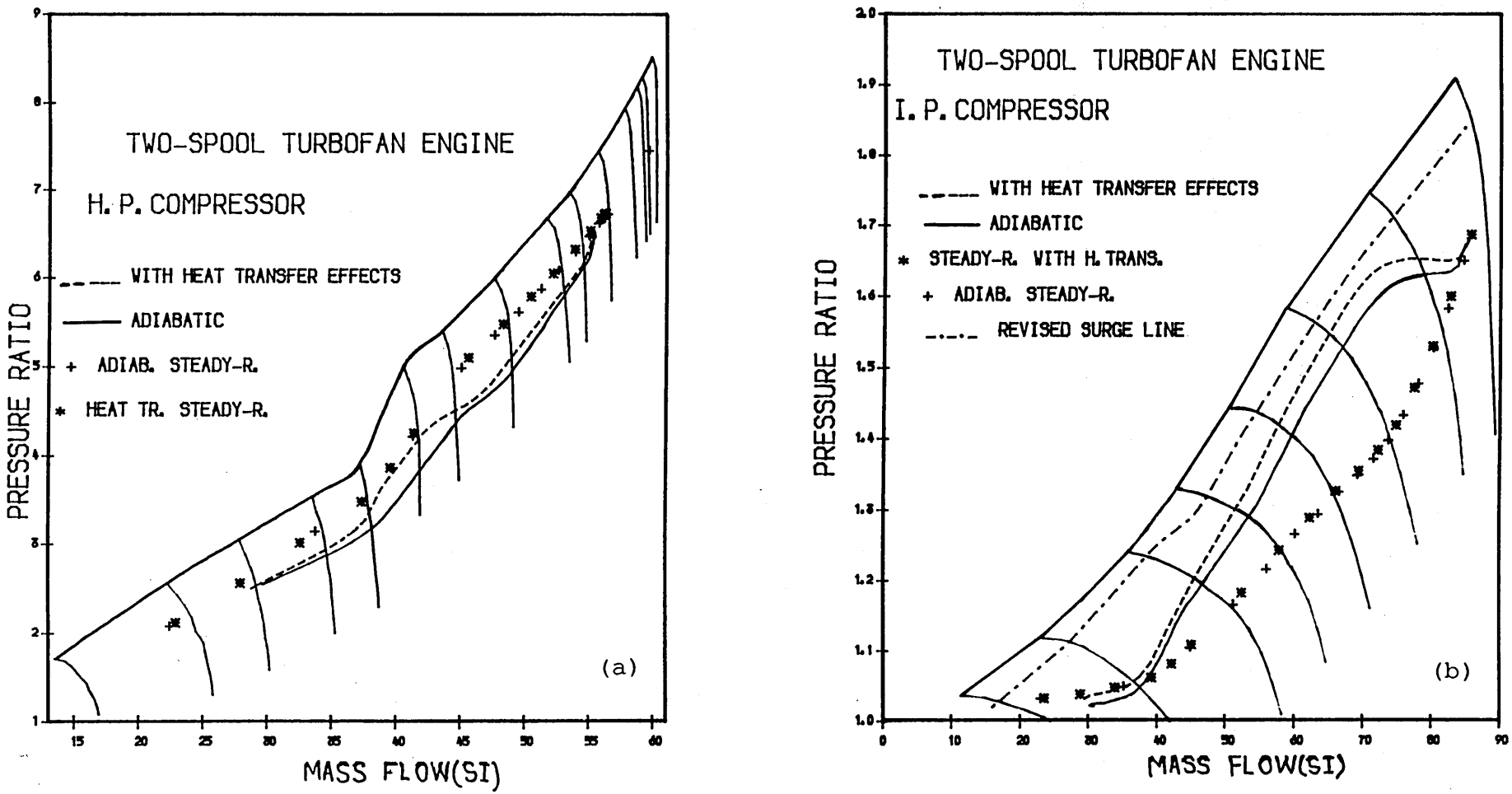

Fig. 41 PREDICTED PATHS OF THE FAN SECTIONS
DURING TRANSIENT DECE. AT 41,000 ft
MACH NUM=0.8

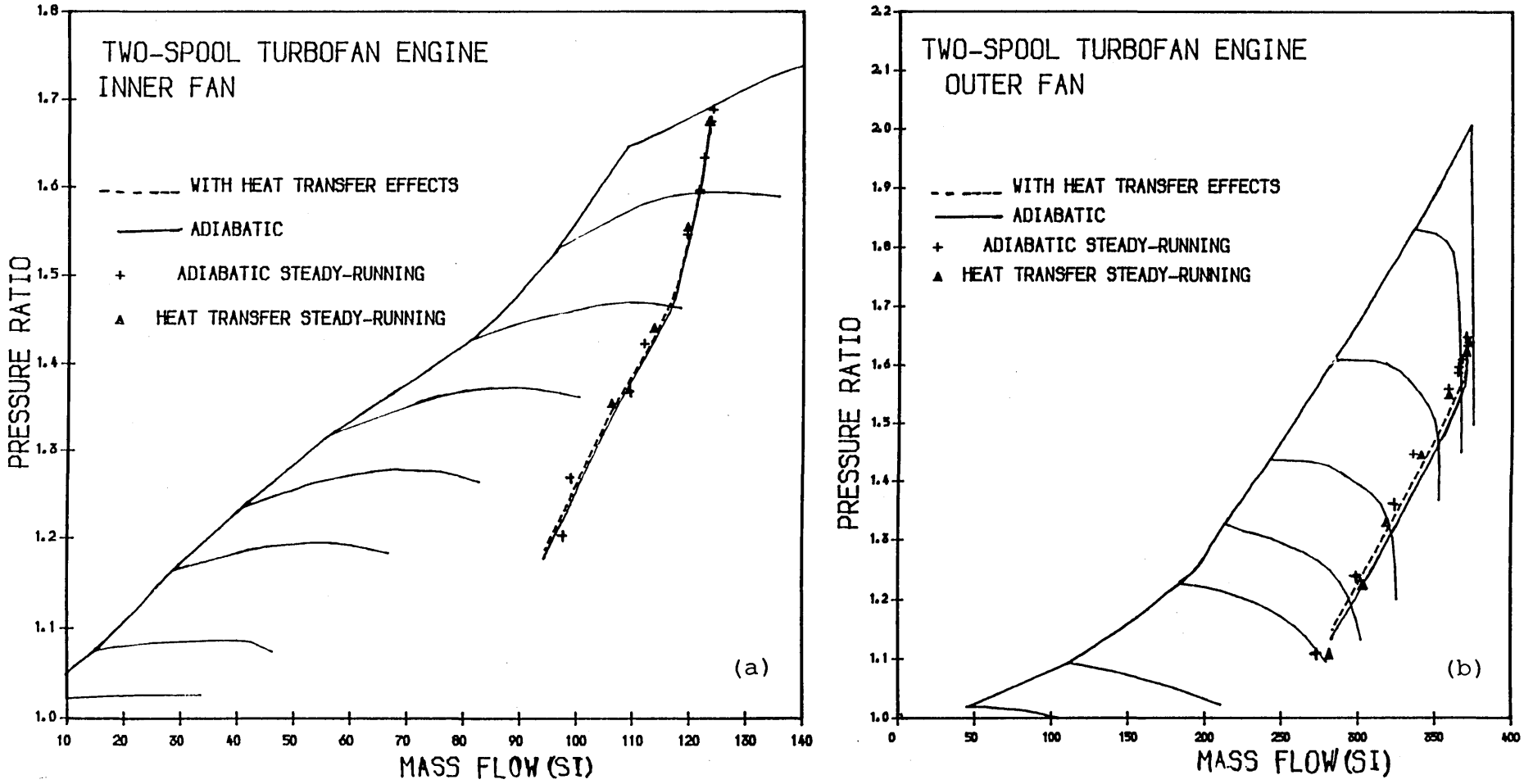

Fig. 42 PREDICTED DECELERATION AT 41,000 FT
MACH NUM=0.8.

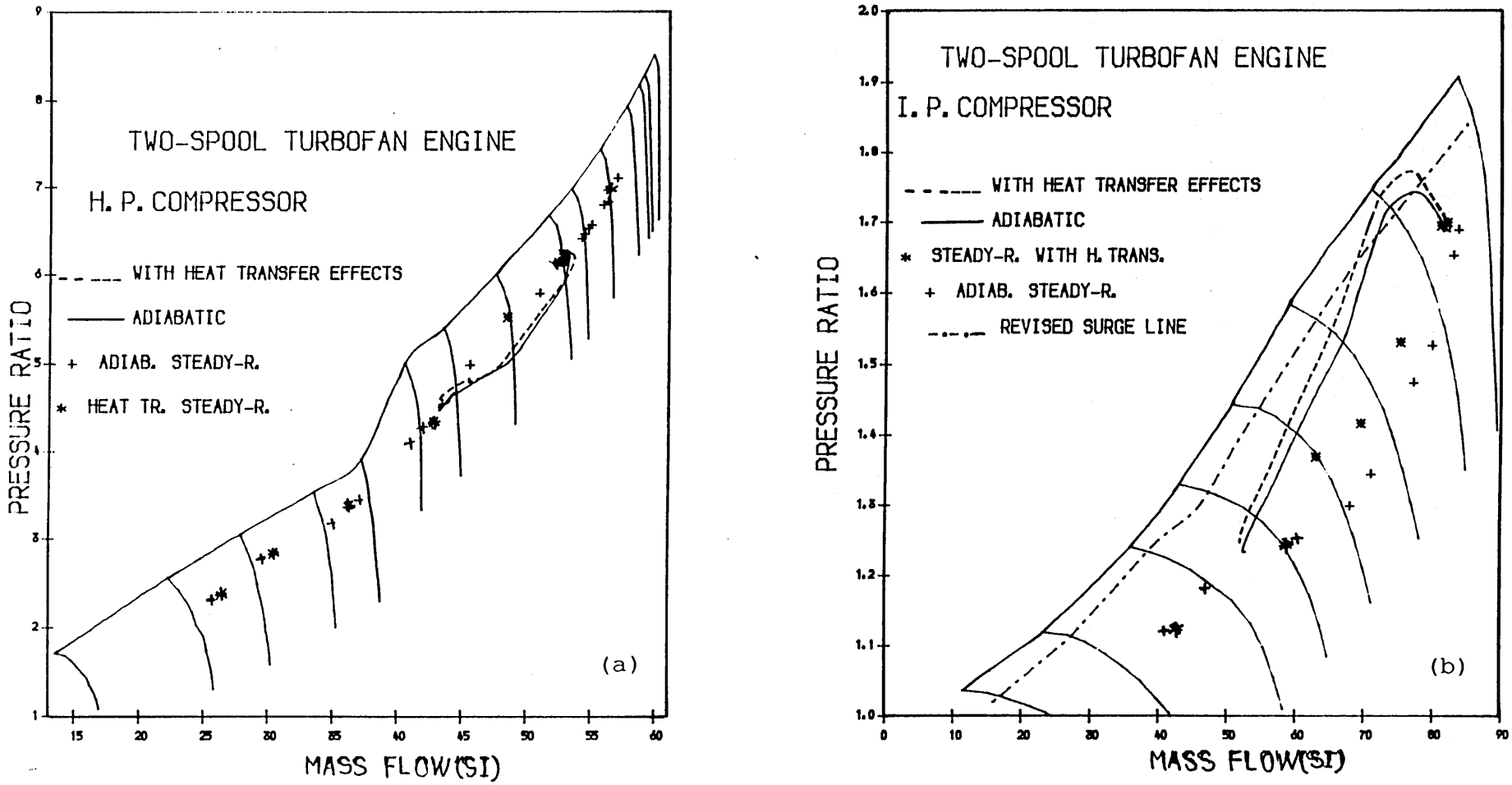

Fig. 43 PREDICTED PATHS OF THE FAN SECTIONS
DURING TRANSIENT DECE. AT 50,000 ft
MACH NUM=0.8

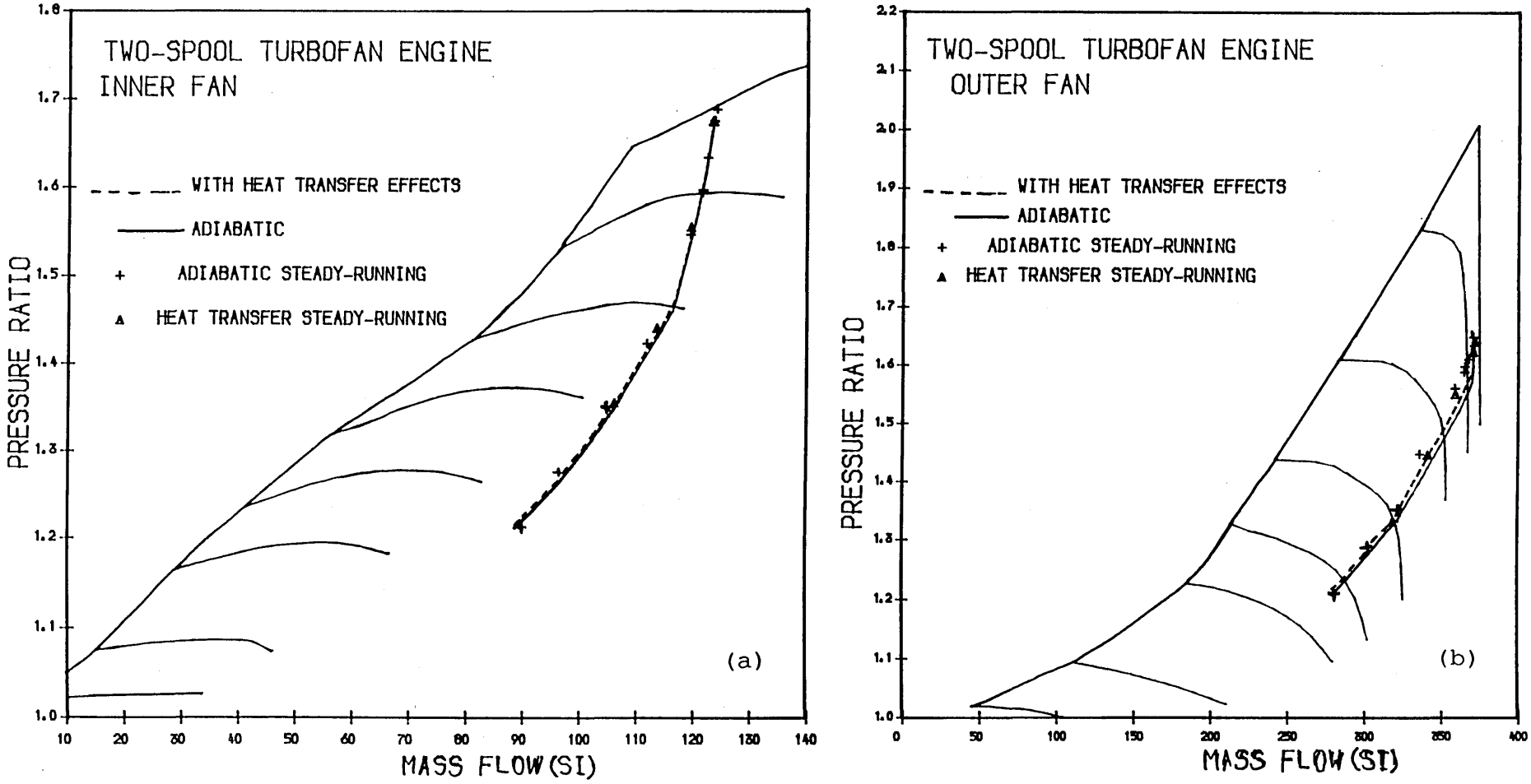

Fig. 44 PREDICTED DECELERATION AT 50,000 FT
MACH NUM=0.8.

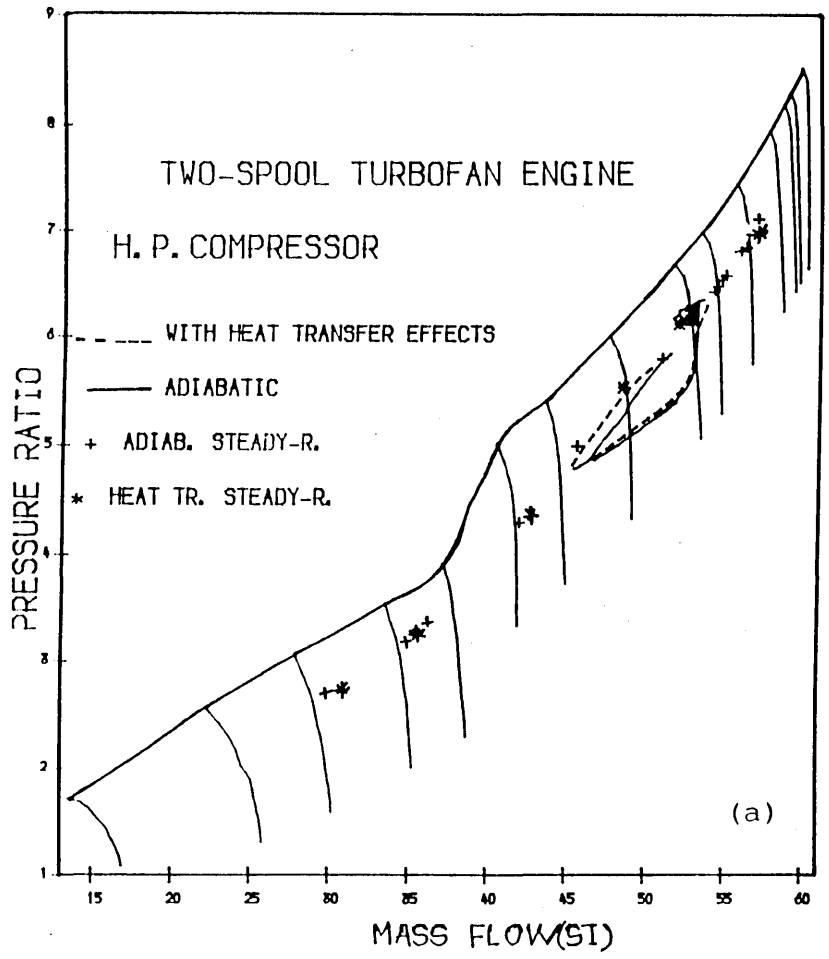

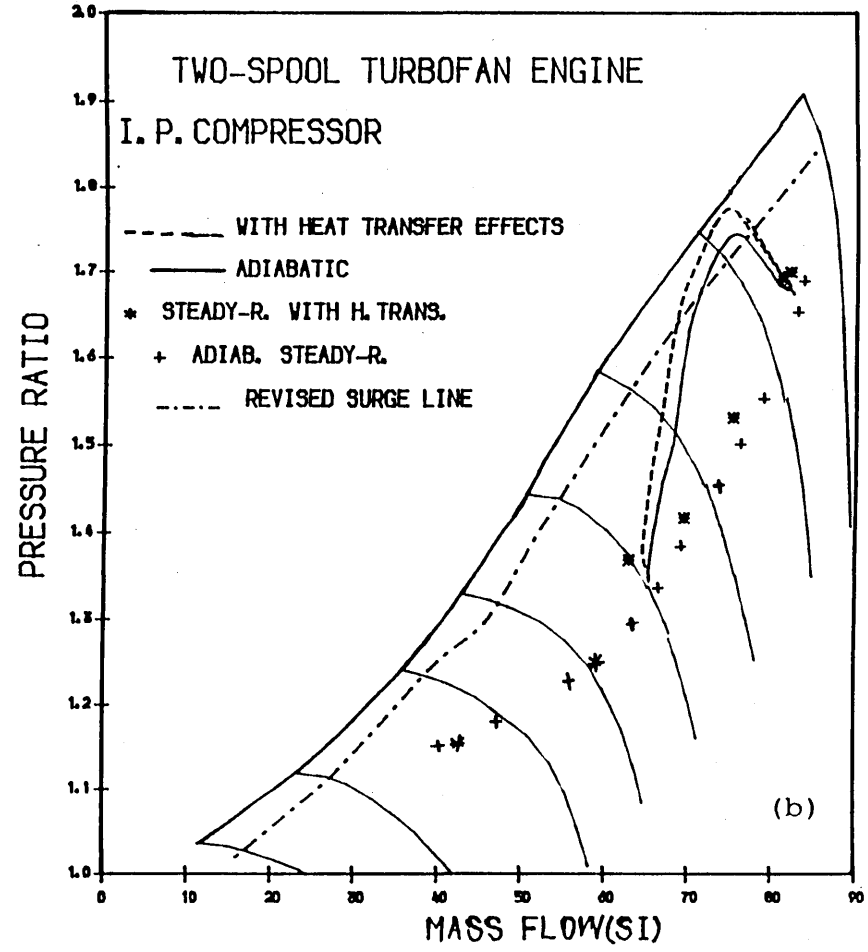

Fig. 45 PREDICTED PATHS OF THE H. P. COMP.
DURING HOT ACC. AT SEA LEVEL

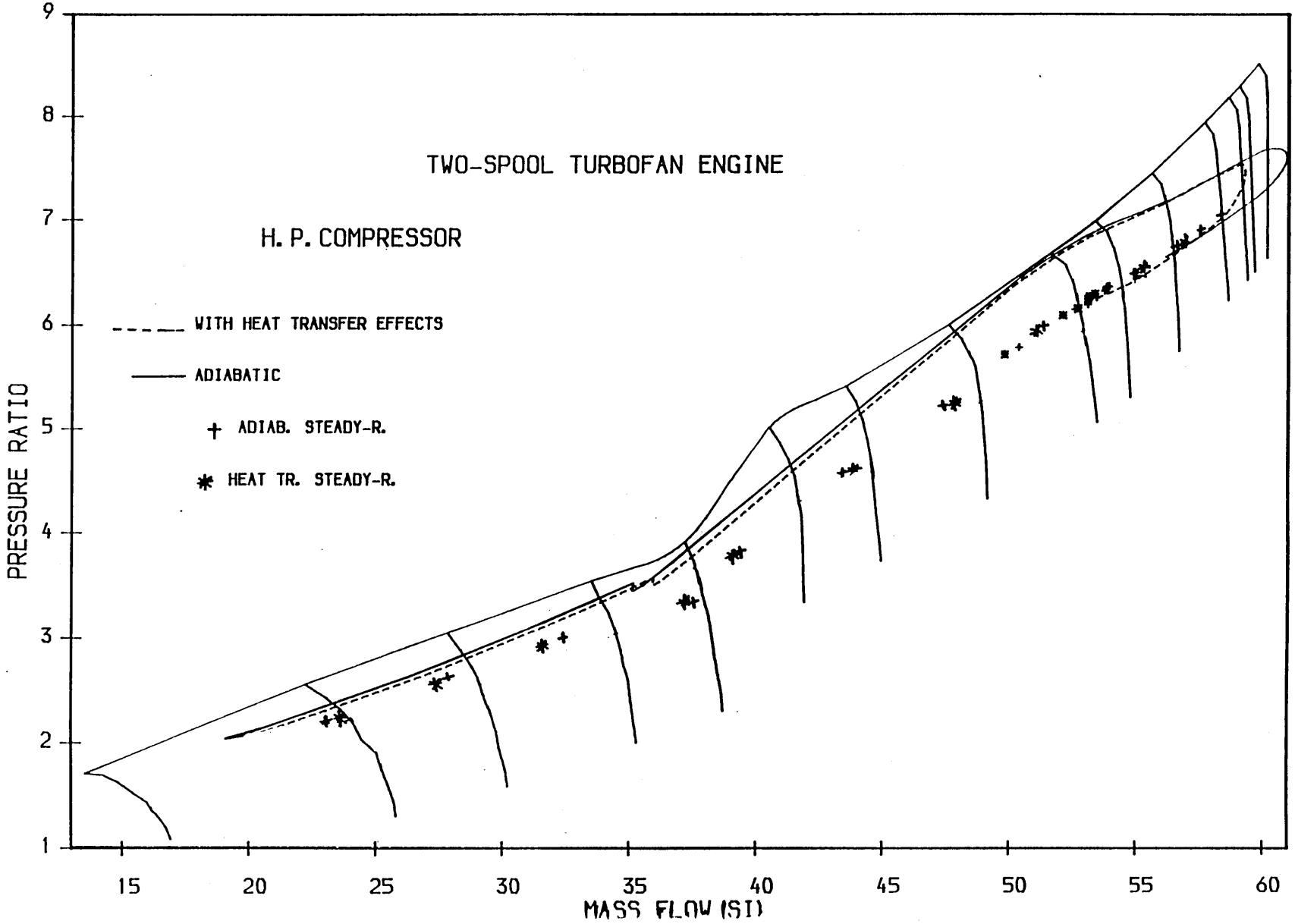

Fig. 46 PREDICTED PATHS OF THE H.P.COMP.
DURING HOT ACC. AT 41,000 FT

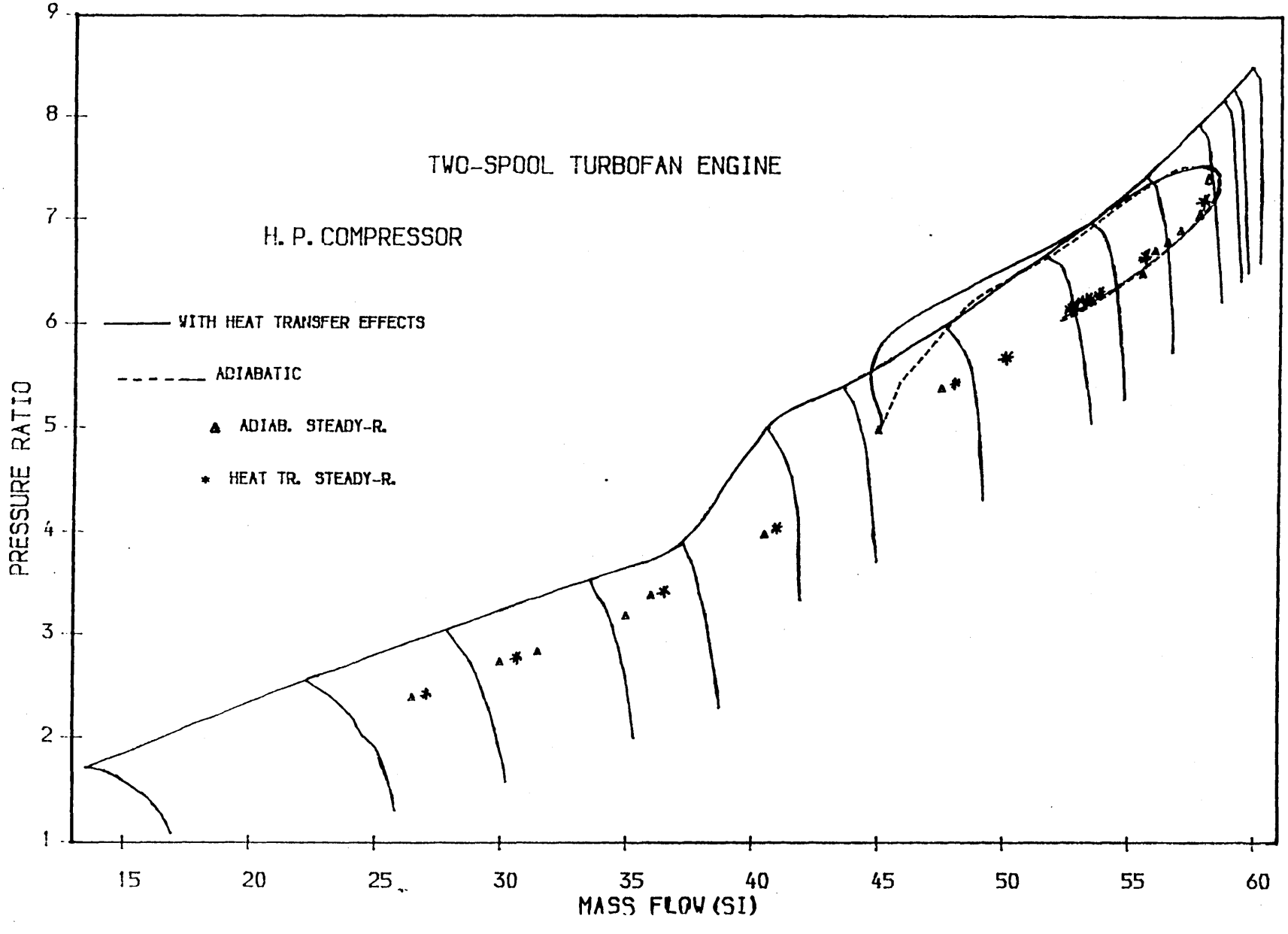

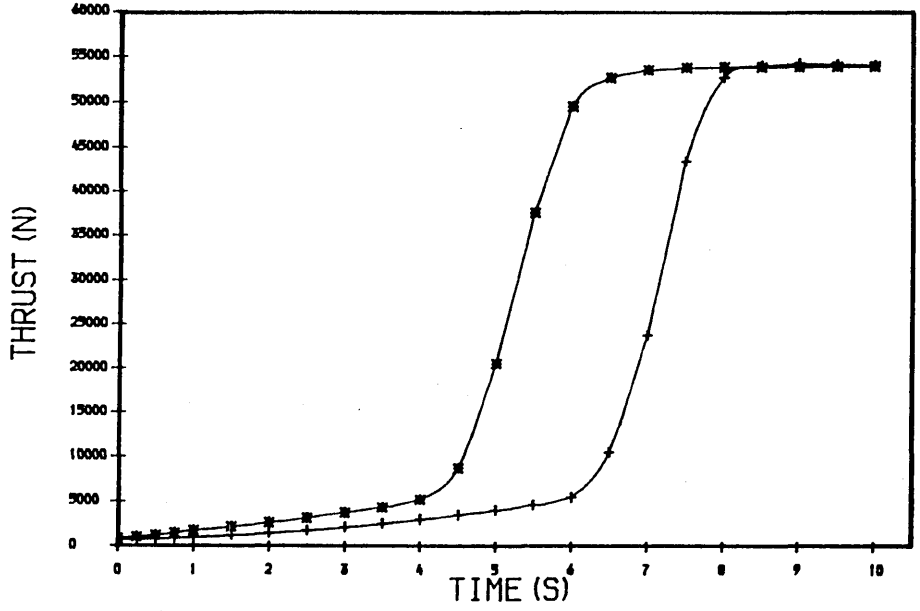

Fig. 47

PREDICTED HOT ACC. AT SEA-LEVEL
MACH NUMBER M = 0.2

* WITH HEAT TRANSFER

\+ ADIABATIC

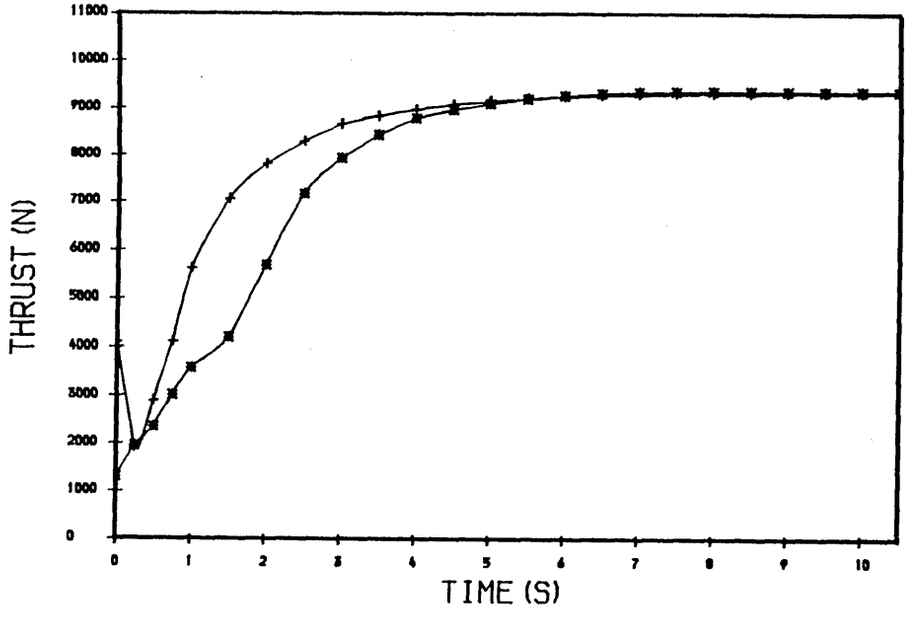

Fig. 48

PREDICTED HOT ACC. AT 41,000 FT
MACH NUM, M = 0·8

\+ WITH HEAT TRANSFER
✱ ADIABATIC

Fig. 49

PREDICTED ACC. AT SEA LEVEL

MACH NUM=0.2.

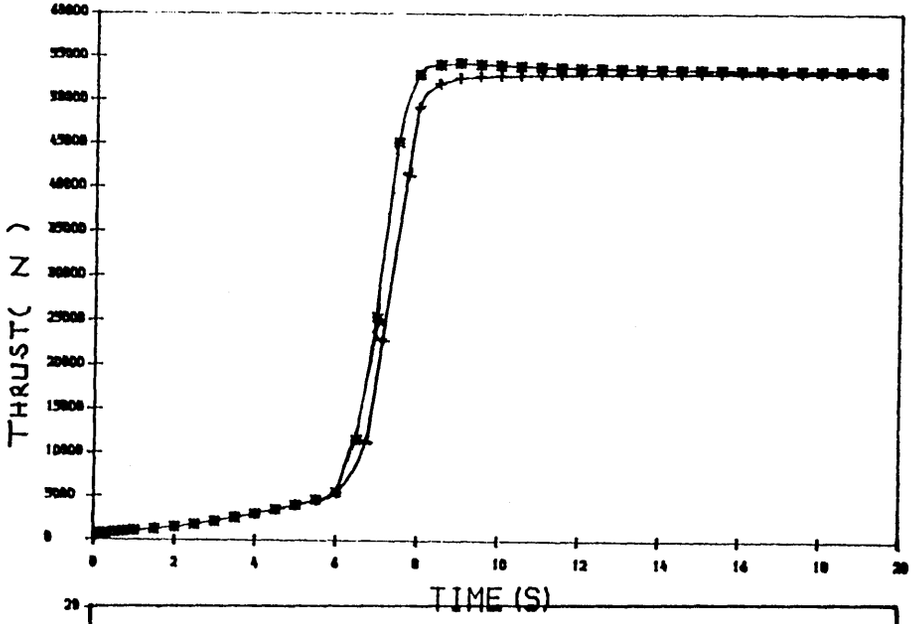

+ WITH HEAT TRANSFER EFFECTS

* ADIABATIC

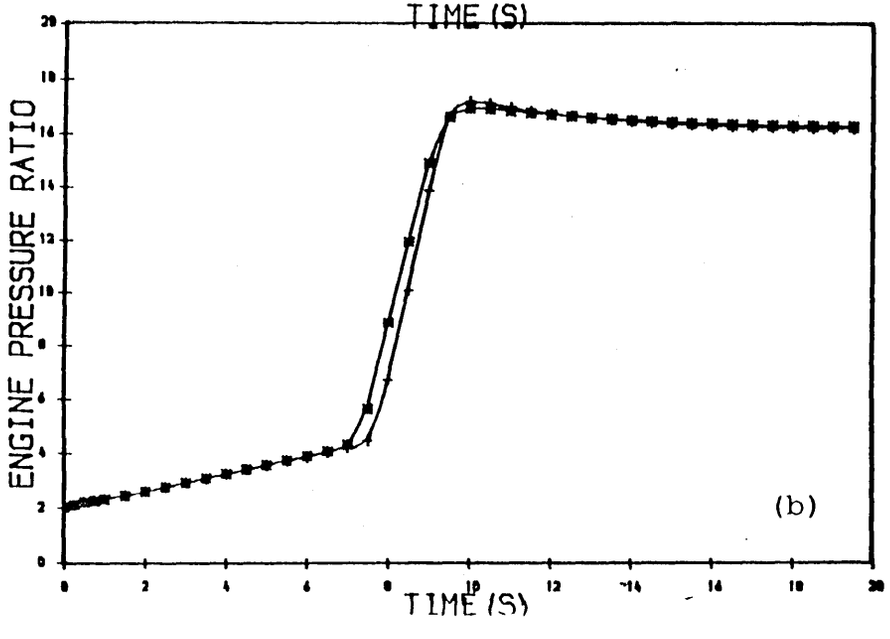

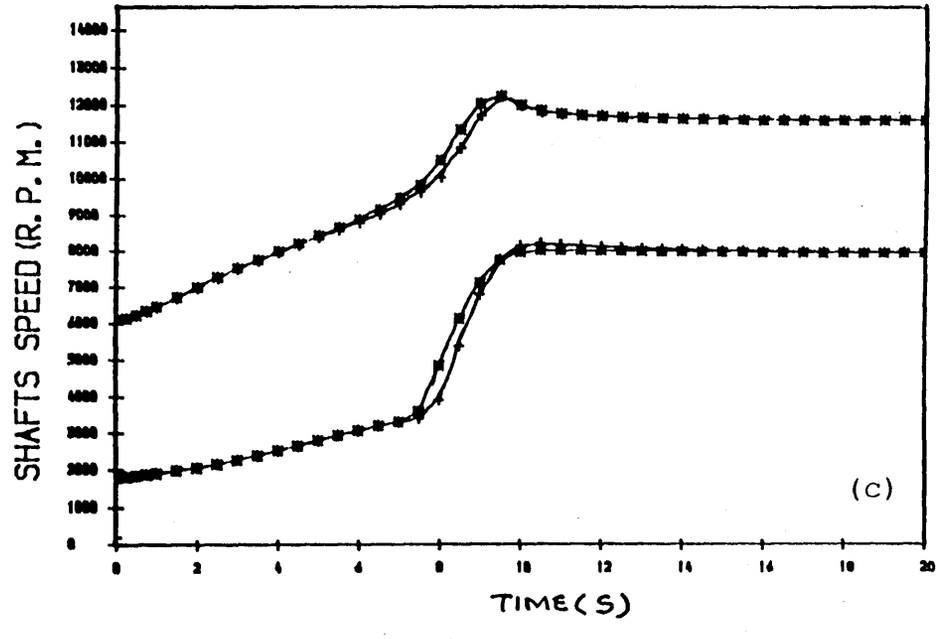

Fig. 50

PREDICTED ACELERATION AT SEA LEVEL CONDITIONS MACH NUM=0.2

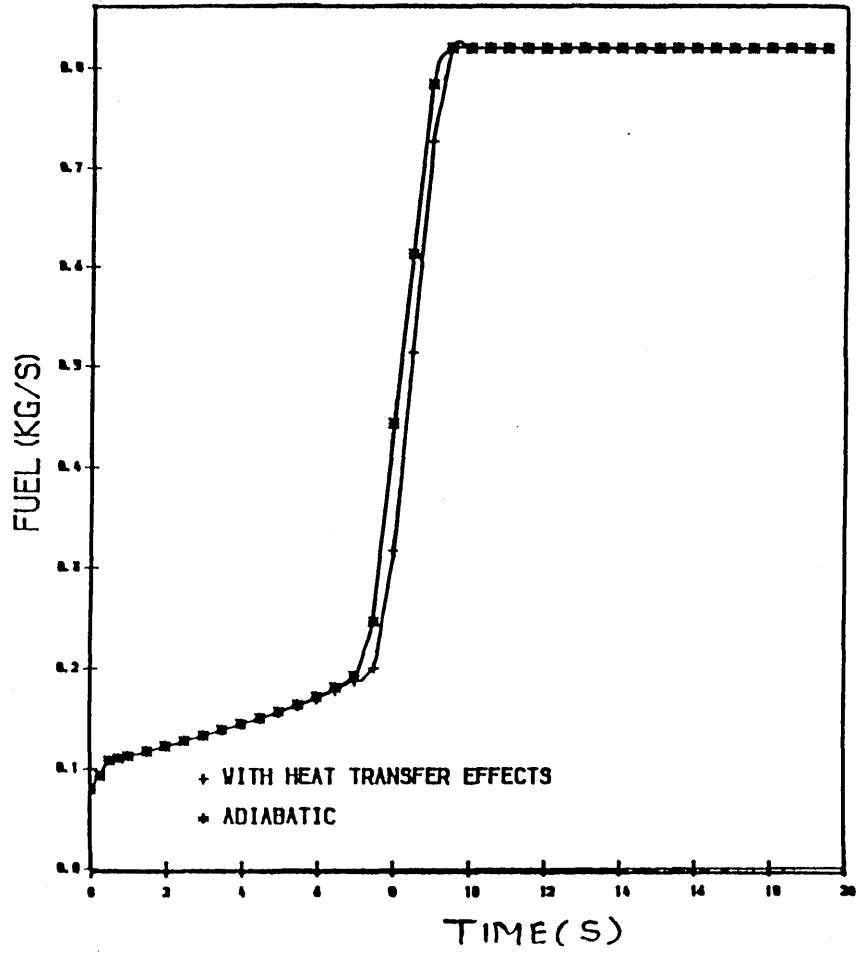

Fig. 51

PREDICTED ACCELERATION AT 41,000 FT

MACH NUM=0.8.

* WITH HEAT TRANSFER EFFECTS

\+ ADIABATIC

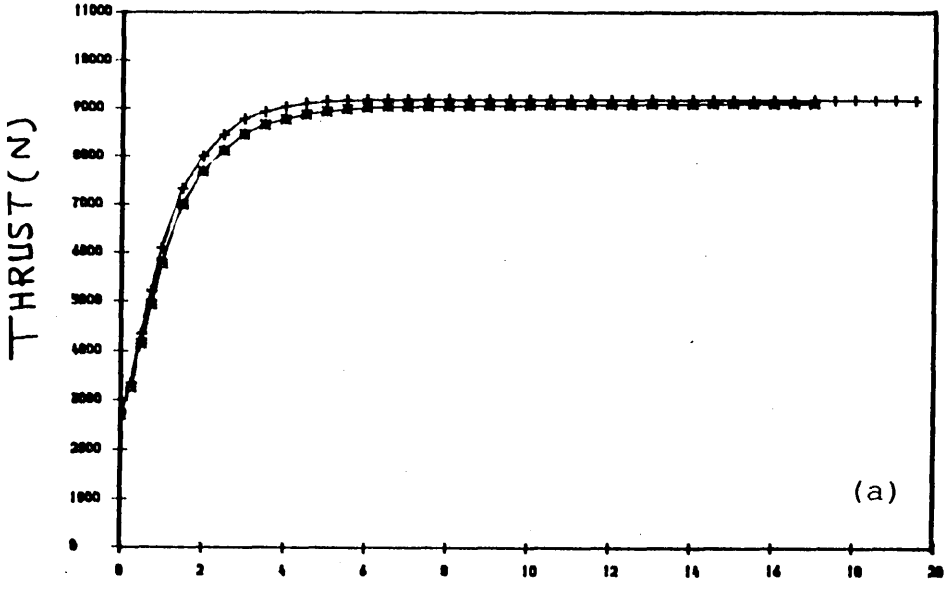

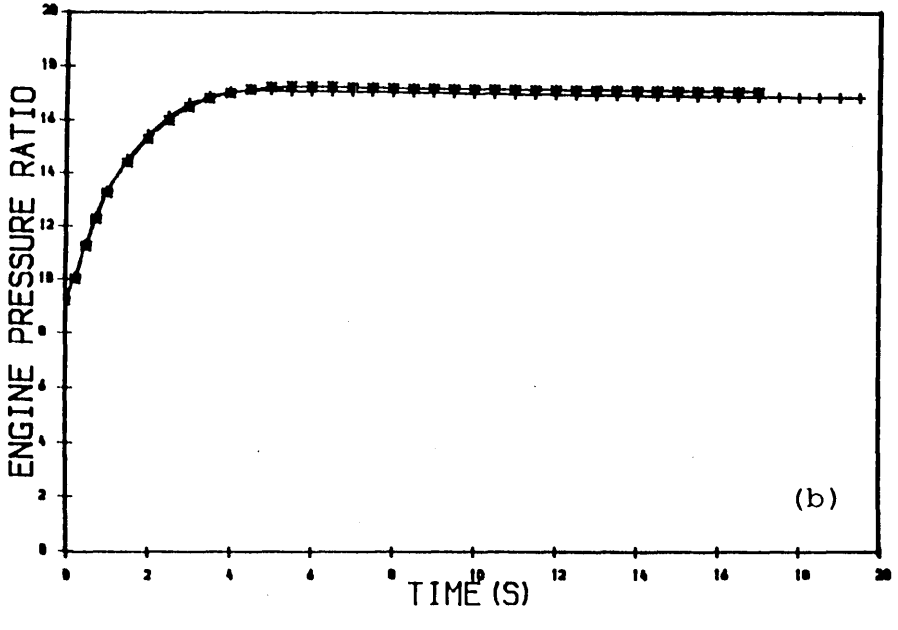

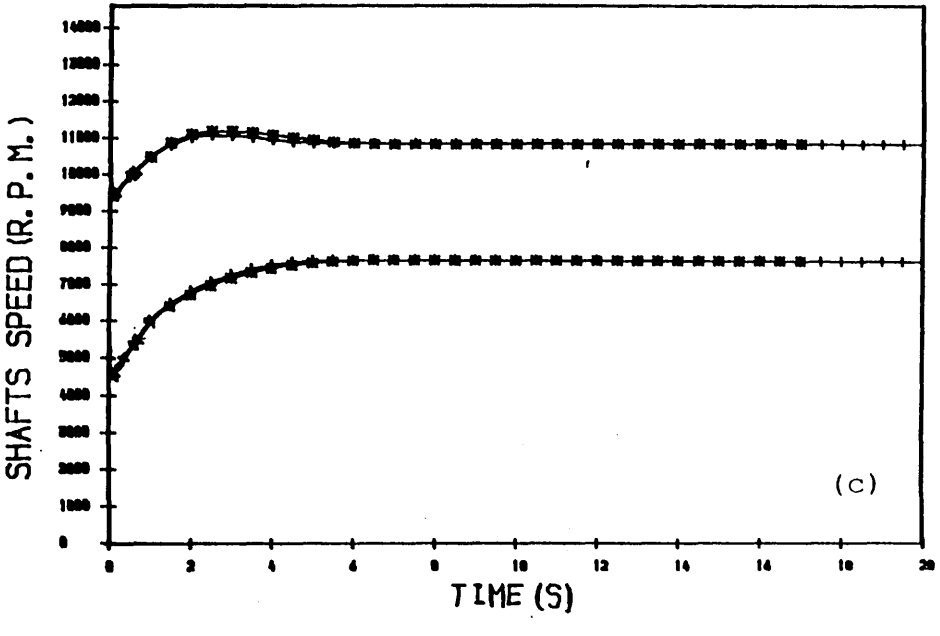

Fig. 52

PREDICTED ACELERATION AT 41,000 FT
CONDITIONS MACH NUM=0.8

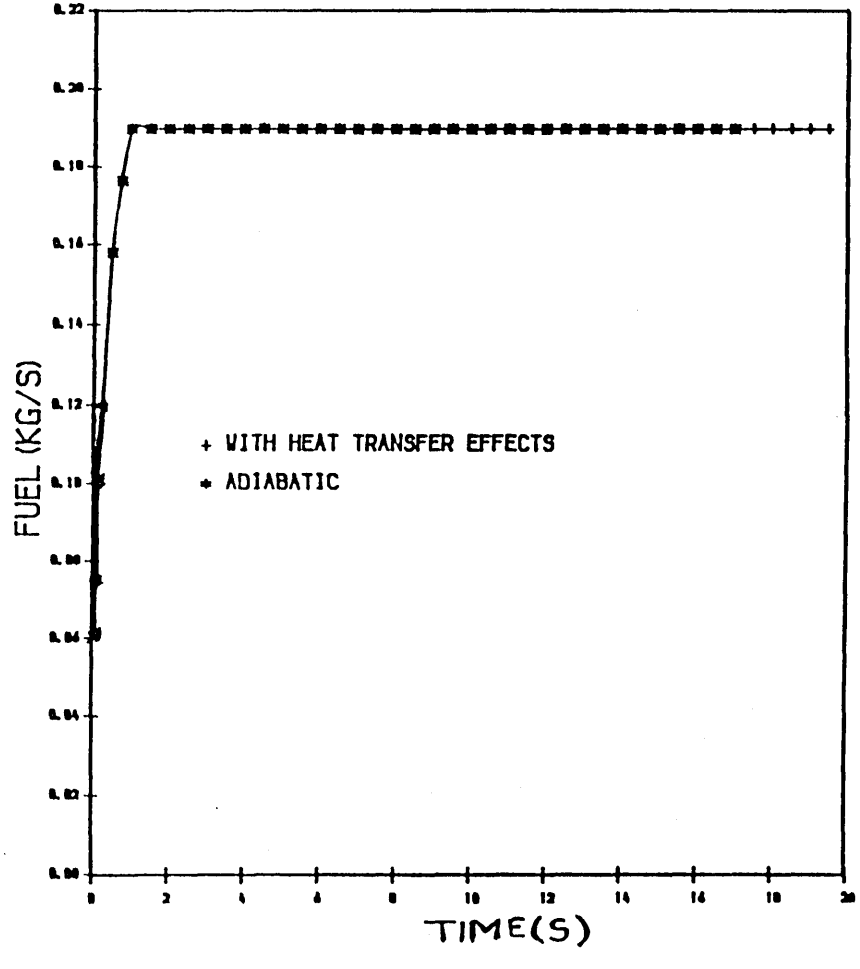

Fig. 53

PREDICTED ACCELERATION AT 50,000 FT

MACH NUM=0.8.

* WITH HEAT TRANSFER EFFECTS
+ ADIABATIC

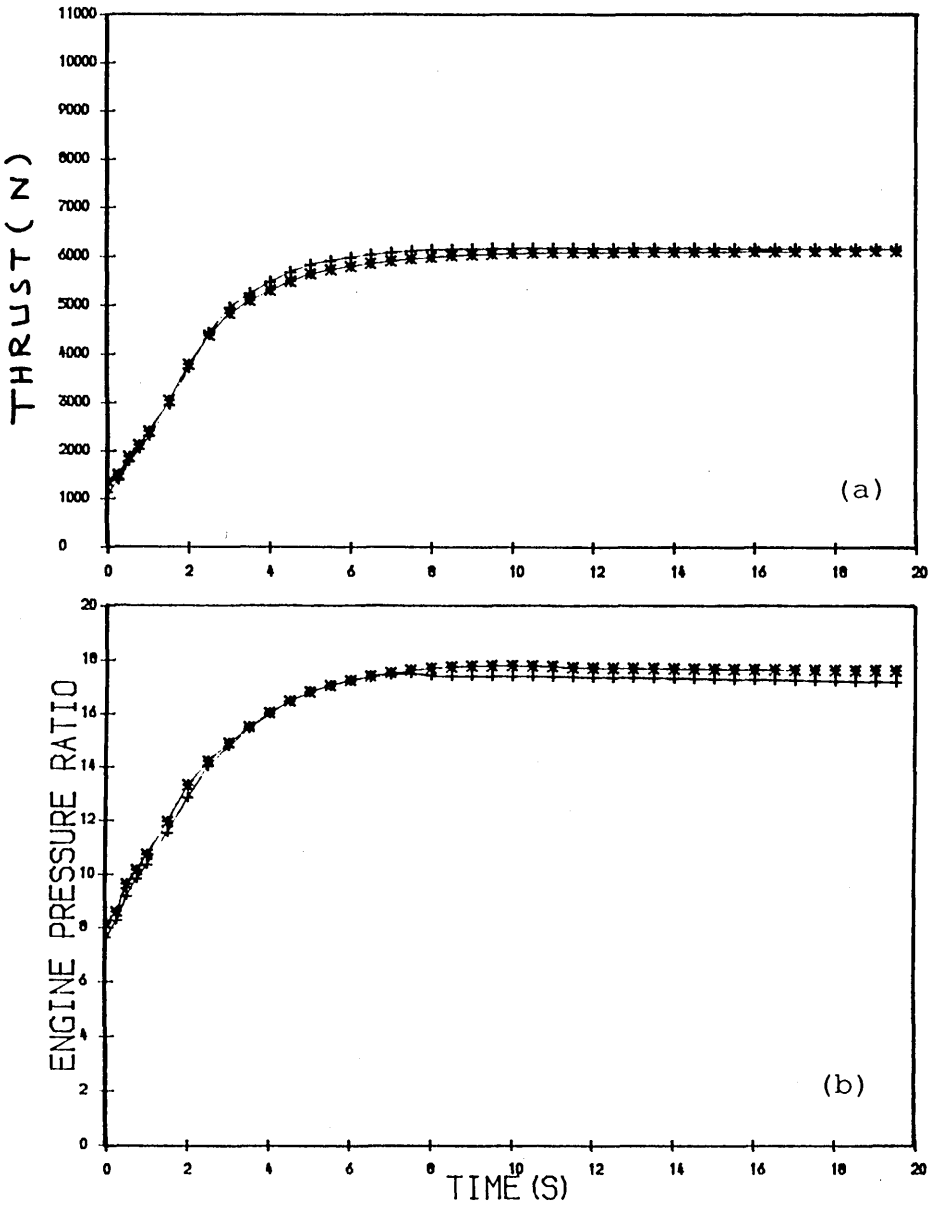

Fig. 54

PREDICTED ACELERATION AT 50,000 FT
CONDITIONS MACH NUM=0.8

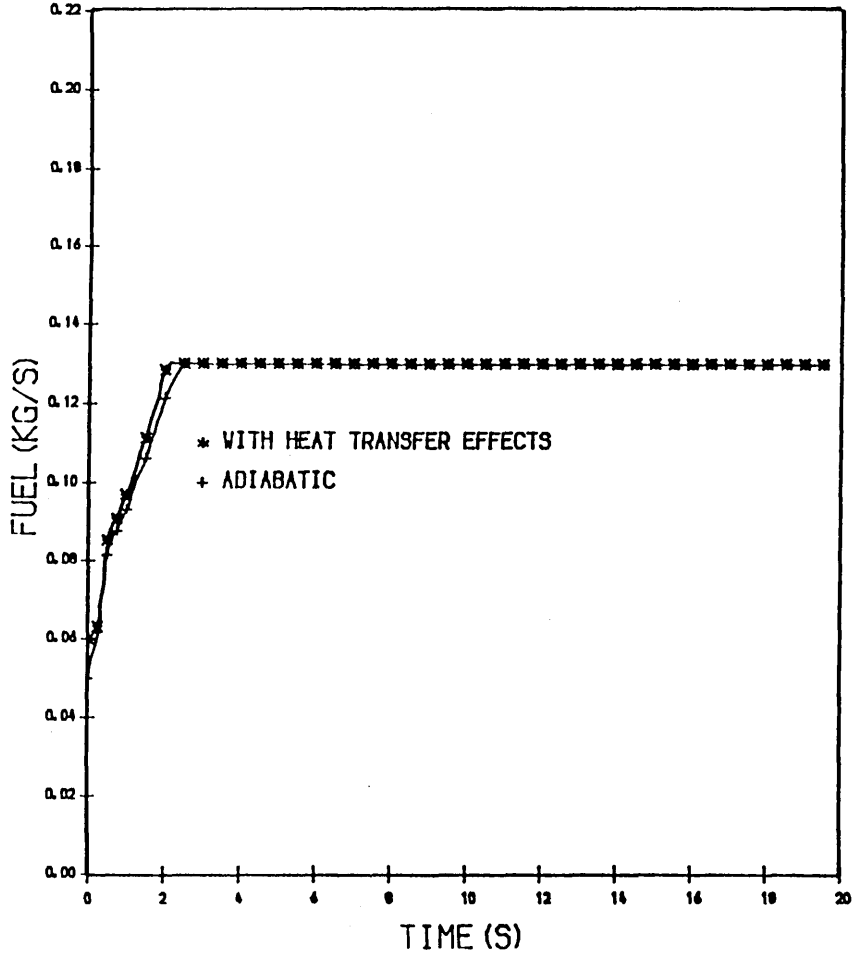

Fig. 55

PREDICTED DECELERATION AT SEA LEVEL

MACH NUM=0.2

* WITH HEAT TRANSFER EFFECTS

\+ ADIABATIC

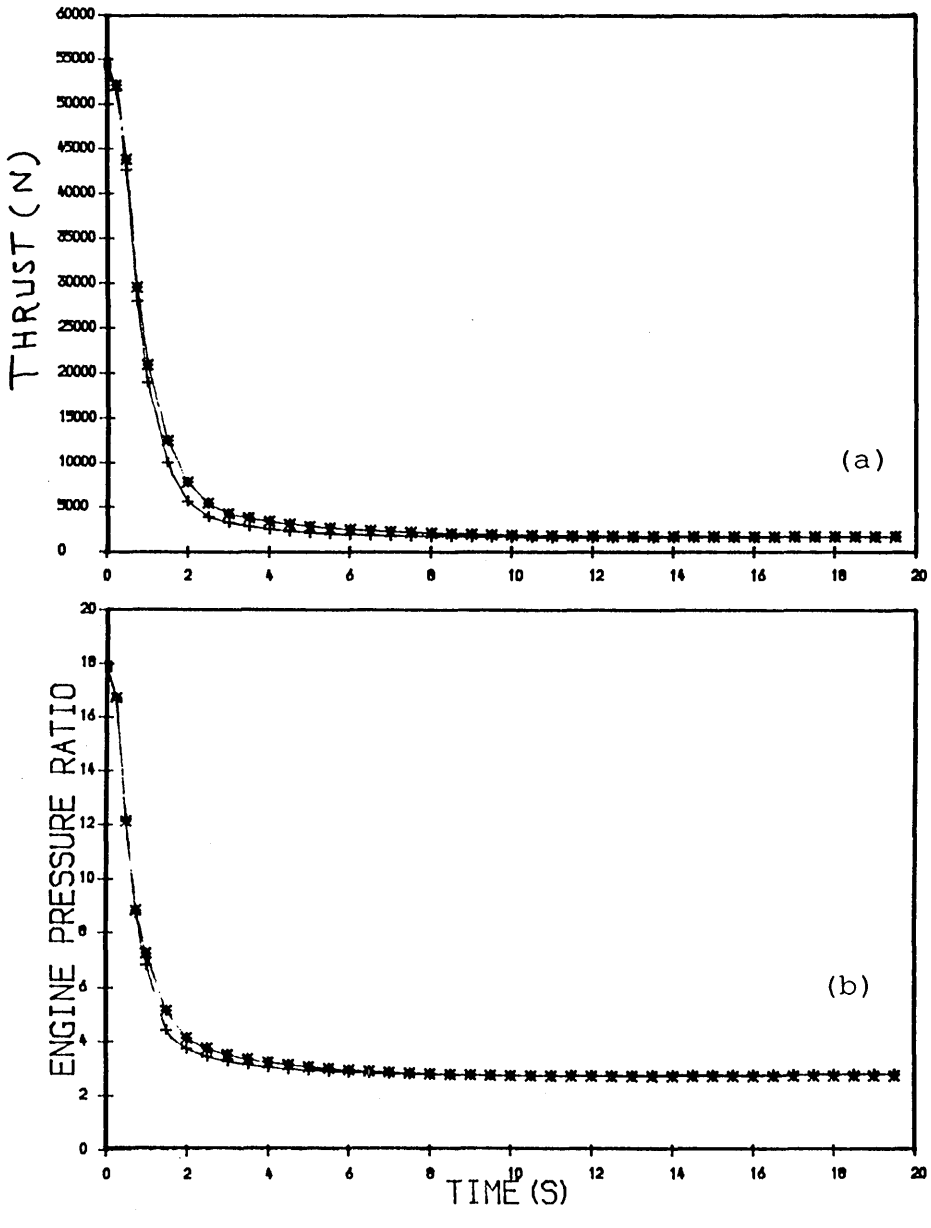

Fig. 56

PREDICTED DECELERATION AT SEA LEVEL CONDITIONS MACH NUM=0.2

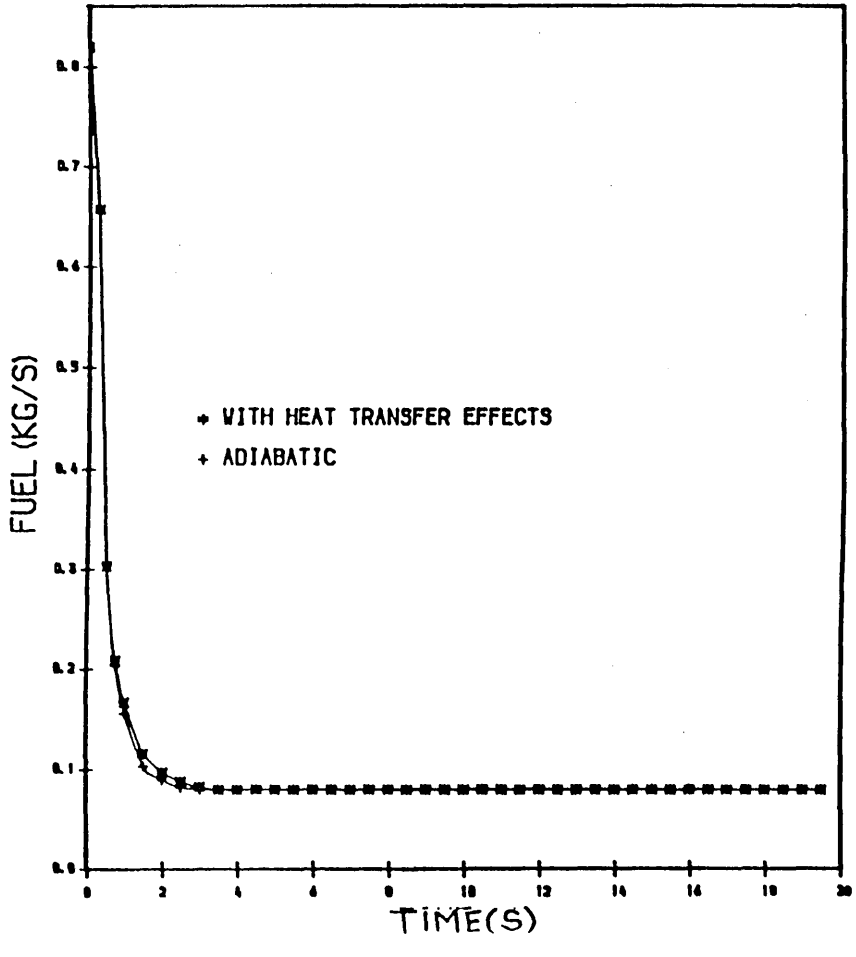

Fig. 57

PREDICTED DECELERATION AT 41,000 FT

MACH NUM=0.8.

* WITH HEAT TRANSFER EFFECTS
+ ADIABATIC

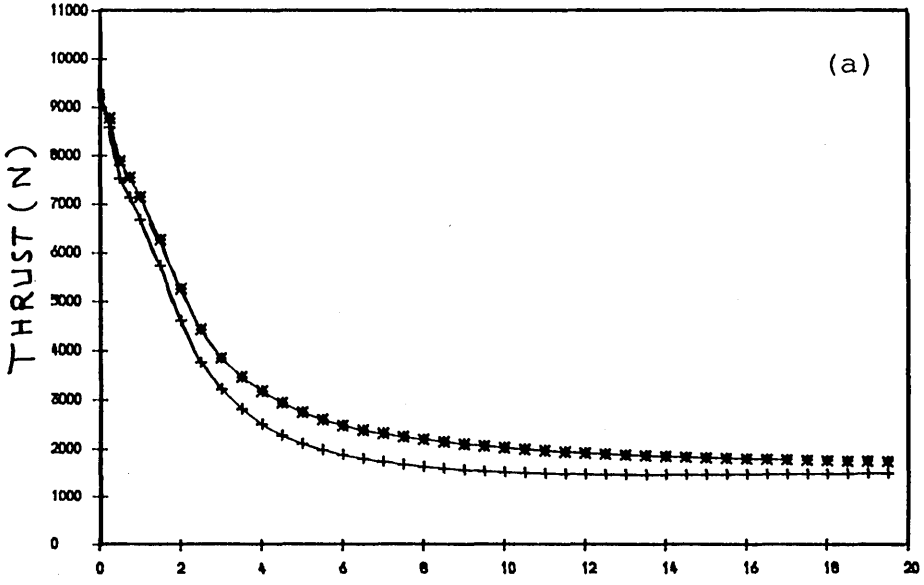

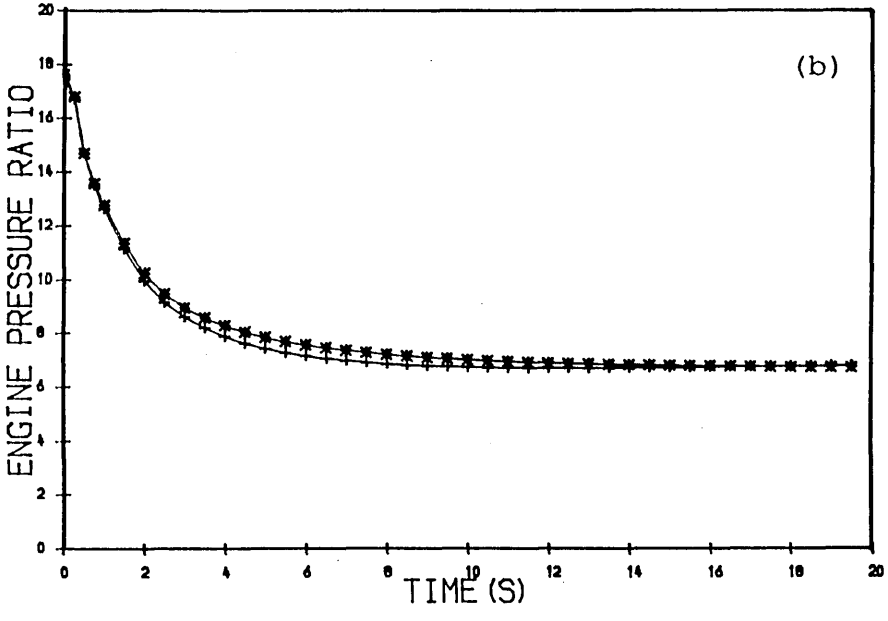

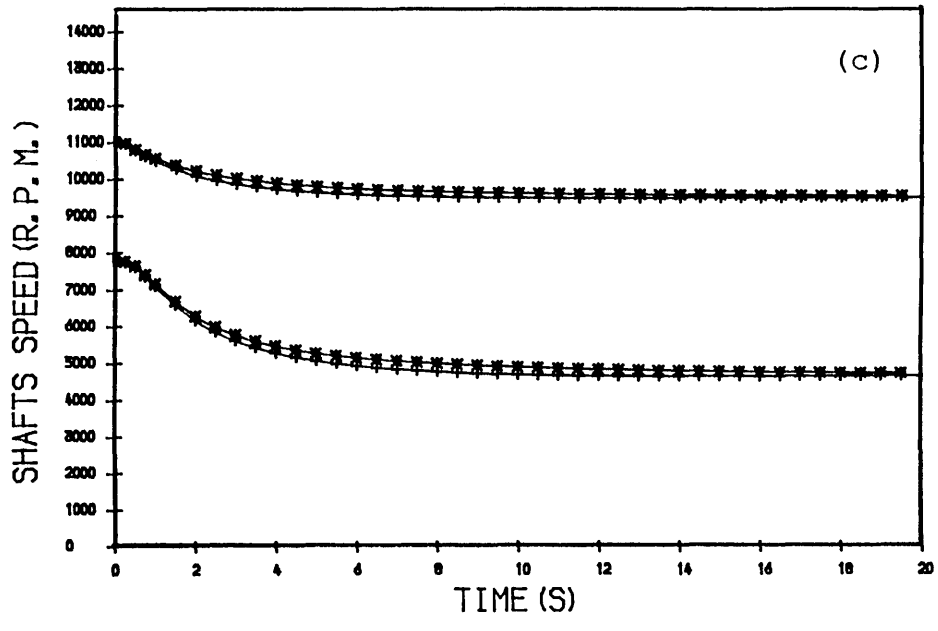

Fig. 58

PREDICTED DECELERATION AT 41,000 FT
CONDITIONS MACH NUM=0.8

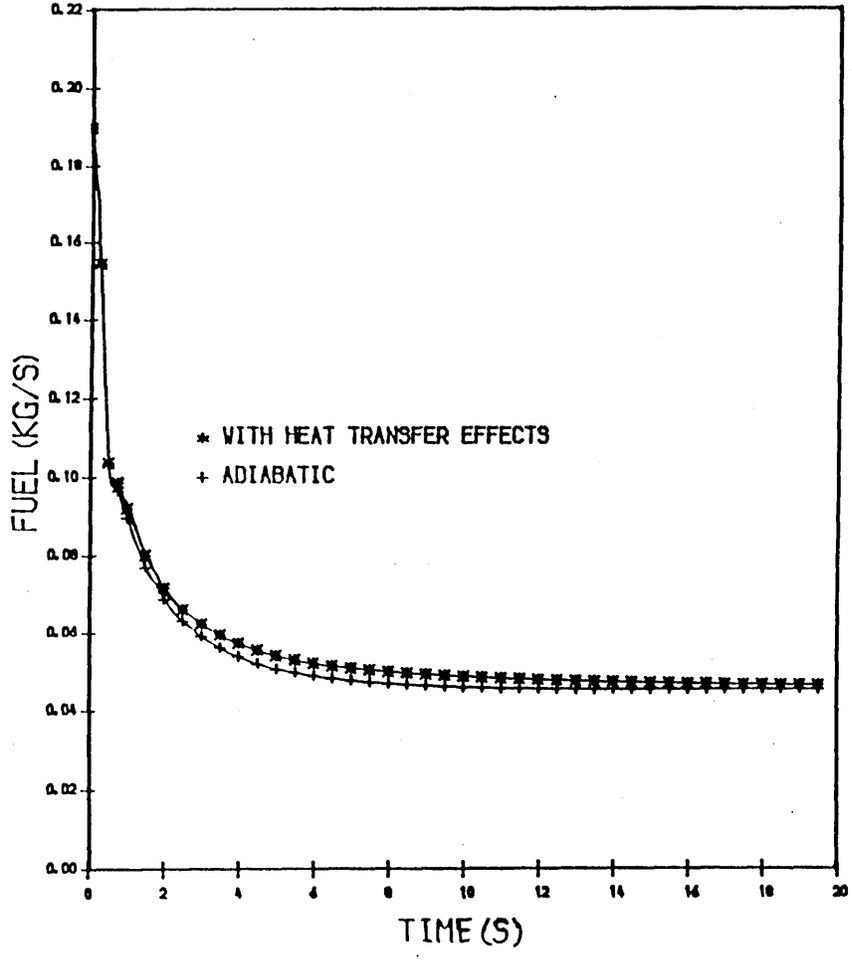

Fig. 59

PREDICTED DECELERATION AT 50,000 FT

MACH NUM=0.8.

* WITH HEAT TRANSFER EFFECTS
+ ADIABATIC

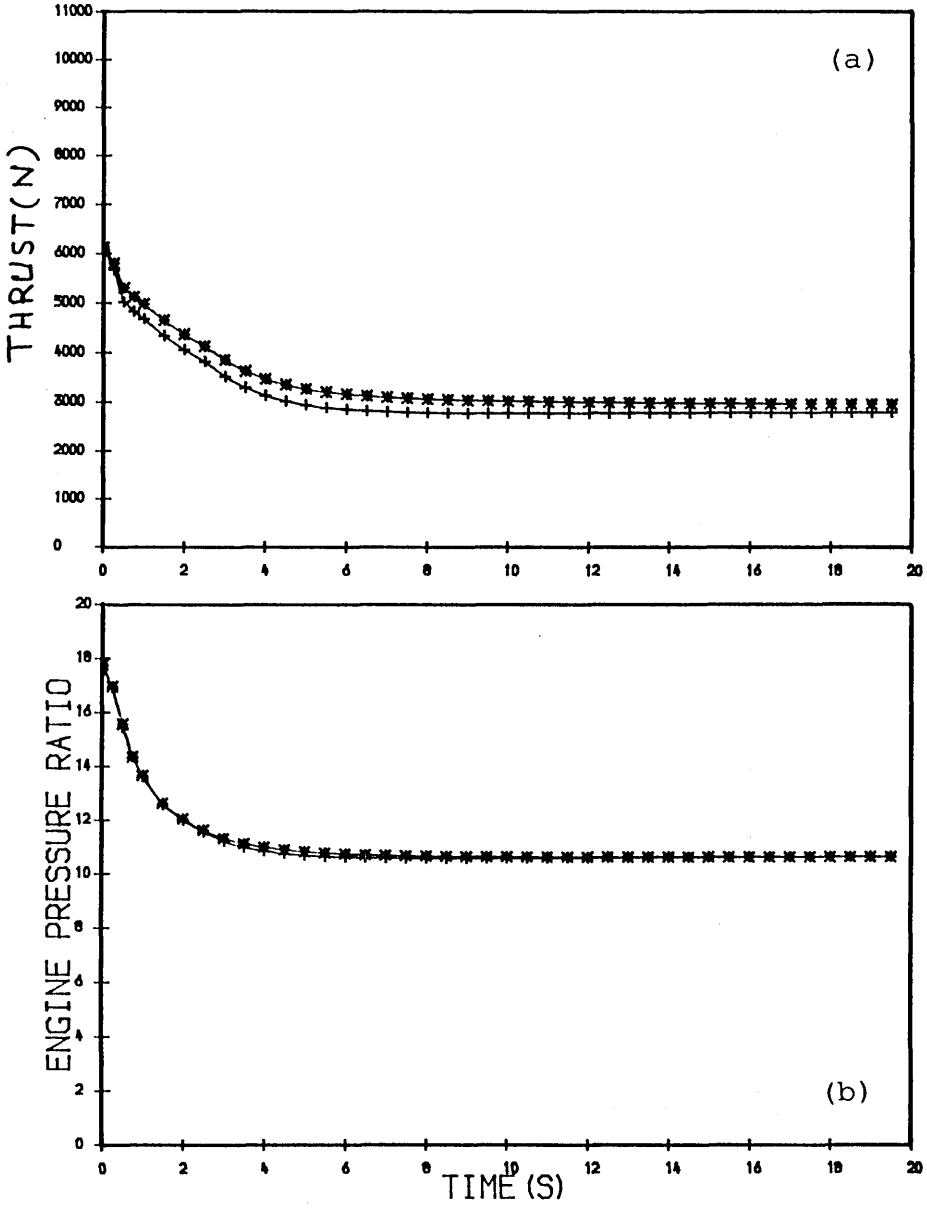

Fig. 60

PREDICTED DECELERATION AT 50,000 FT
CONDITIONS MACH NUM=0.8

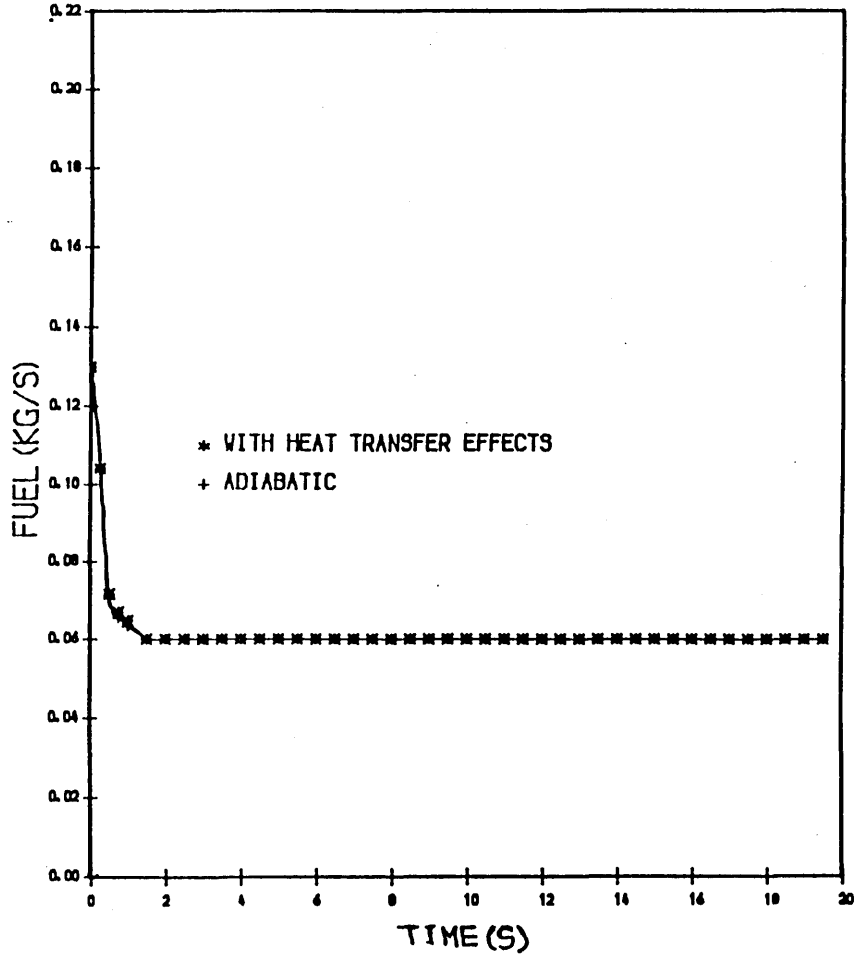

Fig. 61 H.P.C. TIP CLEARANCE MOVEMENTS
AT SEA LEVEL TRANSIENT ACC.

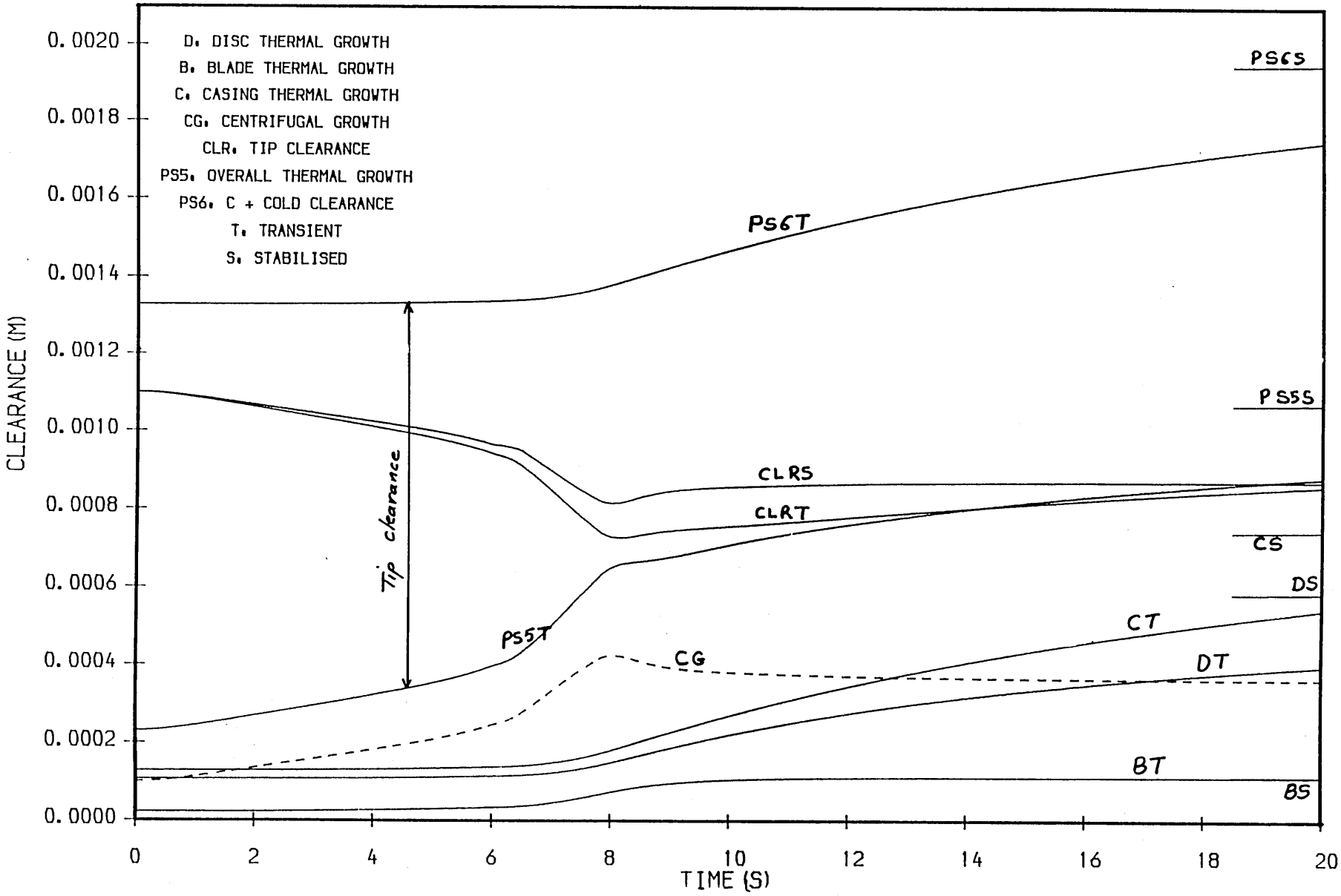

Fig. 62 H.P.T. TIP CLEARANCE MOVEMENTS
AT SEA LEVEL TRANSIENT ACC.

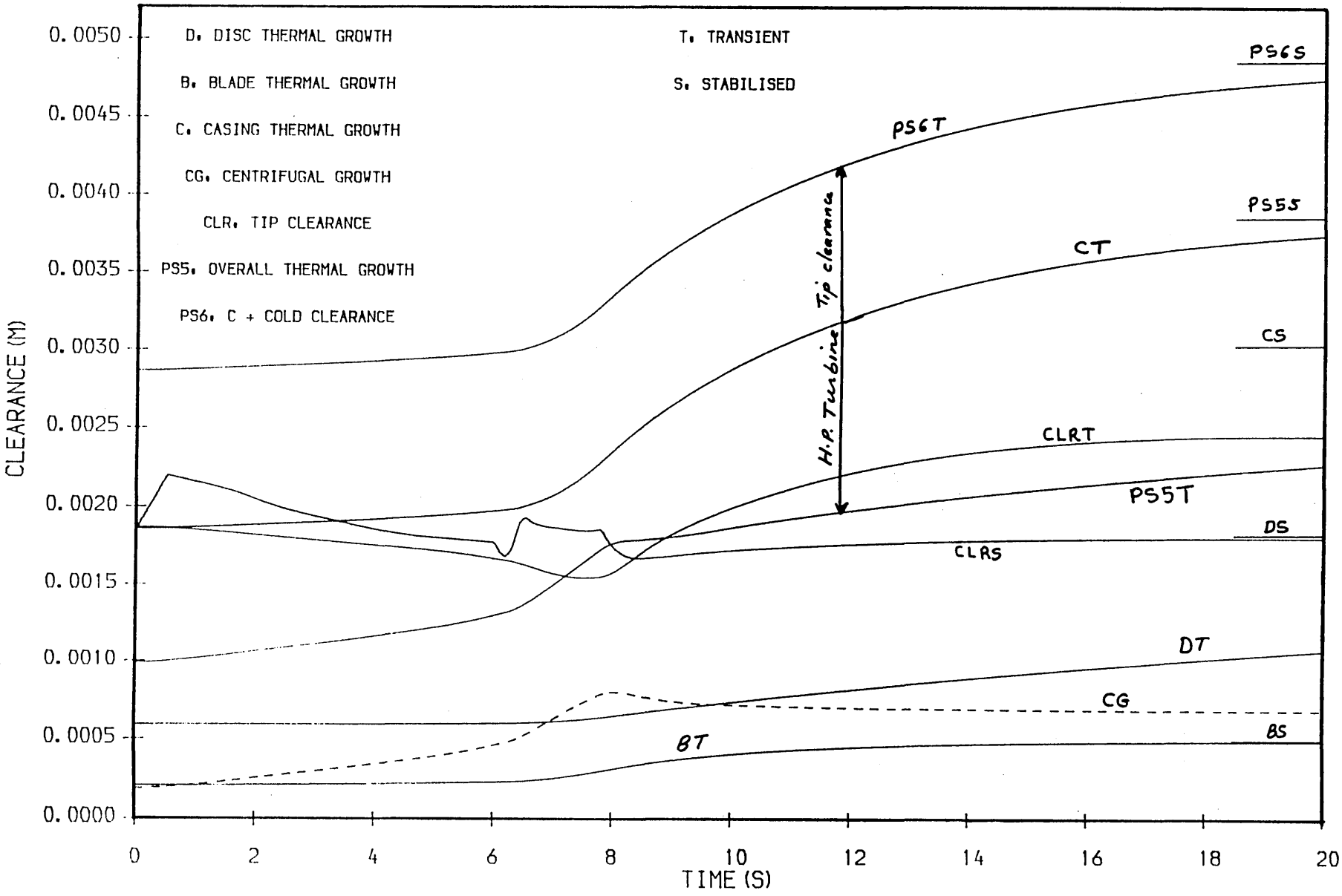

Fig. 63 H.P.C. TIP CLEARANCE MOVEMENTS
AT 41,000 FT TRANSIENT ACC.

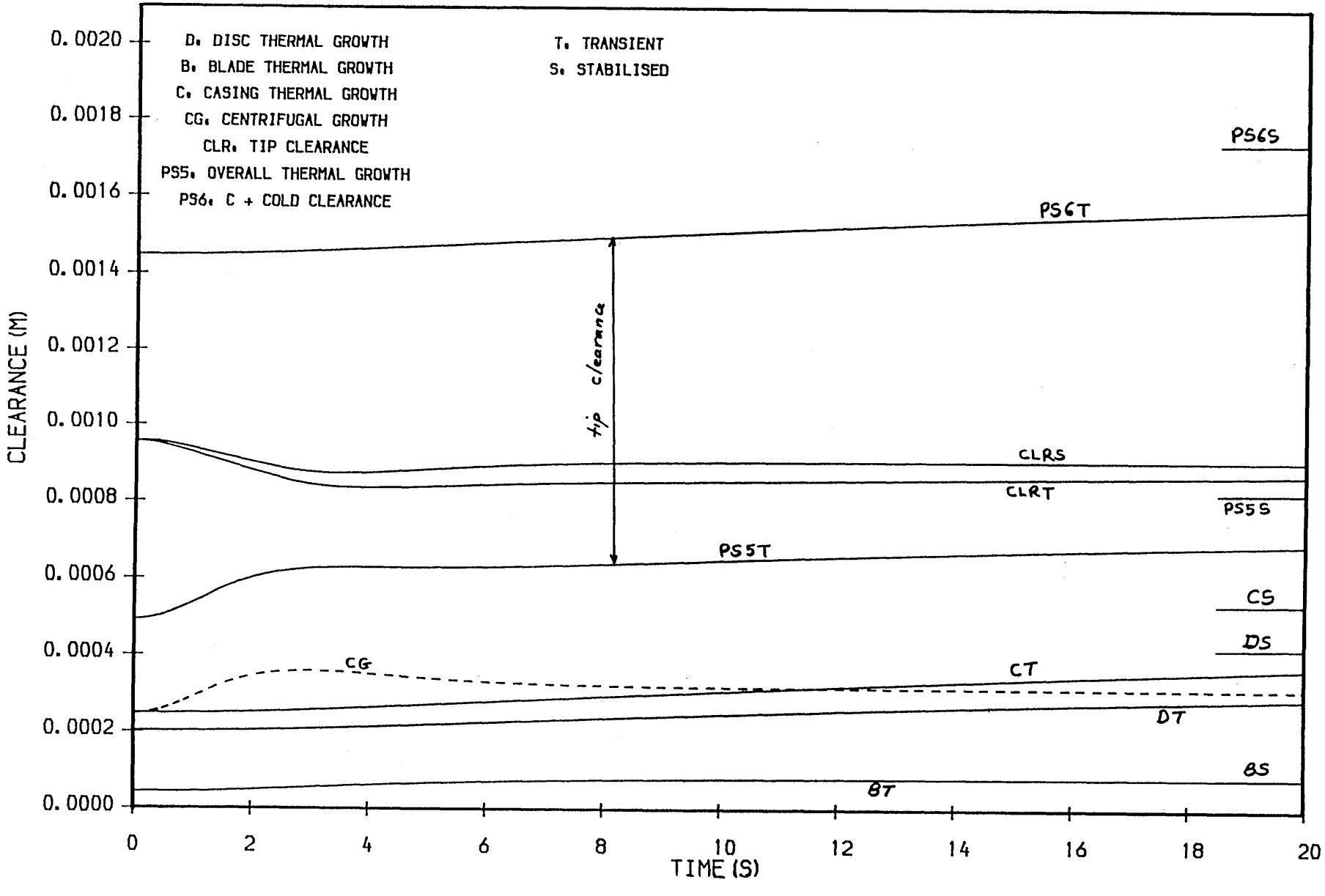

Fig. 64 H.P.T. TIP CLEARANCE MOVEMENTS
AT 41,000 FT TRANSIENT ACC.

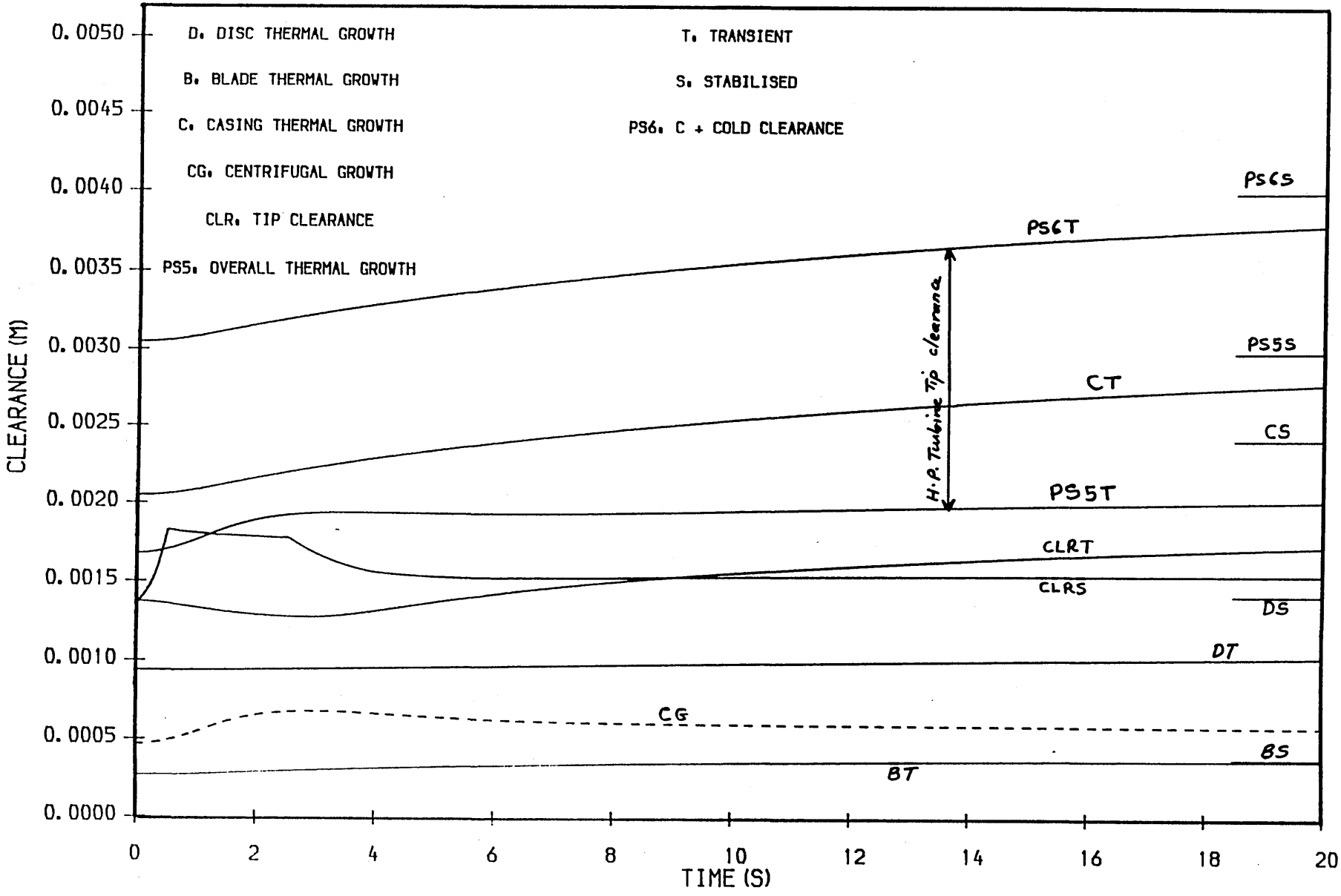

Fig. 65 H.P.C. TIP CLEARANCE MOVEMENTS
AT SEA. LEVEL TRANSIENT DEC.

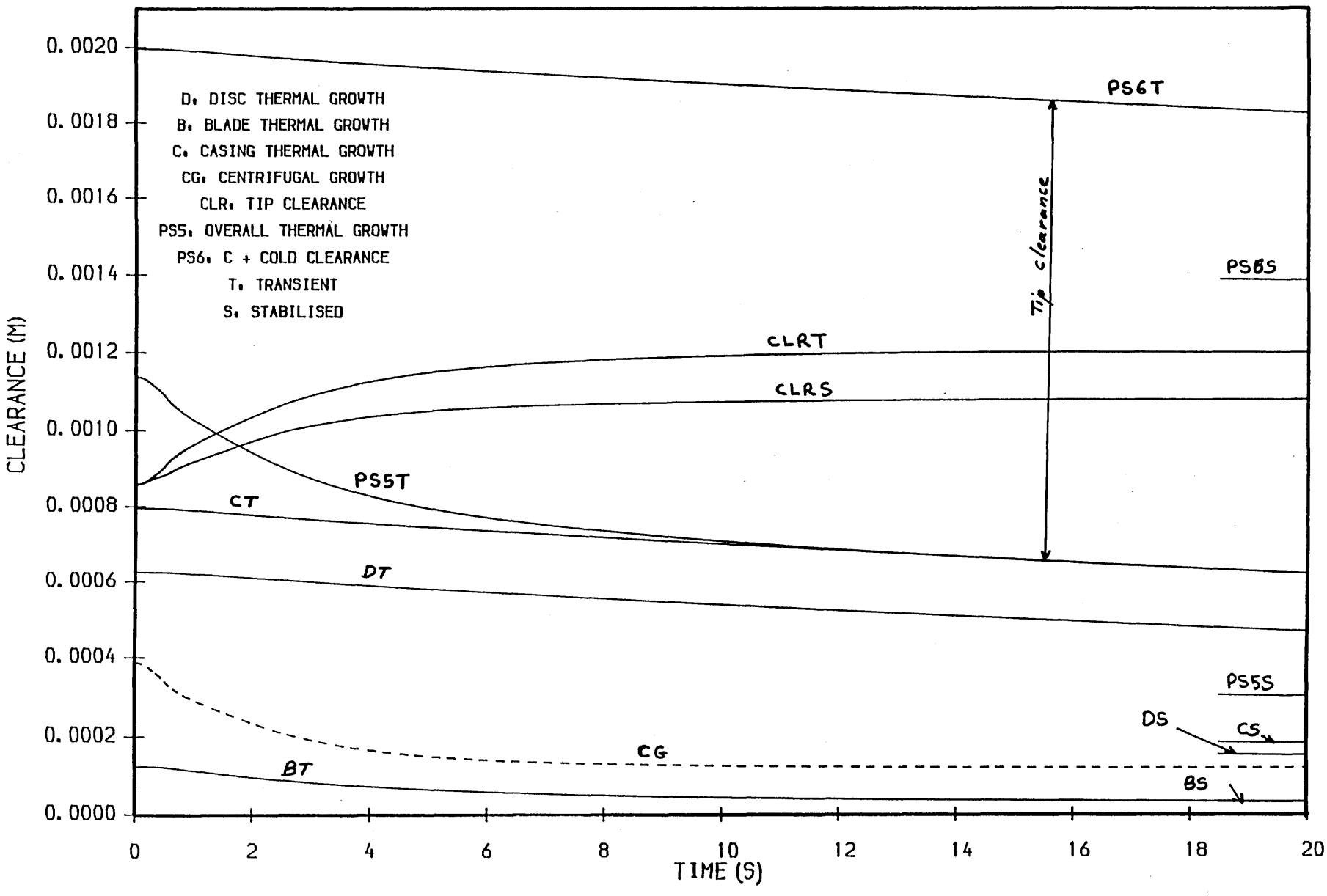

Fig. 66 H.P.T. TIP CLEARANCE MOVEMENTS
AT SEA-LEVEL TRANSIENT DEC.

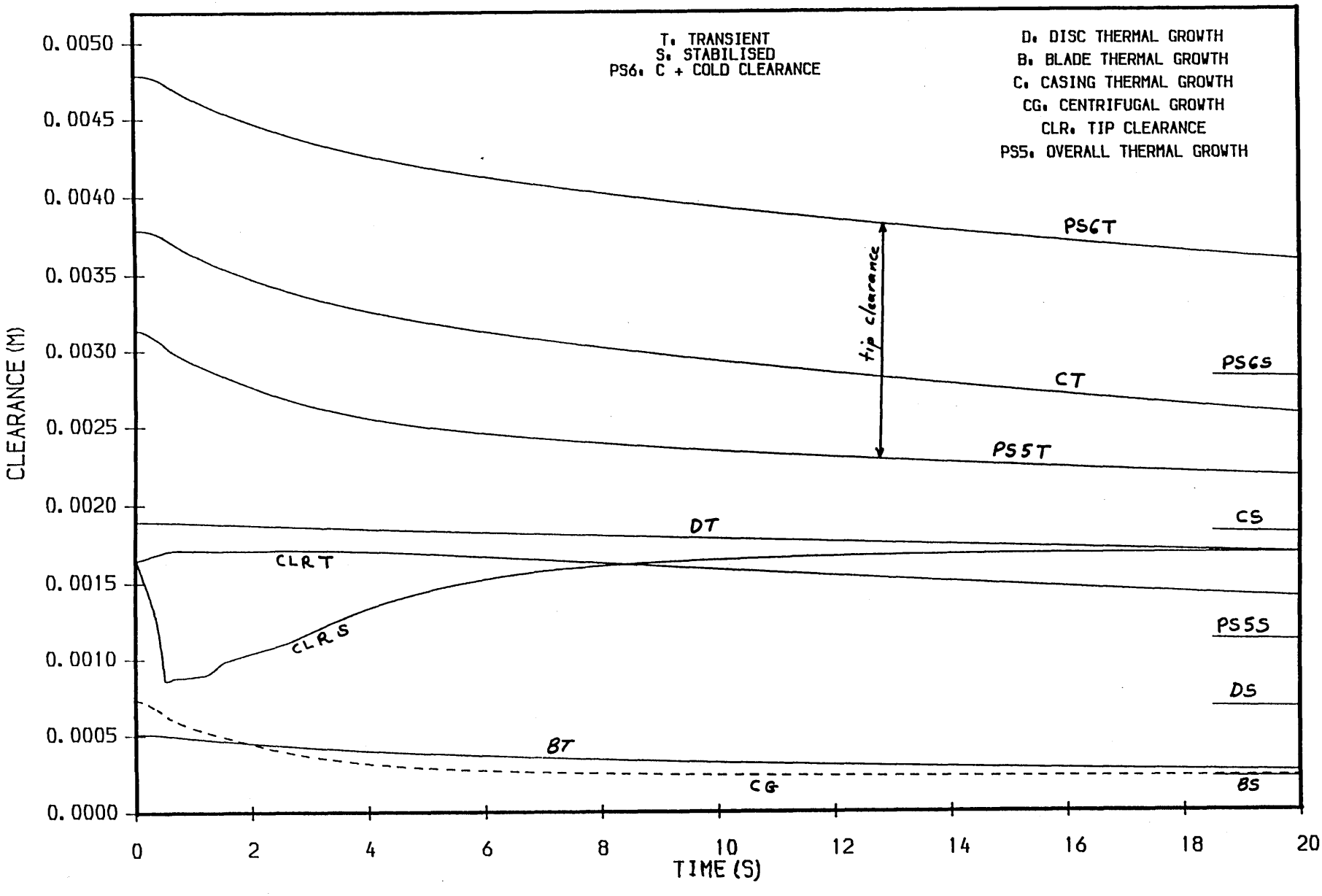

Fig. 67 H.P.C. TIP CLEARANCE MOVEMENTS
AT 41,000 ft TRANSIENT DEC.

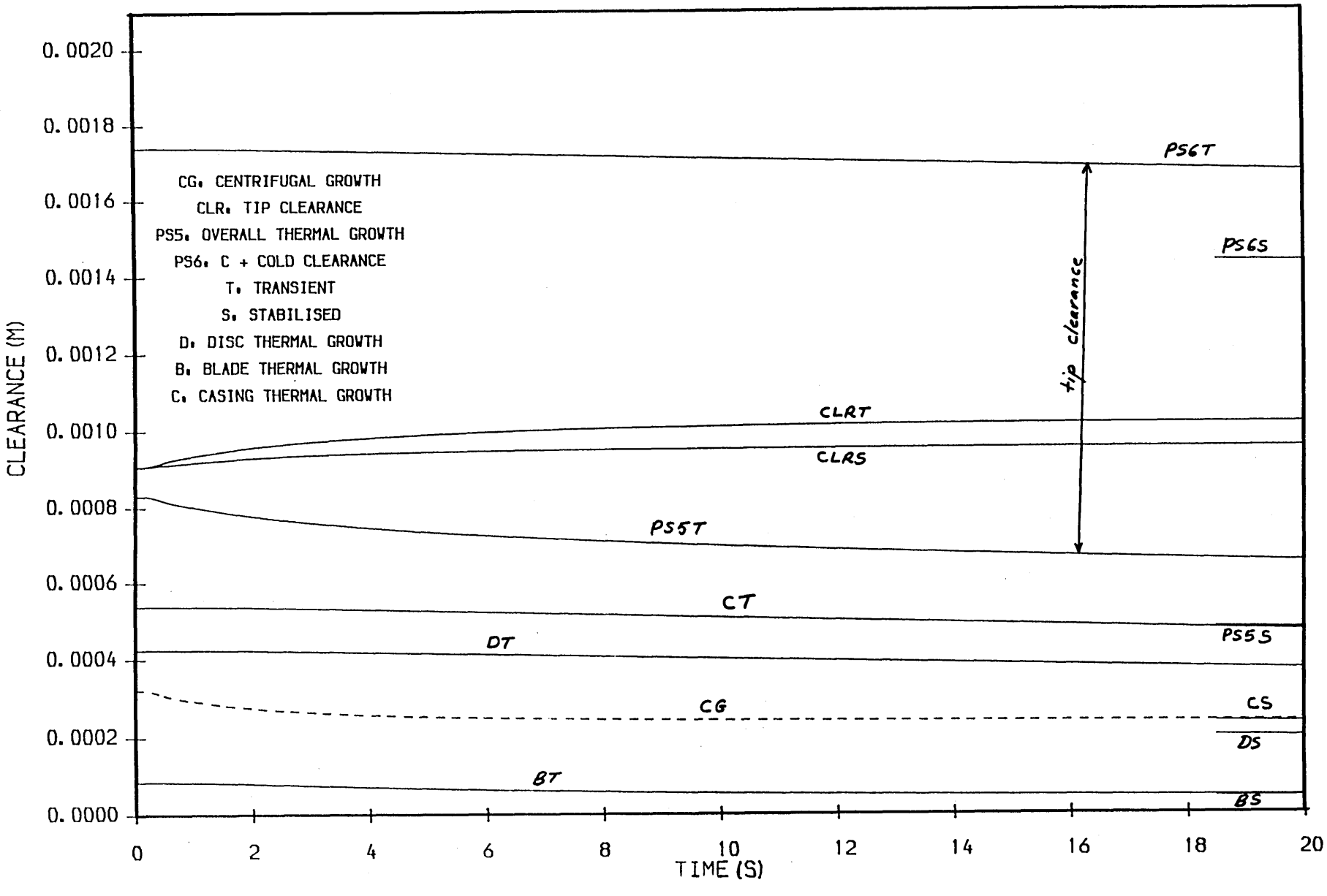

Fig. 68 H.P.T. TIP CLEARANCE MOVEMENTS-
AT 41,000 ft TRANSIENT DEC.

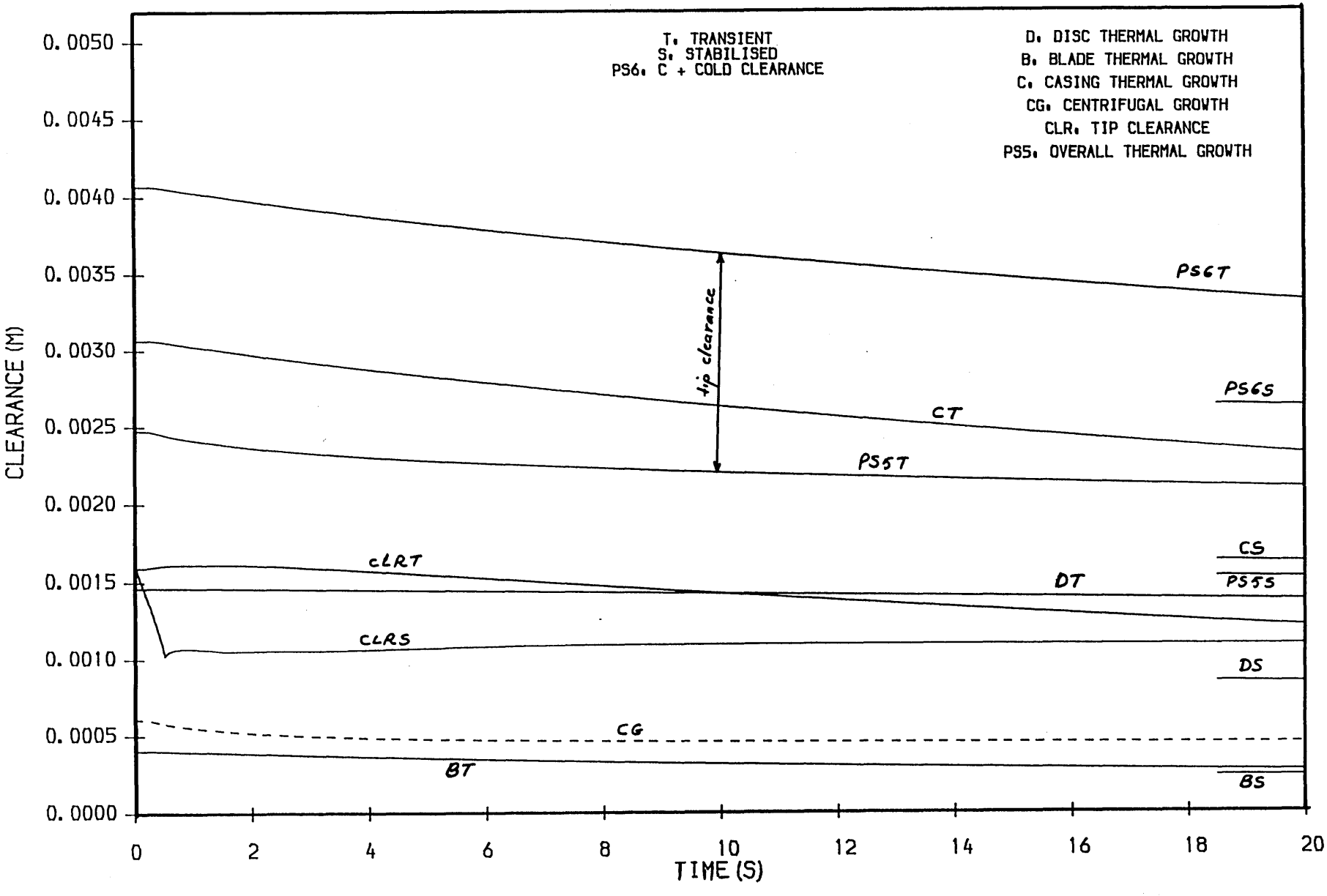

Fig. 69 H.P.C. TIP CLEARANCE MOVEMENTS
AT SEA-LEVEL TRANSIENT HOT ACC.

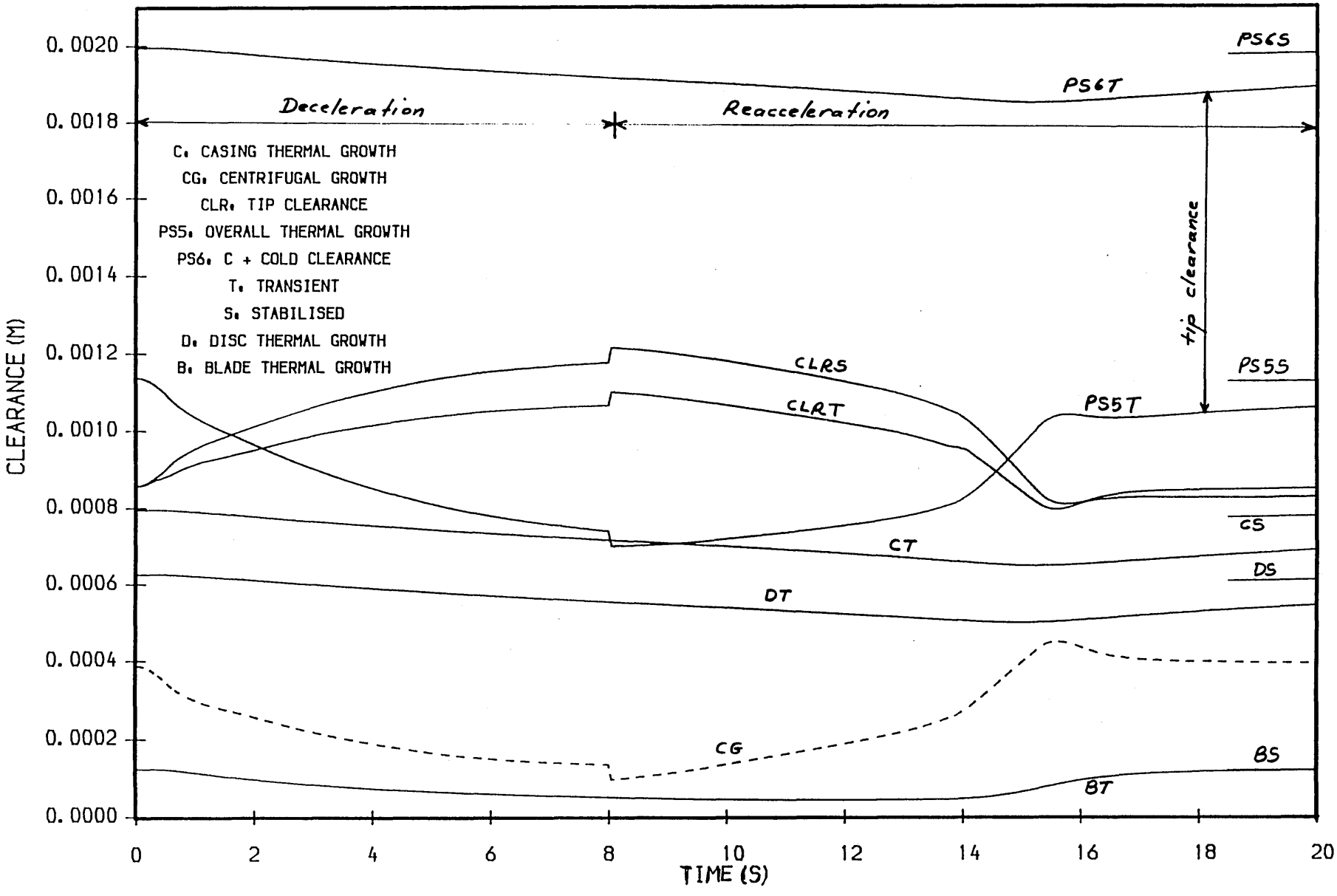

Fig. 70 H.P.T. TIP CLEARANCE MOVEMENTS
AT SEA-LEVEL TRANSIENT HOT ACC.

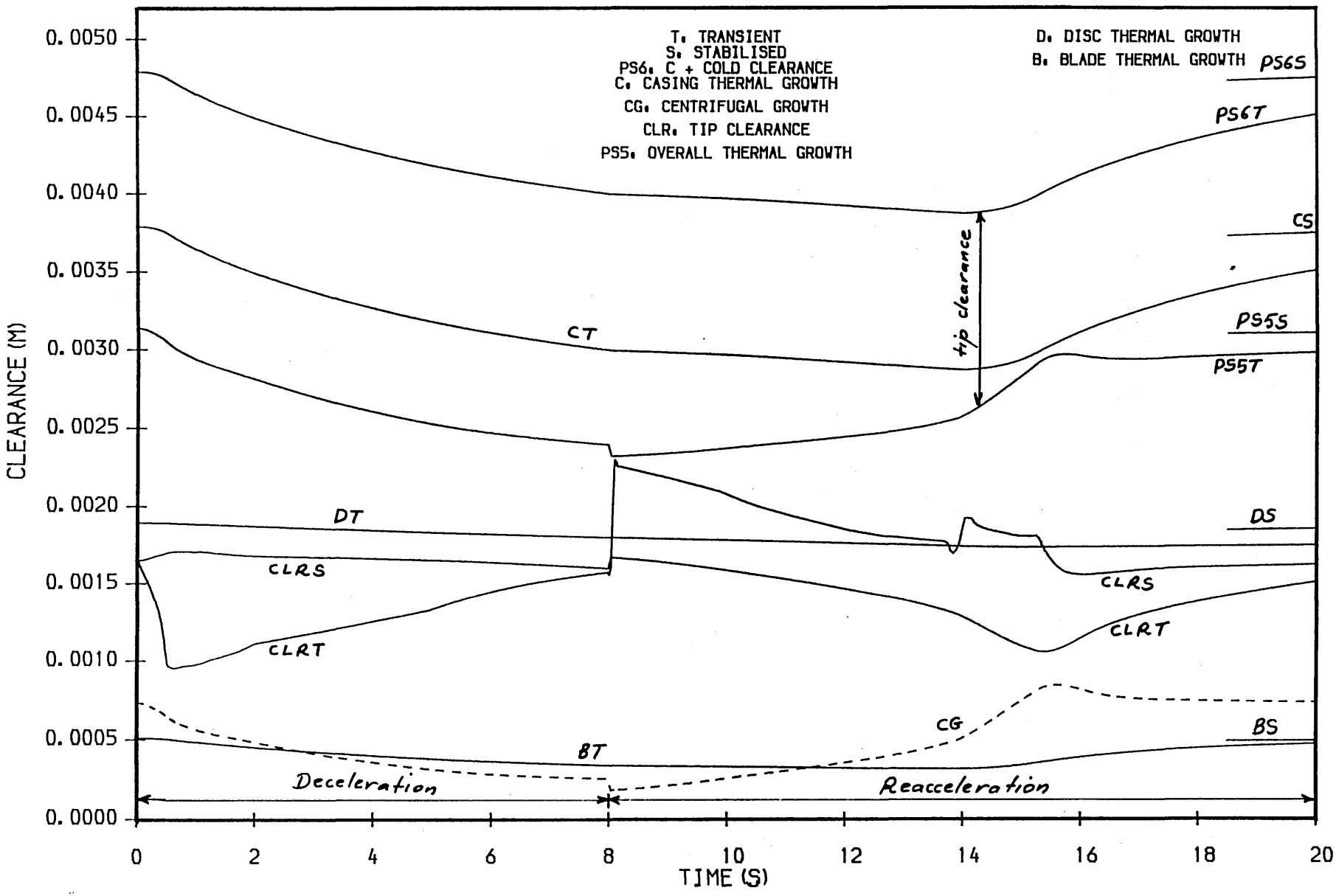

Fig. 71 H.P.C. TIP CLEARANCE MOVEMENTS
AT 41,000 ft TRANSIENT HOT ACC.

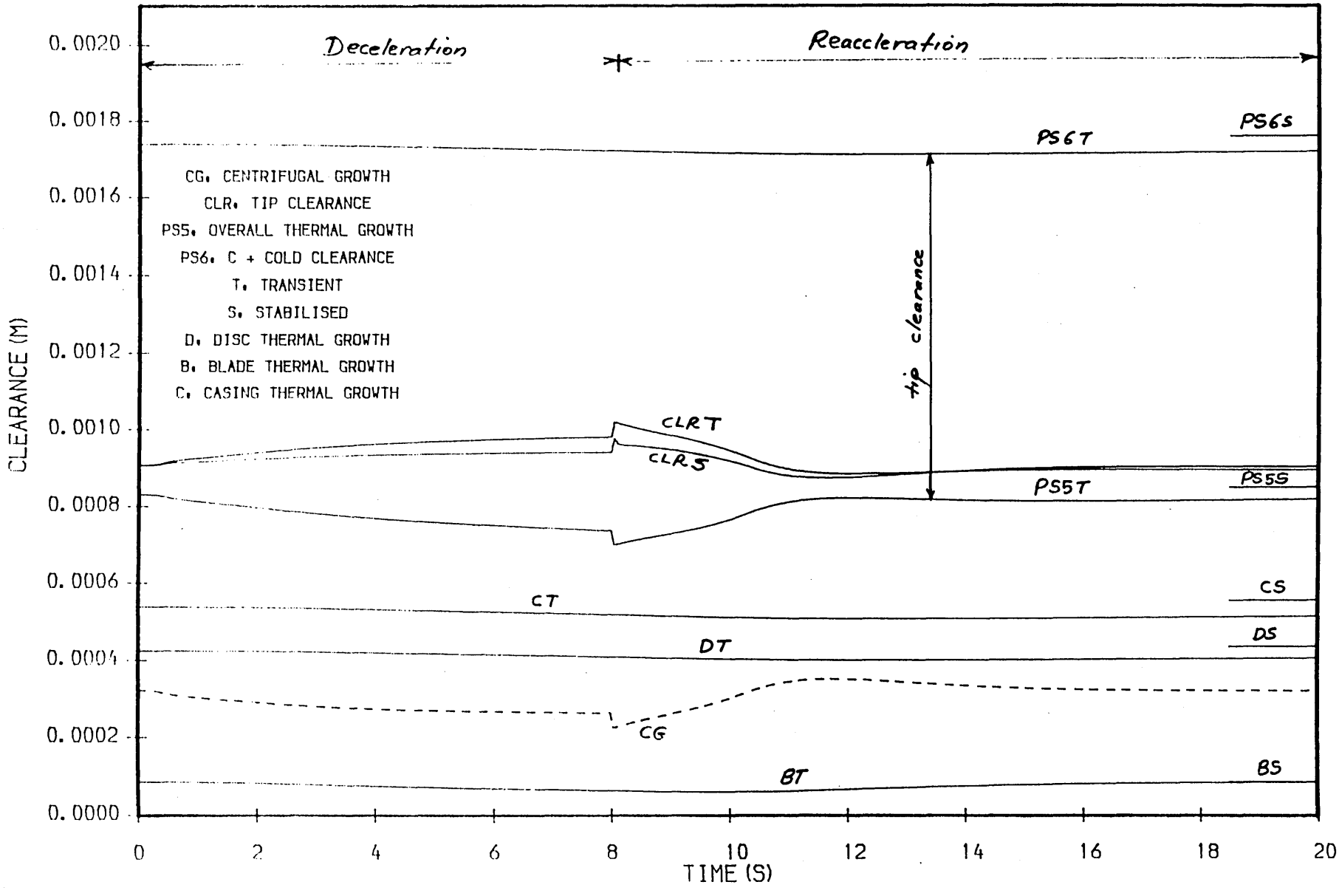

Fig. 72 H.P.T. TIP CLEARANCE MOVEMENTS
AT 41,000 ft TRANSIENT HOT ACC.

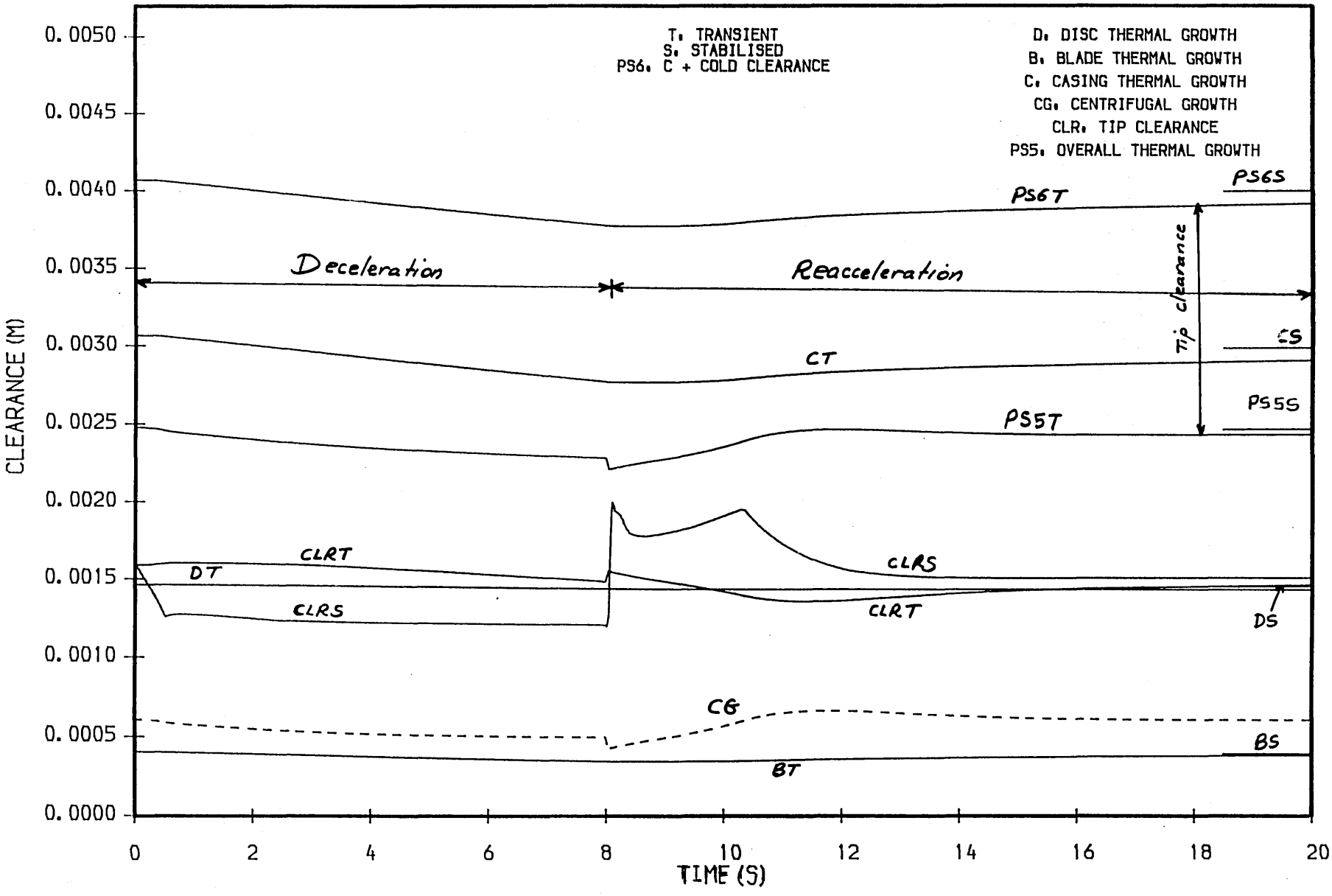

Fig. 73 H.P.C. SEAL CLEARANCE MOVEMENTS
AT SEA LEVEL TRANSIENT ACC.

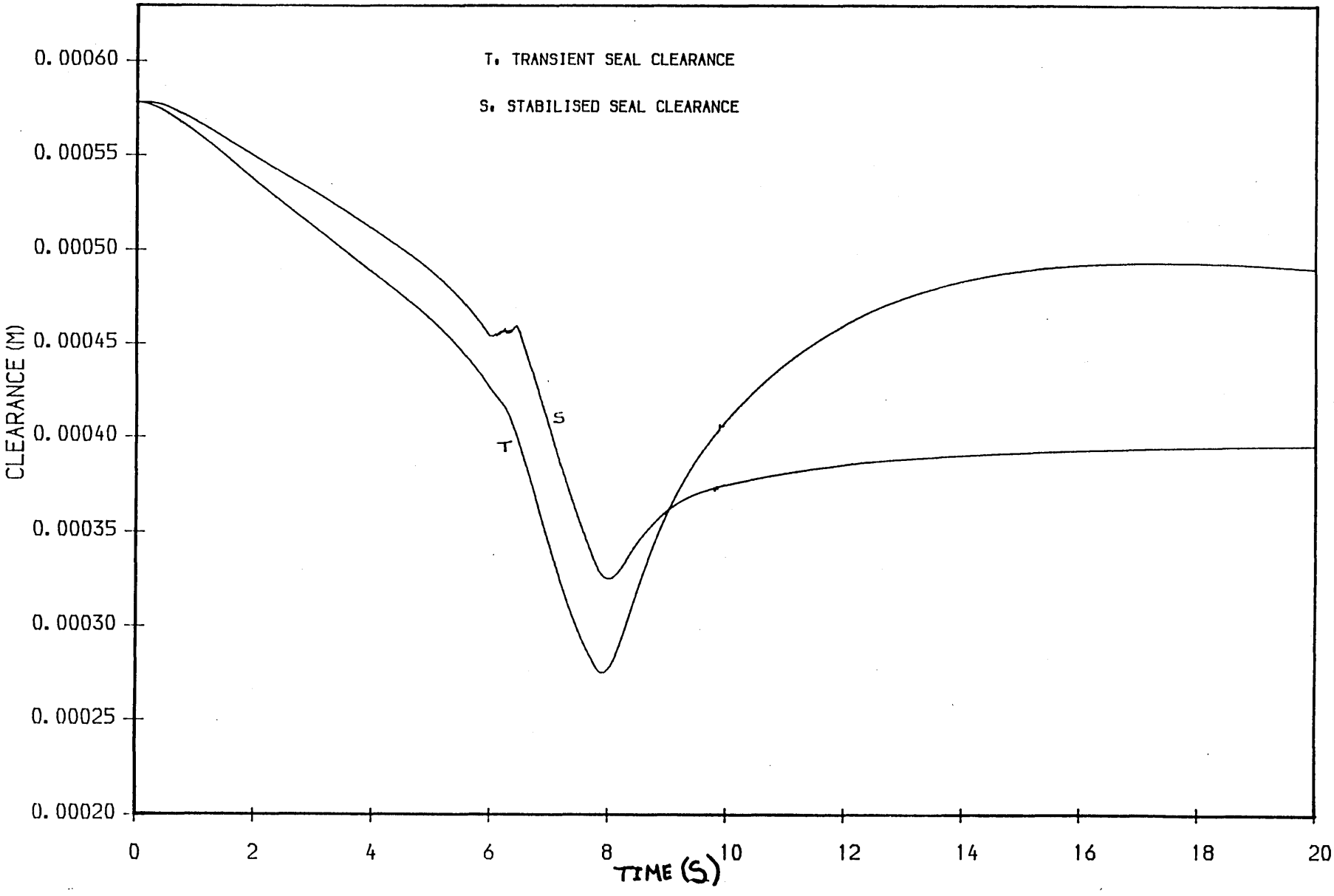

Fig. 74 H.P.T. SEAL CLEARANCE MOVEMENTS
AT SEA LEVEL TRANSIENT ACC.

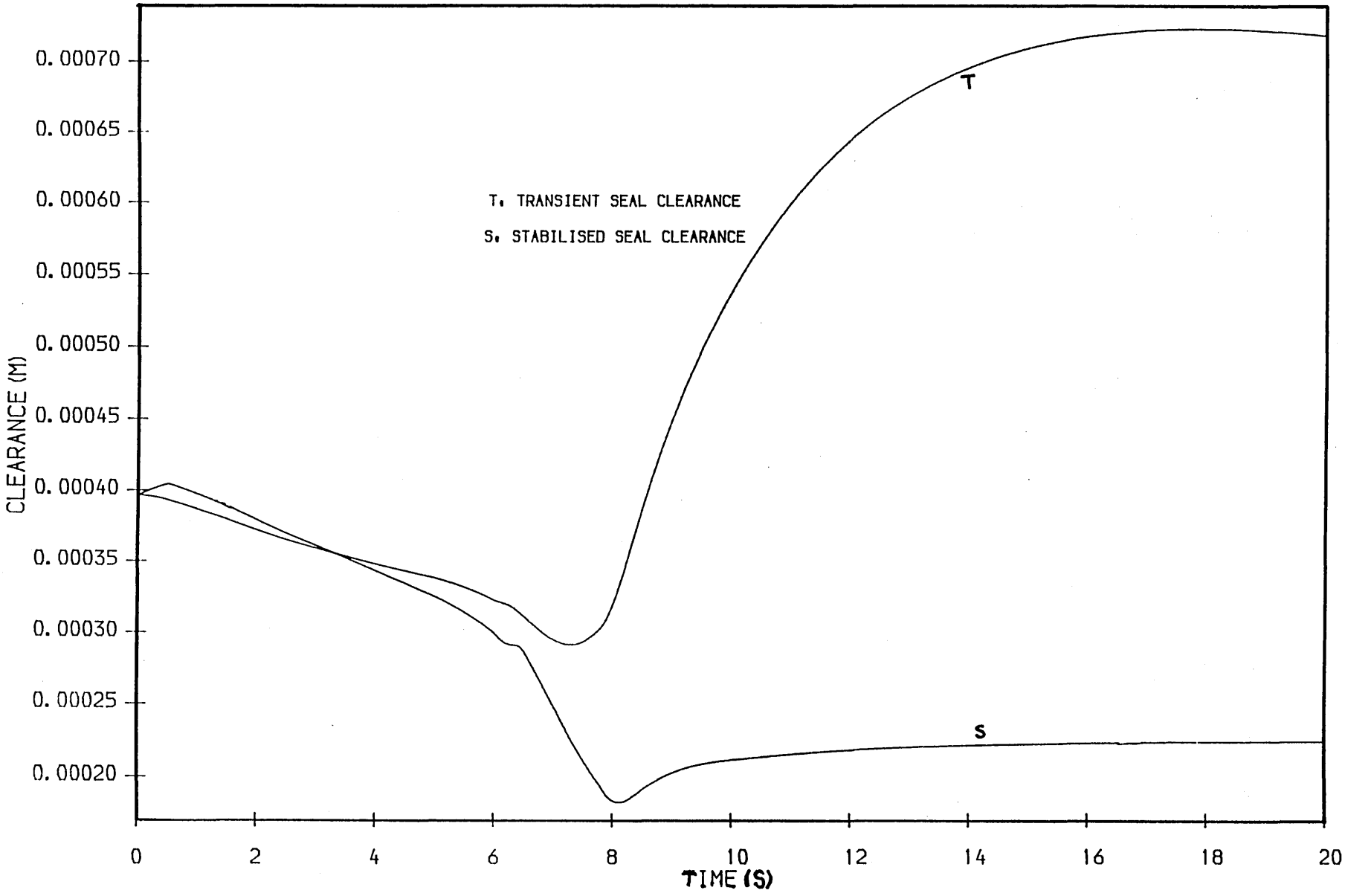

Fig. 75 H.P.C. SEAL CLEARANCE MOVEMENTS
AT 41,000 FT TRANSIENT ACC.

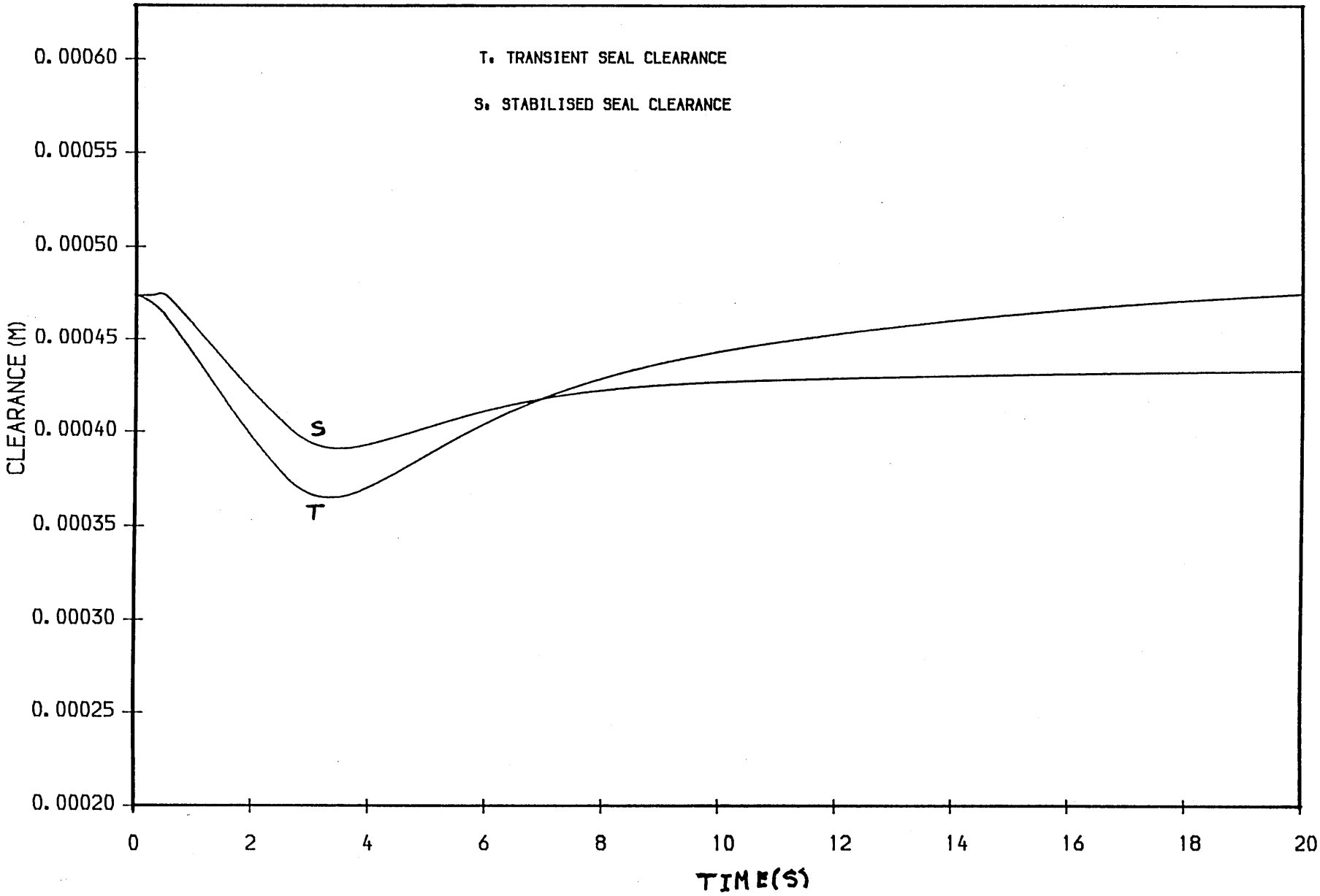

Fig. 76 H.P.T. SEAL CLEARANCE MOVEMENTS
AT 41,000 FT TRANSIENT ACC.

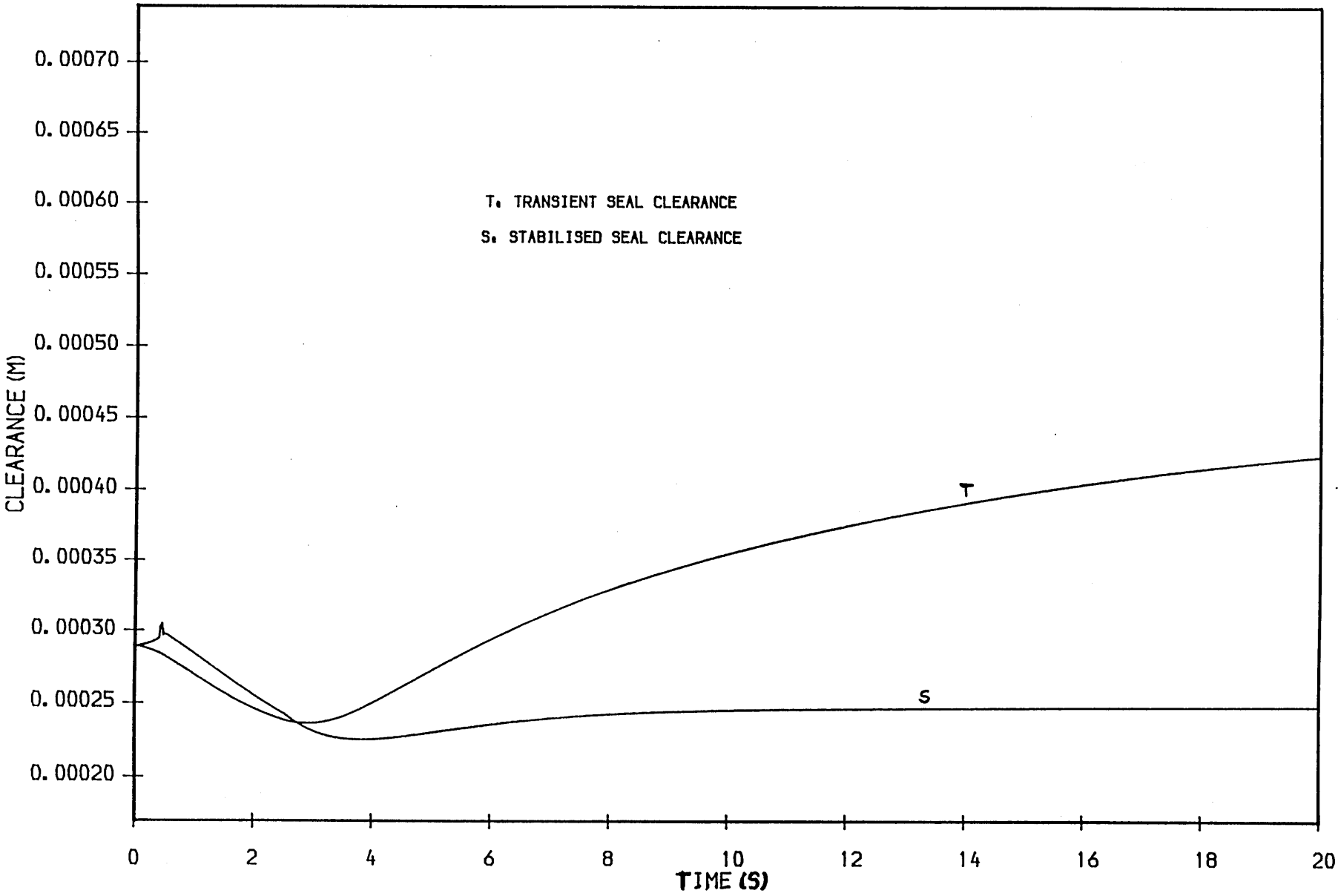

Fig. 77 H.P.C. SEAL CLEARANCE MOVEMENTS
AT SE-LEVEL TRANSIENT DEC.

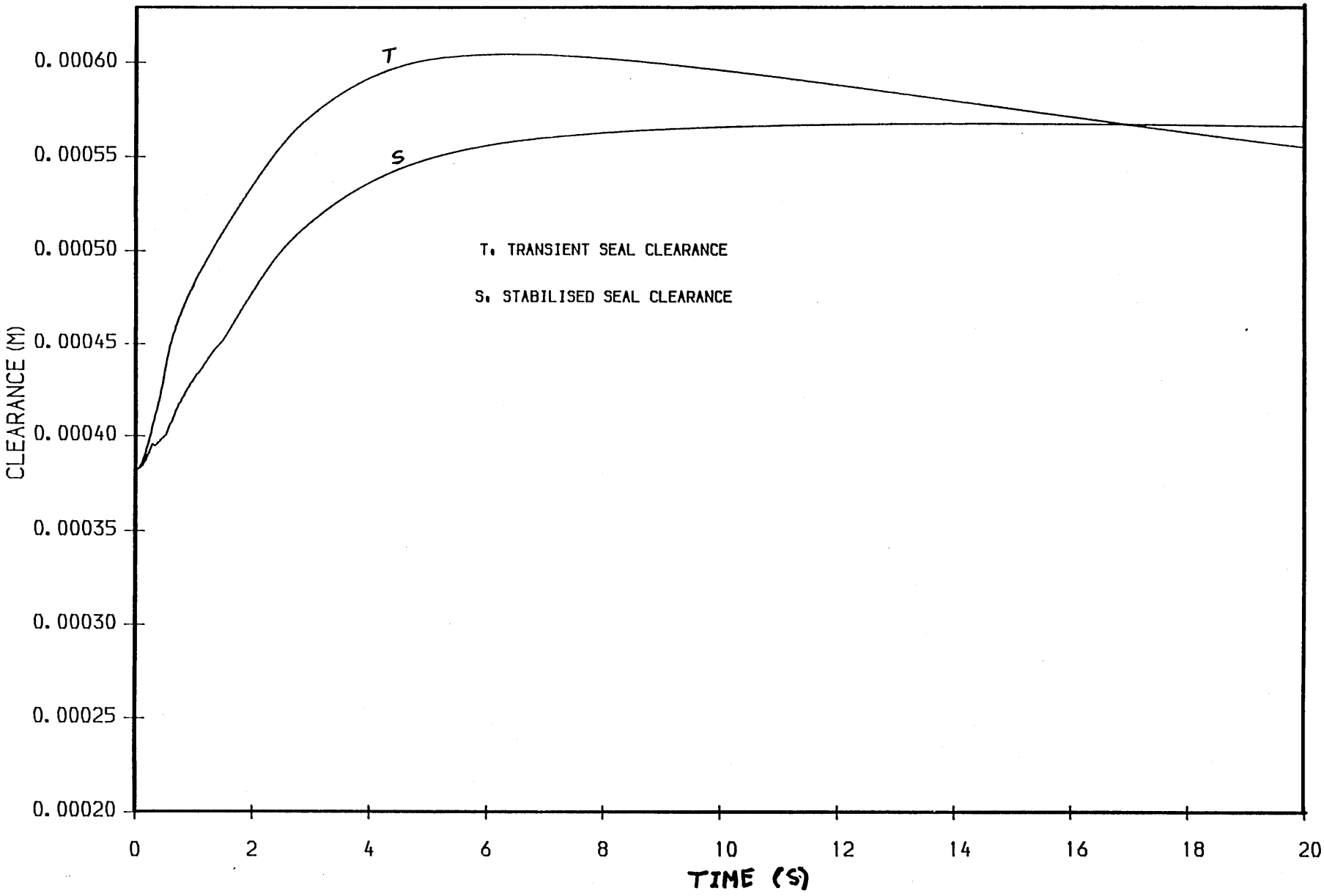

Fig. 78 H.P.T. SEAL CLEARANCE MOVEMENTS
AT SEA-LEVEL TRANSIENT DEC.

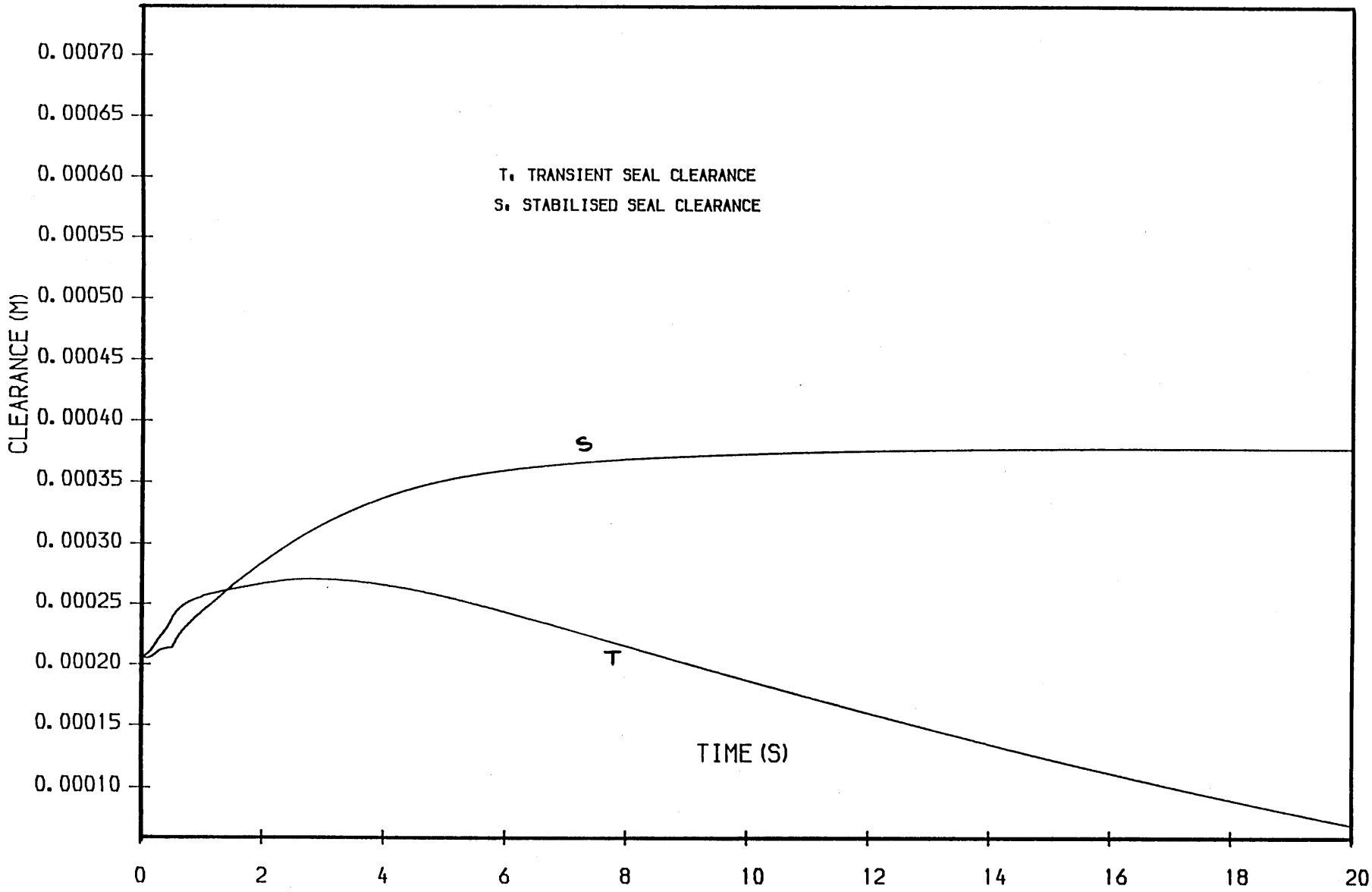

Fig. 79 H.P.C. SEAL CLEARANCE MOVEMENTS
AT 41,000 ft TRANSIENT DEC.

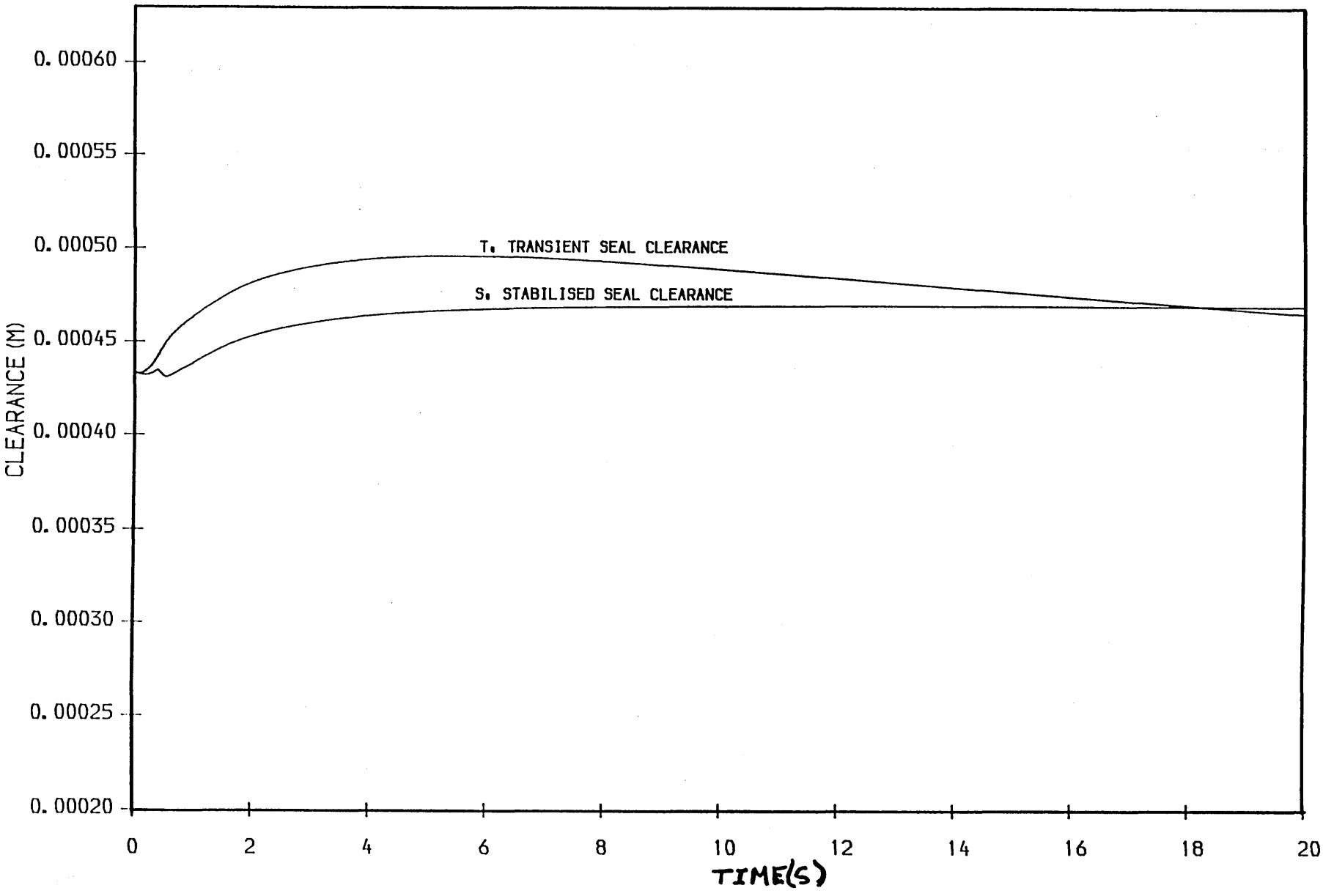

Fig. 80 H.P.T. SEAL CLEARANCE MOVEMENTS
AT 41,000 ft TRANSIENT DEC.

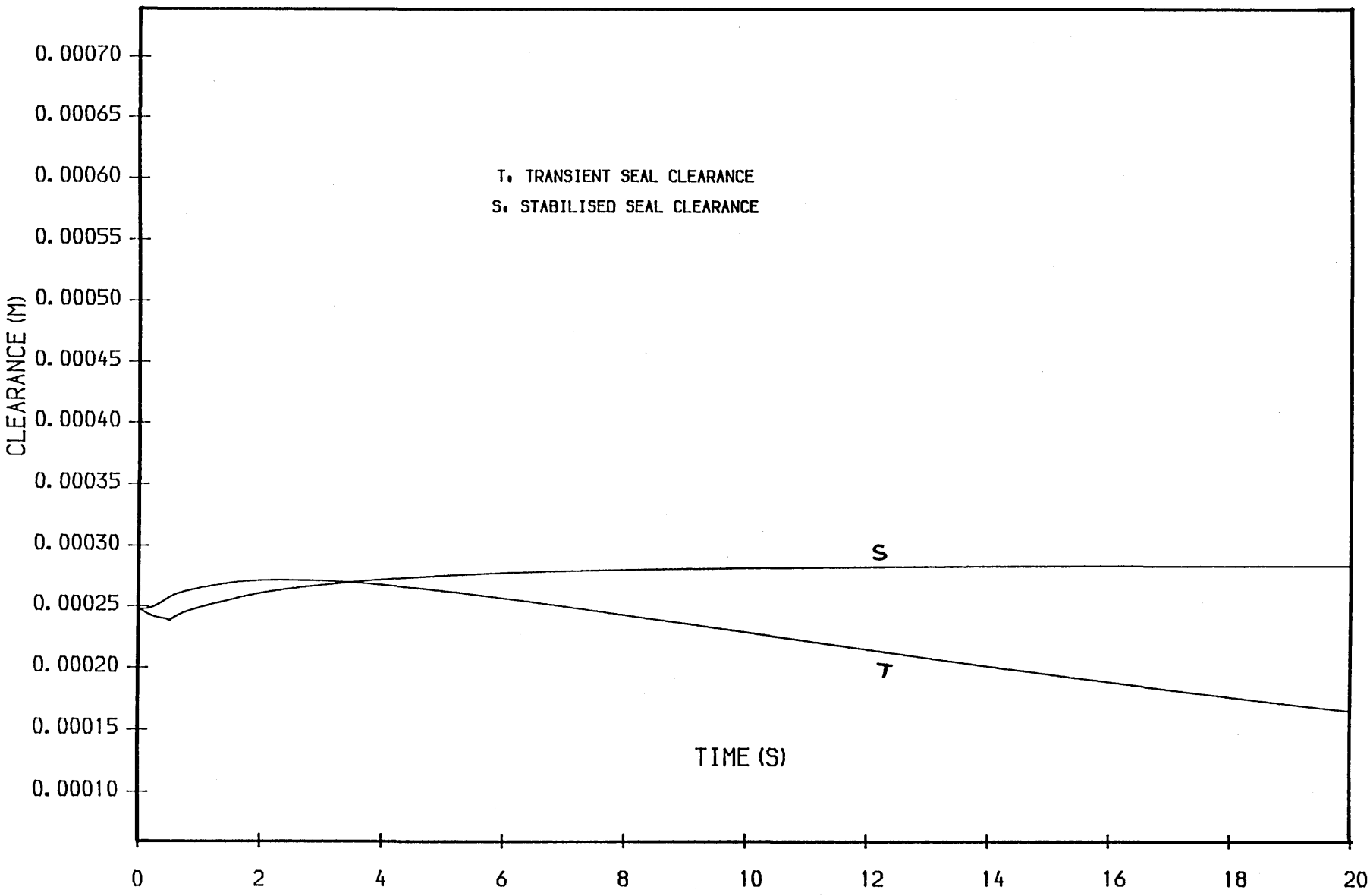

Fig. 81 H.P.C. SEAL CLEARANCE MOVEMENTS
AT SEA-LEVEL TRANSIENT HOT ACC.

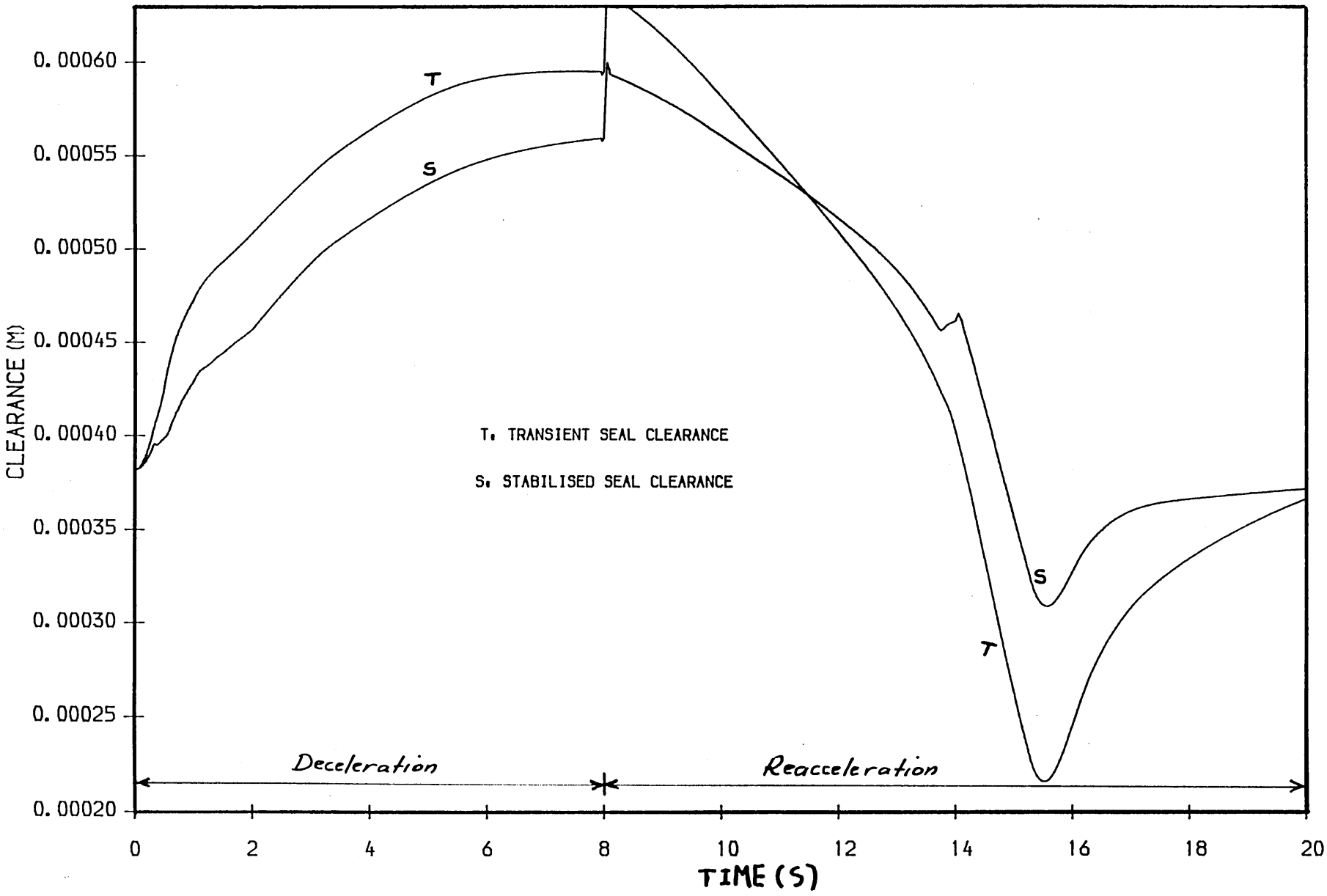

Fig. 82 H.P.T. SEAL CLEARANCE MOVEMENTS
AT SEA-LEVEL TRANSIENT HOT ACC.

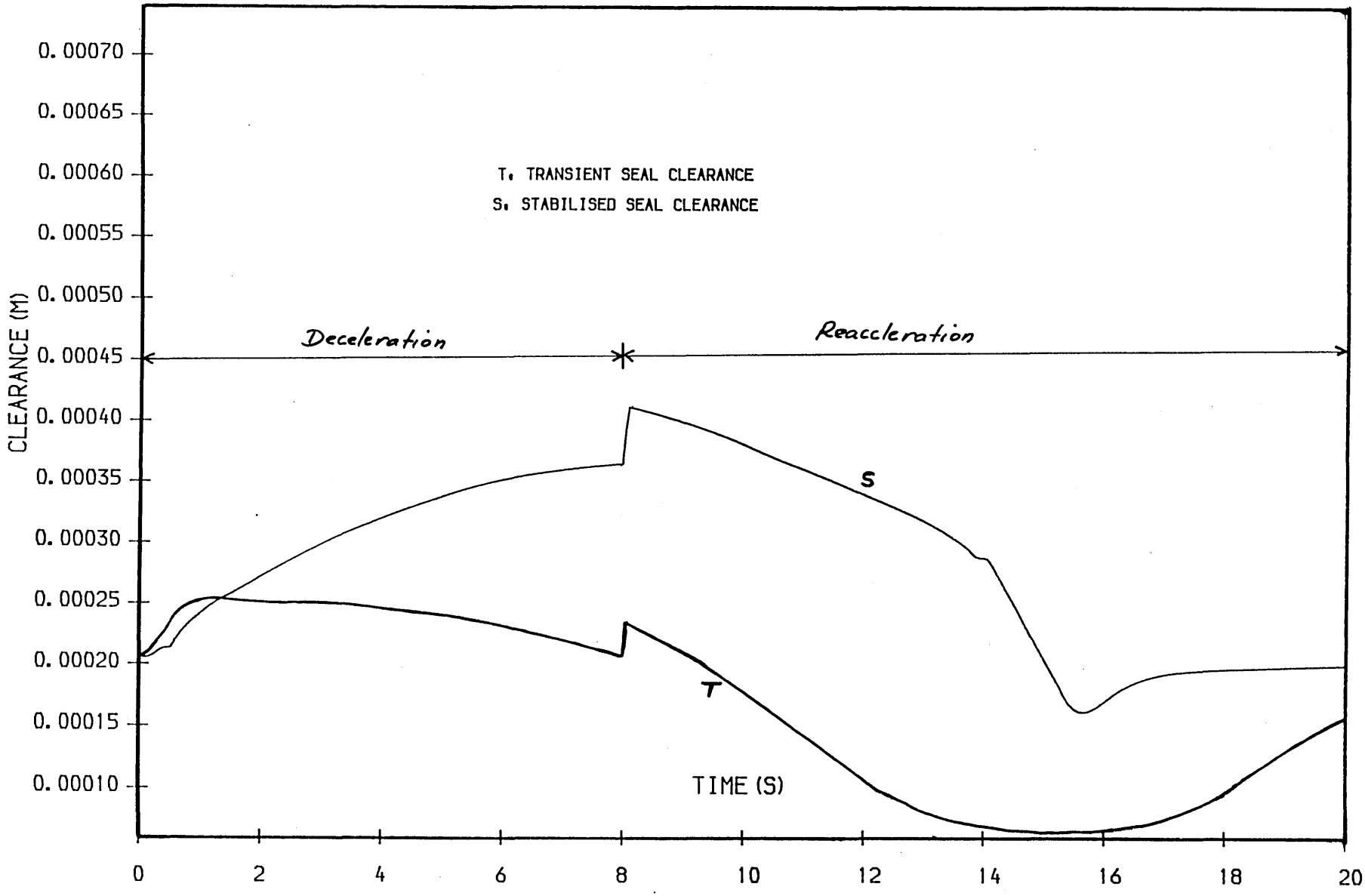

Fig. 83 H.P.C. SEAL CLEARANCE MOVEMENTS
AT 41,000 ft TRANSIENT HOT ACC.

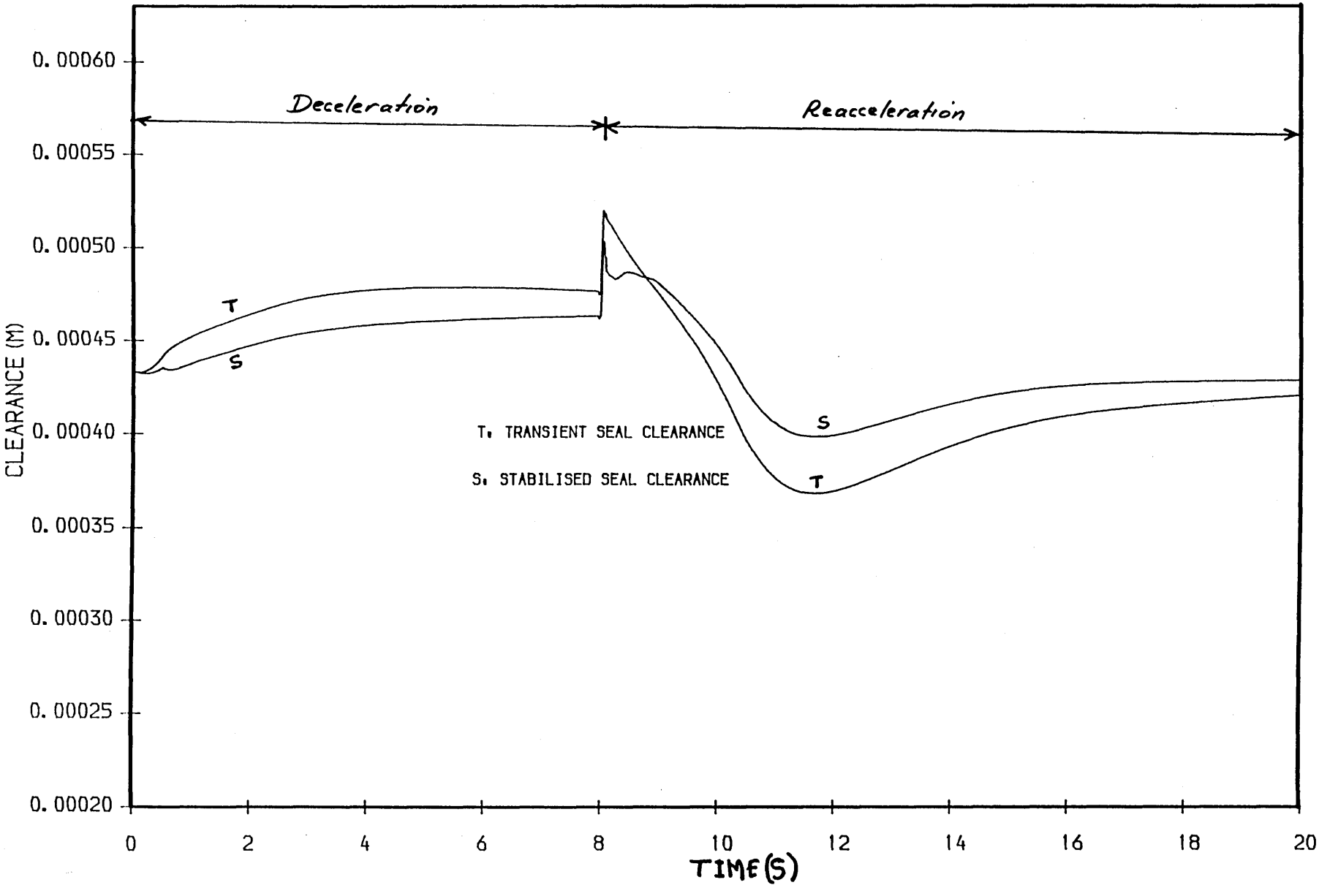

Fig. 84 H.P.T. SEAL CLEARANCE MOVEMENTS
AT 41,000 ft TRANSIENT HOT ACC.

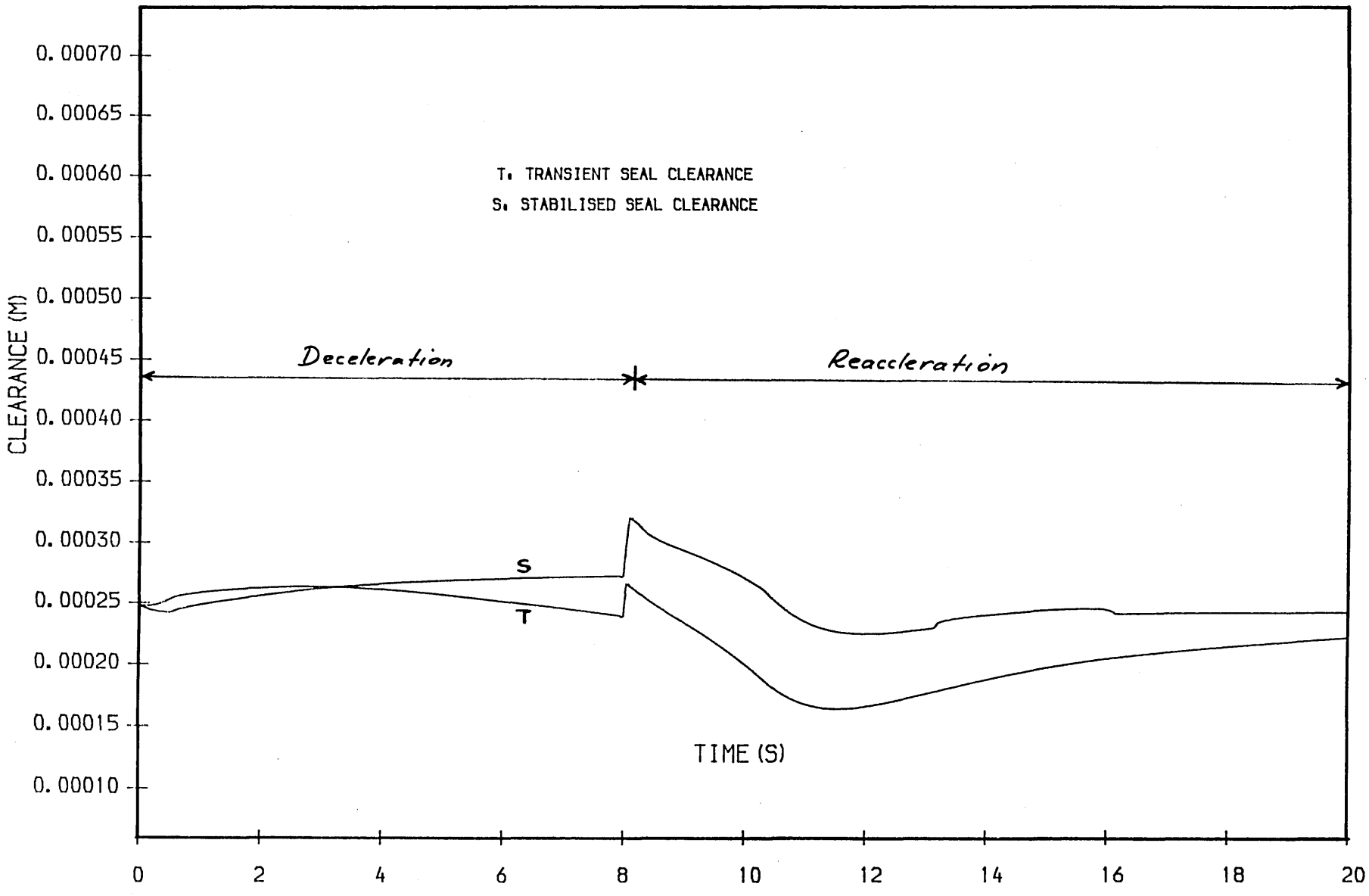

Fig. 85 H.P.C. TIP CLEAR. EFFICIENCY CHANGES AND LOSS AT SEA LEVEL TRANSIENT ACC.

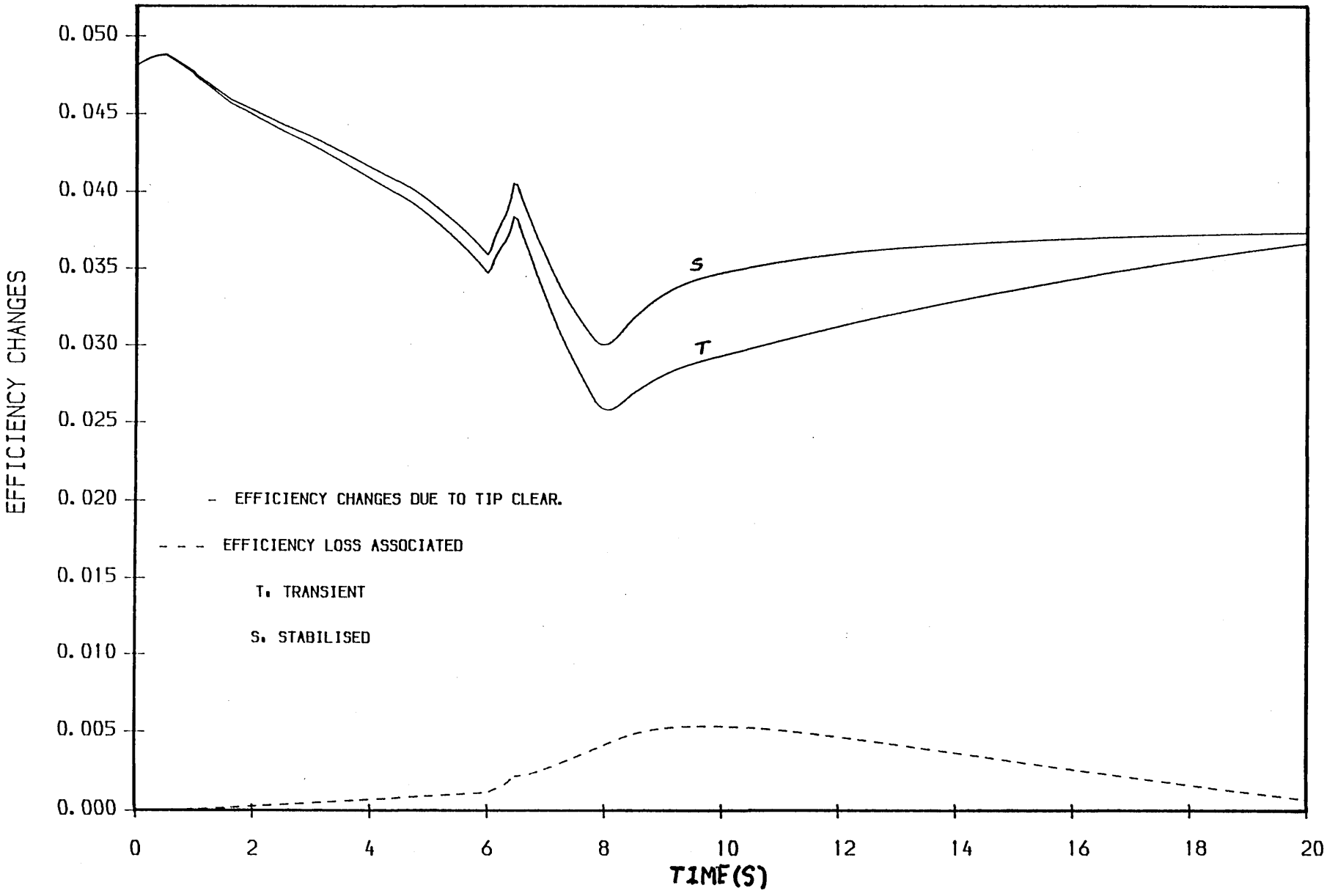

Fig. 86 H.P.C. SEAL CLEARANCE MOVEMENTS
AT 41,000 FT TRANSIENT DEC.

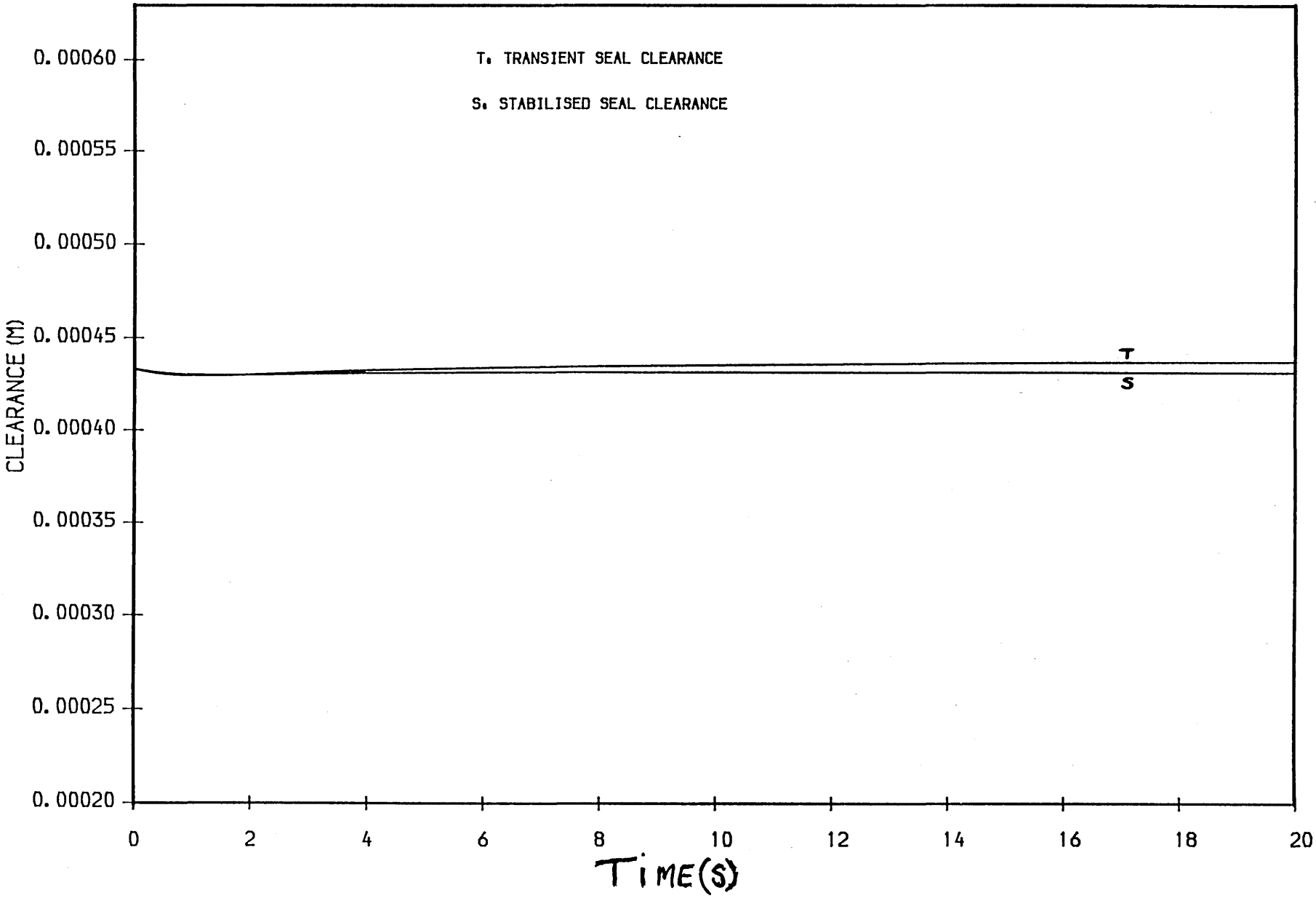

Fig. 87 H.P.T. SEAL CLEARANCE MOVEMENTS
AT 41,000 FT TRANSIENT DEC.

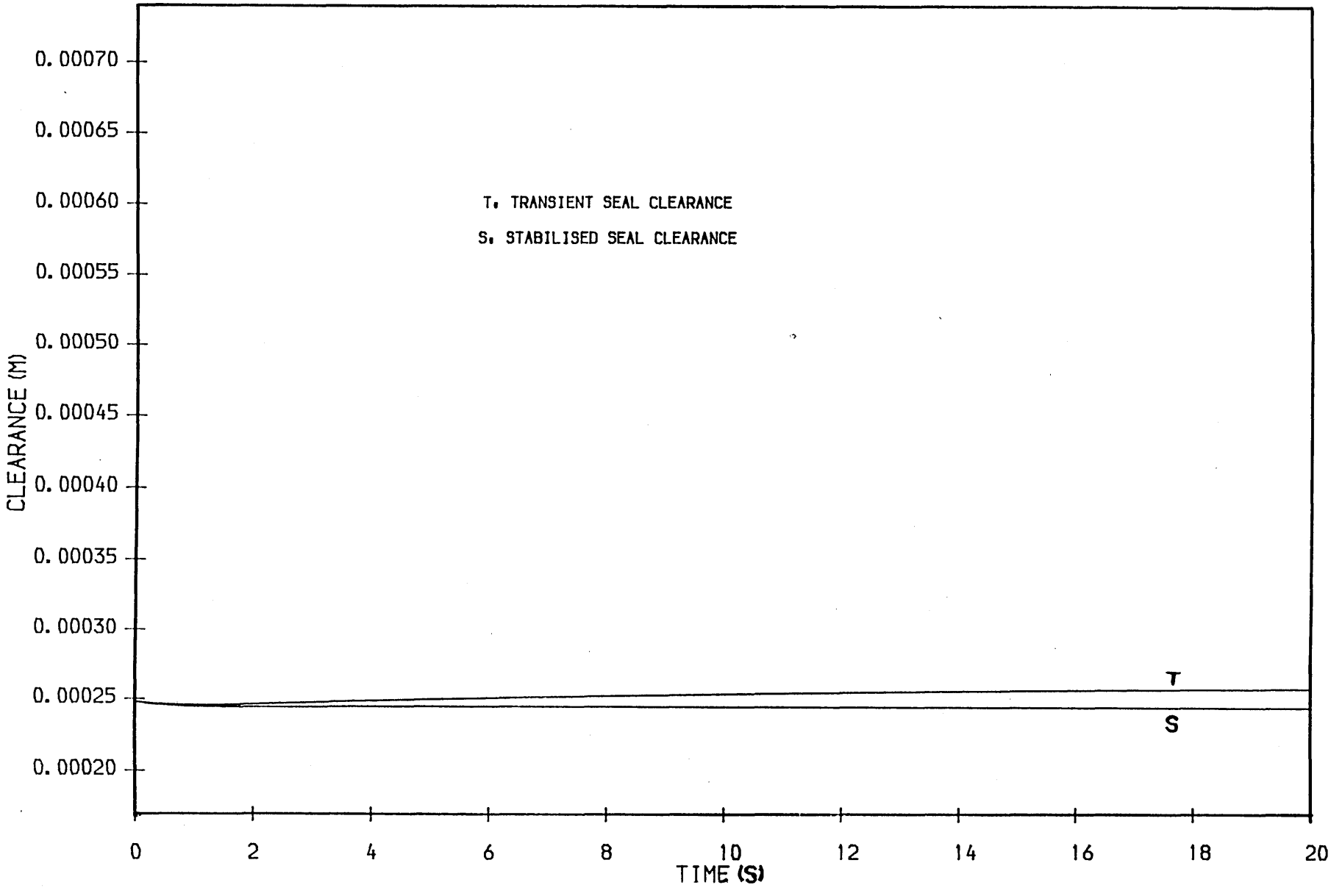

Fig. 88 H.P.T. TIP CLEAR. EFFICIENCY CHANGES AND LOSS AT SEA LEVEL TRANSIENT ACC.

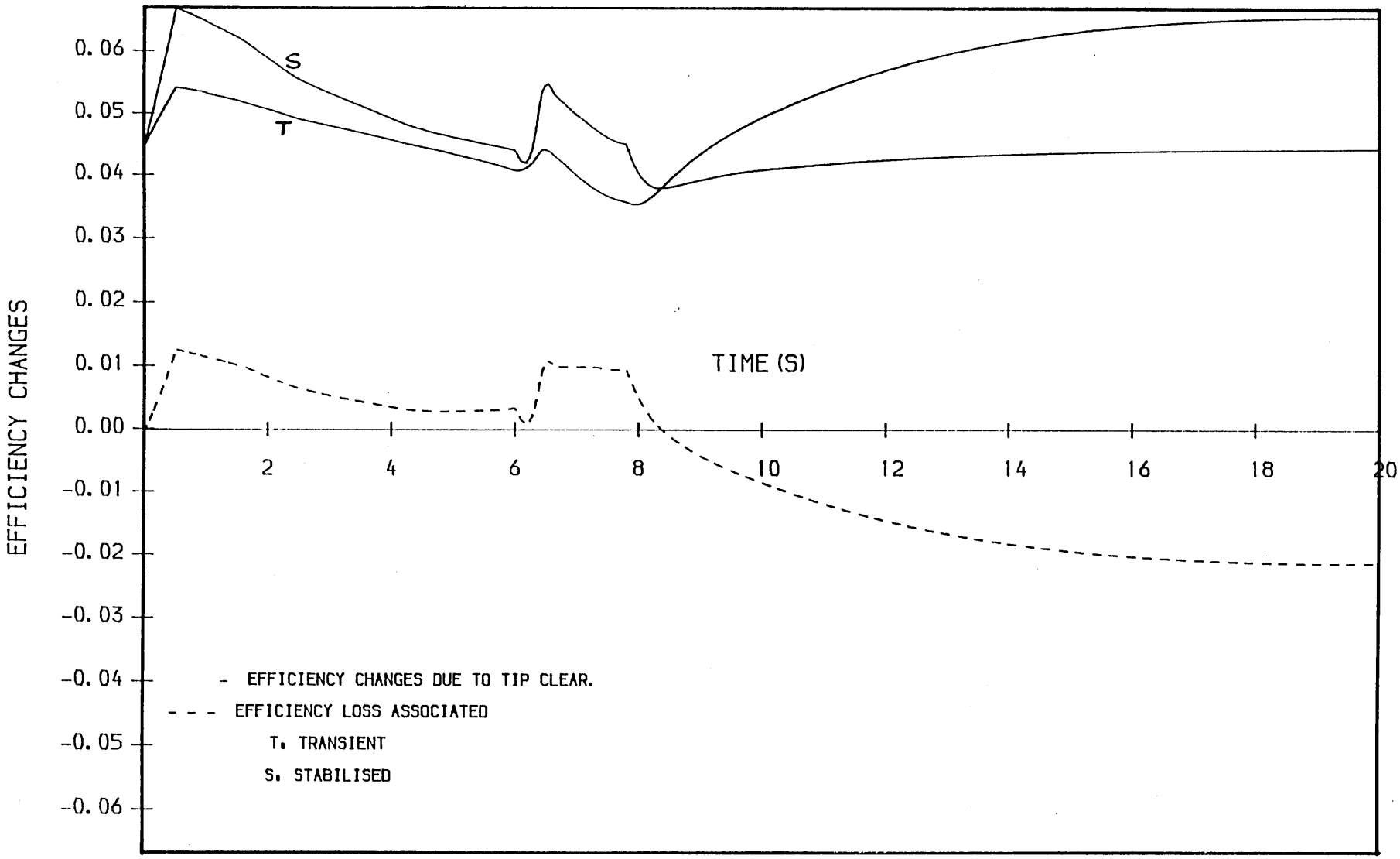

Fig. 89 H.P.C. TIP CLEAR. EFFICIENCY CHANGES AND LOSS AT 41,000 FT TRANSIENT ACC.

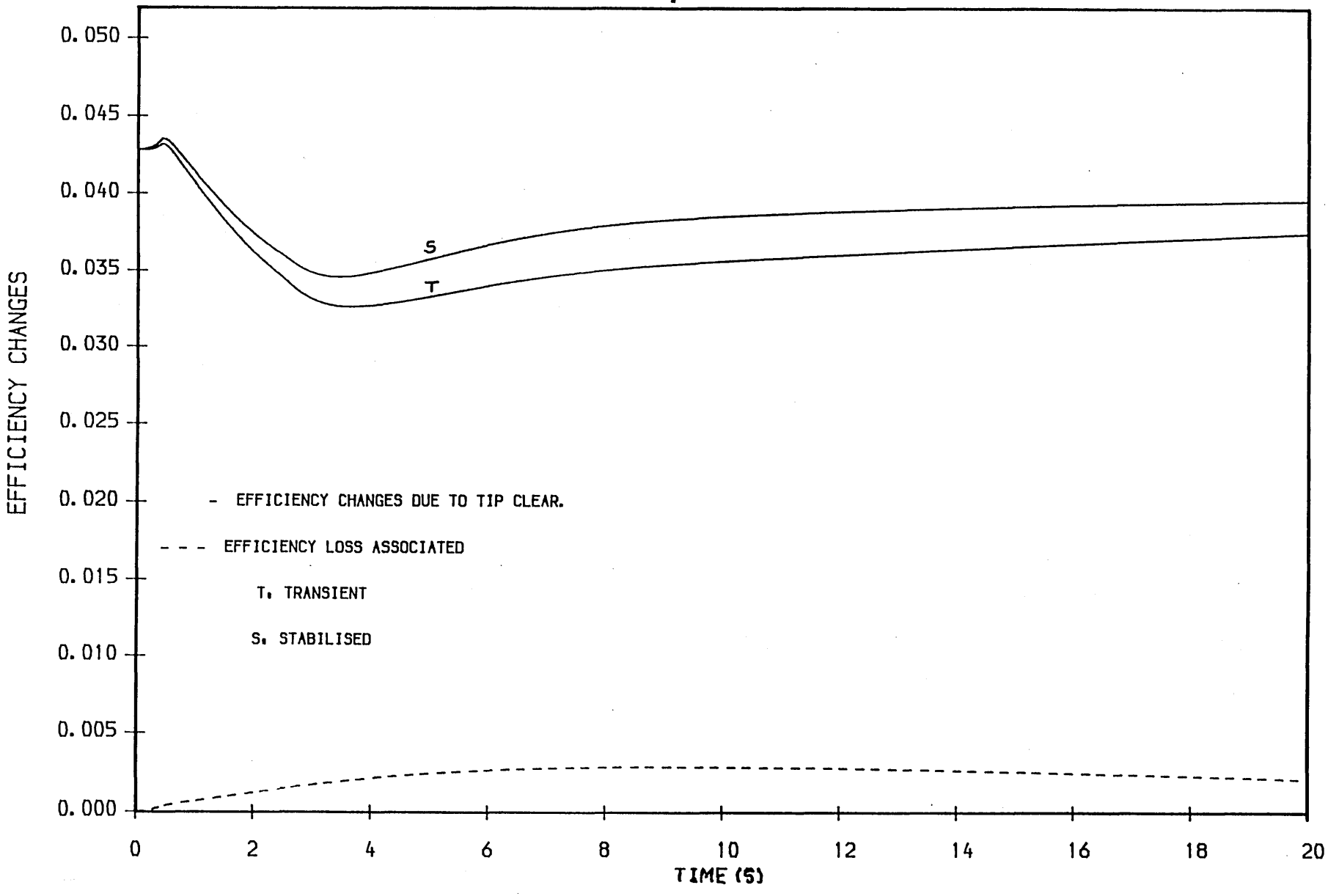

Fig. 90 H.P.T. TIP CLEAR. EFFICIENCY CHANGES AND LOSS AT 41,000 FT TRANSIENT ACC.

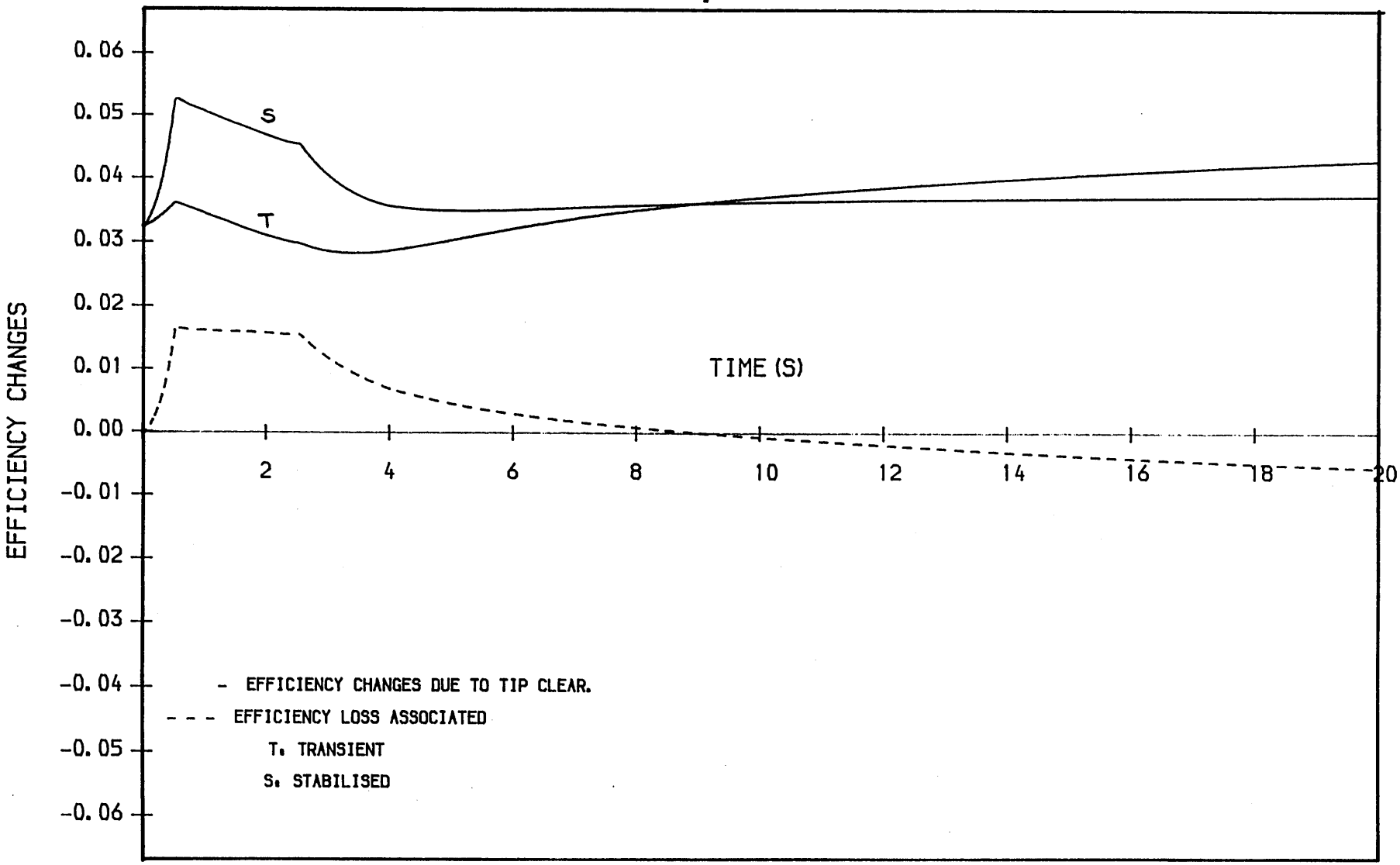

Fig. 91 H.P.C. TIP CLEAR. EFFICIENCY CHANGES
AND LOSS AT SEA-LEVEL TRANSIENT DEC.

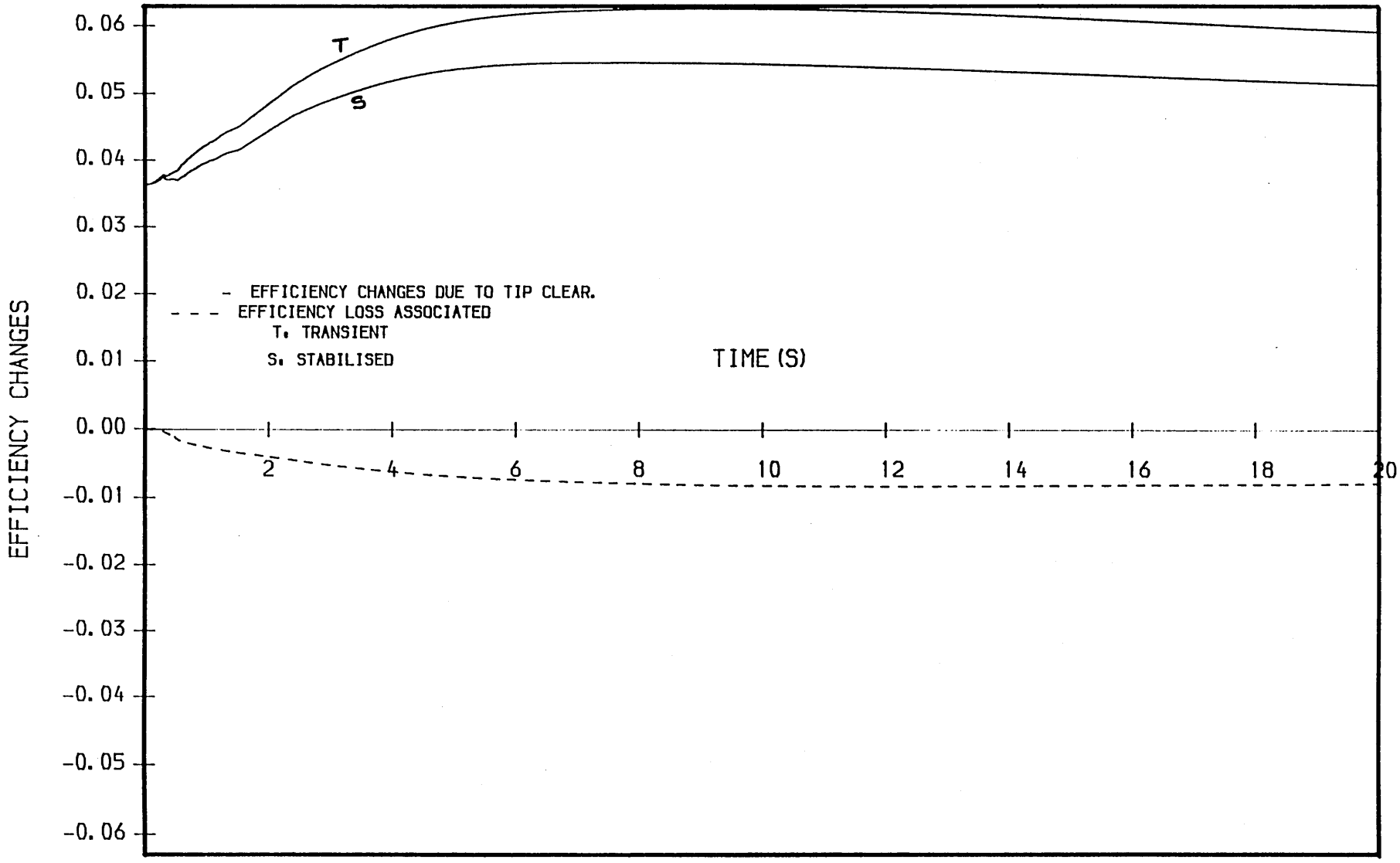

Fig. 92 H.P.T. TIP CLEAR. EFFICIENCY CHANGES AND LOSS AT SEA-LEVEL TRANSIENT DEC.

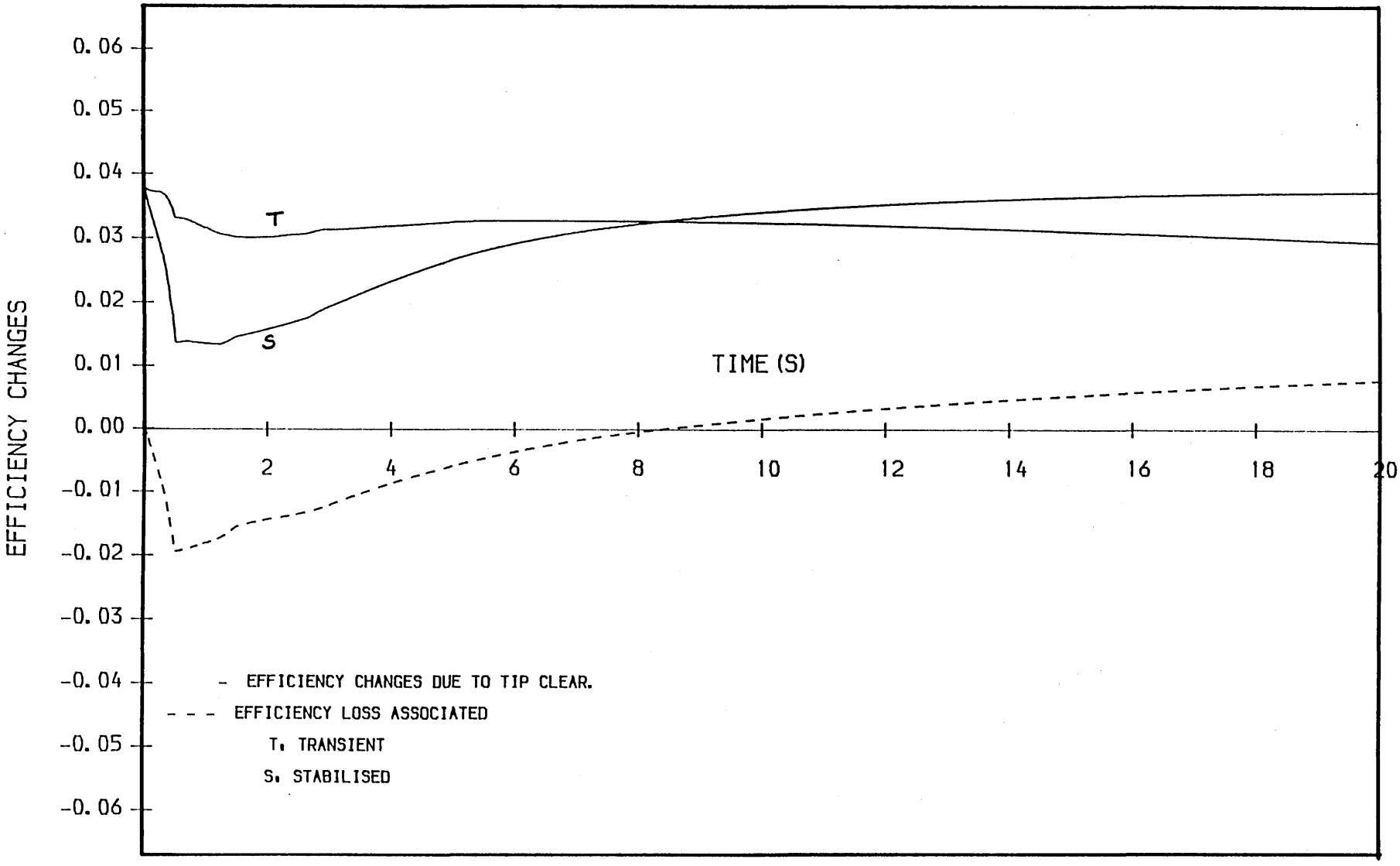

Fig. 93 H.P.C. TIP CLEAR. EFFICIENCY CHANGES AND LOSS AT 41,000 ft TRANSIENT DEC.

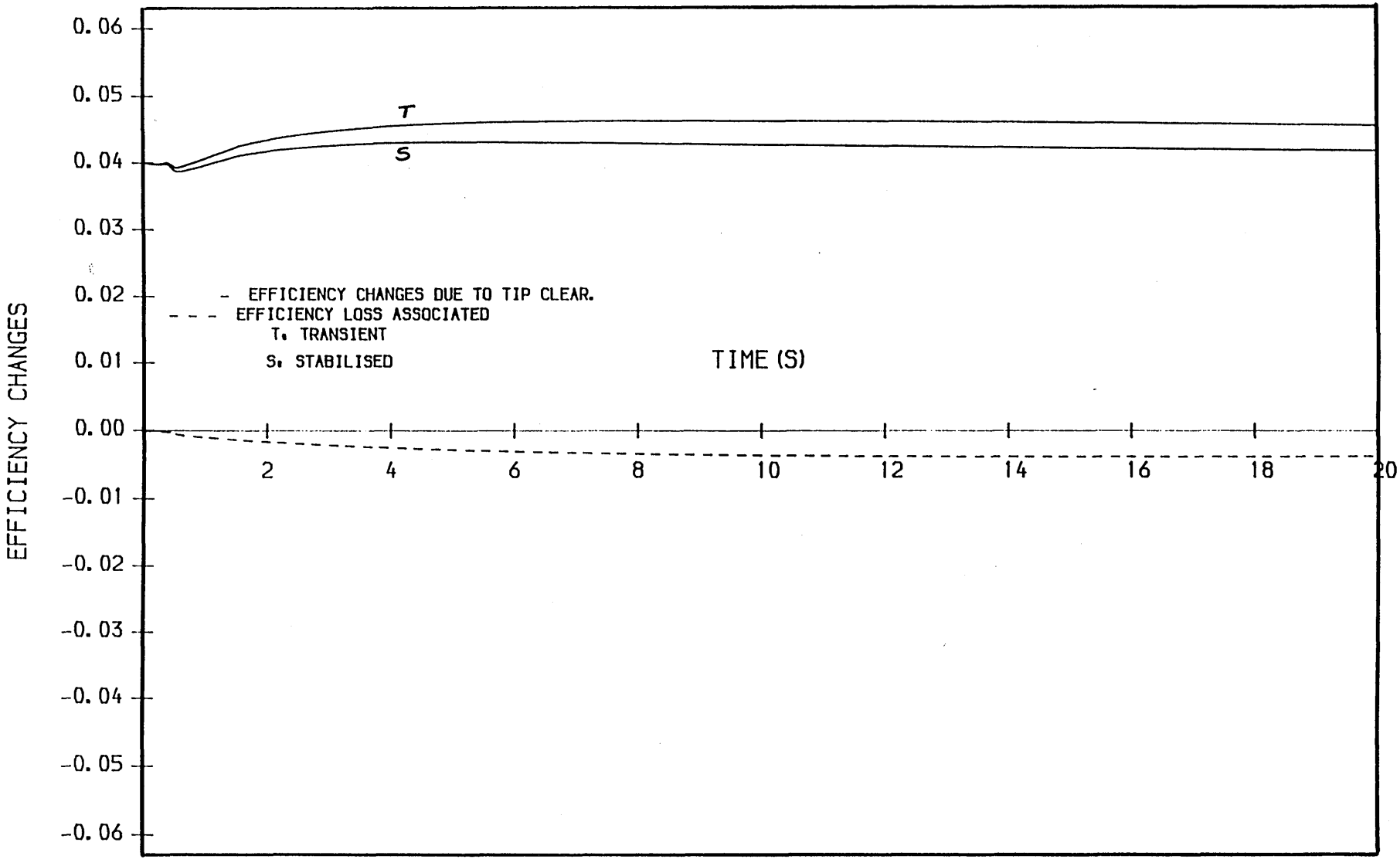

Fig. 94 H.P.T. TIP CLEAR. EFFICIENCY CHANGES AND LOSS AT 41,000 ft TRANSIENT DEC.

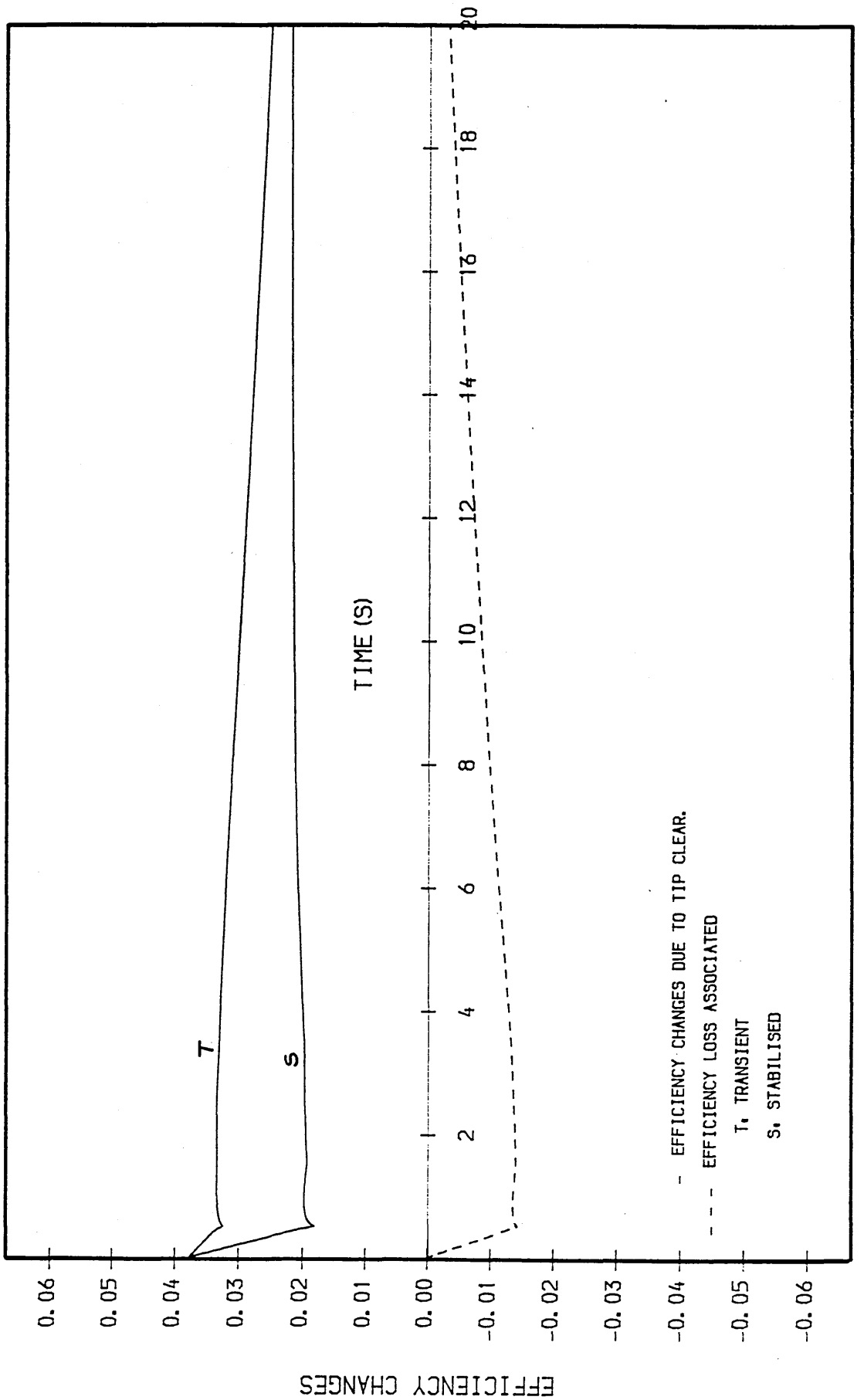

Fig. 95 H.P.C. TIP CLEAR. EFFICIENCY CHANGES AND LOSS AT SEA-LEVEL TRANS. HOT ACC.

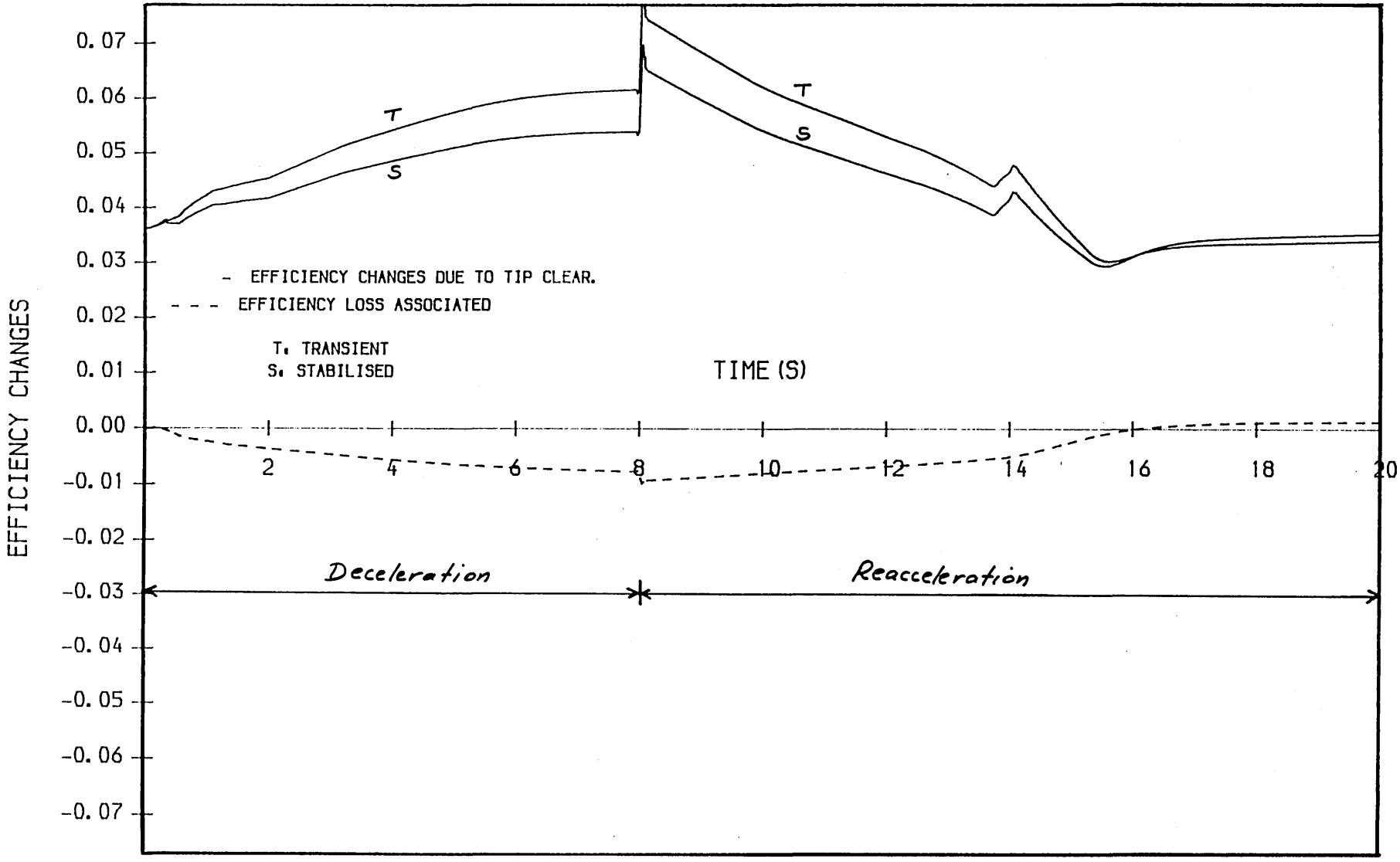

Fig. 96 H.P.T. TIP CLEAR. EFFICIENCY CHANGES AND LOSS AT SEA-LEVEL TRANS. HOT ACC.

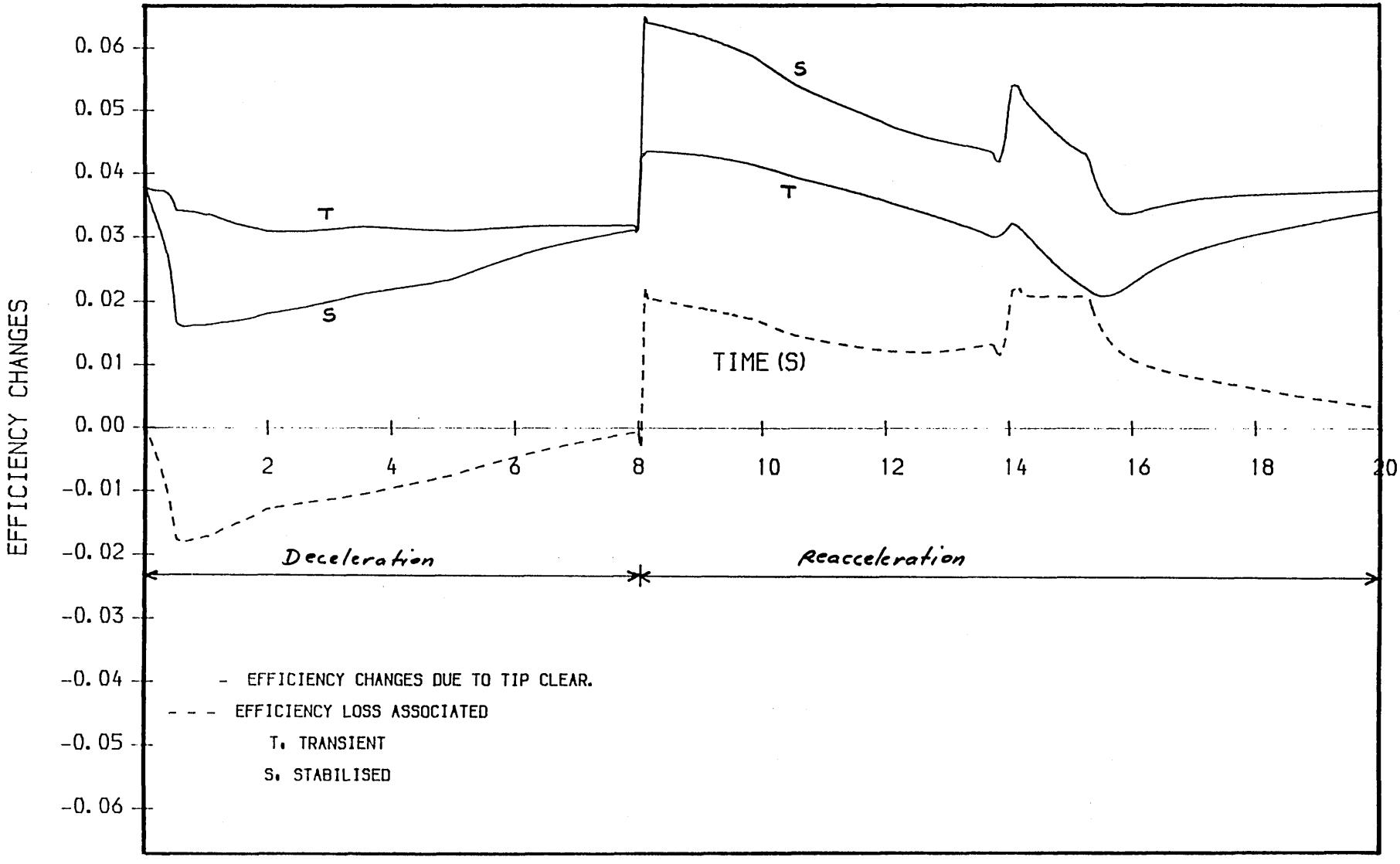

Fig. 97 H.P.C. TIP CLEAR. EFFICIENCY CHANGES
AND LOSS AT 41,000 ft TRANS. HOT ACC.

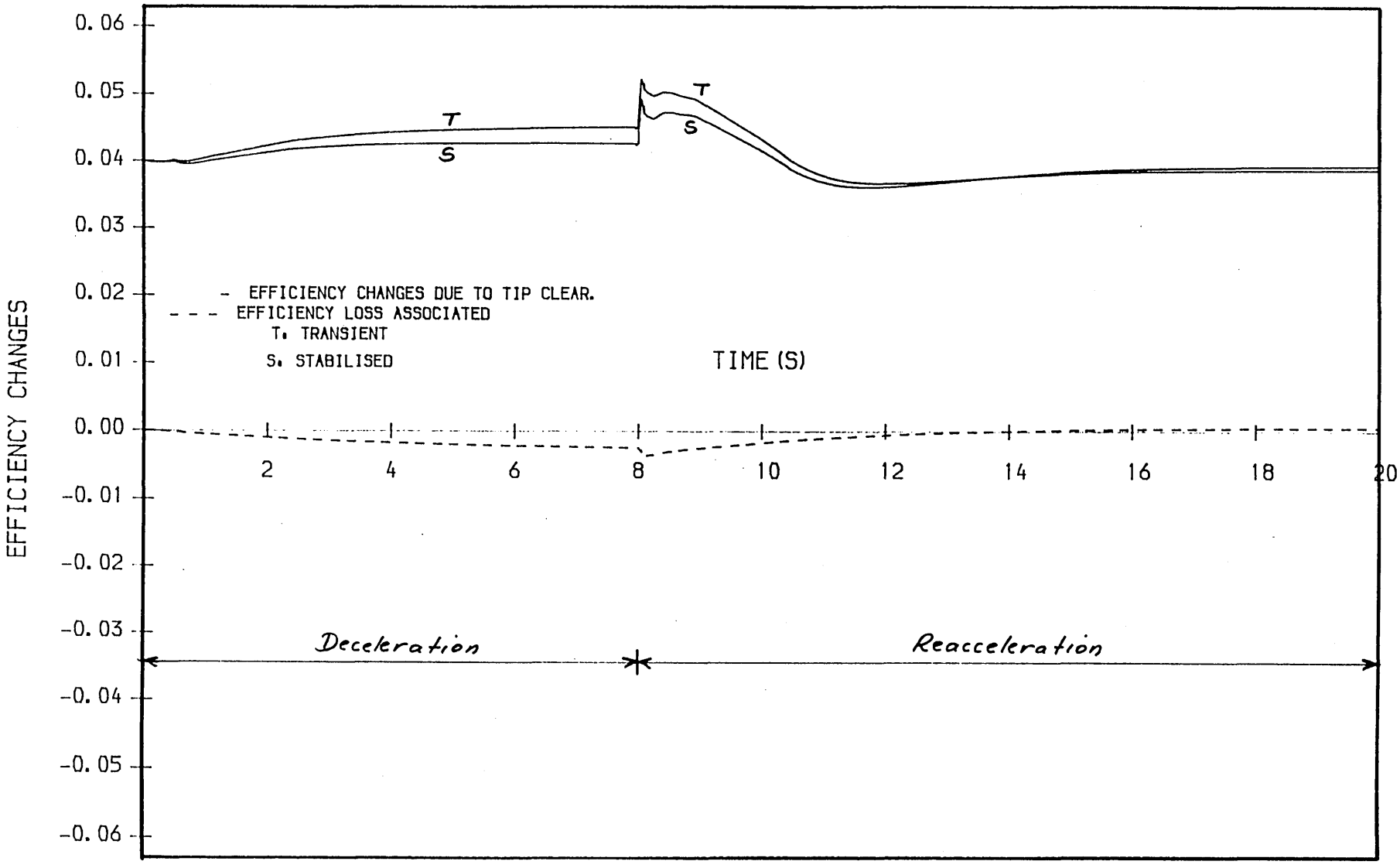

Fig. 98 H.P.T. TIP CLEAR. EFFICIENCY CHANGES
AND LOSS AT 41,000 ft TRANS. HOT ACC.

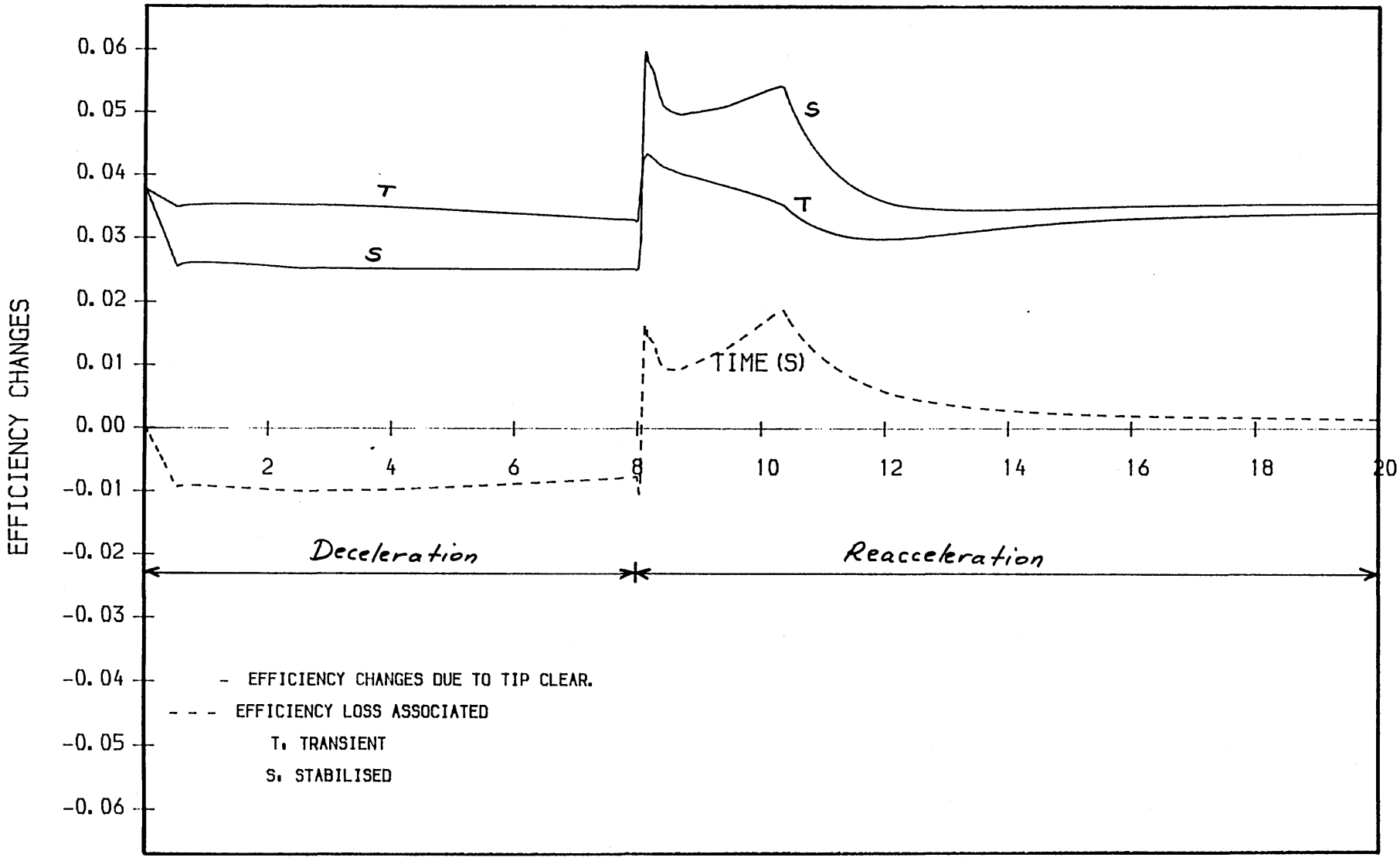

Fig. 99 ACCELERATION AND DECELERATION FUEL SCHEDULES OF A TWO-SPOOL TURBOFAN ENGINE DEFINED AS FRACTIONS OF CASC-211

(a) AT SEA-LEVEL; MACH 0.2

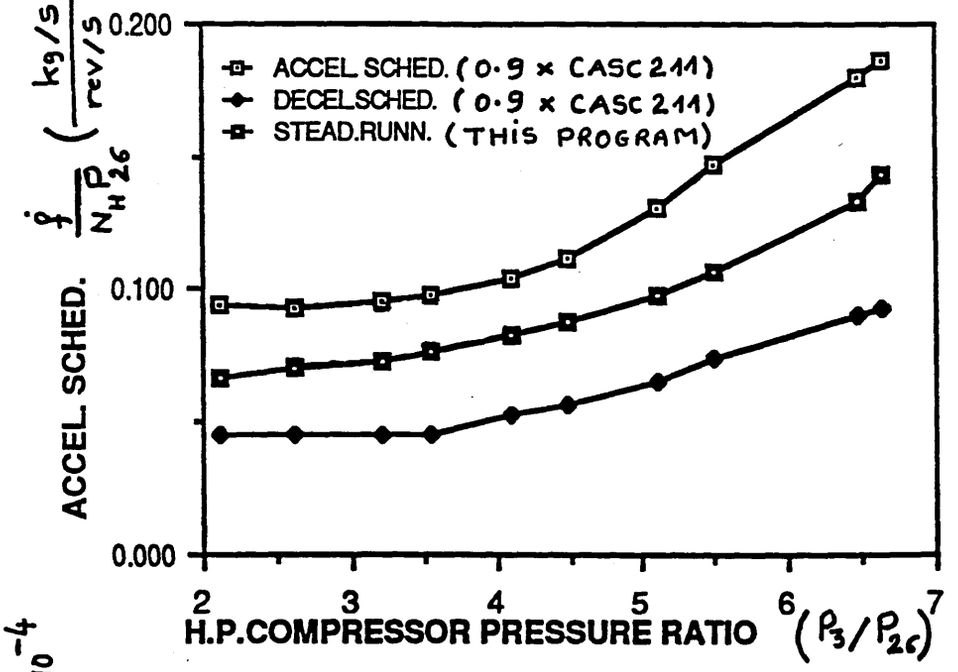

(b) AT 41,000 ft ; MACH 0.8

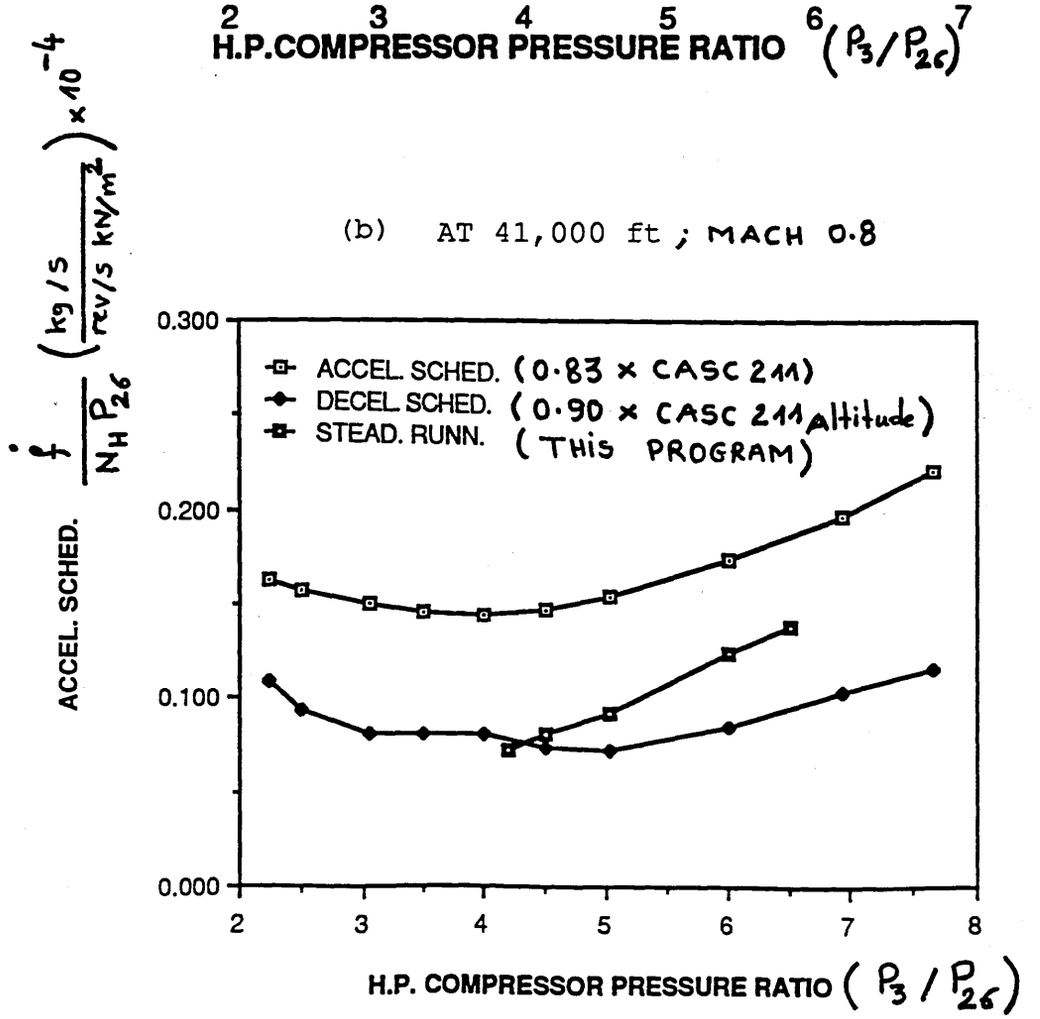

Fig. 100

PREDICTED PATHS OF THE H. P. COMP. DURING COLD ACCEL. AT SEA LEVEL FUEL SCHEDULE COMPENSATED WITH A FUNCT. OF H. P. C. BLADE TEMP. COMP.

------ WITH FUEL SCHEDULE COMPENSATED
——— HEAT TRAN. WITHOUT COMPENSATION
▲ STEADY-RUNNING

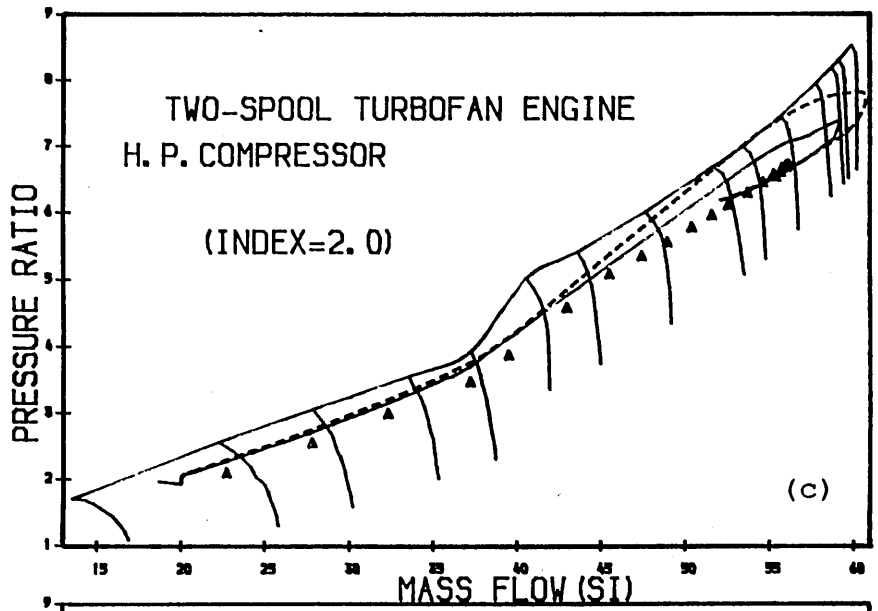

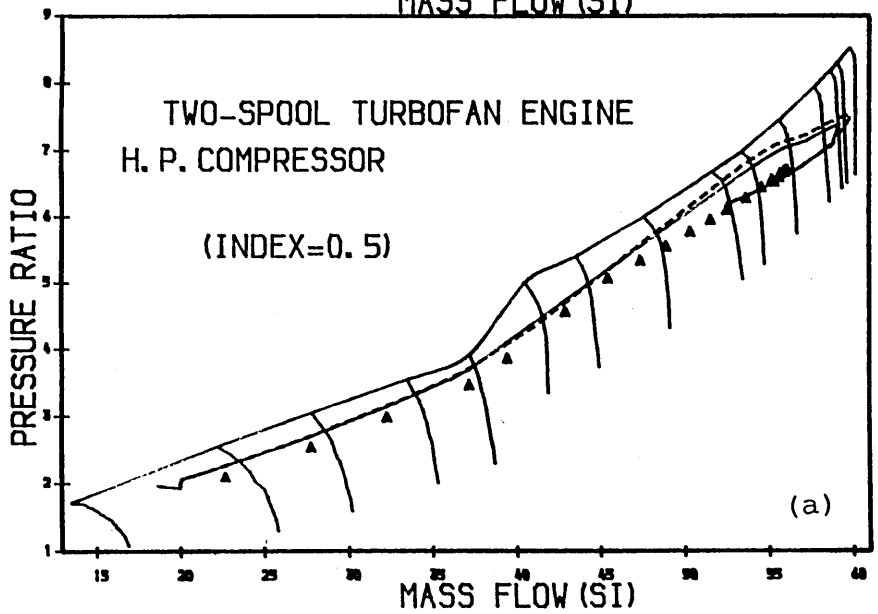

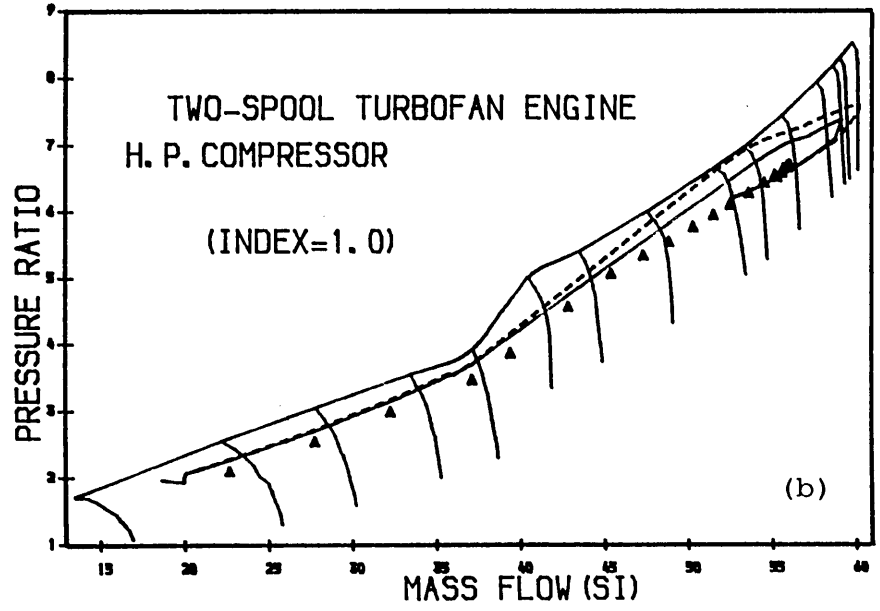

Fig. 101

PREDICTED COLD ACC. AT SEA LEVEL

FUEL SCHED. H.P.C. BLADE TEMP. COMP.

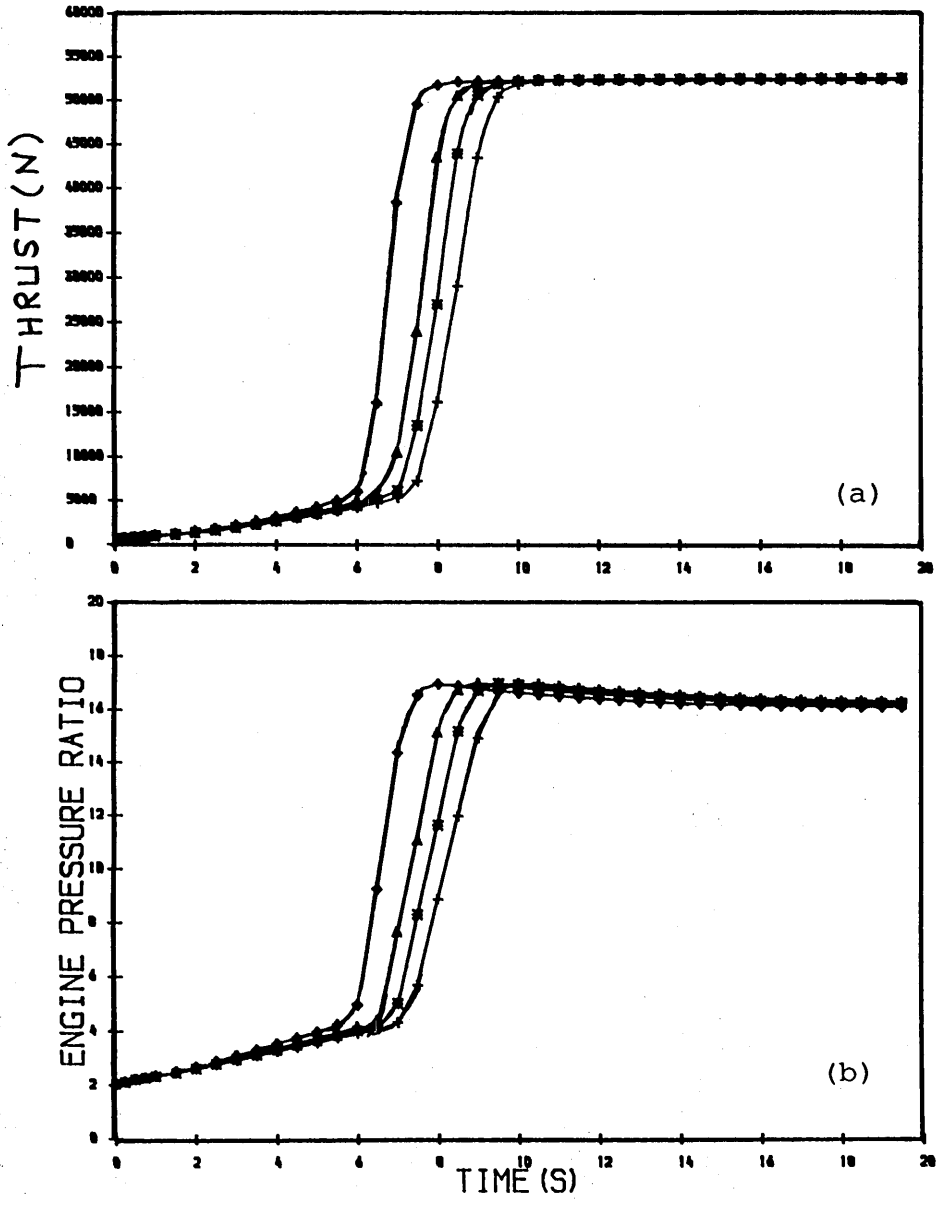

◆ FUEL COMPENSATED (INDEX=2.0)

▲ FUEL COMPENSATED (INDEX=1.0)

✱ WITH FUEL COMPENS. (INDEX=0.50)

\+ WITHOUT COMPENSATION

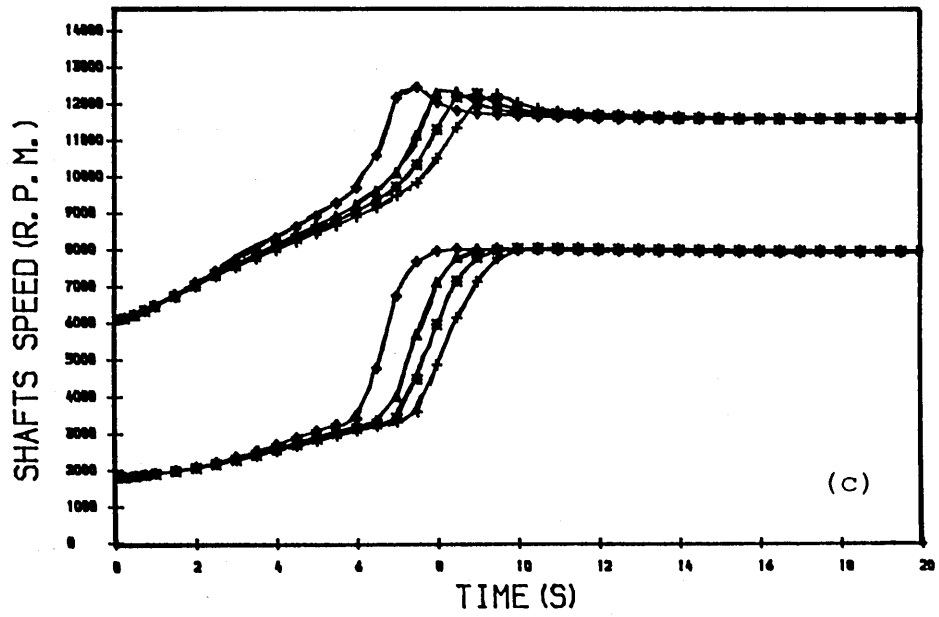

Fig. 102

PREDICTED PATHS OF THE H.P. COMP. DURING HOT ACCEL. AT SEA LEVEL FUEL SCHEDULE COMPENSATED WITH A FUNCT. OF H.P.C. BLADE TEMP. COMP.

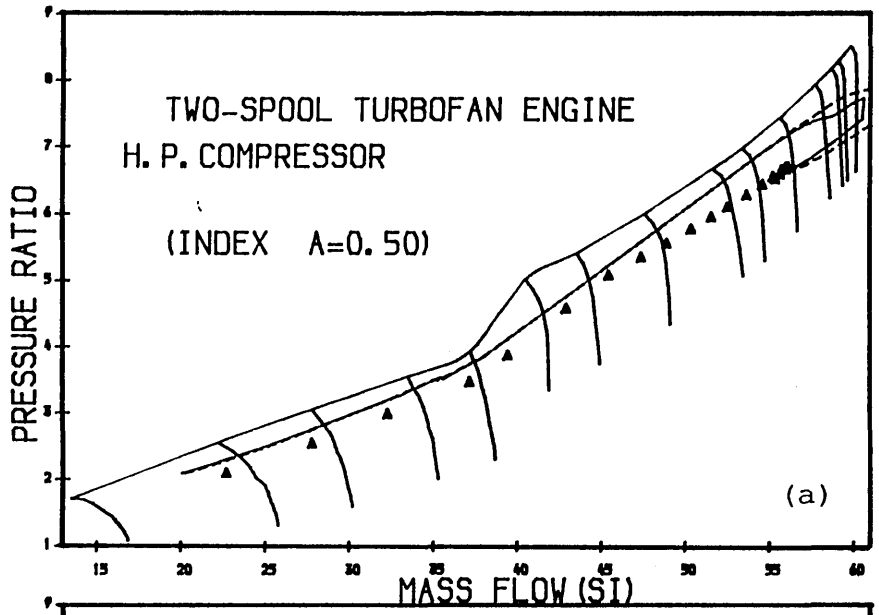

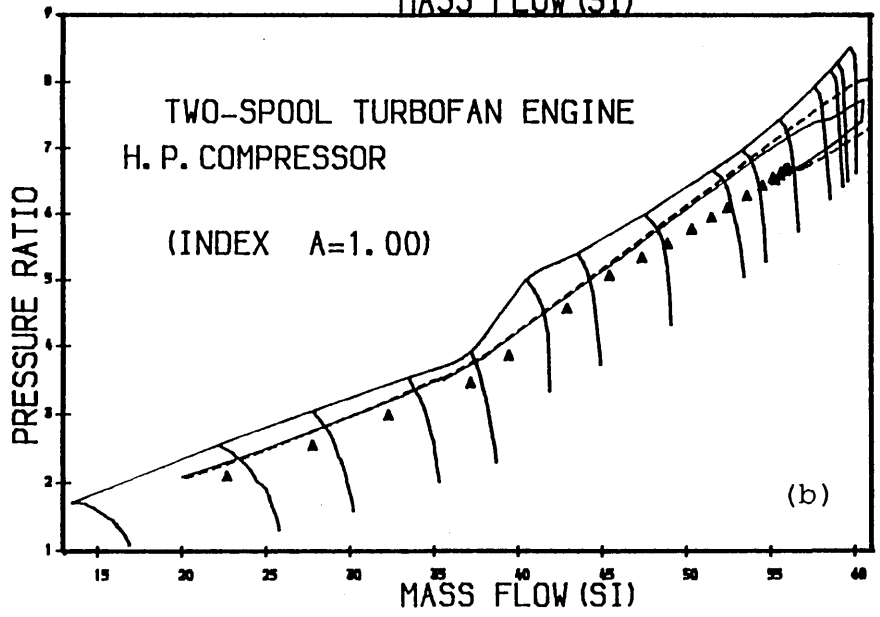

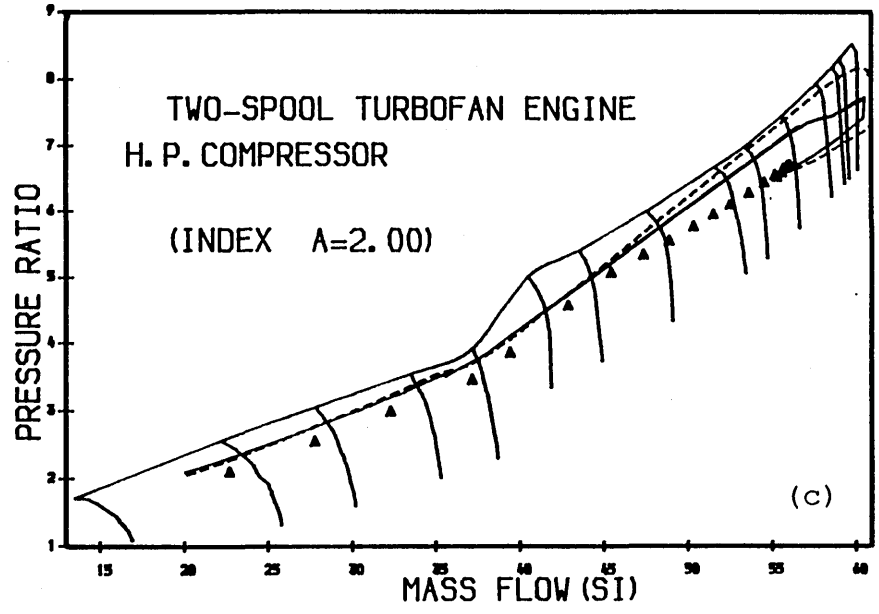

WITH FUEL SCHEDULE COMPENSATED
HEAT TRAN. WITHOUT COMPENSATION
▲ STEADY-RUNNING

Fig. 103

PREDICTED HOT ACC. AT SEA LEVEL

FUEL SCHED. H.P.C. BLADE TEMP. COMP.

◆ FUEL COMPENSATED (INDEX=2.00)

▲ FUEL COMPENSATED (INDEX=1.00)

● FUEL COMPENSATED (INDEX=0.50)

+ WITHOUT COMPENSATION

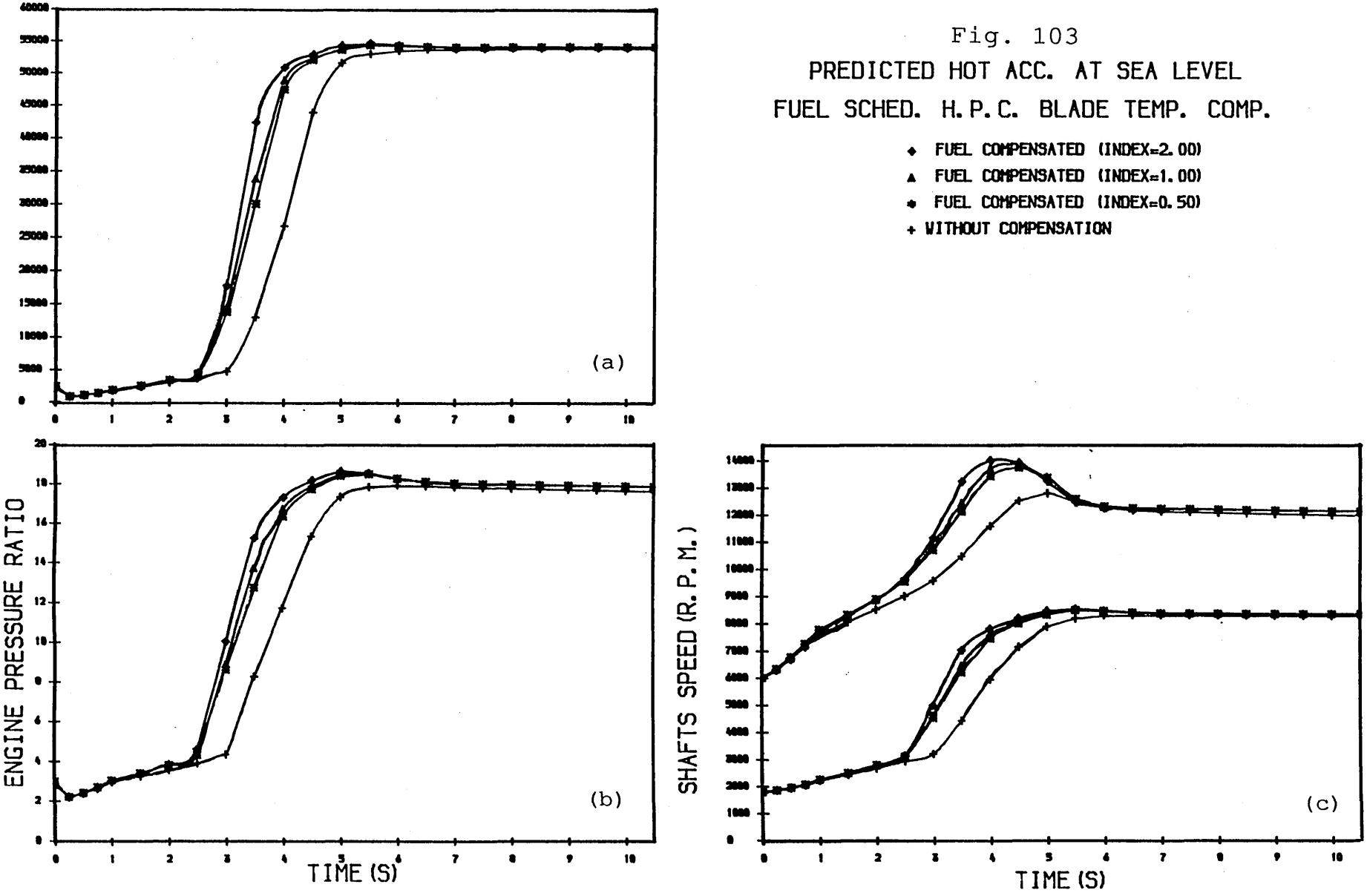

Fig. 104 TRANSIENT ACC. AT SEA LEVEL
H. P. C. BLADE TEMP. COMP.

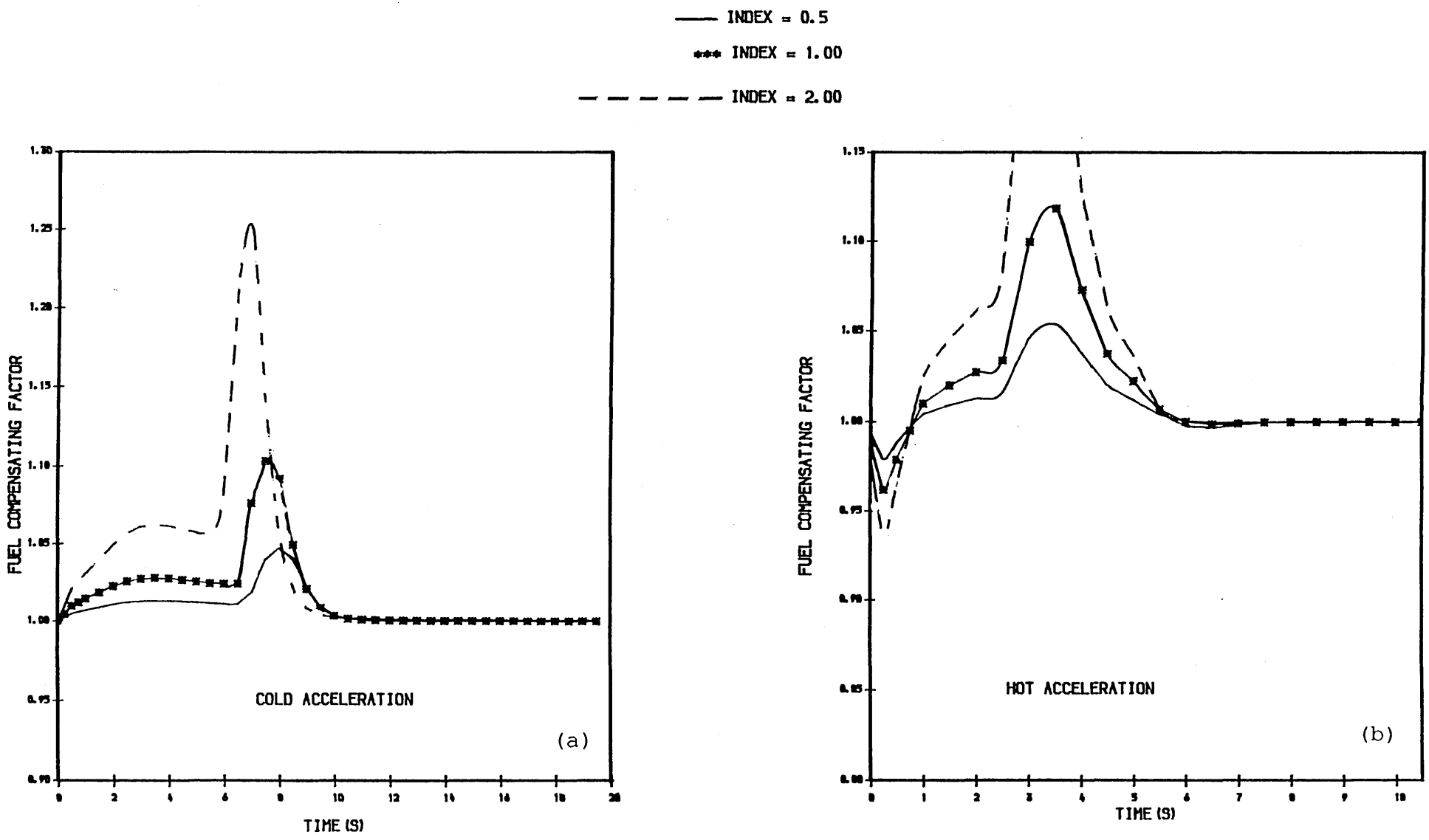

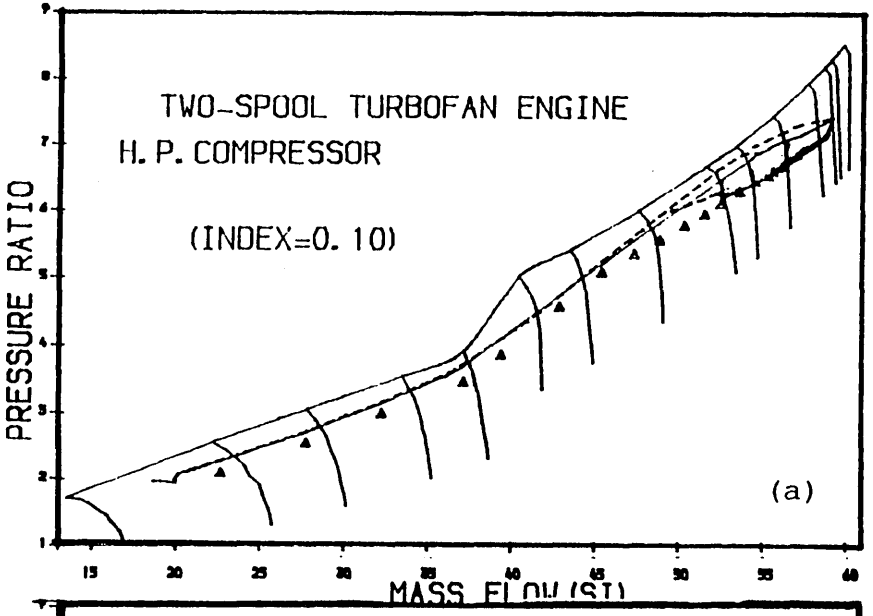

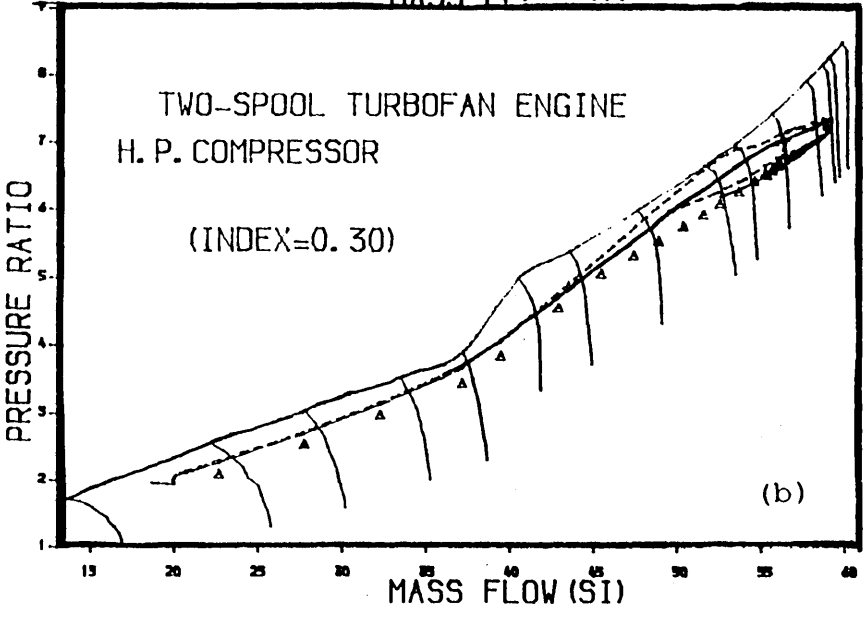

Fig. 105

PREDICTED PATHS OF THE H. P. COMP. DURING COLD ACCEL. AT SEA LEVEL FUEL SCHEDULE COMPENSATED WITH A FUNCT. OF H. P. T. BLADE TEMP. COMP.

------ WITH FUEL SCHEDULE COMPENSATED
——— HEAT TRAN. WITHOUT COMPENSATION
▲ STEADY-RUNNING

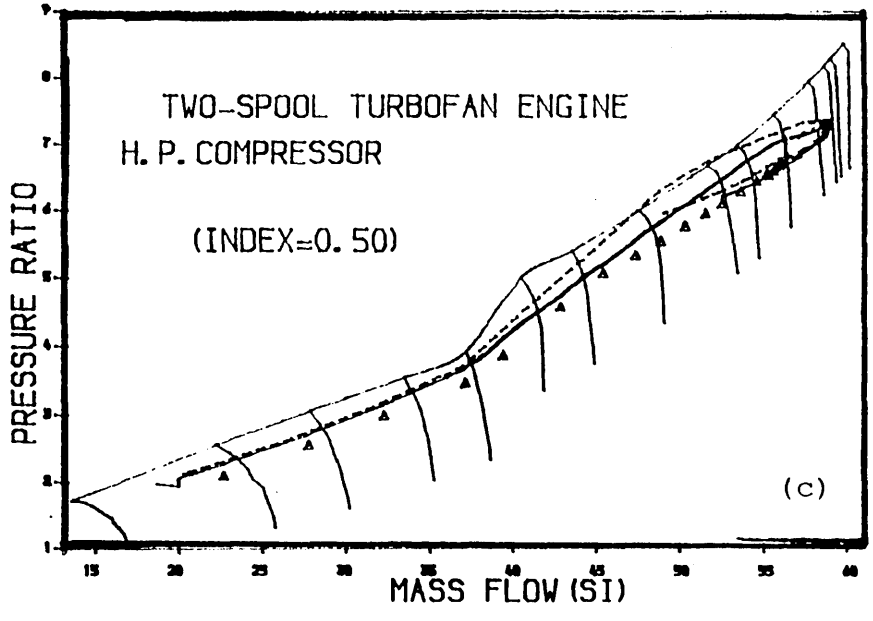

Fig. 106

PREDICTED COLD ACC. AT SEA LEVEL

FUEL SCHED. H.P.T. BLADE TEMP. COMP.

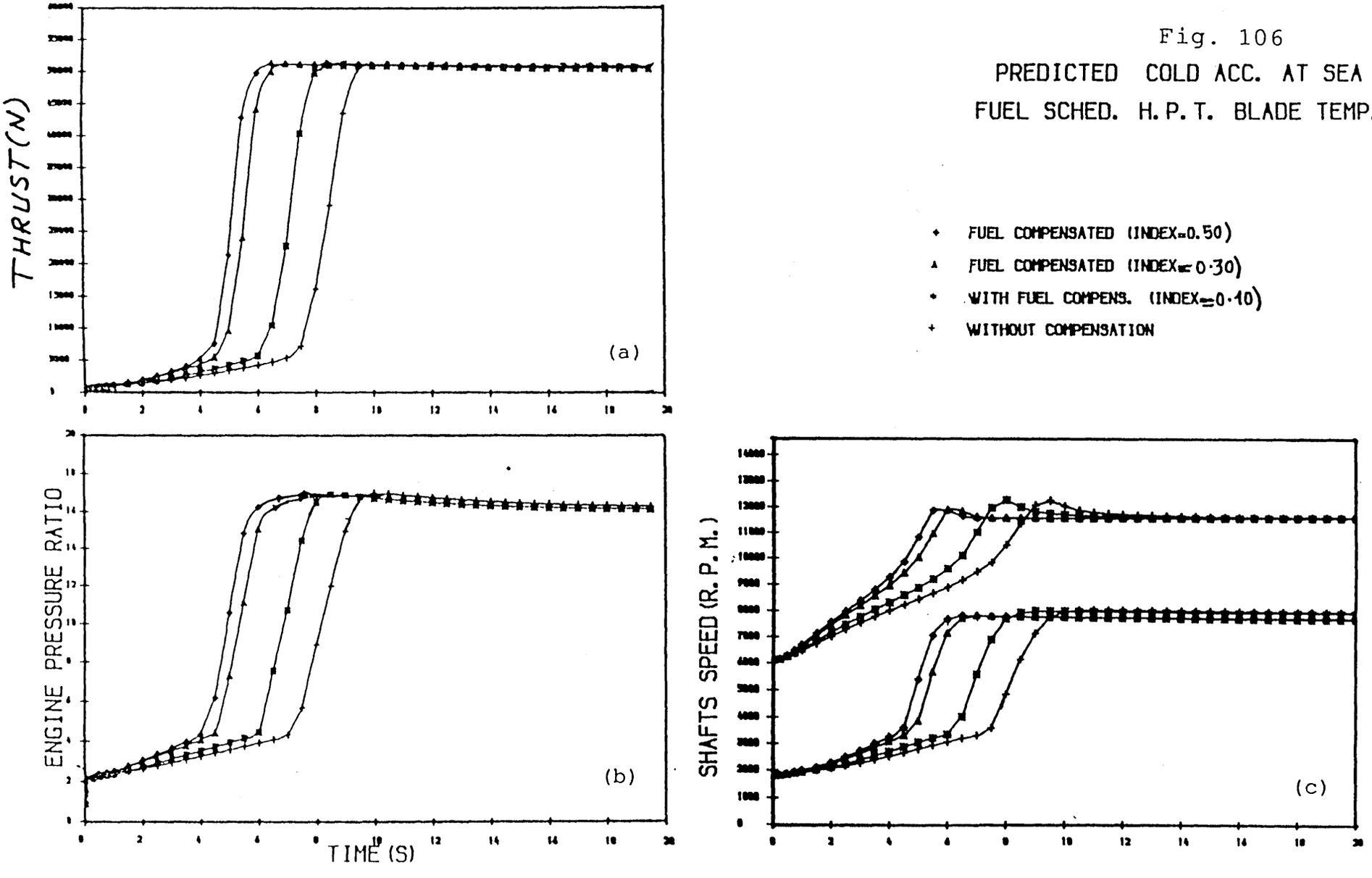

Fig. 107

PREDICTED PATHS OF THE H.P. COMP. DURING HOT ACCEL. AT SEA LEVEL FUEL SCHEDULE COMPENSATED WITH A FUNCT. OF H.P.T. BLADE TEMP. COMP.

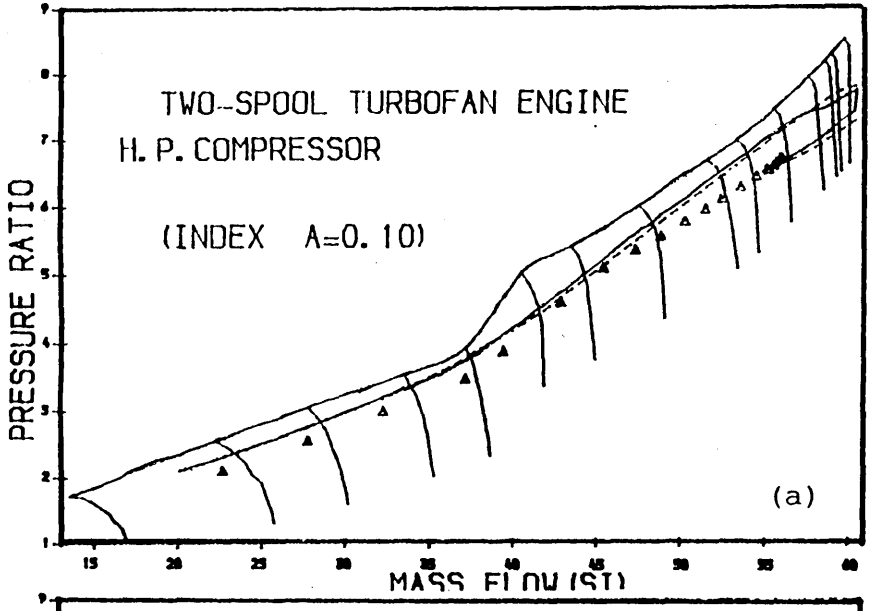

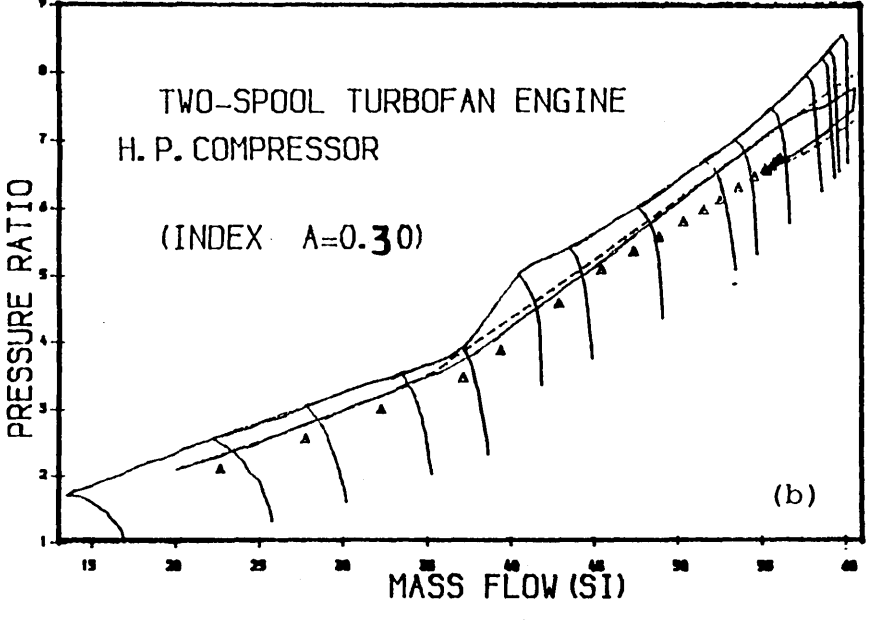

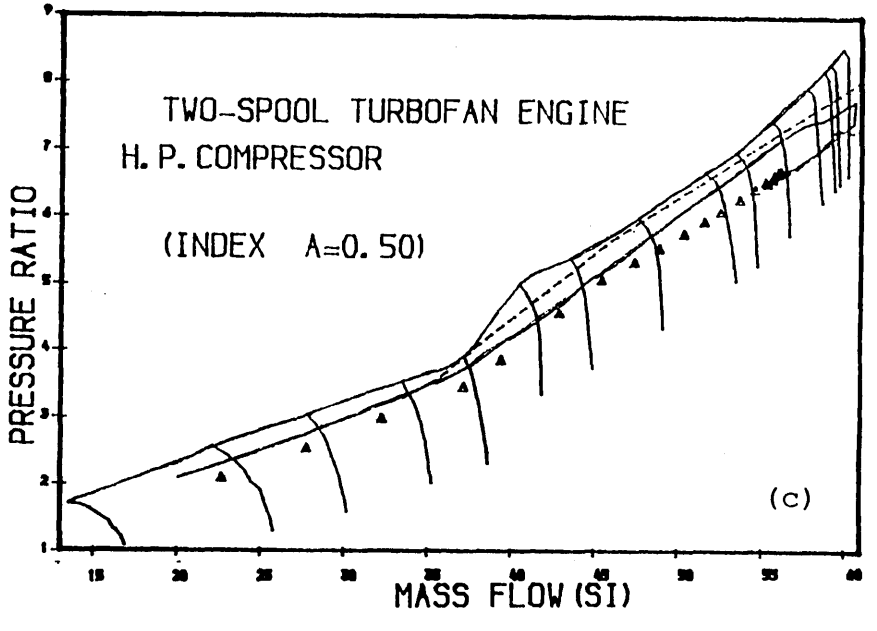

WITH FUEL SCHEDULE COMPENSATED
HEAT TRAN. WITHOUT COMPENSATION
▲ STEADY-RUNNING

Fig. 108

PREDICTED HOT ACC. AT SEA LEVEL

FUEL SCHED. H.P.T. BLADE TEMP. COMP.

◆ FUEL COMPENSATED (INDEX=0.50)

▲ FUEL COMPENSATED (INDEX=0.30)

* FUEL COMPENSATED (INDEX=0.10)

+ WITHOUT COMPENSATION

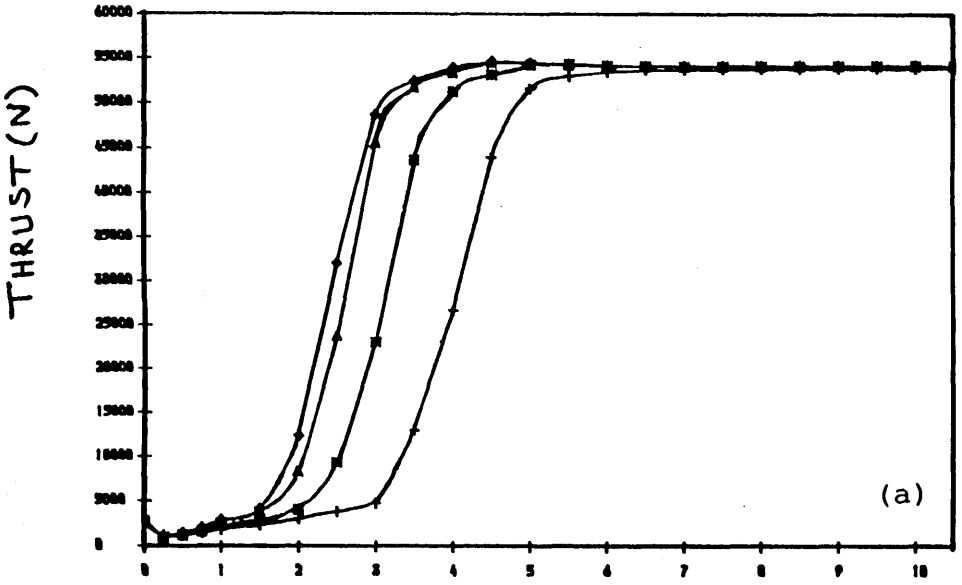

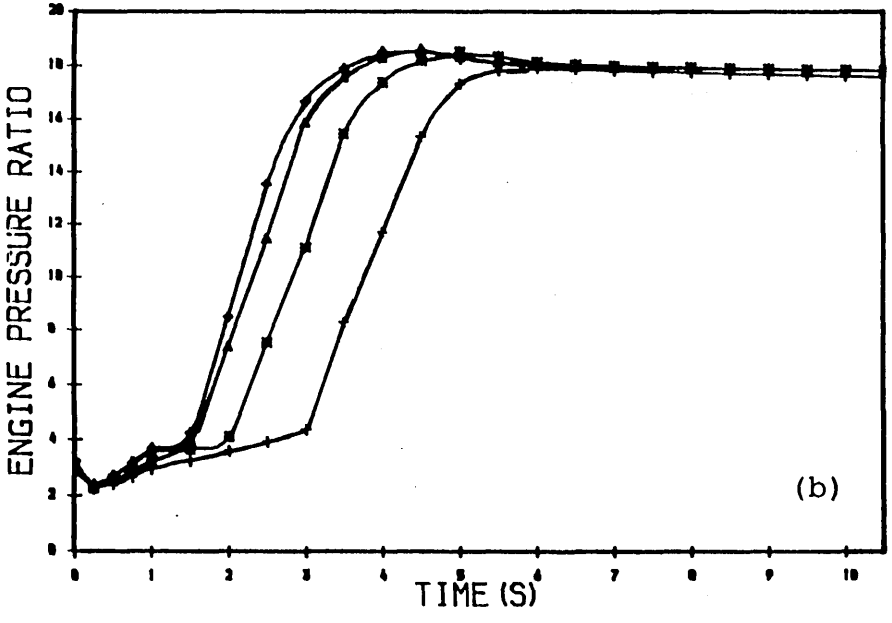

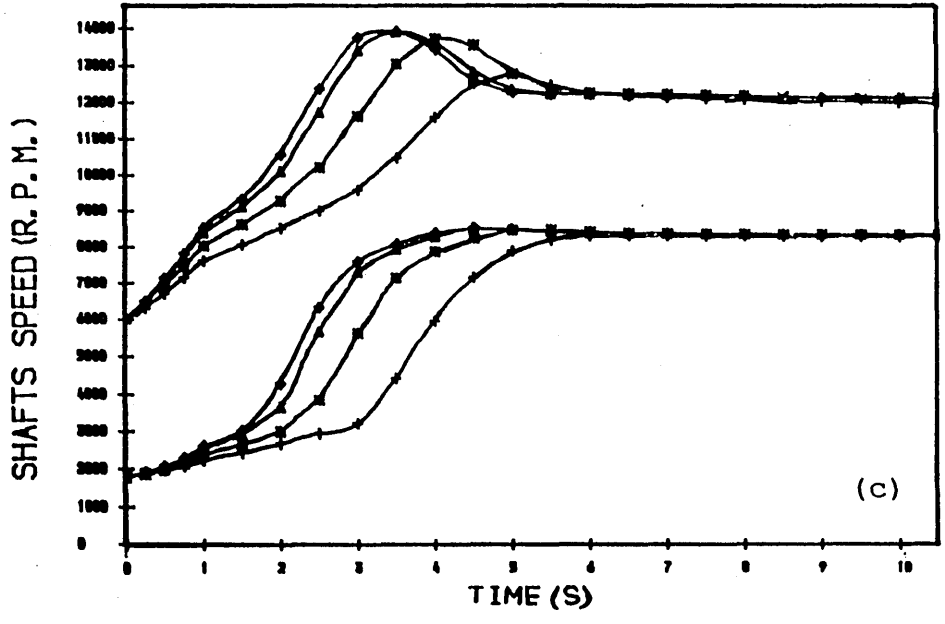

Fig. 109 TRANSIENT ACC. AT SEA LEVEL
H.P.T. BLADE TEMP. COMP.

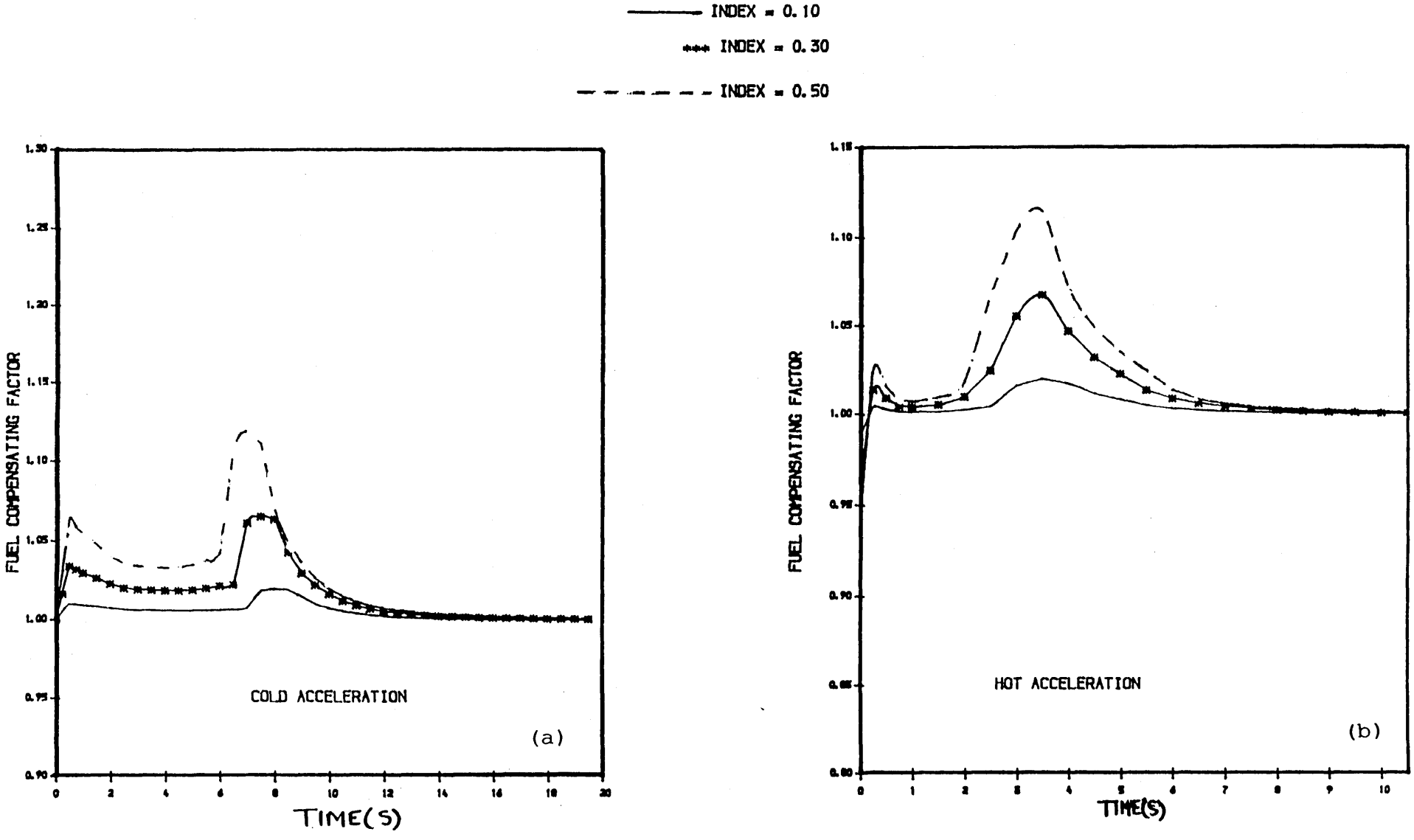

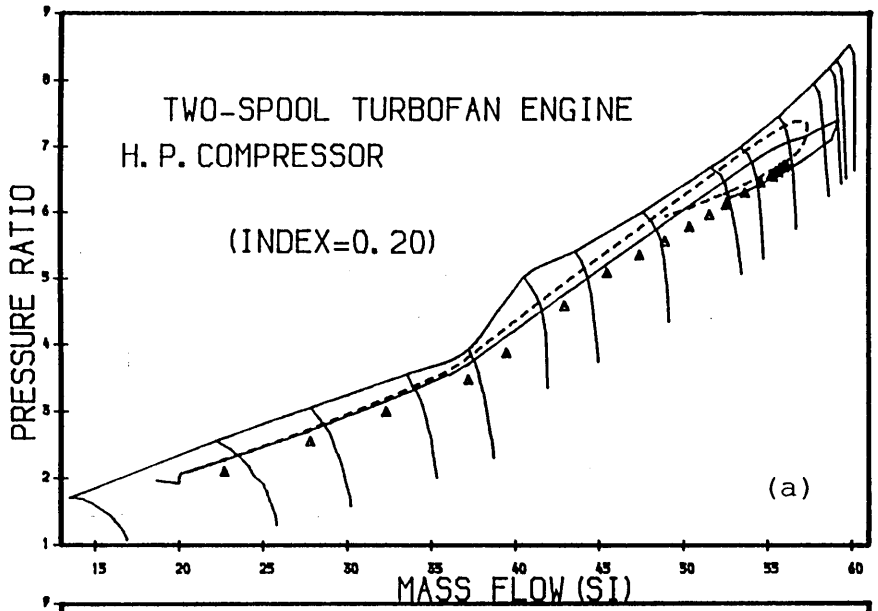

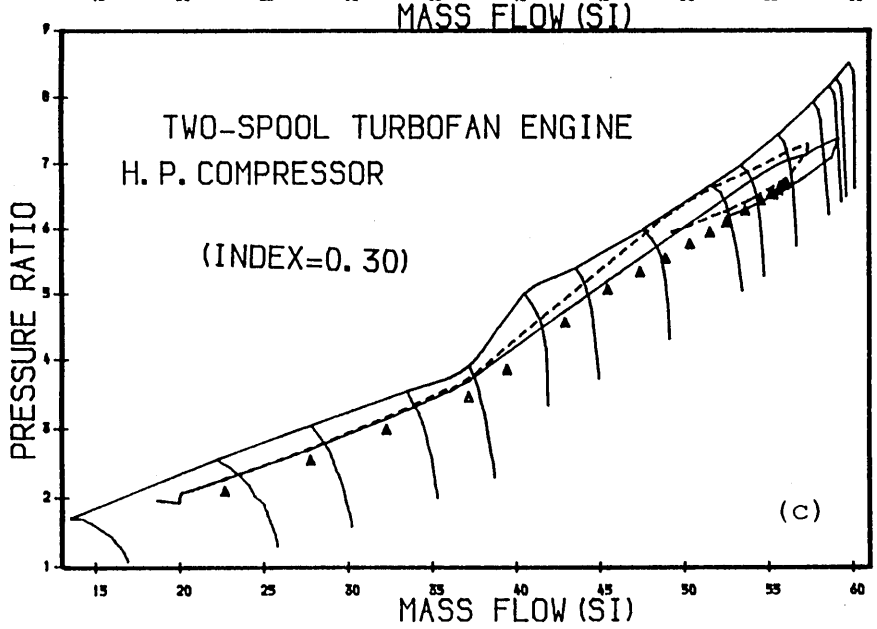

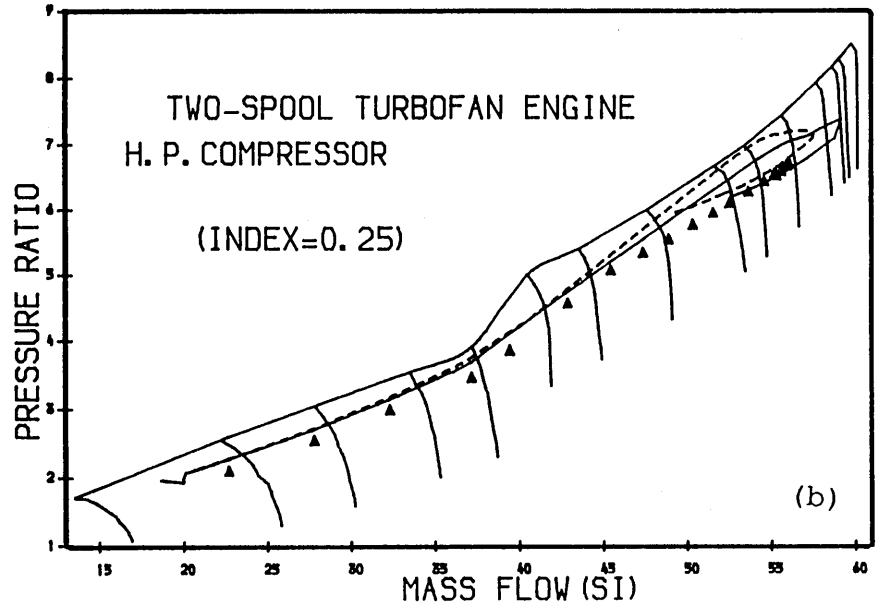

Fig. 110

PREDICTED PATHS OF THE H. P. COMP.
DURING COLD ACCEL. AT SEA LEVEL
FUEL SCHEDULE COMPENSATED WITH
A FUNCT. OF H. P. T. DISC (HUB) TP. COMP.

------ WITH FUEL SCHEDULE COMPENSATED
——— HEAT TRAN. WITHOUT COMPENSATION
▲ STEADY-RUNNING

Fig. 111

PREDICTED COLD ACC. AT SEA LEVEL

FUEL SCHED. H.P.T. DISC (HUB) TEMP.

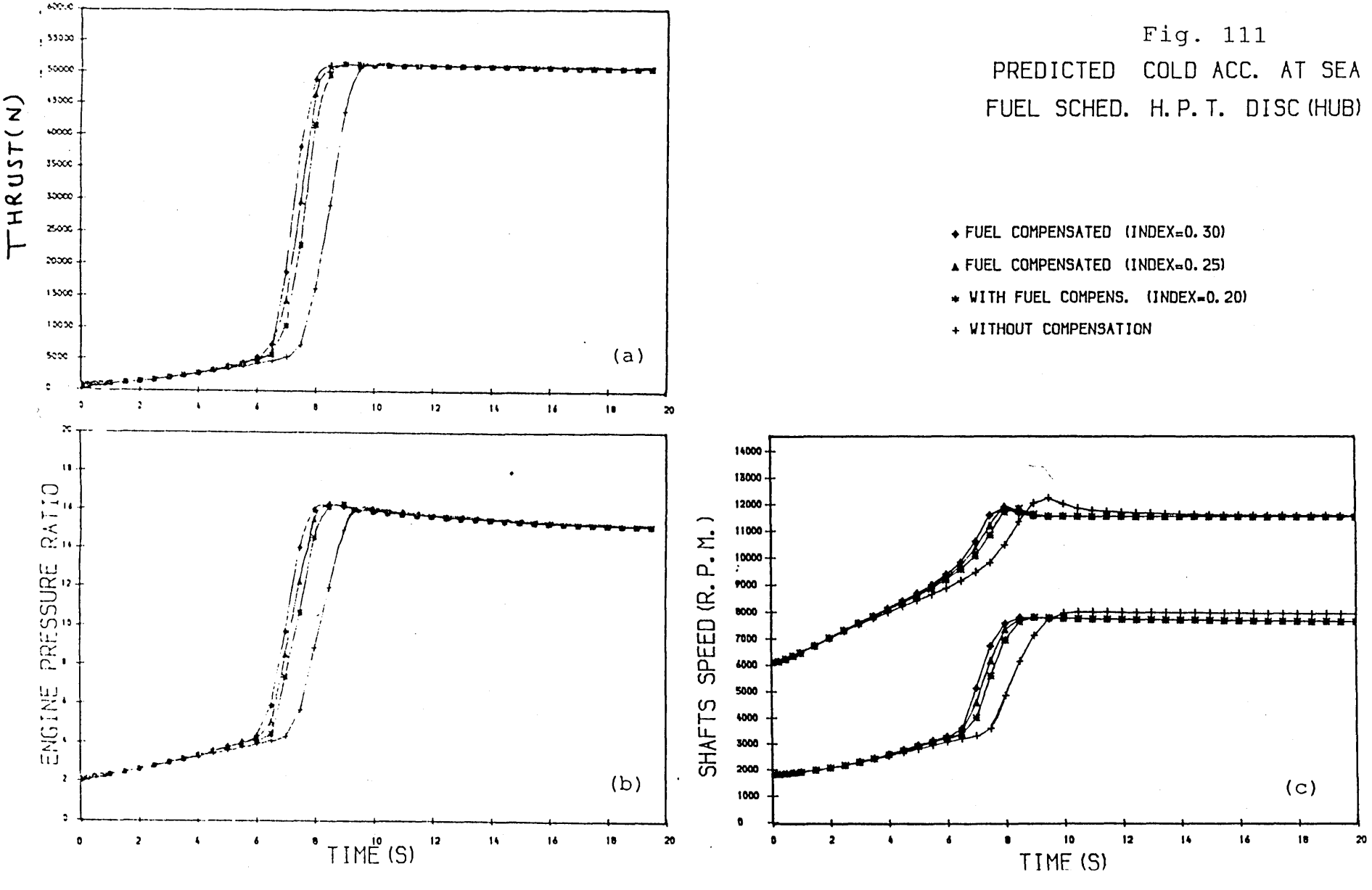

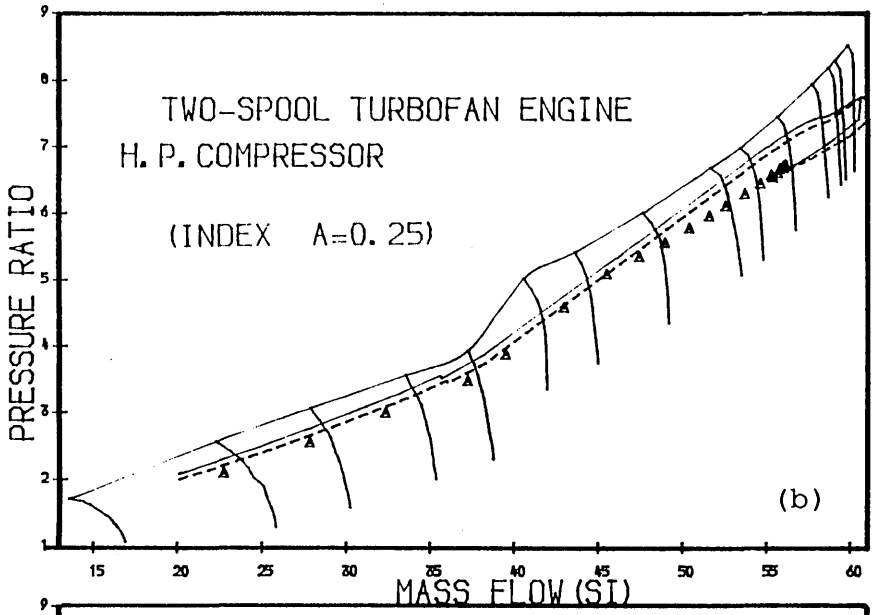

Fig. 112

PREDICTED PATHS OF THE H. P. COMP. DURING HOT ACCEL. AT SEA LEVEL FUEL SCHEDULE COMPENSATED WITH A FUNCT. OF H. P. T. DISC (HUB) TP. COMP.

------ WITH FUEL SCHEDULE COMPENSATED
——— HEAT TRAN. WITHOUT COMPENSATION
▲ STEADY-RUNNING

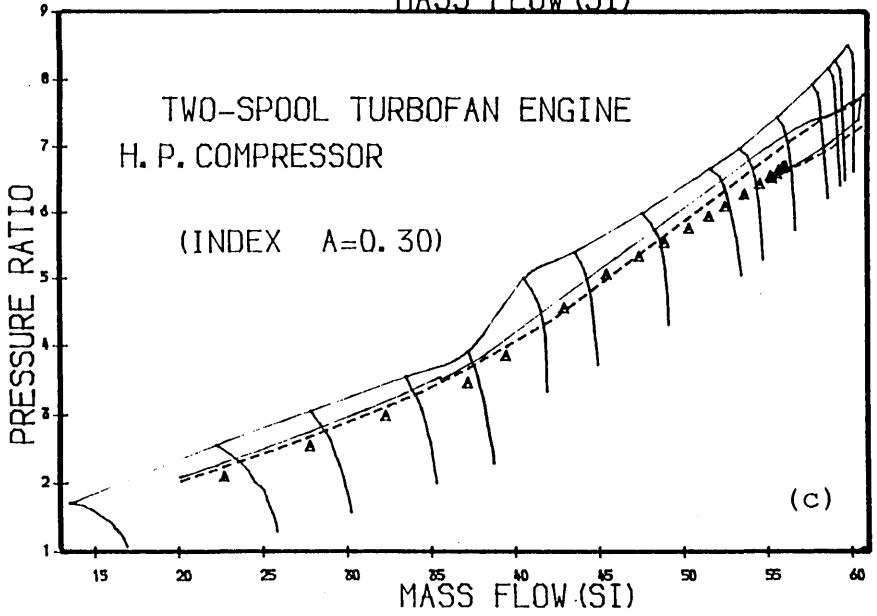

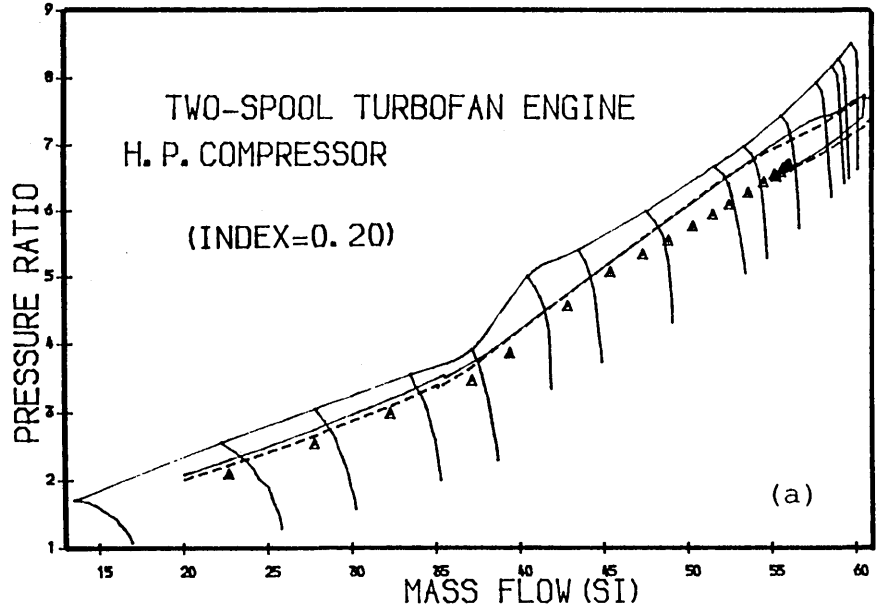

Fig. 113

PREDICTED HOT ACC. AT SEA LEVEL

FUEL SCHED. H.P.T. DISC (HUB) TP. CMP.

◆ FUEL COMPENSATED (INDEX=0.30)

▲ FUEL COMPENSATED (INDEX=0.25)

✱ FUEL COMPENSATED (INDEX=0.20)

\+ WITHOUT COMPENSATION

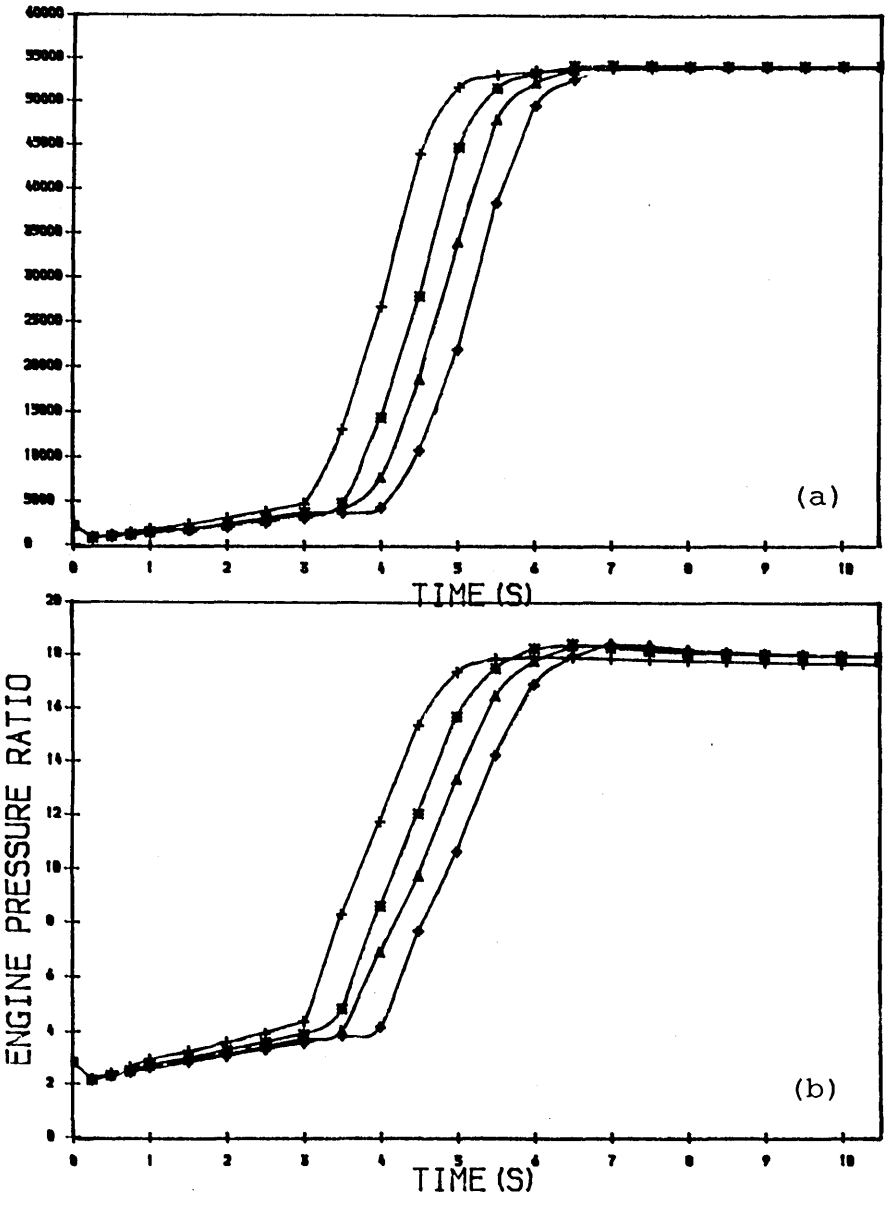

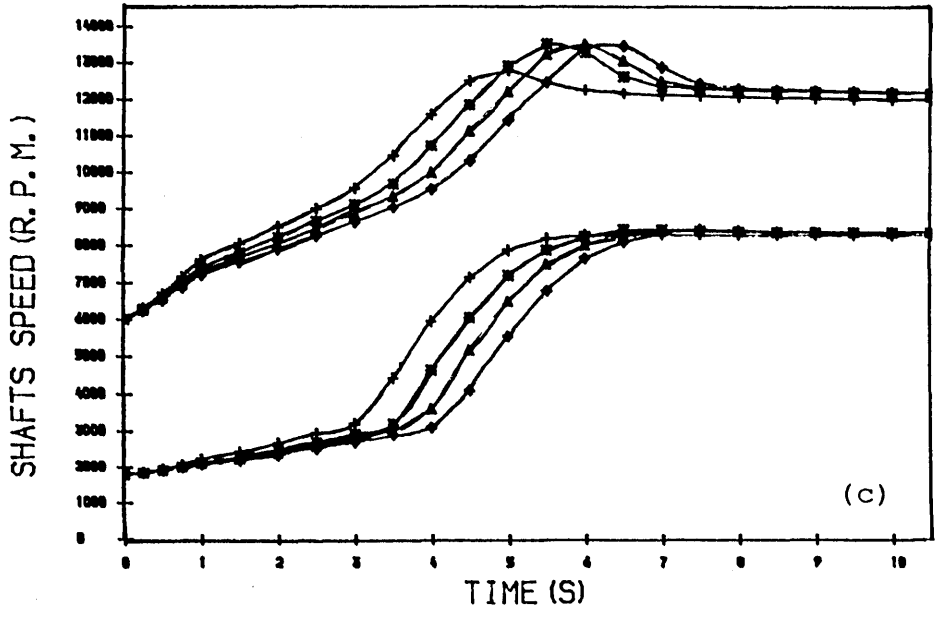

Fig. 114 TRANSIENT ACC. AT SEA LEVEL
H. P. T. DISC (HUB) TEMP. COMP.

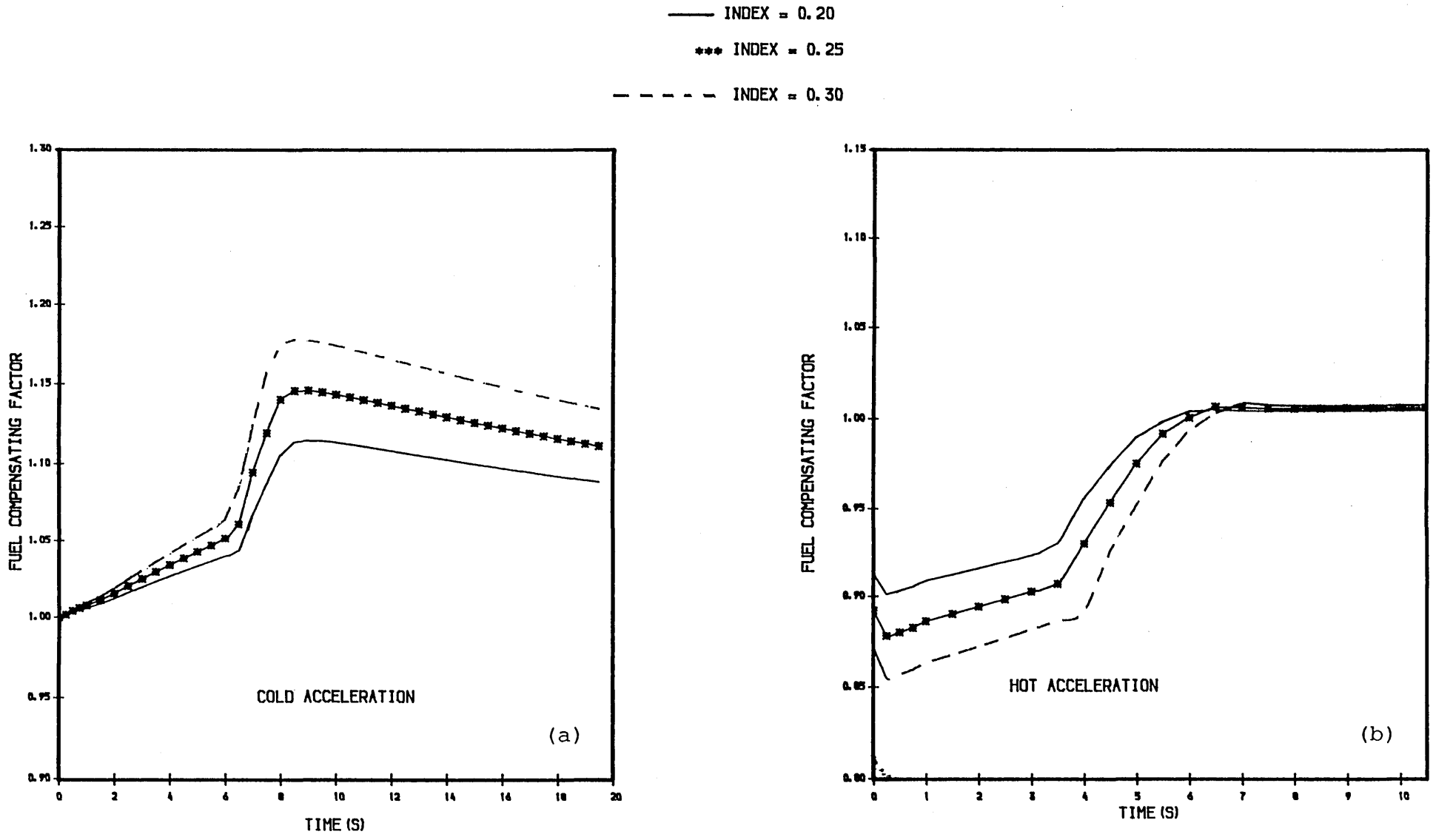

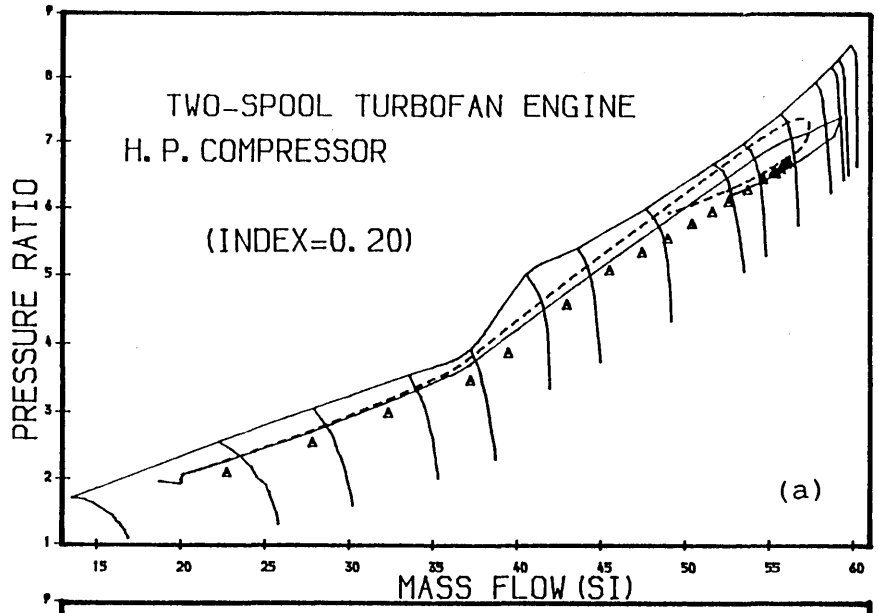

Fig. 115

PREDICTED PATHS OF THE H. P. COMP.
DURING COLD ACCEL. AT SEA LEVEL
FUEL SCHEDULE COMPENSATED WITH
A FUNCT. OF H. P. T. DISC (DGM) TP. CMP.

------ WITH FUEL SCHEDULE COMPENSATED
——— HEAT TRAN. WITHOUT COMPENSATION
▲ STEADY-RUNNING

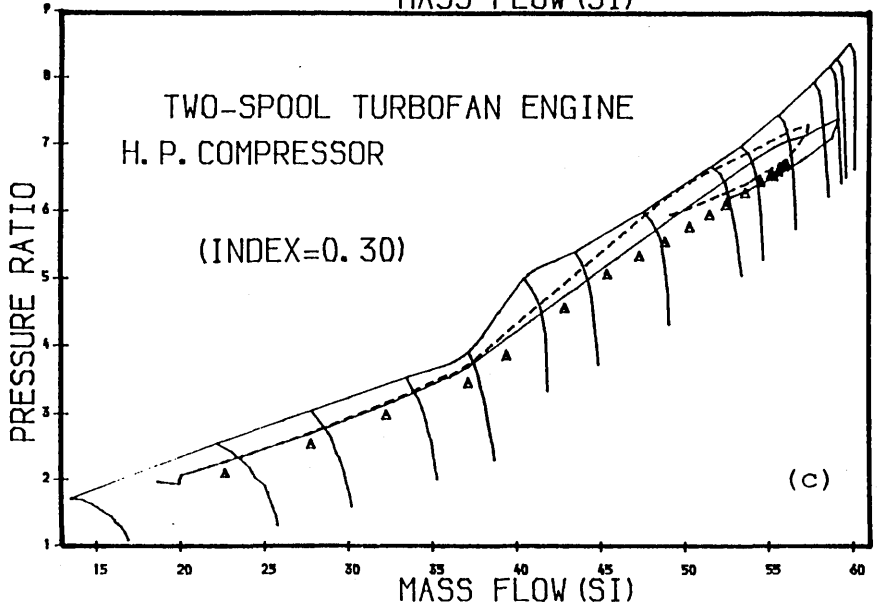

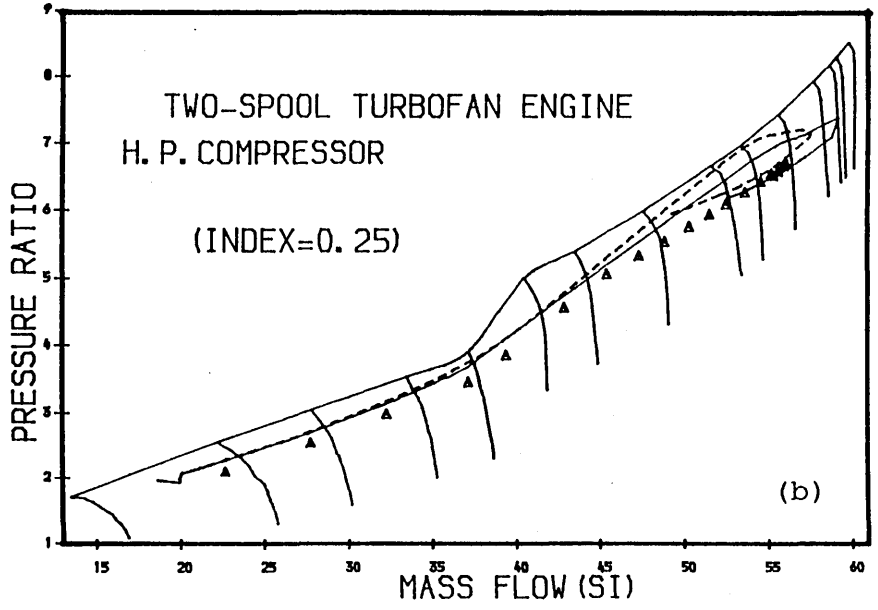

Fig. 116

PREDICTED COLD ACC. AT SEA LEVEL

FUEL SCHED. H.P.T. DISC (DGM) TEMP.

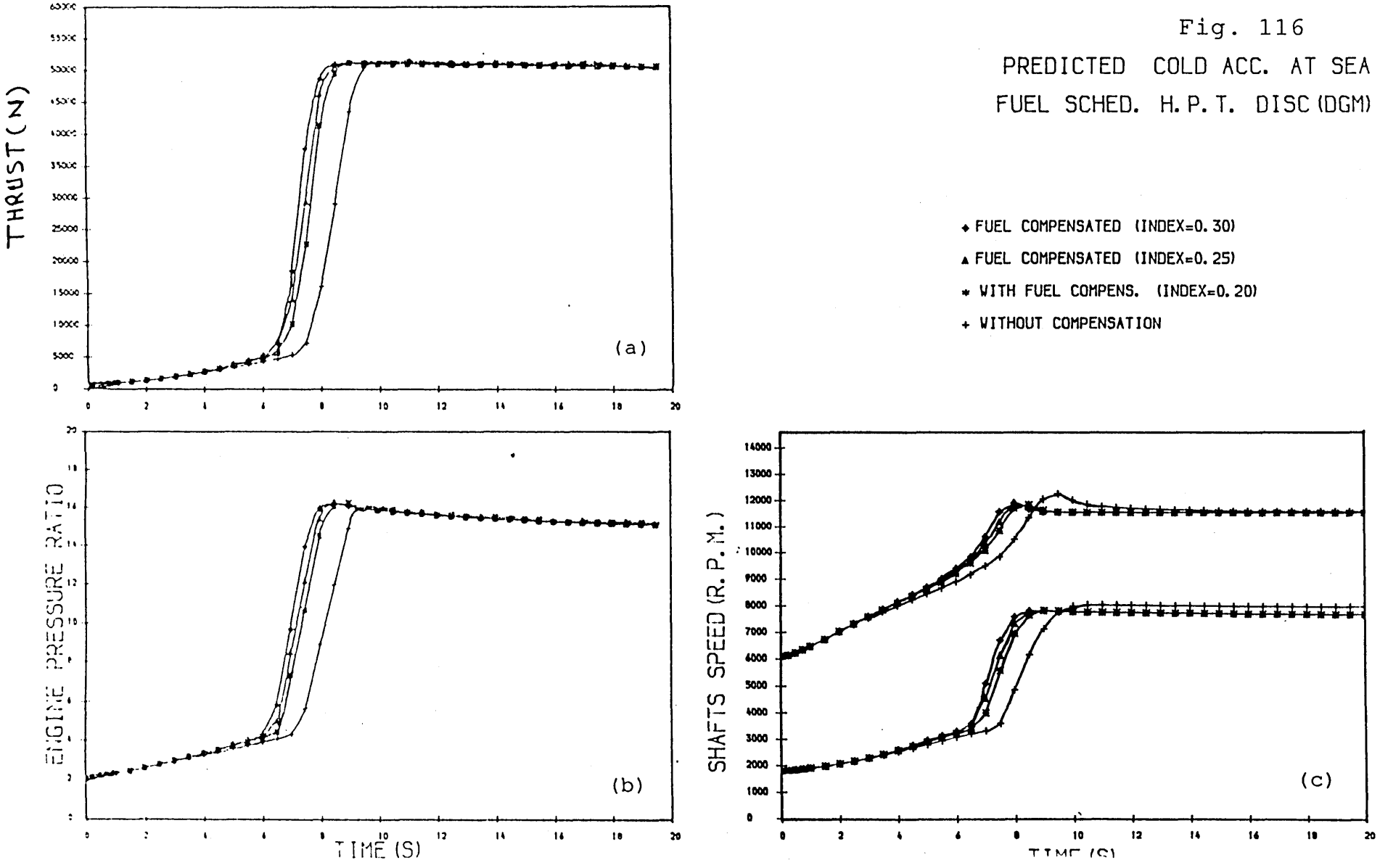

◆ FUEL COMPENSATED (INDEX=0.30)

▲ FUEL COMPENSATED (INDEX=0.25)

✱ WITH FUEL COMPENS. (INDEX=0.20)

\+ WITHOUT COMPENSATION

Fig. 117

PREDICTED PATHS OF THE H.P. COMP. DURING HOT ACCEL. AT SEA LEVEL FUEL SCHEDULE COMPENSATED WITH A FUNCT. OF H.P.T. DISC (DGM) TP. COMP.

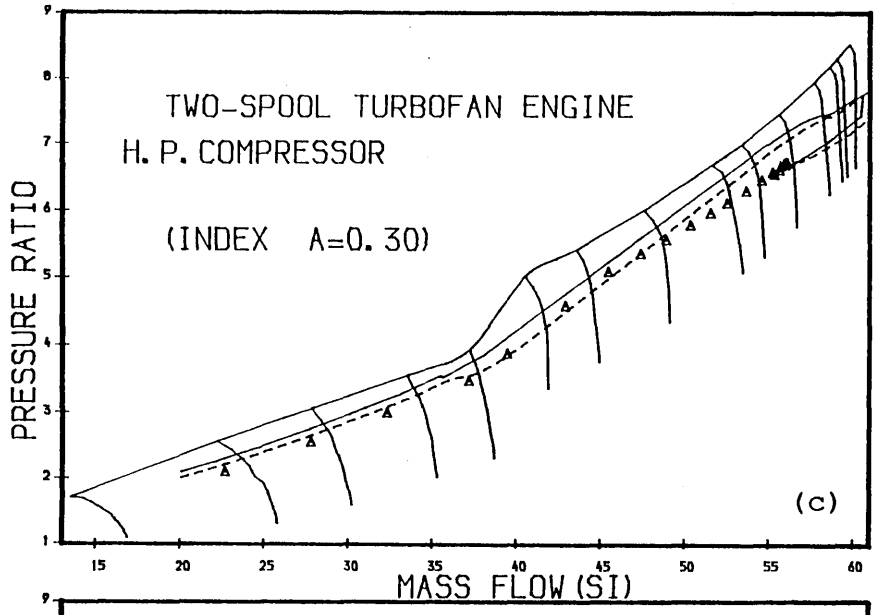

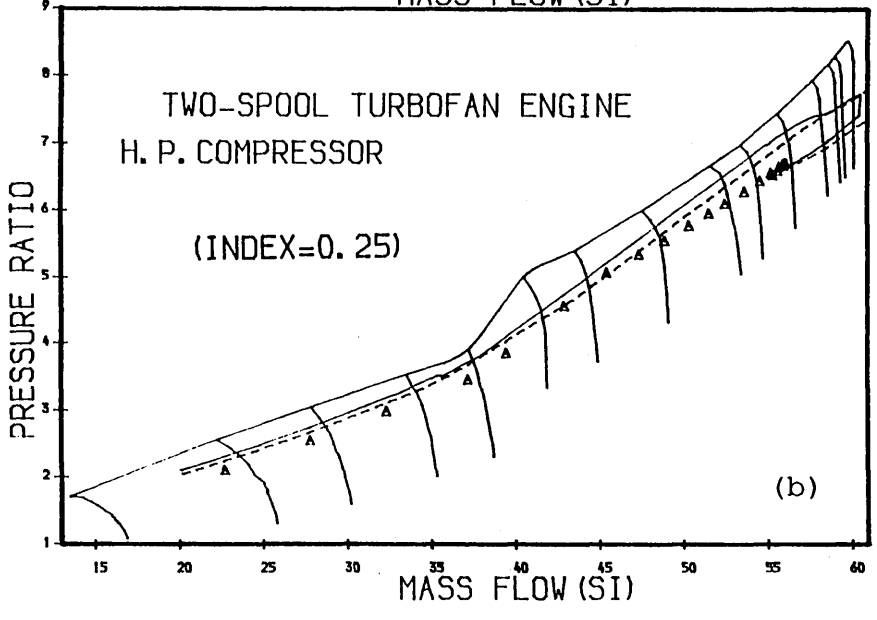

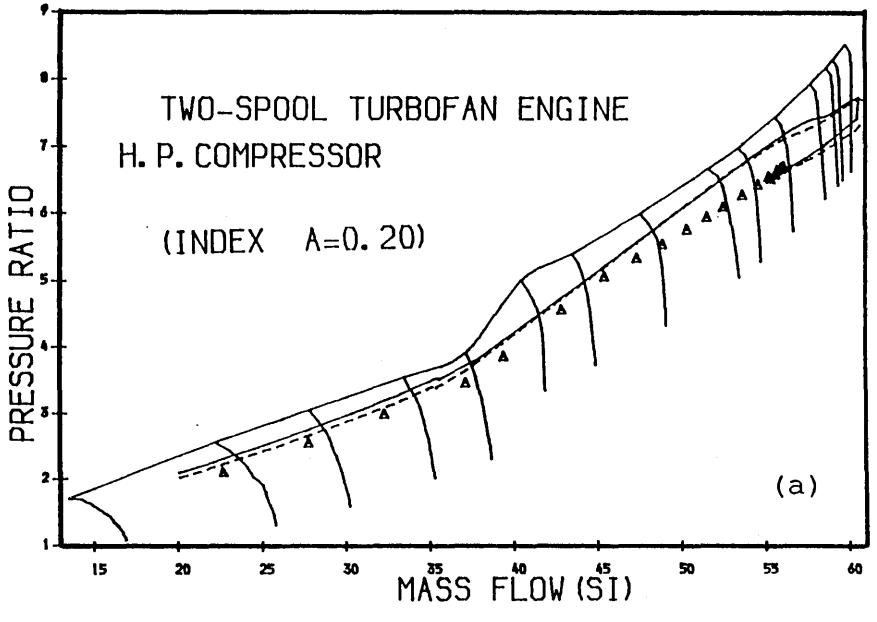

------ WITH FUEL SCHEDULE COMPENSATED
——— HEAT TRAN. WITHOUT COMPENSATION
▲ STEADY-RUNNING

Fig. 118

PREDICTED HOT ACC. AT SEA LEVEL

FUEL SCHED. H.P.T. DISC (DGM) TP. CMP.

- ◆ FUEL COMPENSATED (INDEX=0.30)
- ▲ FUEL COMPENSATED (INDEX=0.25)
- ✱ FUEL COMPENSATED (INDEX=0.20)
- \+ WITHOUT COMPENSATION

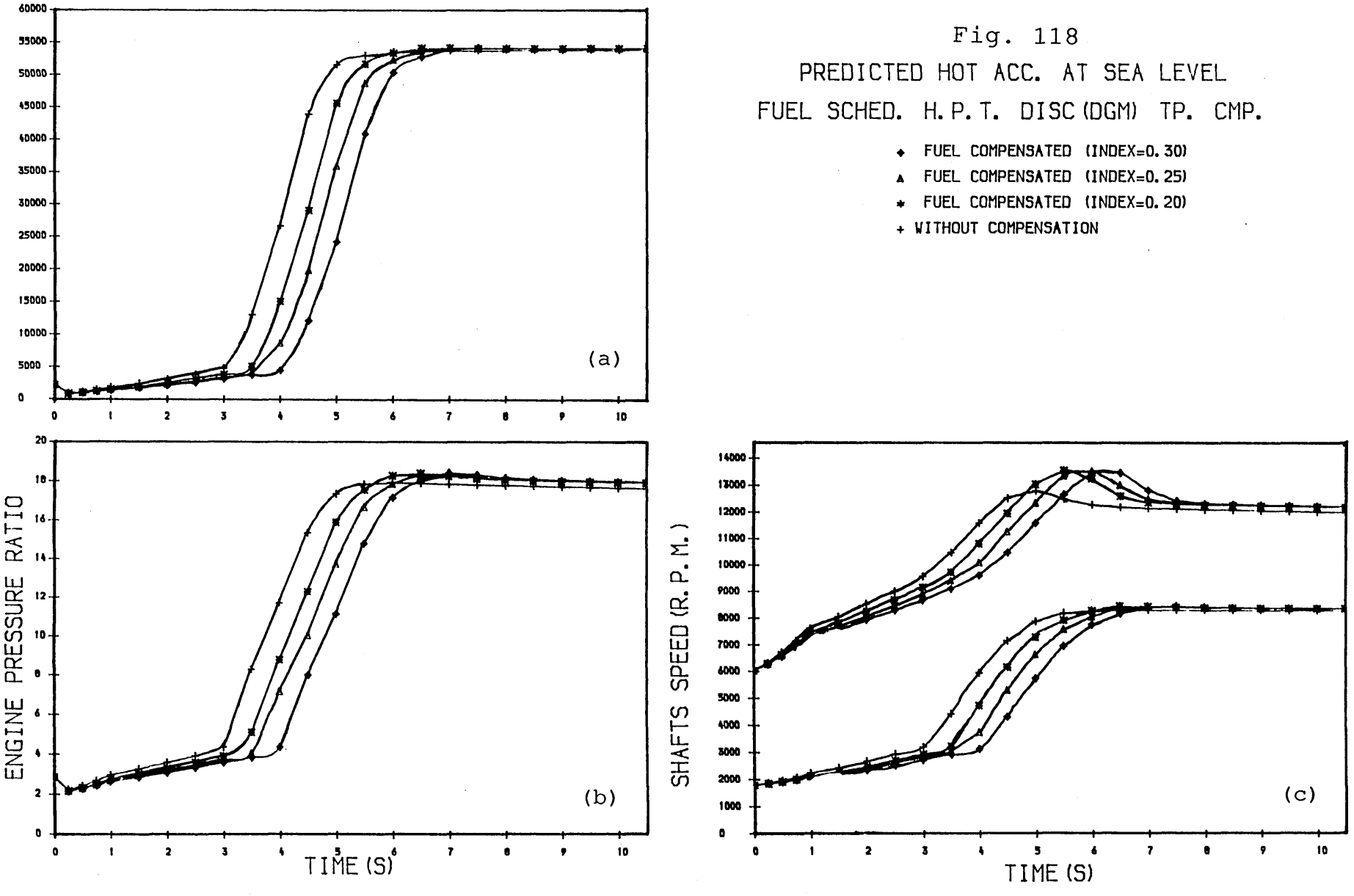

Fig. 119 TRANSIENT ACC. AT SEA LEVEL
H. P. T. DISC (DGM) TEMP. COMP.

—— INDEX = 0.20

*** INDEX = 0.25

— — — — · INDEX = 0.30

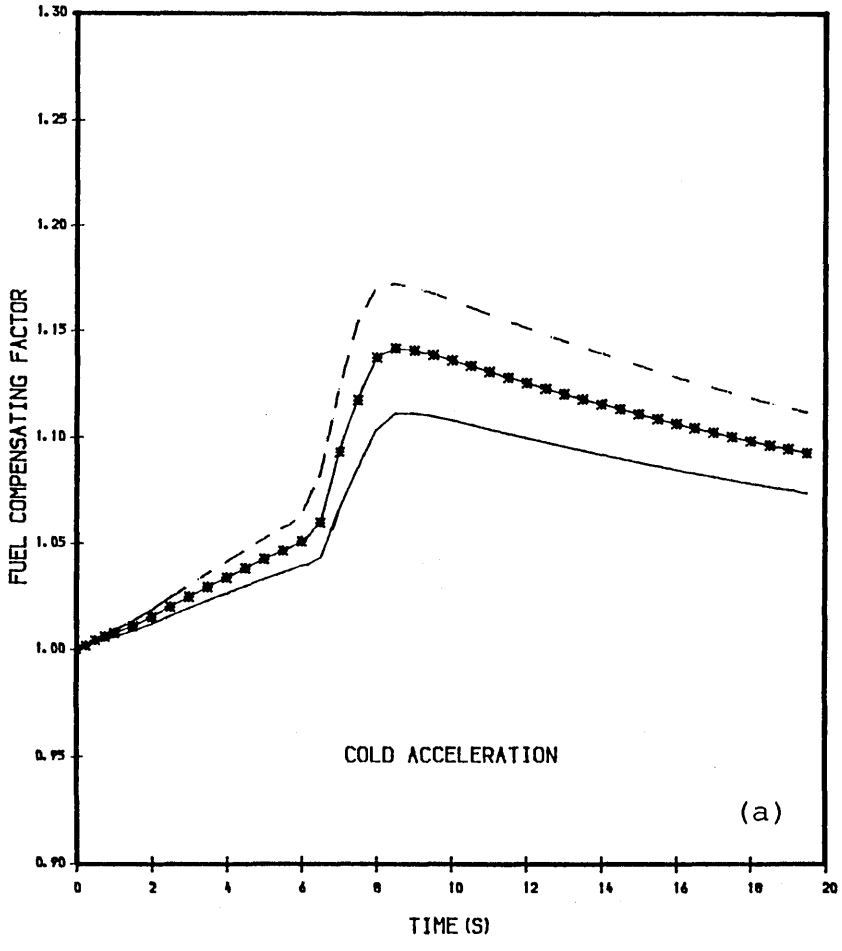

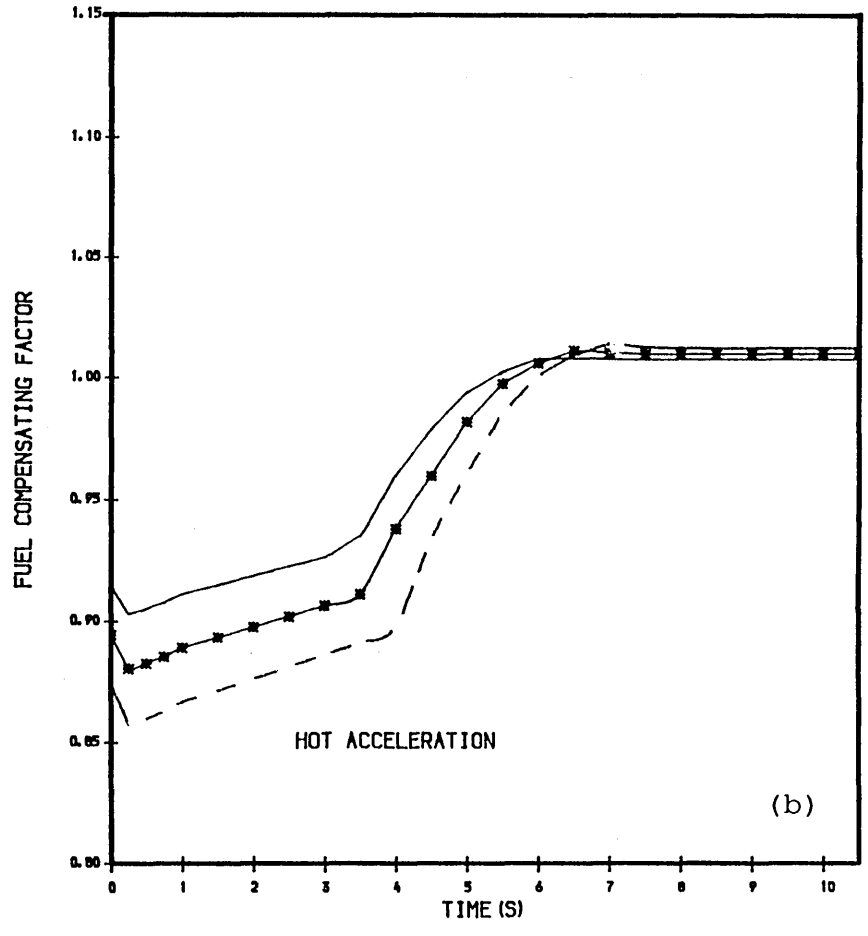

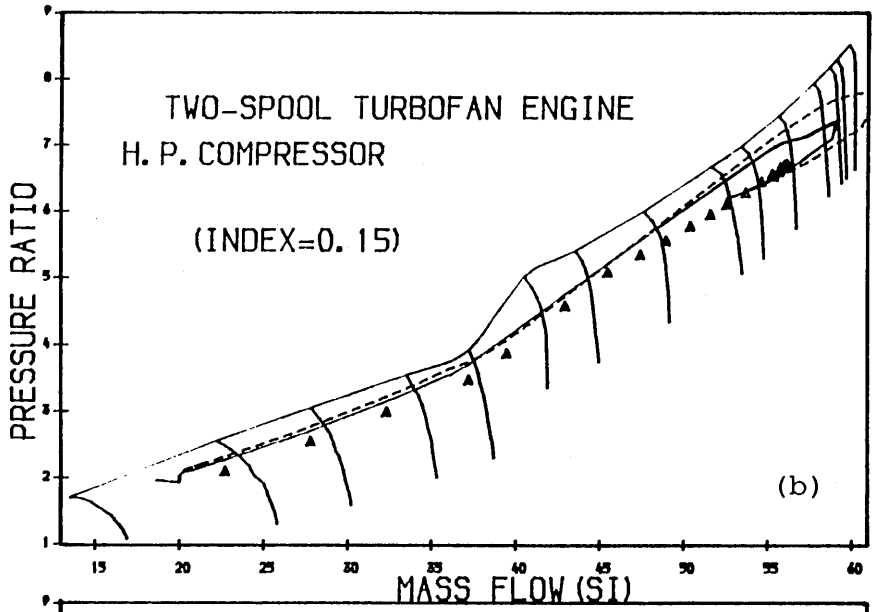

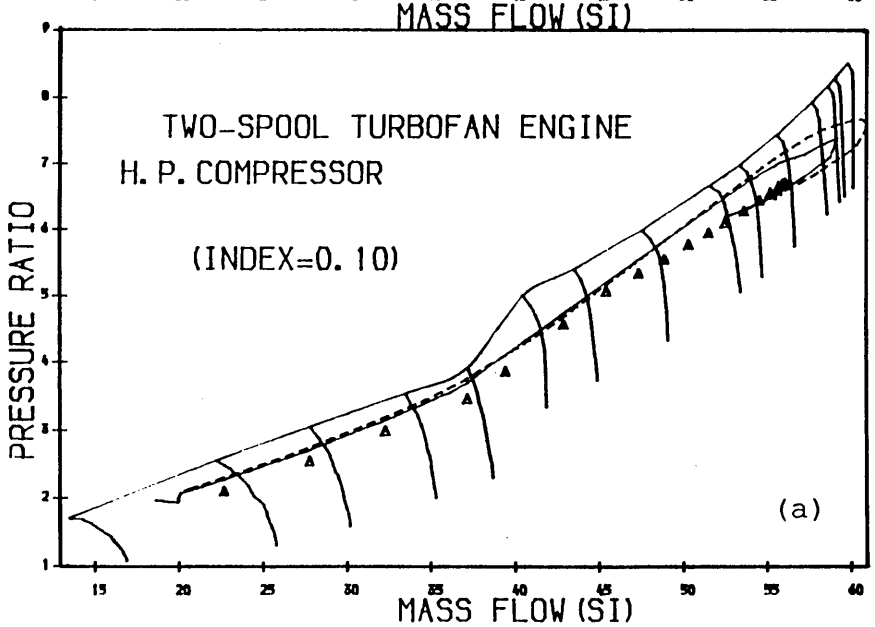

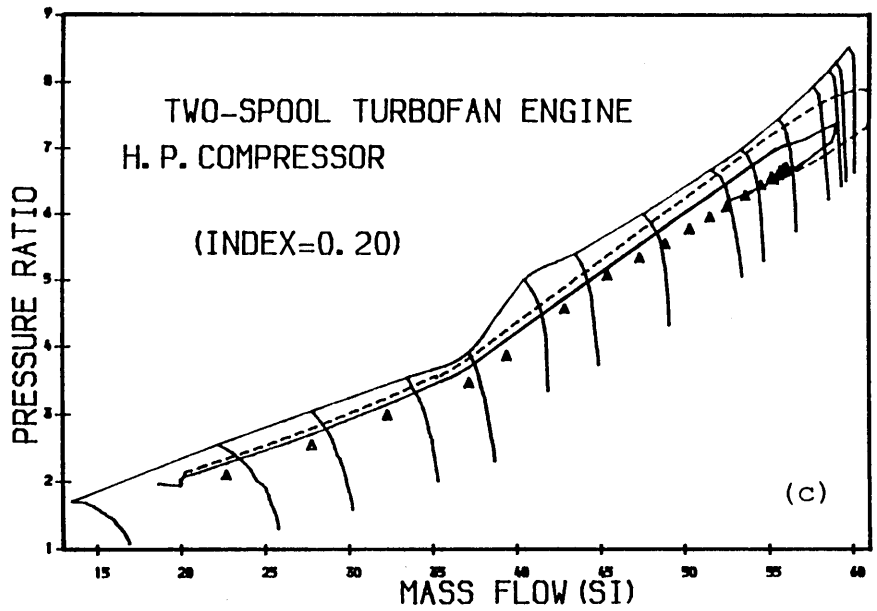

Fig. 120

PREDICTED PATHS OF THE H. P. COMP. DURING COLD ACCEL. AT SEA-LEVEL FUEL SCHEDULE COMPENSATED WITH A FUNCT. OF H. P. T. DISC (PLT) TEMP.

- - - - - - WITH FUEL SCHEDULE COMPENSATED
——— HEAT TRAN. WITHOUT COMPENSATION
▲ STEADY-RUNNING

Fig. 121

PREDICTED COLD ACC. AT SEA LEVEL

FUEL SCHED. H.P.T. DISC(PLT) TP. CMP.

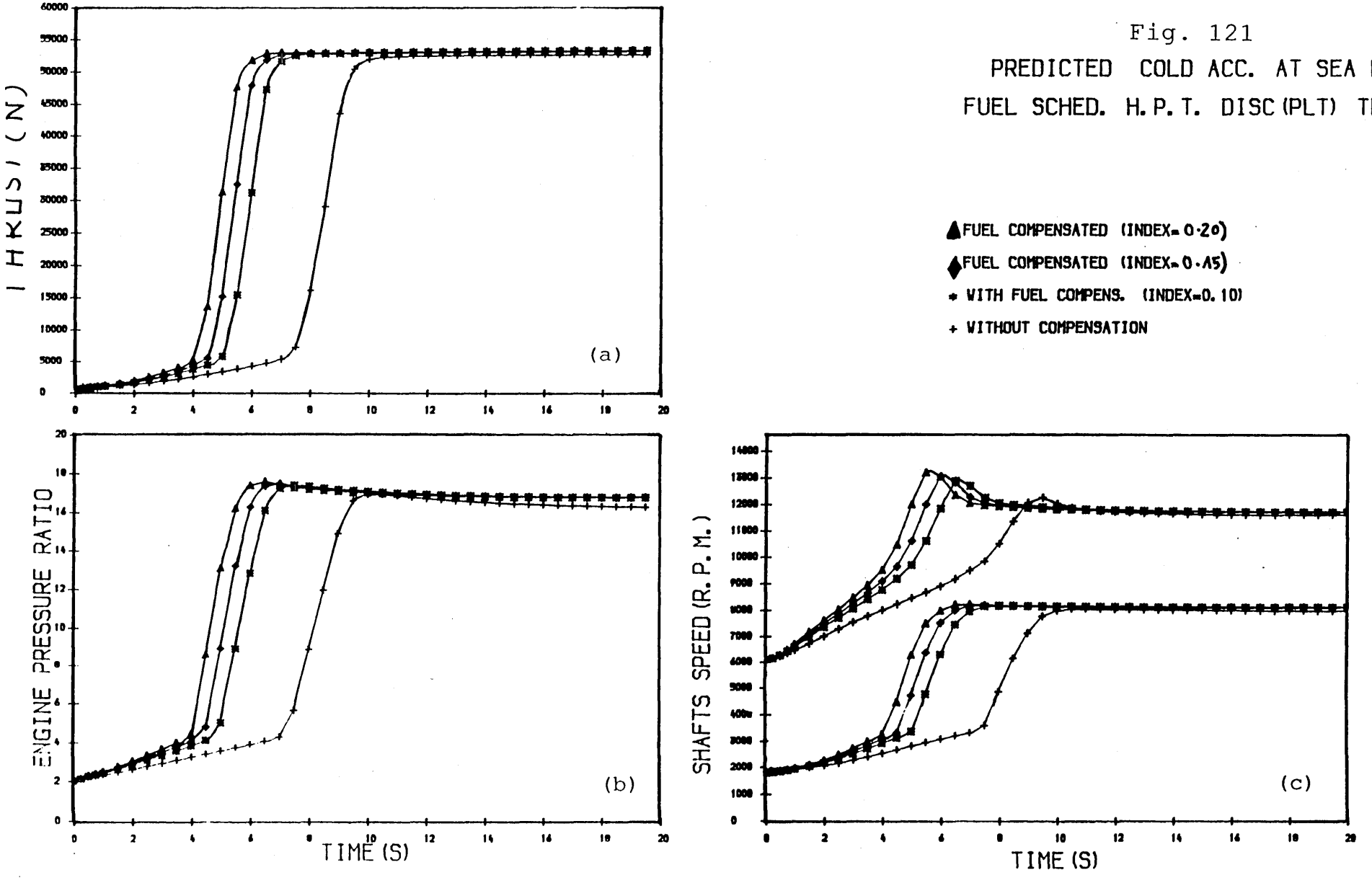

Fig. 122

PREDICTED PATHS OF THE H.P. COMP. DURING HOT ACCEL. AT SEA-LEVEL FUEL SCHEDULE COMPENSATED WITH A FUNCT. OF H.P.T. DISC (PLT) TEMP.

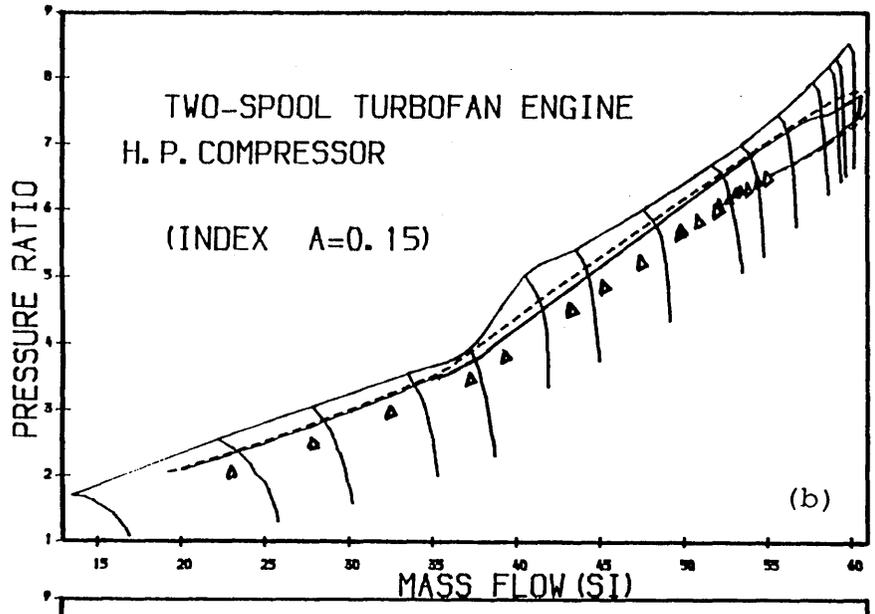

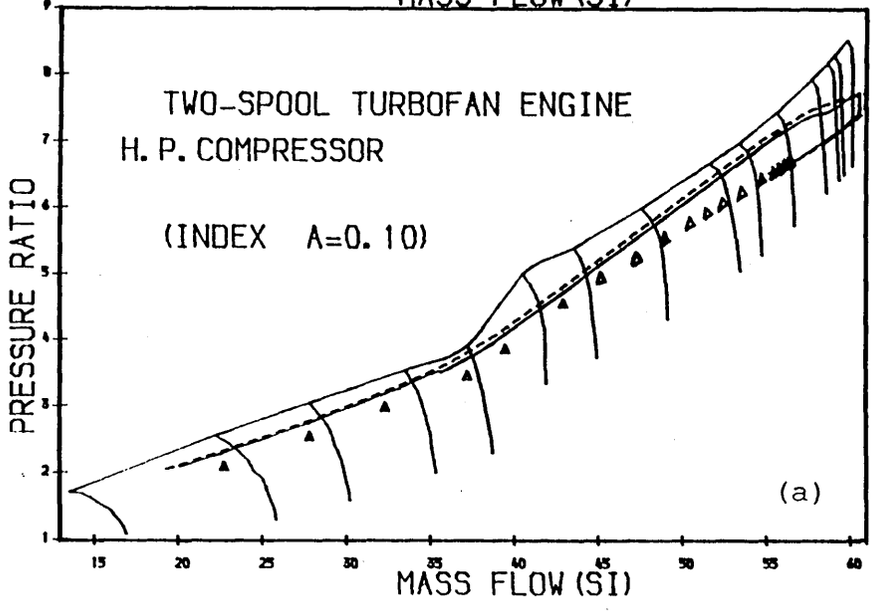

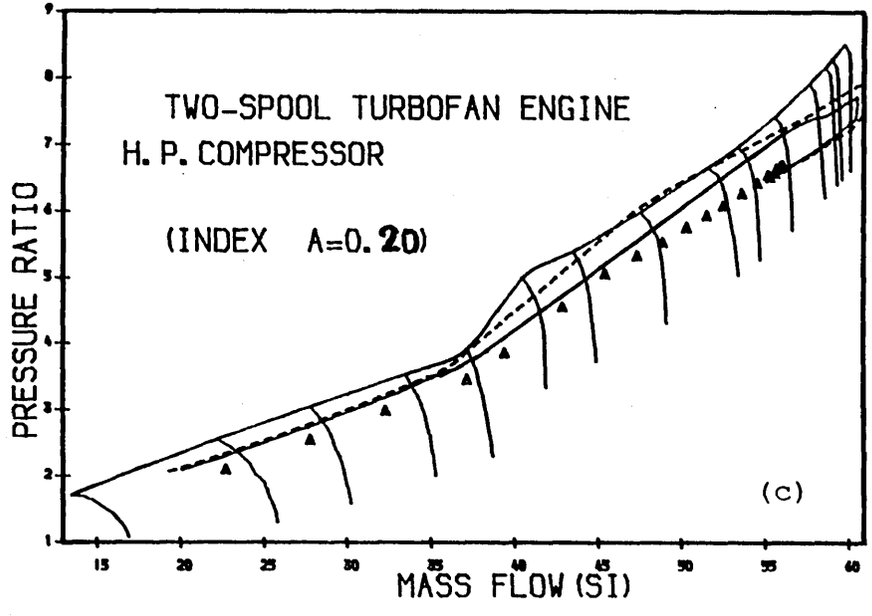

WITH FUEL SCHEDULE COMPENSATED
HEAT TRAN. WITHOUT COMPENSATION
▲ STEADY-RUNNING

Fig. 123

PREDICTED HOT ACC. AT SEA LEVEL

FUEL SCHED. H.P.T. DISC (PLT) TEMP.

▲ FUEL COMPENSATED (INDEX= 0·20)

◆ FUEL COMPENSATED (INDEX= 0·15)

• FUEL COMPENSATED (INDEX=0.10)

+ WITHOUT COMPENSATION

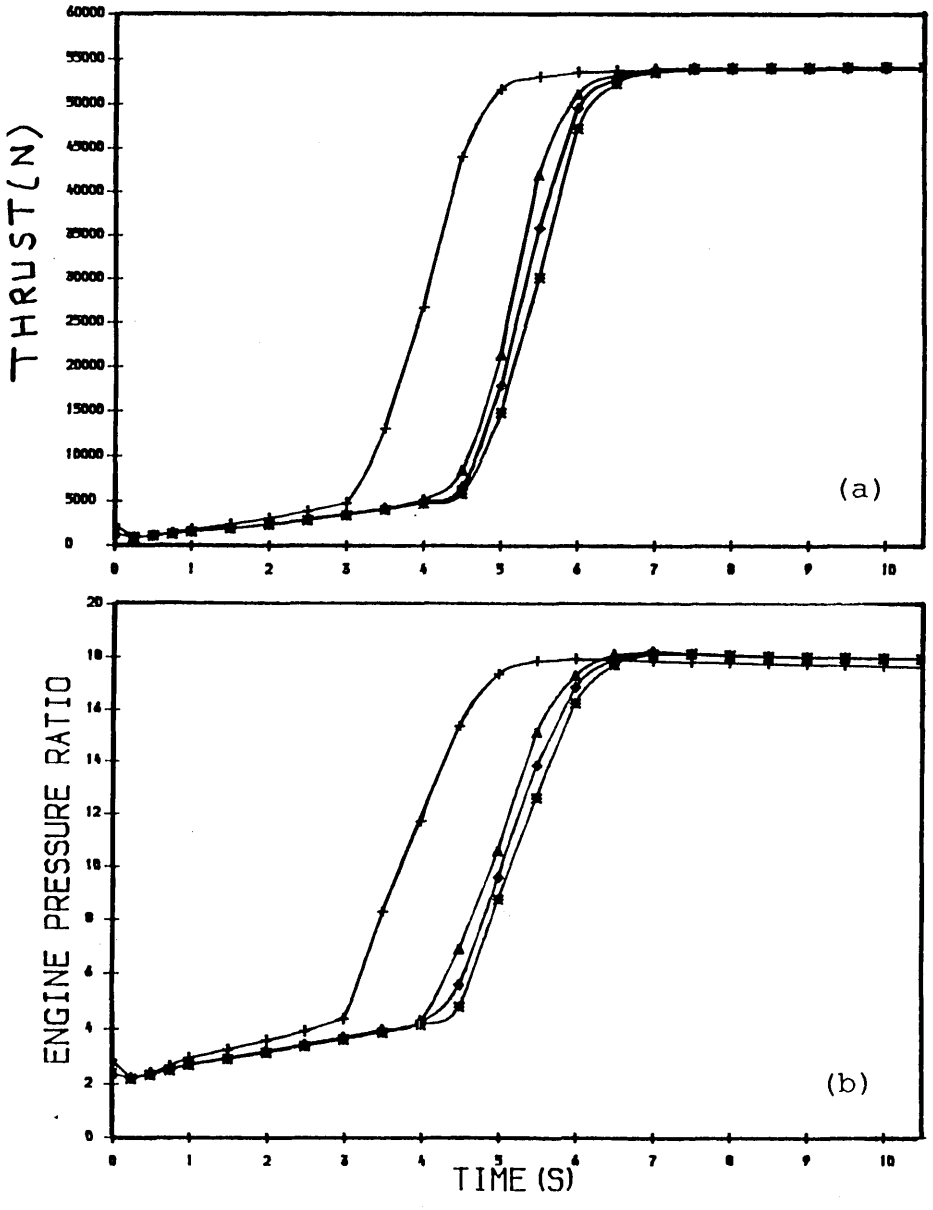

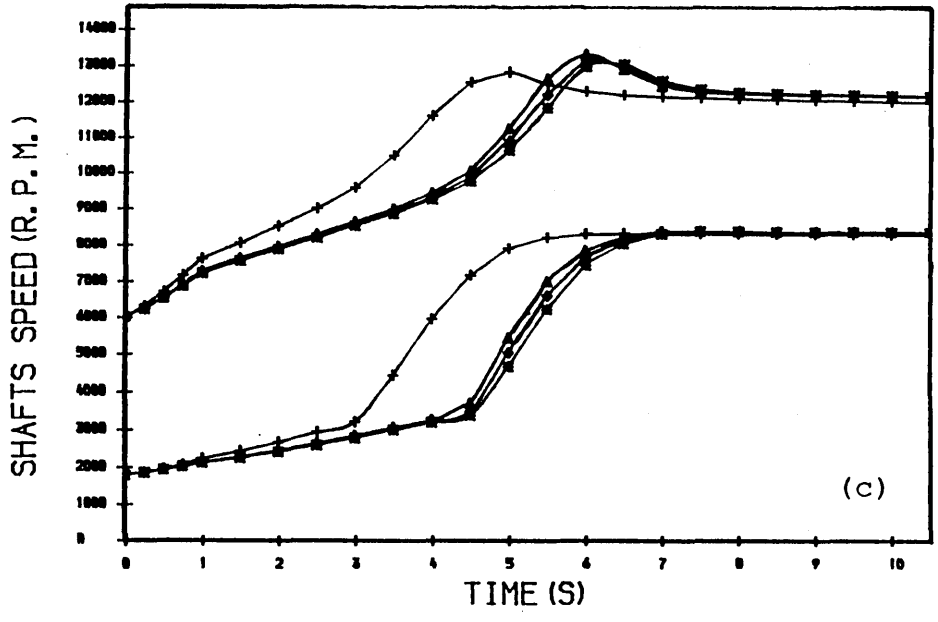

Fig. 124 TRANSIENT ACC. AT SEA-LEVEL
H. P. T. DISC (PLT) TEMP. COMP.

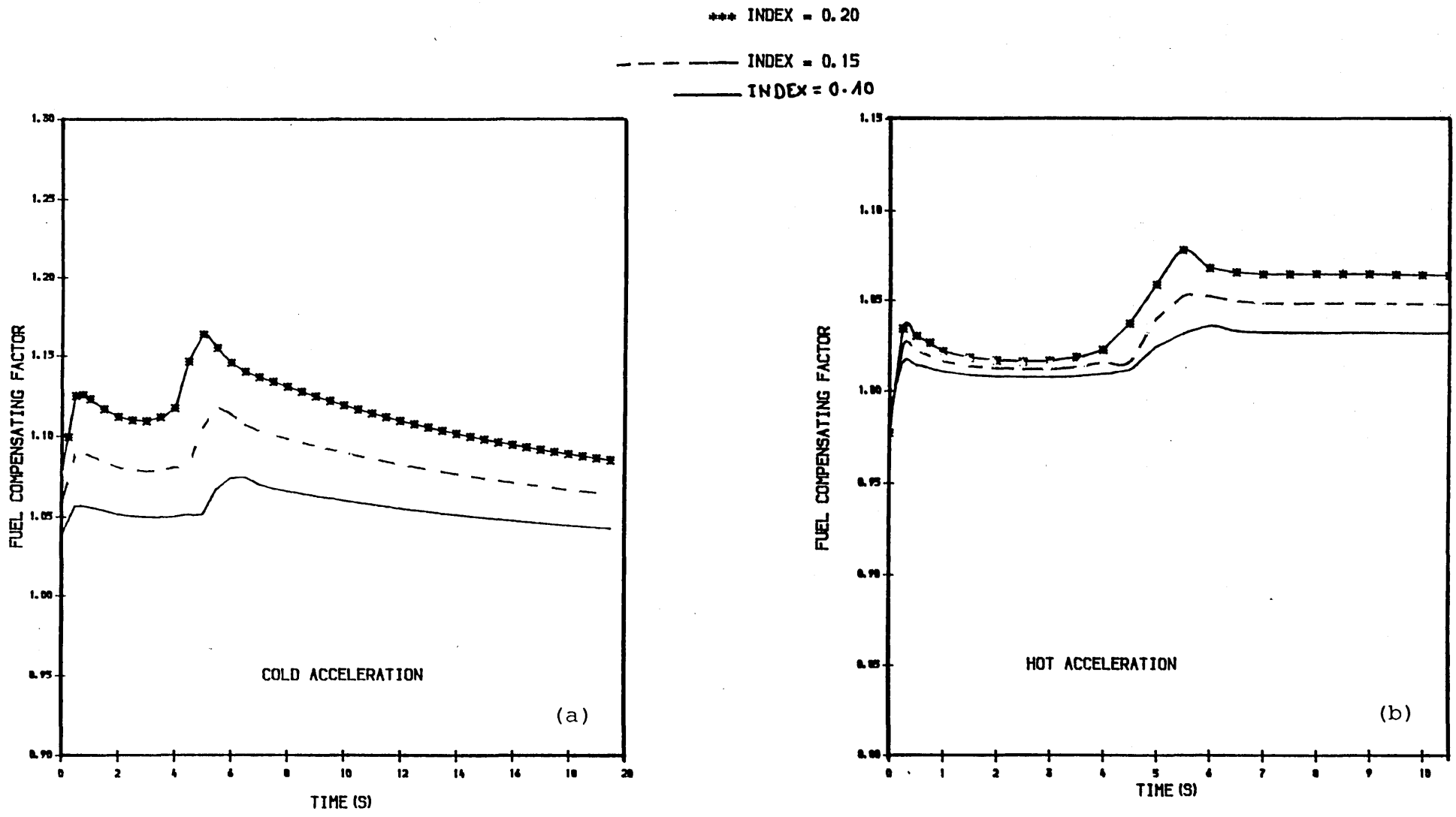

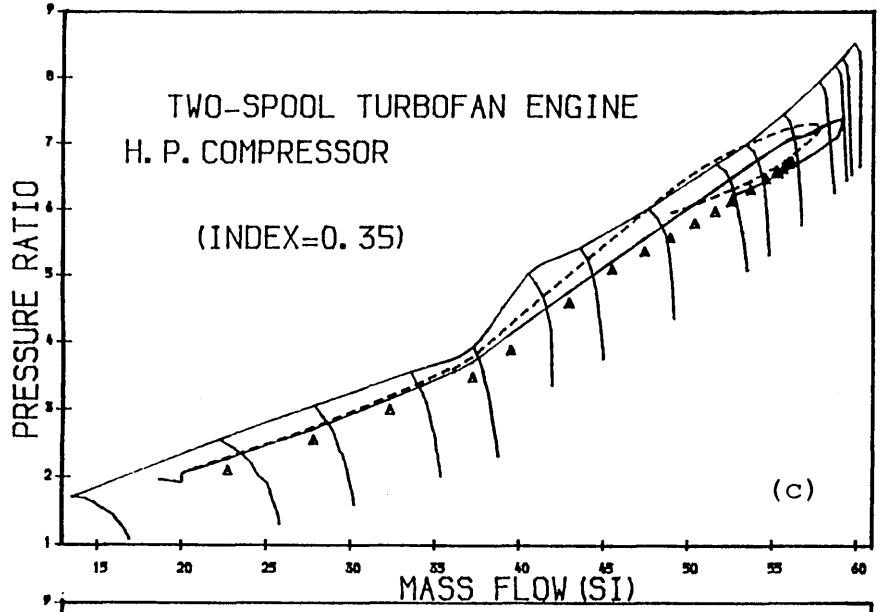

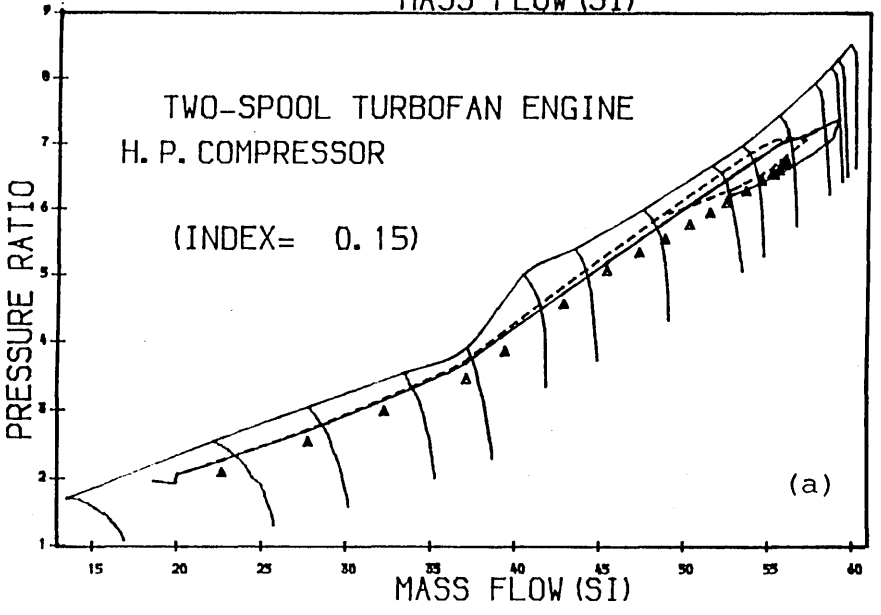

Fig. 125

PREDICTED PATHS OF THE H. P. COMP. DURING COLD ACCEL. AT SEA LEVEL FUEL SCHEDULE COMPENSATED WITH A FUNCT. OF H. P. T. DISC TEMP. COMP.

------ WITH FUEL SCHEDULE COMPENSATED
——— HEAT TRAN. WITHOUT COMPENSATION
▲ STEADY-RUNNING

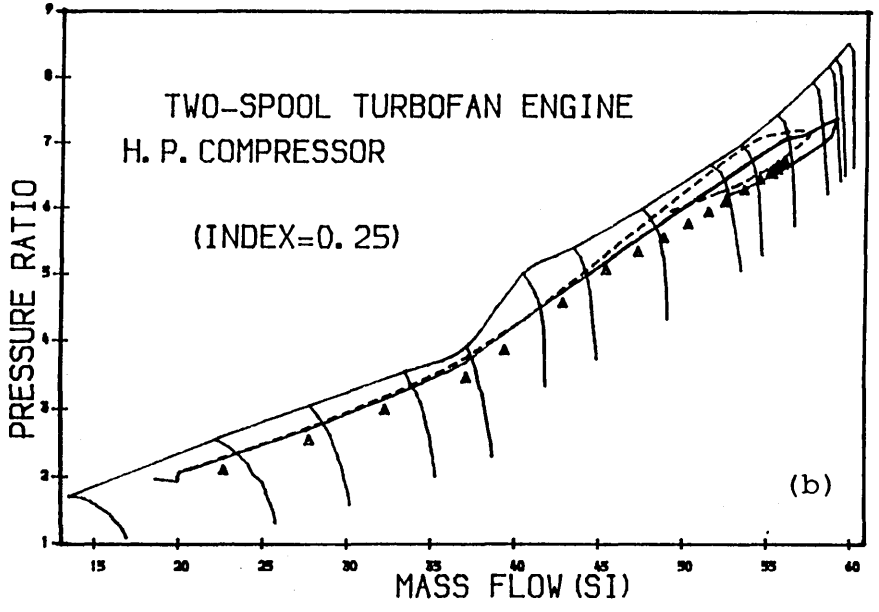

Fig. 126

PREDICTED COLD ACC. AT SEA LEVEL

FUEL SCHED. H.P.T. DISC TEMP. COMP.

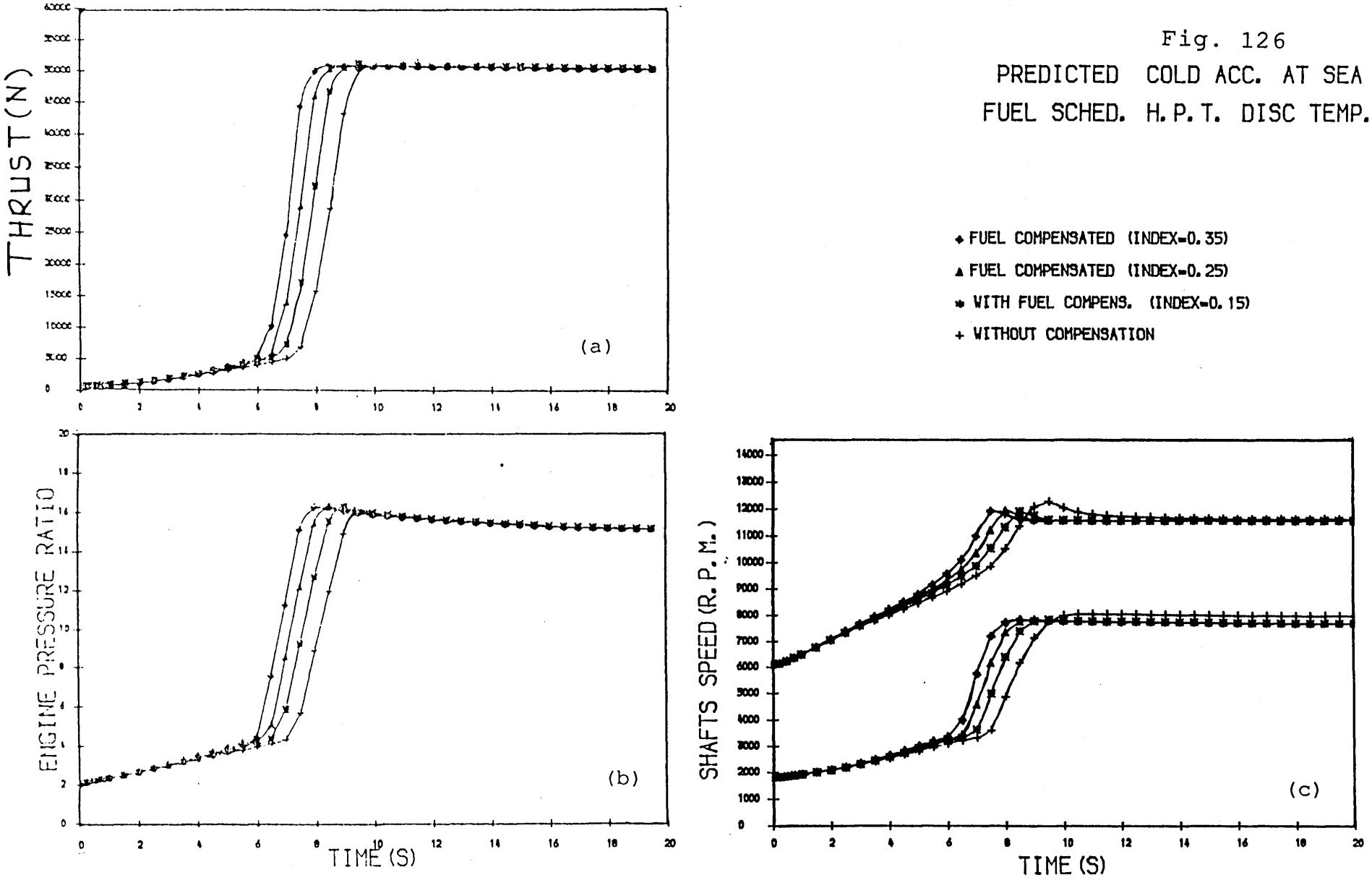

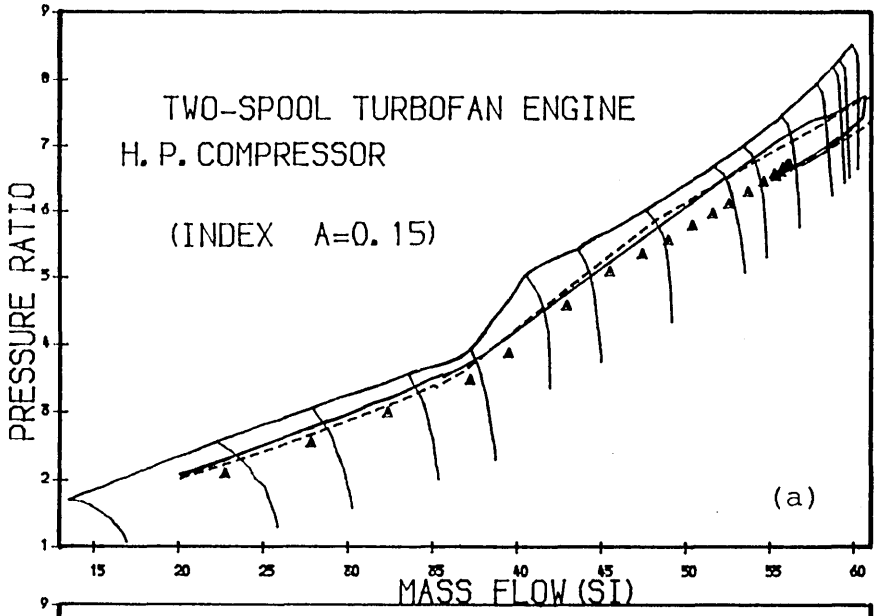

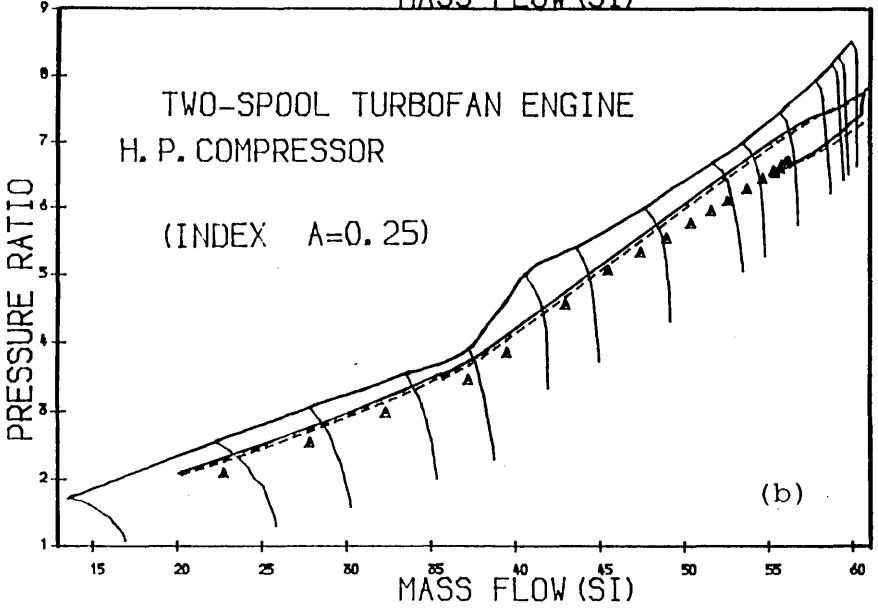

Fig. 127

PREDICTED PATHS OF THE H. P. COMP. DURING HOT ACCEL. AT SEA LEVEL FUEL SCHEDULE COMPENSATED WITH A FUNCT. OF H. P. T. DISC TEMP. COMP.

------- WITH FUEL SCHEDULE COMPENSATED
——— HEAT TRAN. WITHOUT COMPENSATION
▲ STEADY-RUNNING

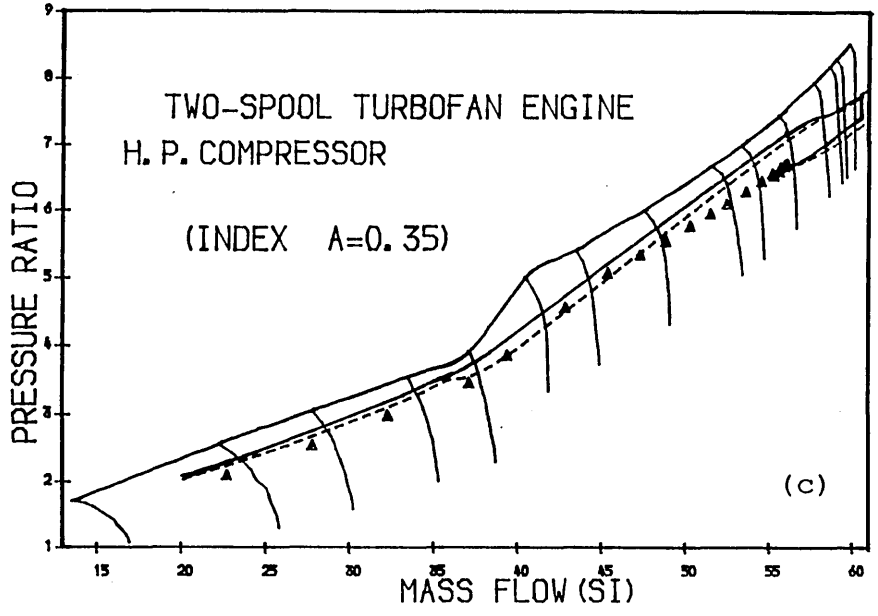

Fig. 128

PREDICTED HOT ACC. AT SEA LEVEL

FUEL SCHED. H.P.T. DISC TEMP. COMP.

- ◆ FUEL COMPENSATED (INDEX=0.35)
- ▲ FUEL COMPENSATED (INDEX=0.25)
- ✱ FUEL COMPENSATED (INDEX=0.15)
- \+ WITHOUT COMPENSATION

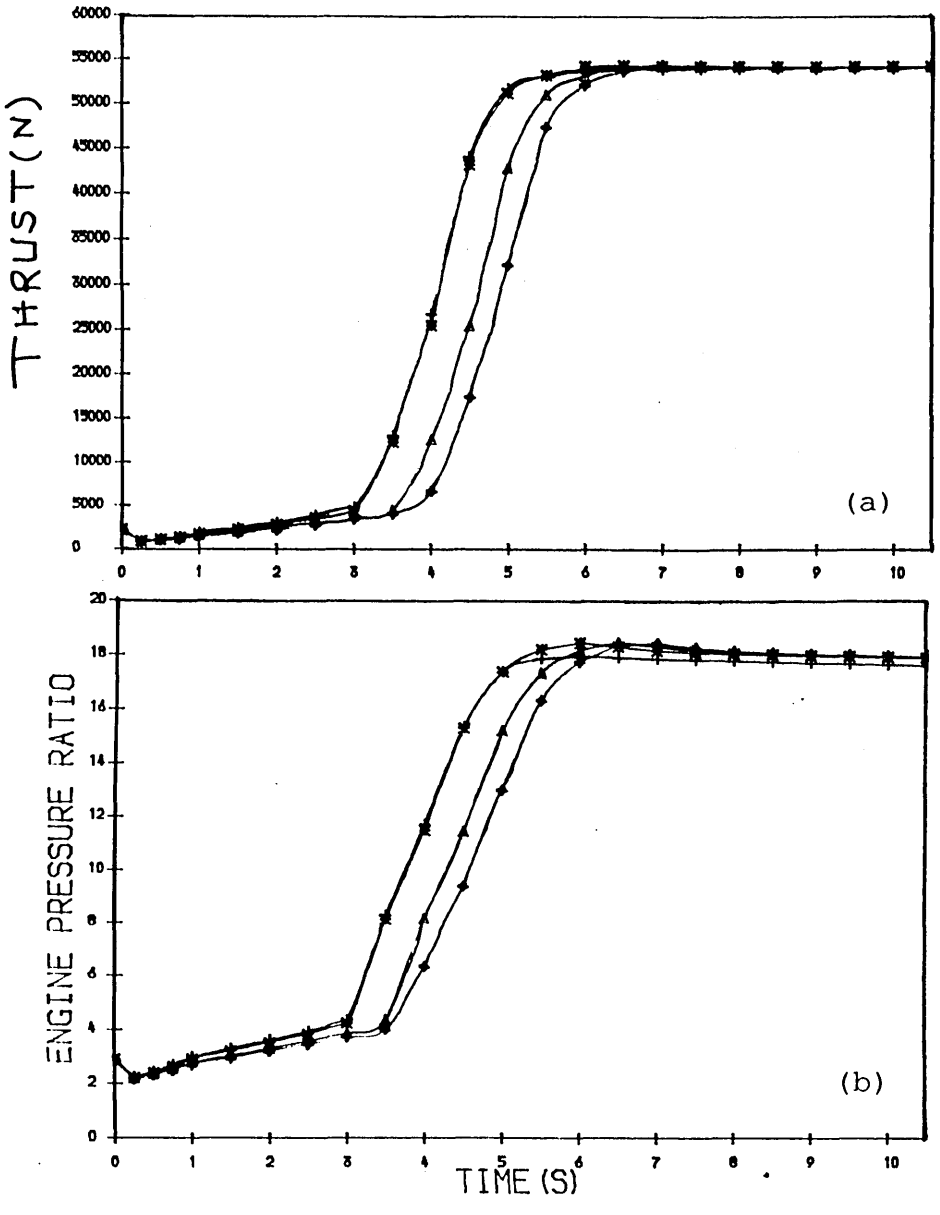

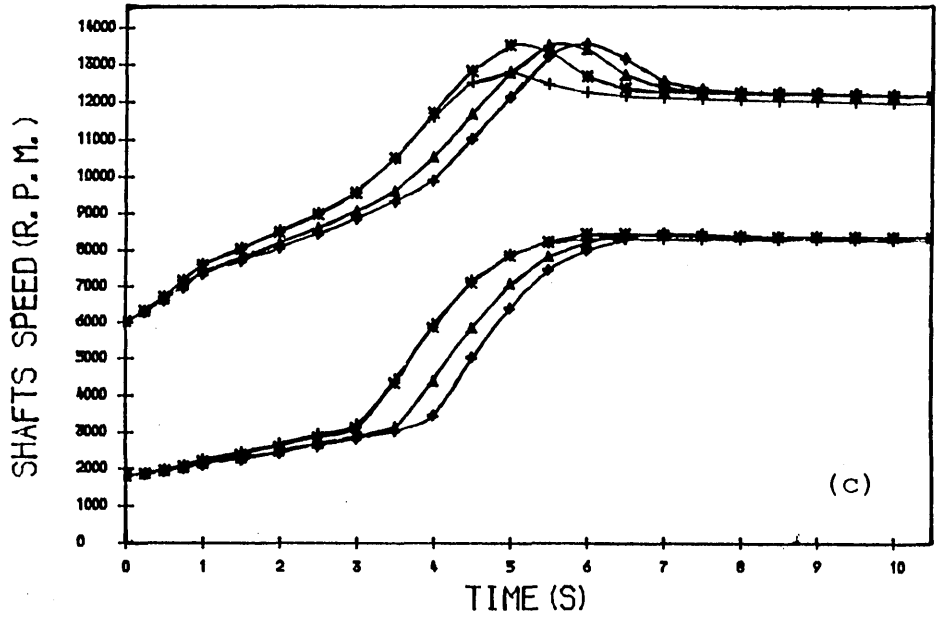

Fig. 129 TRANSIENT ACC. AT SEA LEVEL
H.P.T. DISC TEMP. COMP.

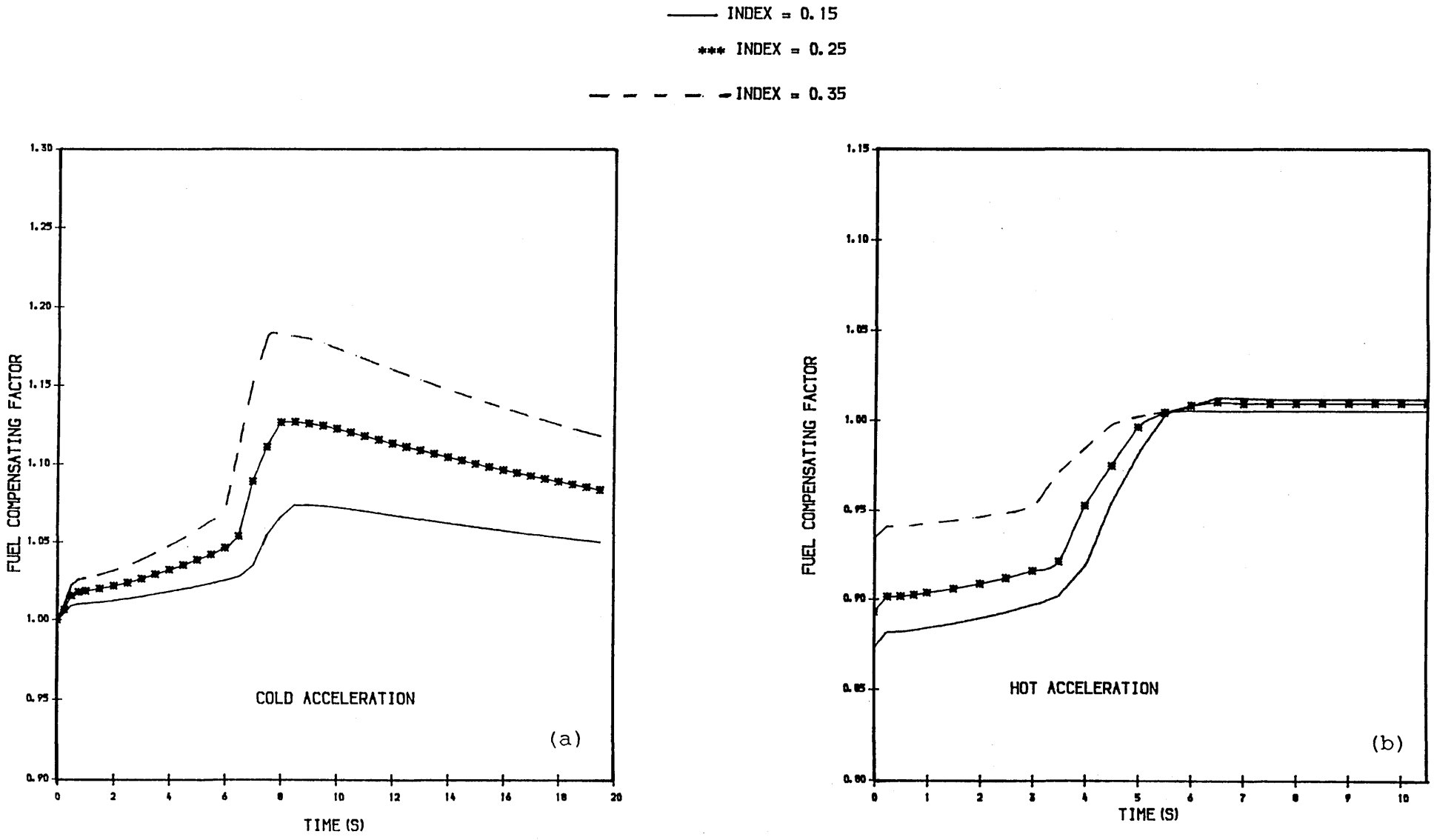

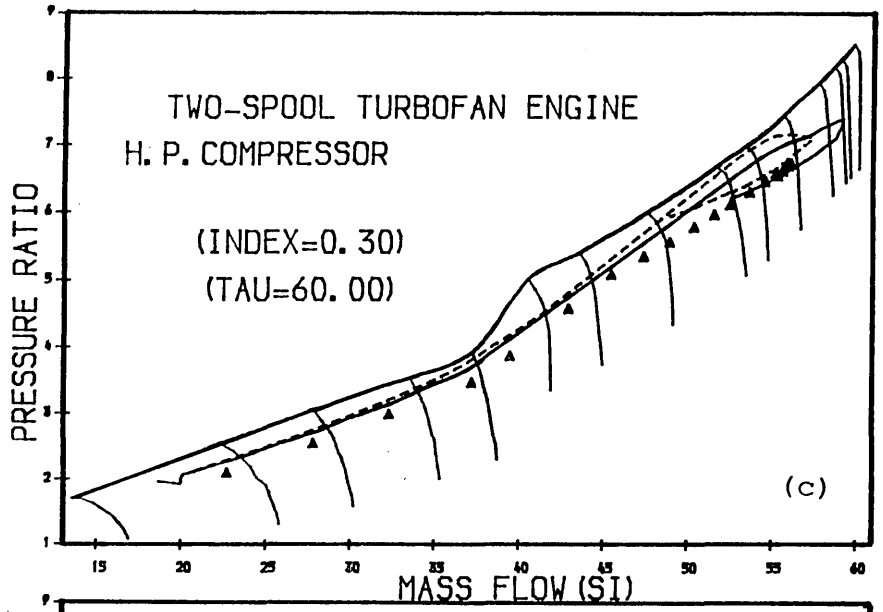

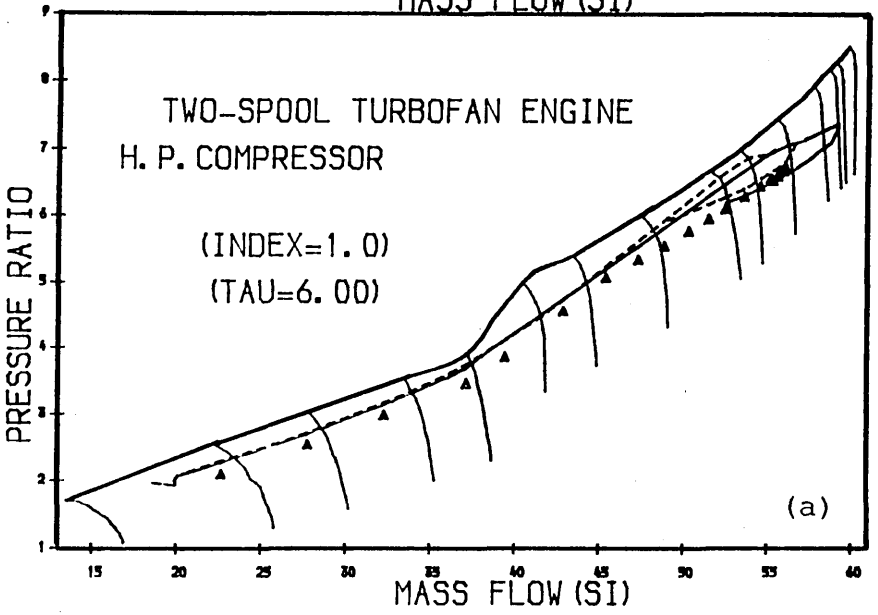

Fig. 130

PREDICTED PATHS OF THE H. P. COMP.
DURING COLD ACCEL. AT SEA LEVEL
FUEL SCHEDULE COMPENSATED WITH
A FUNCT. OF H. P. SHAFT DELAYED SPEED .

------ WITH FUEL SCHEDULE COMPENSATED
——— HEAT TRAN. WITHOUT COMPENSATION
▲ STEADY-RUNNING

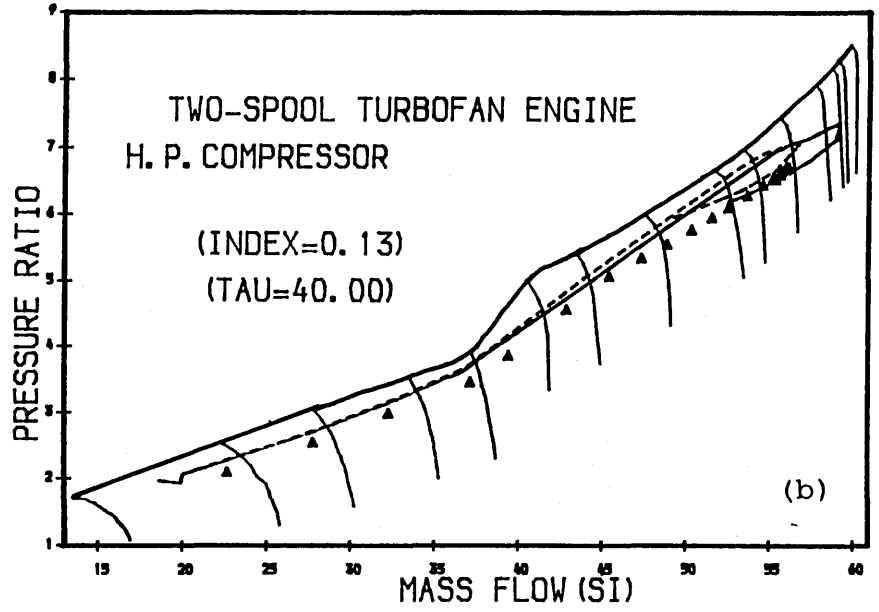

Fig. 131

PREDICTED COLD ACC. AT SEA LEVEL

FUEL SCHED. H. P. SHAFT DELAYED SPEED

◆ FUEL COMPENSATED (INDEX=0.30) ; τ = 60.00

▲ FUEL COMPENSATED (INDEX=0.13) ; τ = 40.00

✱ WITH FUEL COMPENS. (INDEX=1.00) ; τ = 6.00

+ WITHOUT COMPENSATION

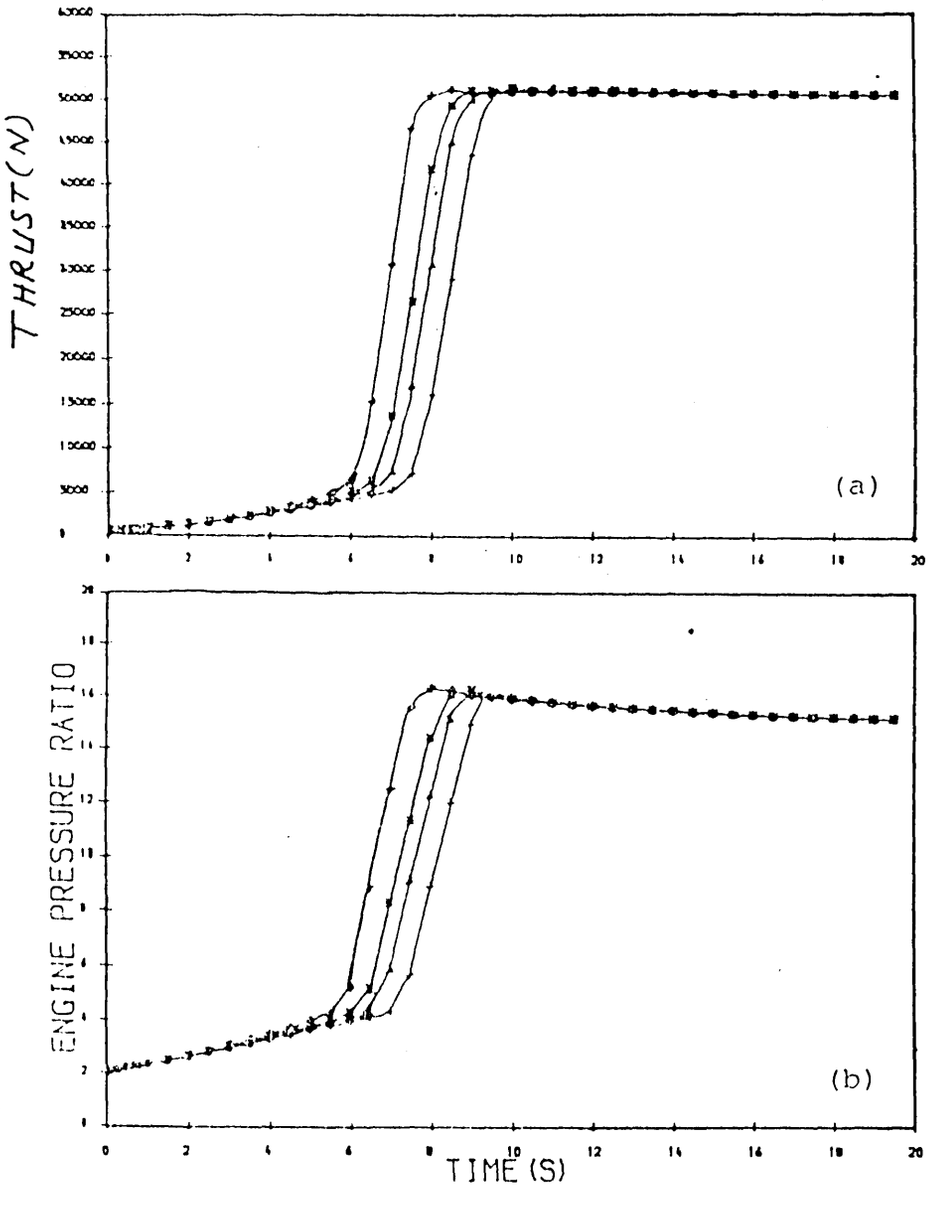

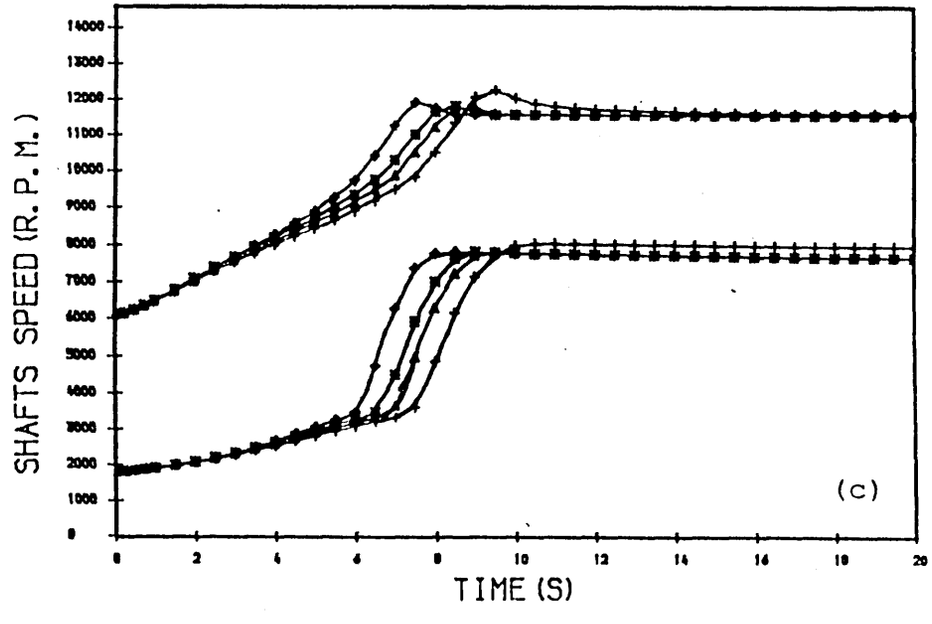

Fig. 132

PREDICTED PATHS OF THE H. P. COMP. DURING HOT ACCEL. AT SEA LEVEL FUEL SCHEDULE COMPENSATED WITH A FUNCT. OF H. P. SHAFT DELAYED SPEED

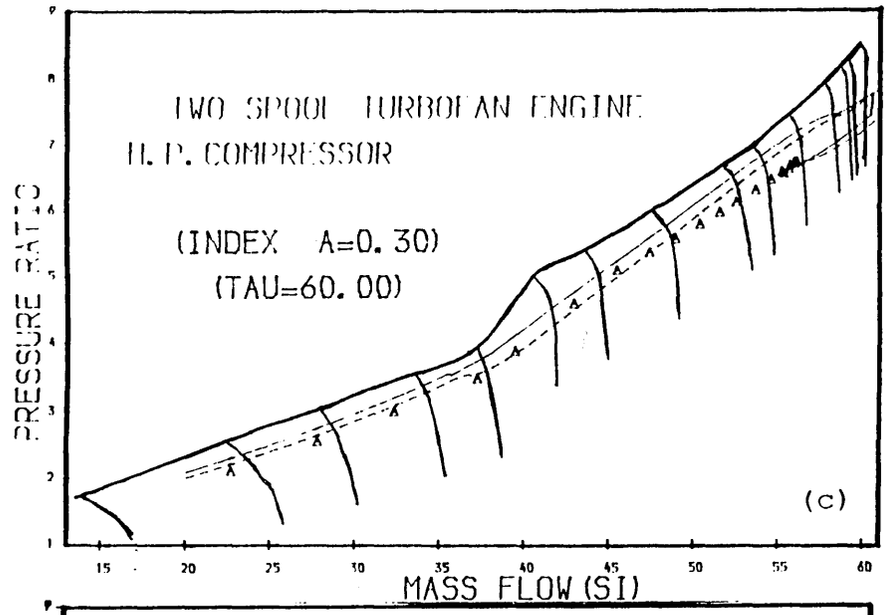

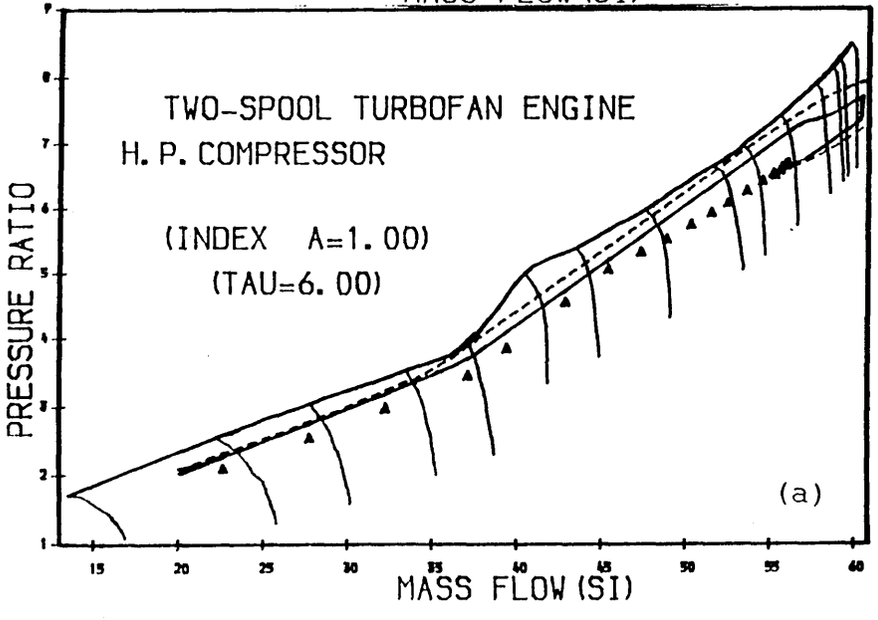

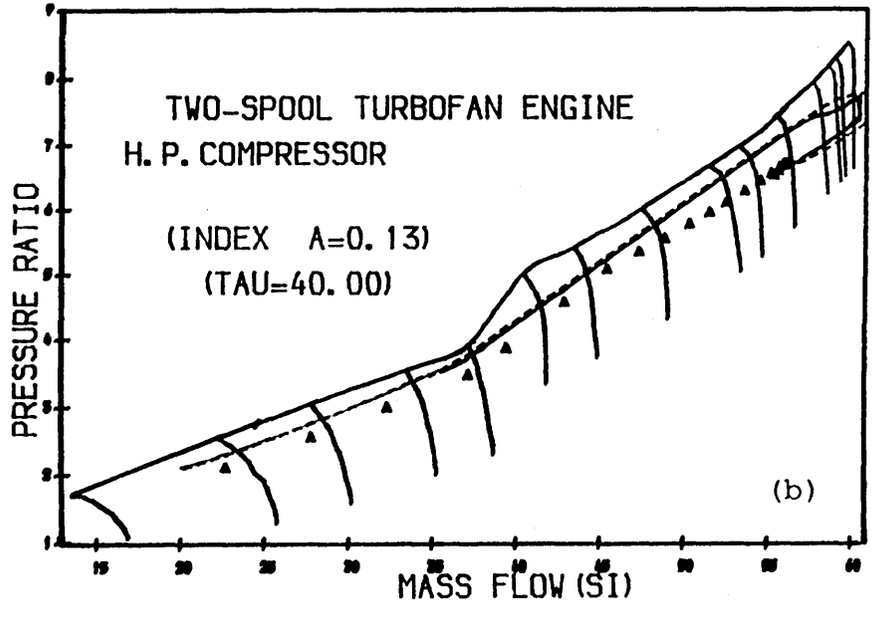

------ WITH FUEL SCHEDULE COMPENSATED

——— HEAT TRAN. WITHOUT COMPENSATION

▲ STEADY-RUNNING

Fig. 133

PREDICTED HOT ACC. AT SEA LEVEL

FUEL SCHED. H.P. SHAFT DELAYED SPEED

▲ FUEL COMPENSATED (INDEX=0.30) ; τ = 60.00

* FUEL COMPENSATED (INDEX=0.13) ; τ = 40.00

◆ FUEL COMPENSATED (INDEX=1.00) ; τ = 6.00

\+ WITHOUT COMPENSATION

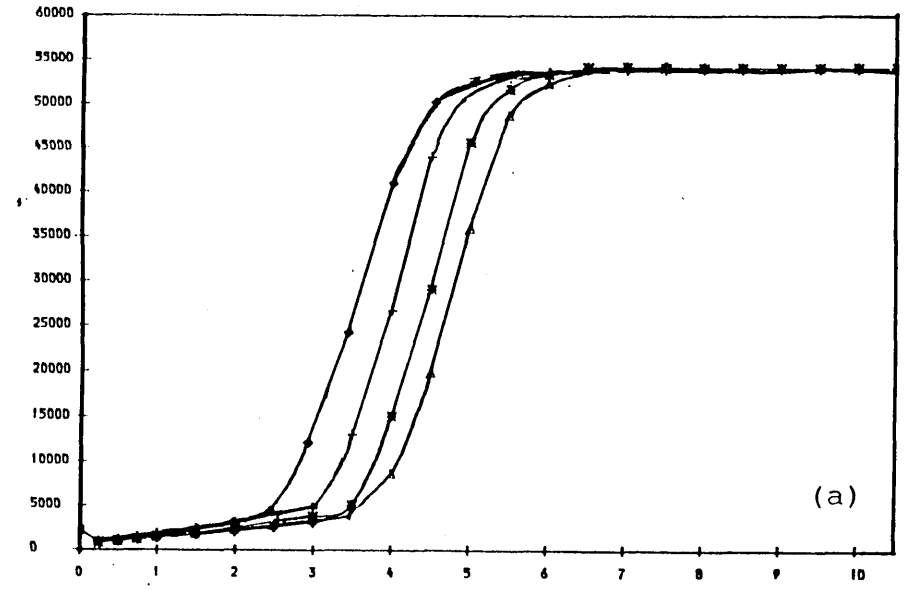

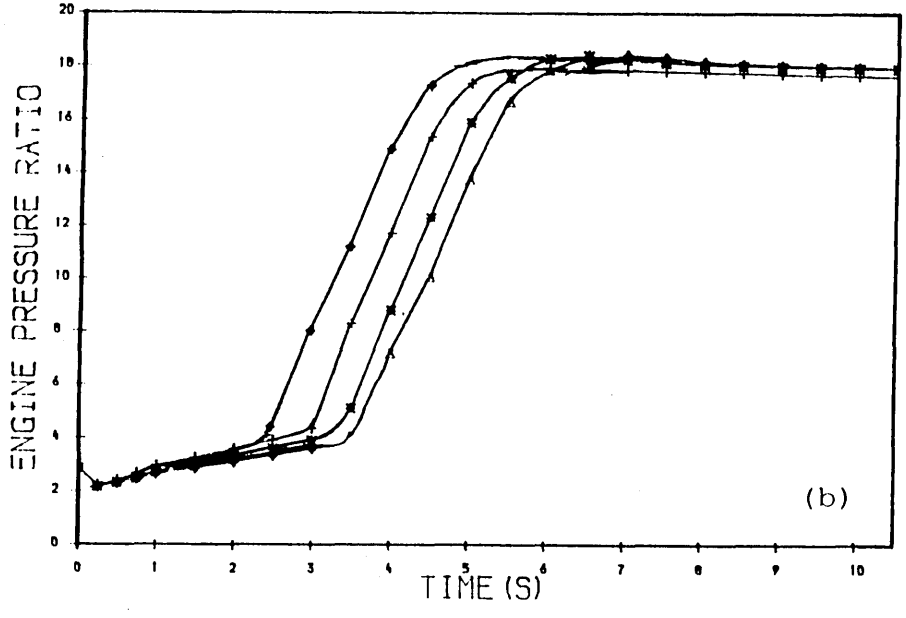

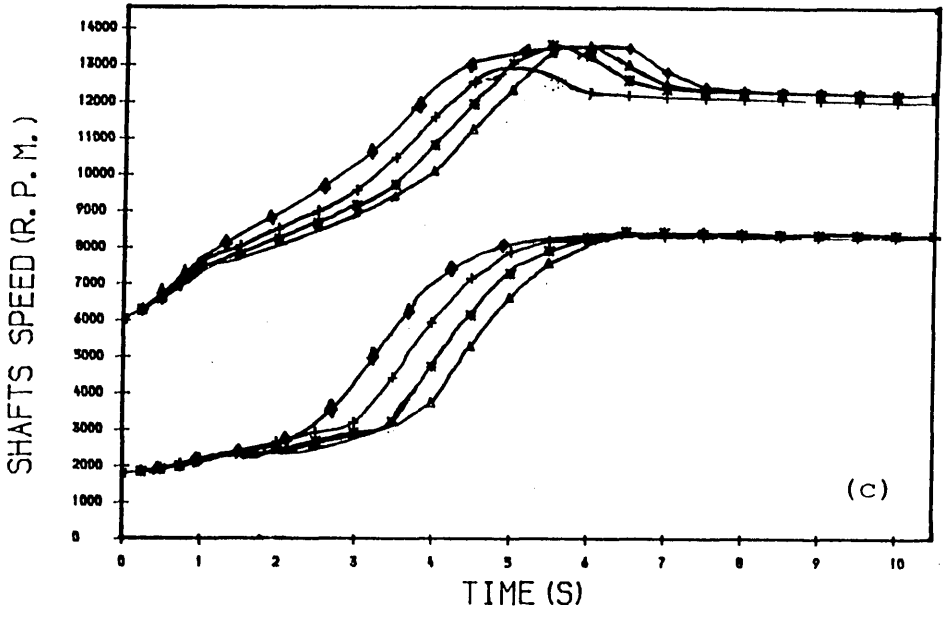

Fig. 134 TRANSIENT ACC. AT SEA LEVEL
H. P. SHAFT DELAYED SPEED COMP.

——— INDEX = 1.0 ; τ = 6.00

*** INDEX = 0.13 ; τ = 40.00

– – – – – – INDEX = 0.30 ; τ = 60.00

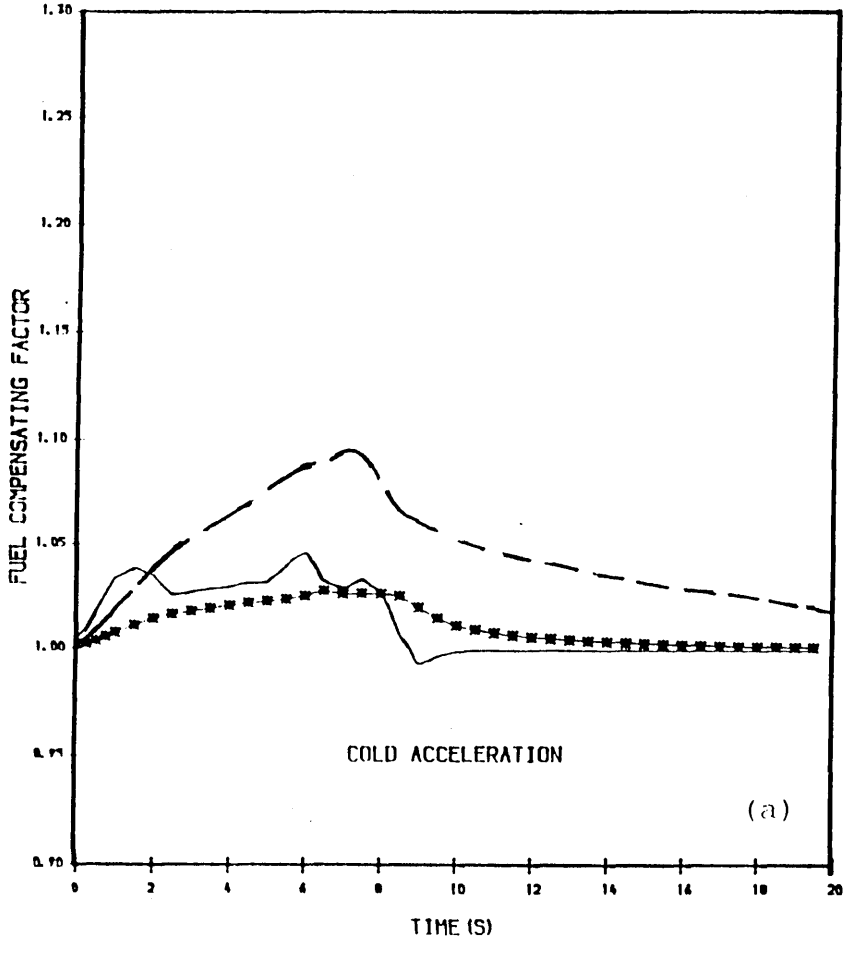

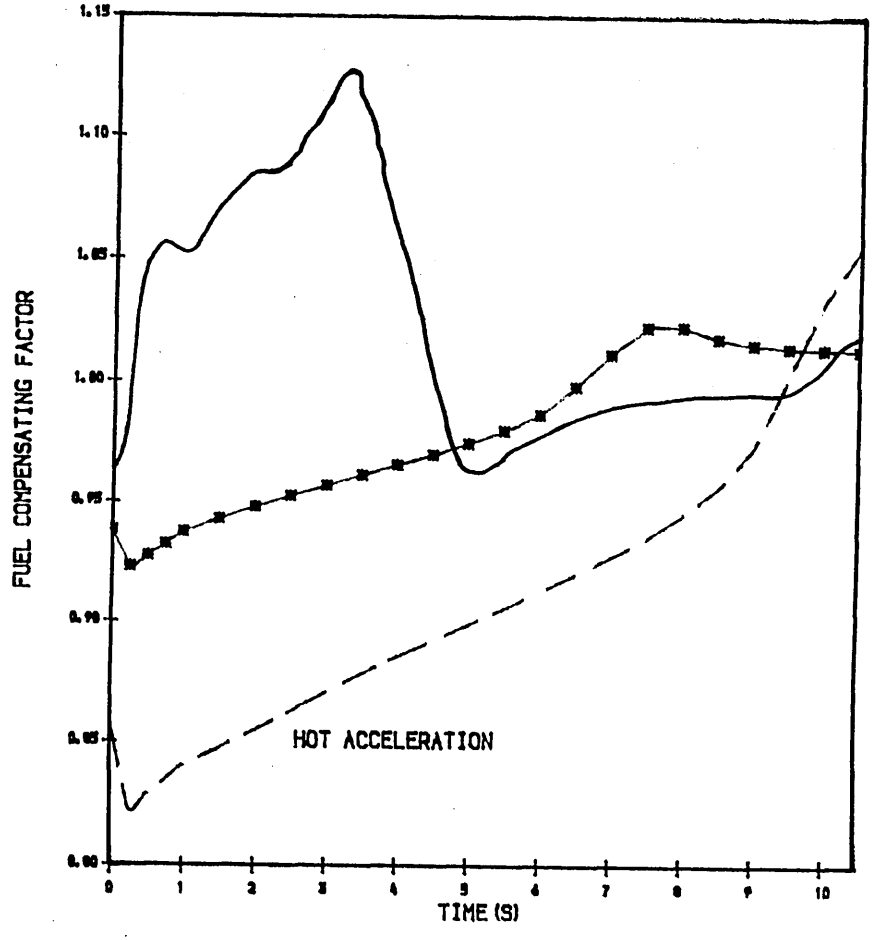

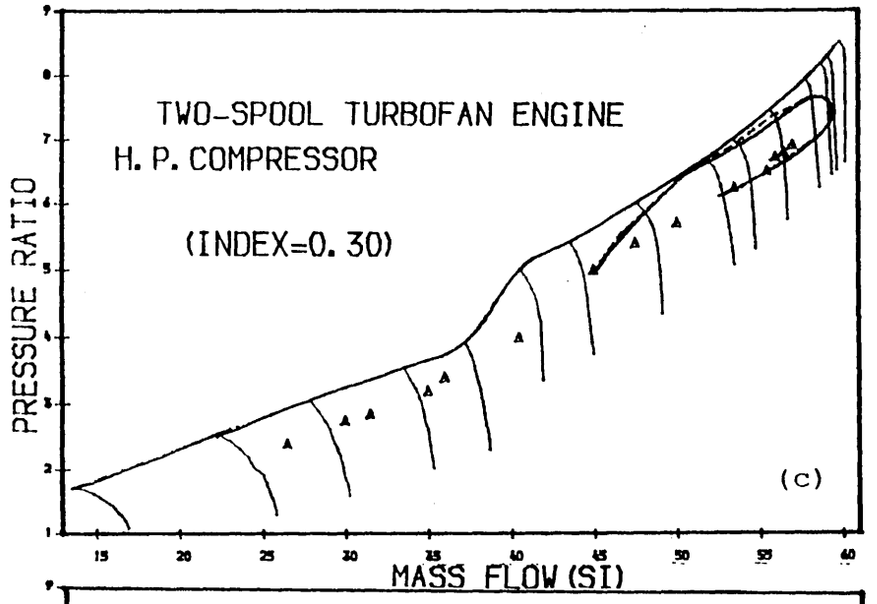

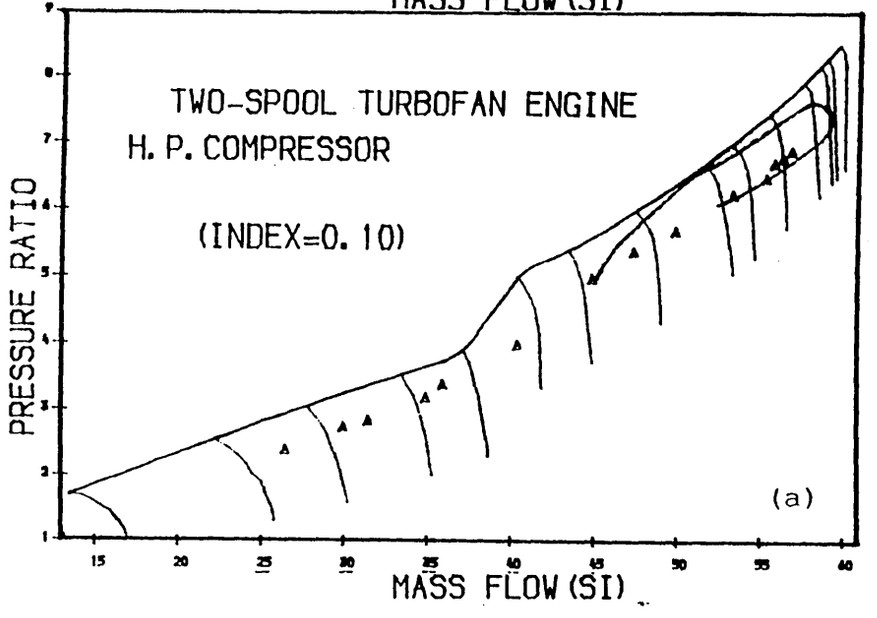

Fig. 135

PREDICTED PATHS OF THE H. P. COMP.
DURING COLD ACCEL. AT 41,000 FT
FUEL SCHEDULE COMPENSATED WITH
A FUNCT. OF H. P. T. DISC (HUB) TP. CP.

---- WITH FUEL SCHEDULE COMPENSATED
——— HEAT TRAN. WITHOUT COMPENSATION
▲ STEADY-RUNNING

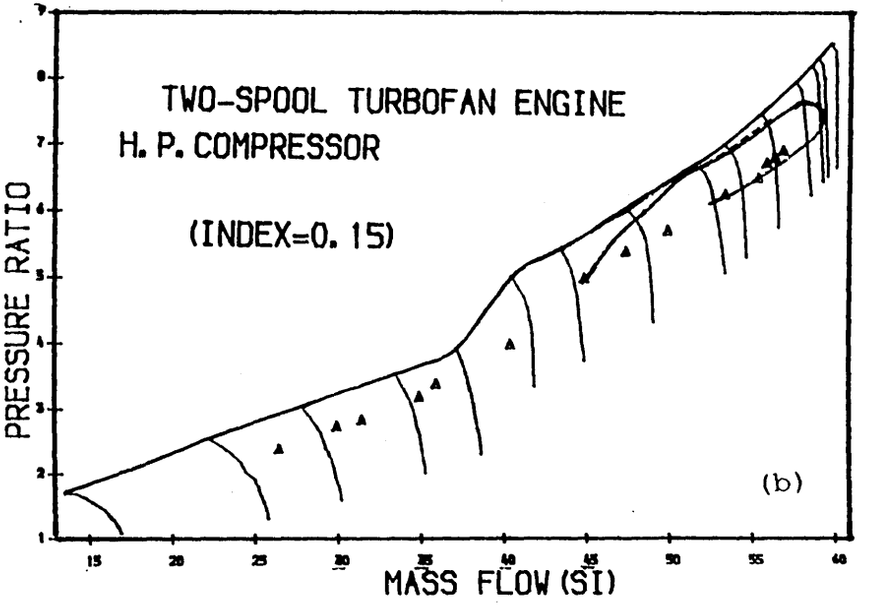

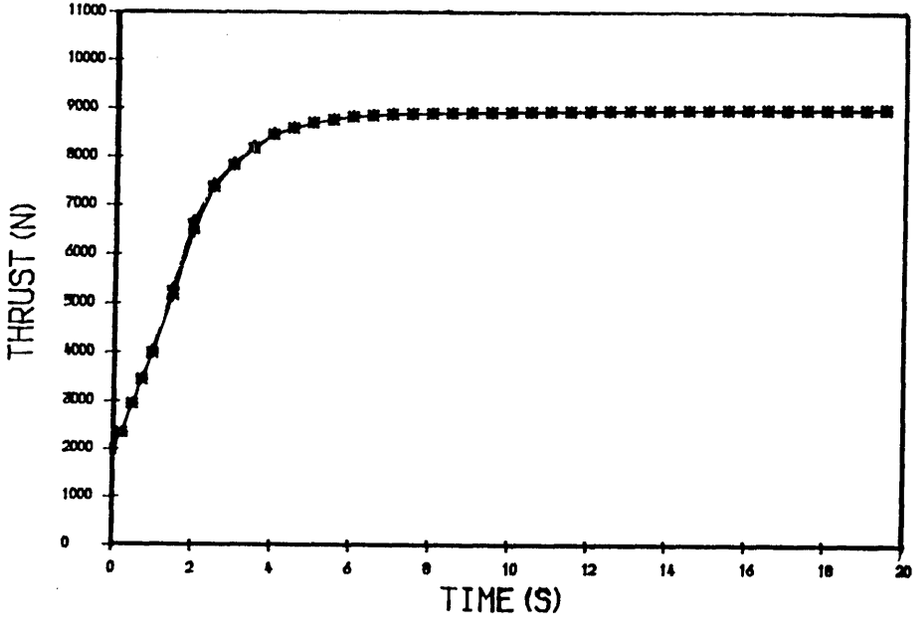

Fig. 136

PREDICTED COLD ACC. AT 41,000 FT
FUEL SCHED. H.P.T. DISC (HUB) TP. CMP.

◆ FUEL COMPENSATED (INDEX=0.30)
▲ FUEL COMPENSATED (INDEX=0.15)
✱ WITH FUEL COMPENS. (INDEX=0.10)
+ WITHOUT COMPENSATION

Fig. 137

PREDICTED PATHS OF THE H. P. COMP.
DURING HOT ACCEL. AT 41,000FT
FUEL SCHEDULE COMPENSATED WITH
A FUNCT. OF H.P.T. DISC(HUB) TP. COMP.

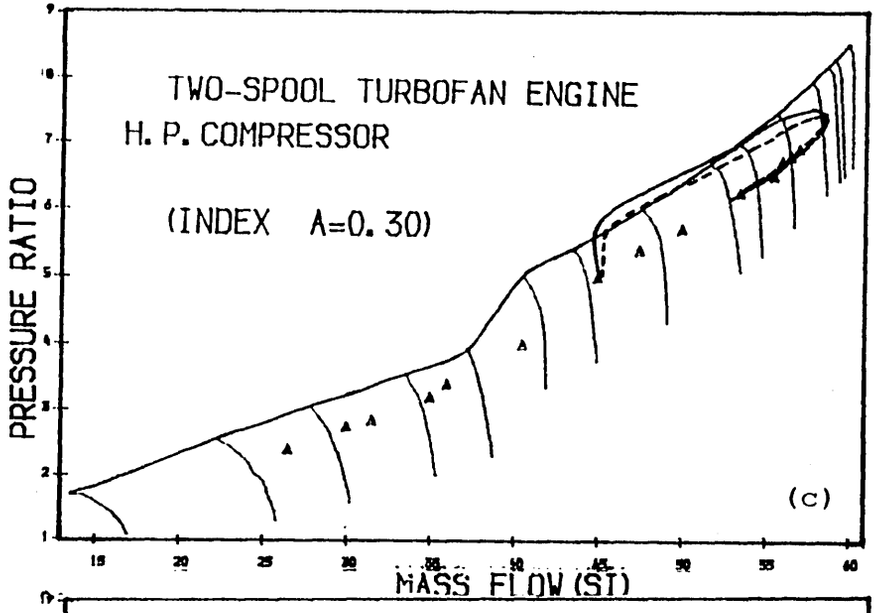

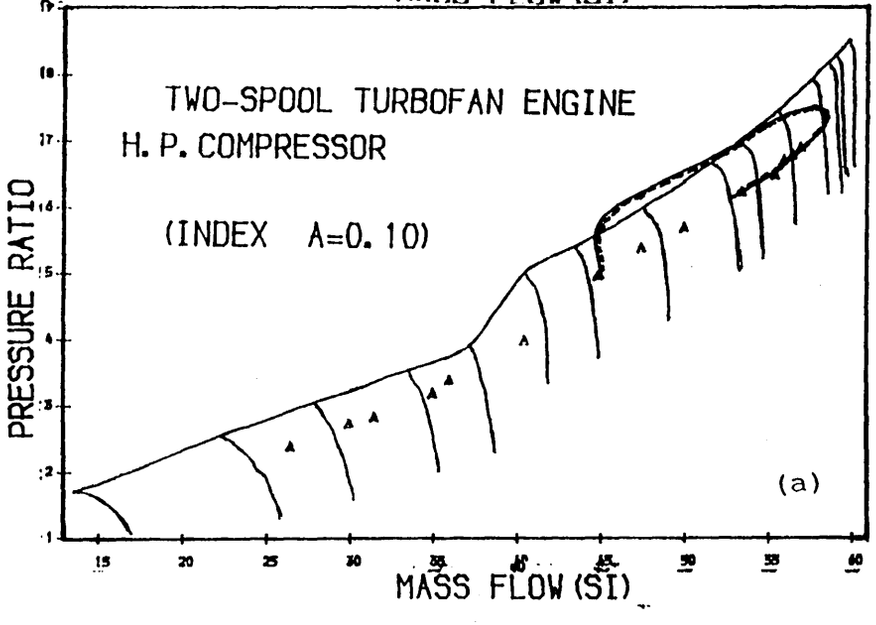

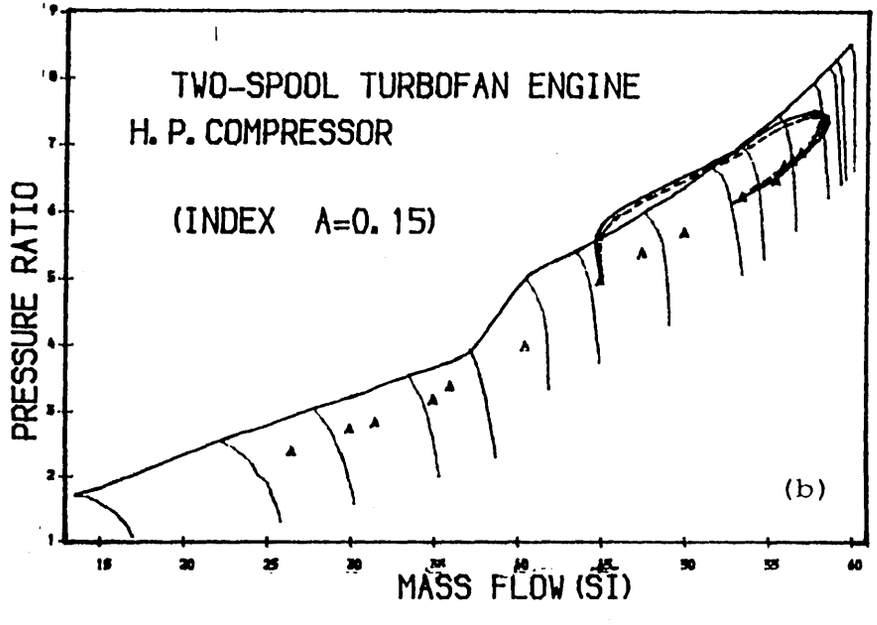

WITH FUEL SCHEDULE COMPENSATED
HEAT TRAN. WITHOUT COMPENSATION
▲ STEADY-RUNNING

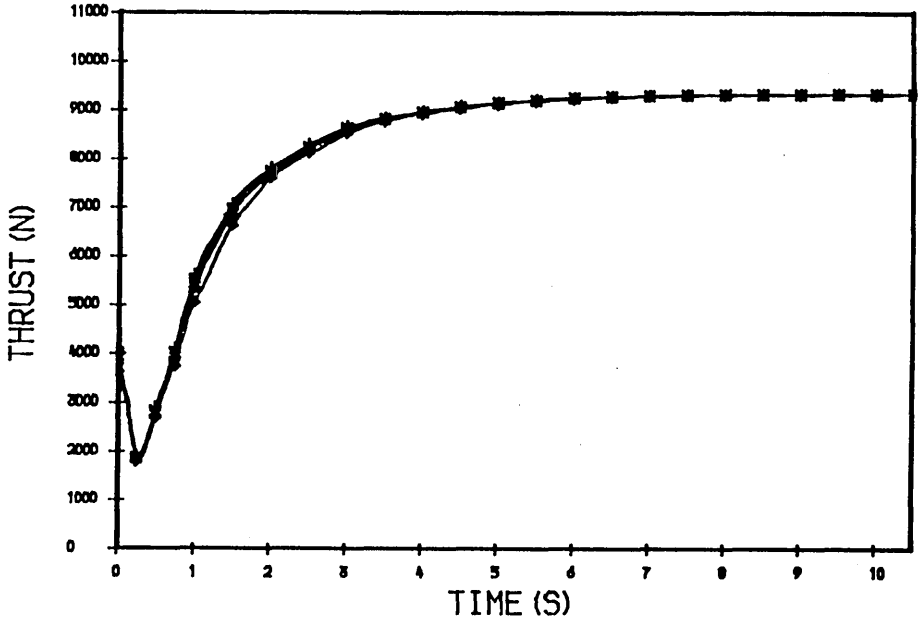

Fig. 138

PREDICTED HOT ACC. AT 41,000 FT
FUEL SCHED. H.P.T. DISC (HUB) TP. COMP.

◆ FUEL COMPENSATED (INDEX=0.30)
▲ FUEL COMPENSATED (INDEX=0.15)
✱ FUEL COMPENSATED (INDEX=0.10)
+ WITHOUT COMPENSATION

Fig. 139 TRANSIENT ACC. AT 41,000 FT
H. P. T. DISC (HUB) TEMP. COMP.

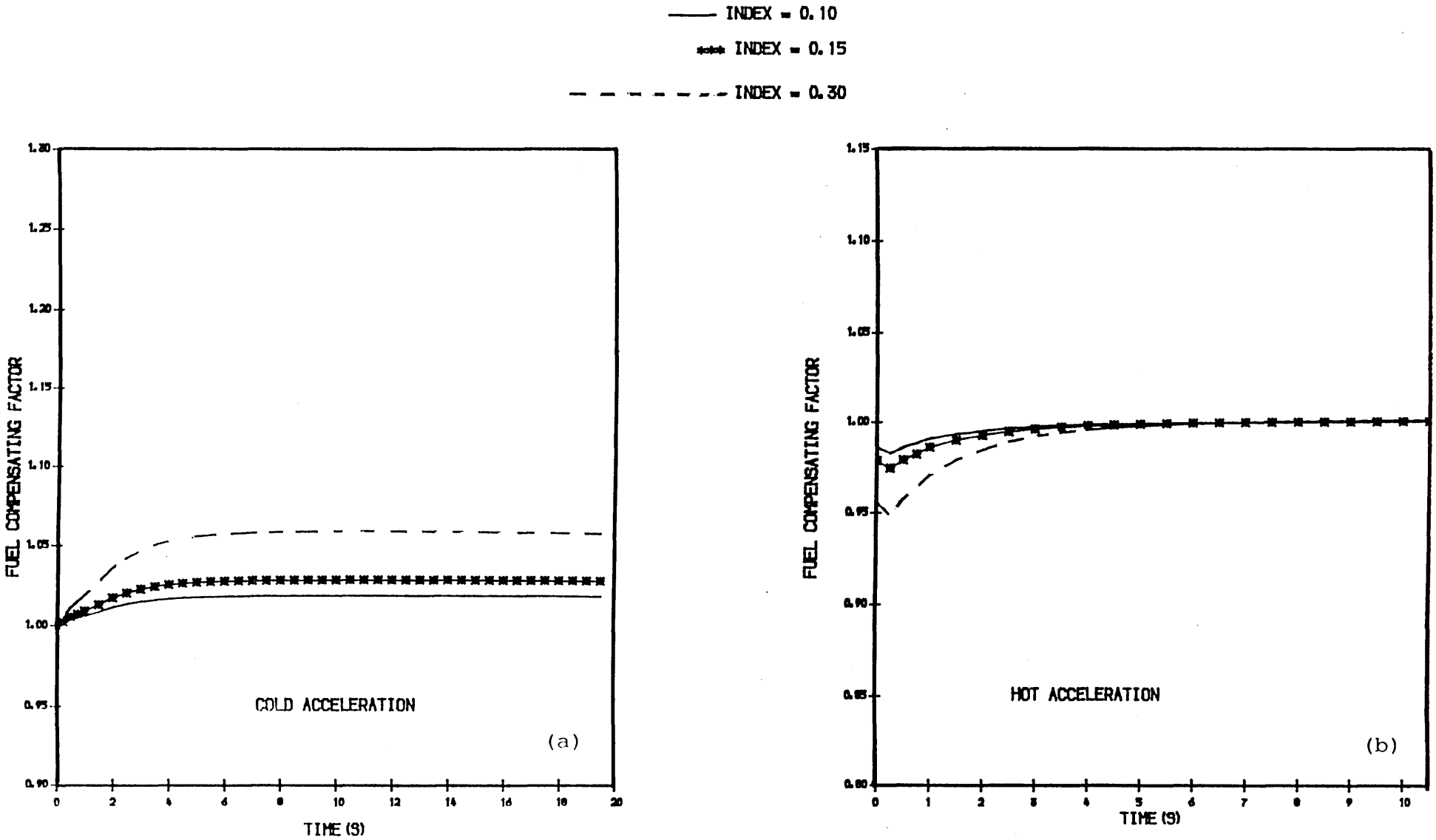

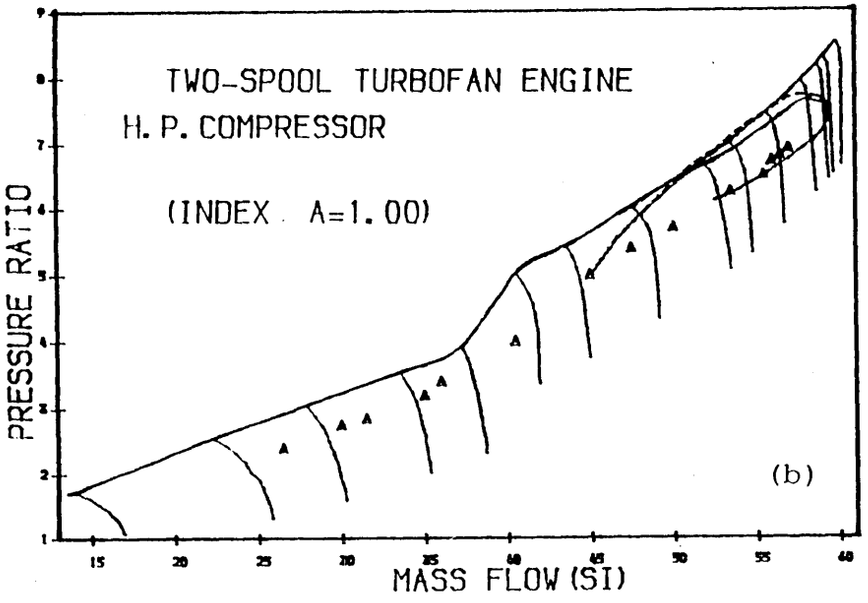

Fig. 140

PREDICTED PATHS OF THE H. P. COMP.
DURING COLD ACCEL. AT 41,000 FT
FUEL SCHEDULE COMPENSATED WITH
A FUNCT. OF H. P. T. DISC (HUB) TP. CP.

- - - — WITH FUEL SCHEDULE COMPENSATED
——— HEAT TRAN. WITHOUT COMPENSATION
▲ STEADY-RUNNING

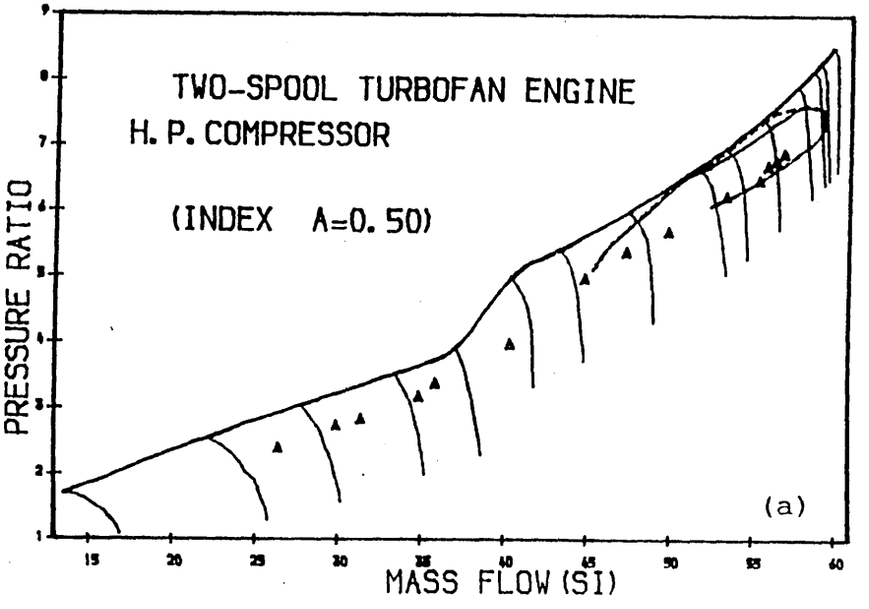

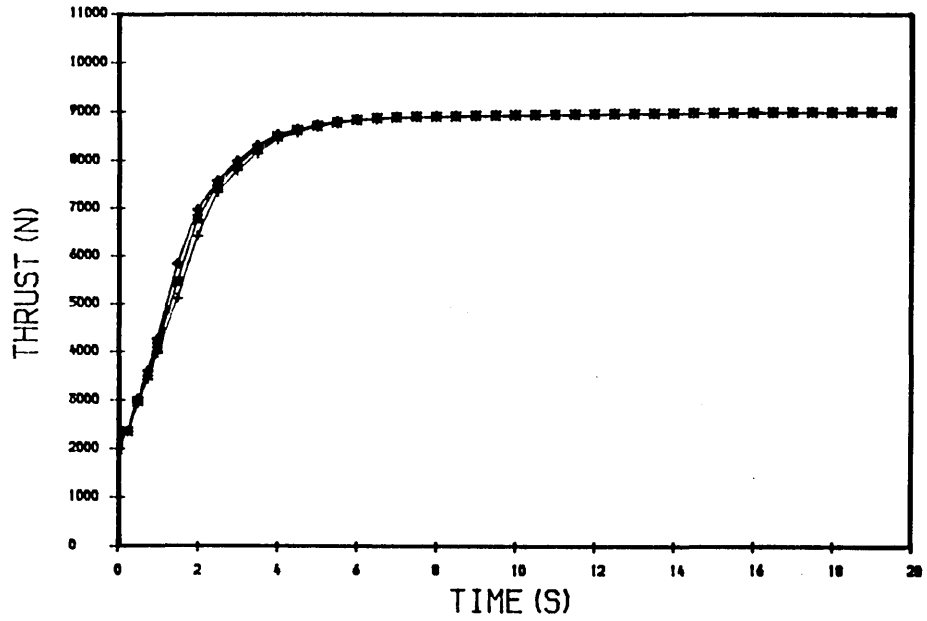

Fig. 141

PREDICTED COLD ACC. AT 41,000 FT
FUEL SCHED. H.P.T. DISC (HUB) TP. CMP.

◆ FUEL COMPENSATED (INDEX=1.00)

✱ WITH FUEL COMPENS. (INDEX=0.50)

\+ WITHOUT COMPENSATION

Fig. 142

PREDICTED PATHS OF THE H. P. COMP. DURING HOT ACCEL. AT 41,000FT FUEL SCHEDULE COMPENSATED WITH A FUNCT. OF H. P. T. DISC (HUB) TP. COMP.

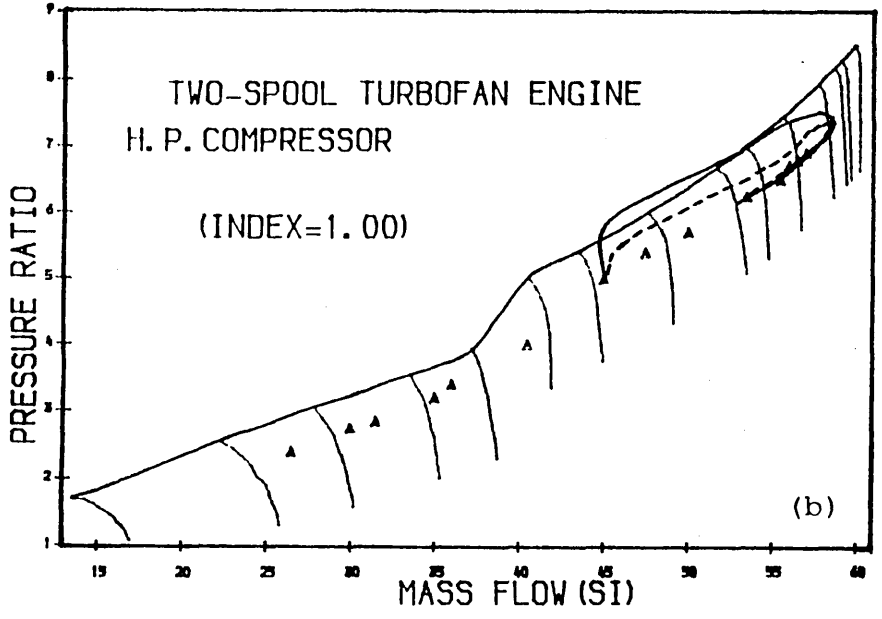

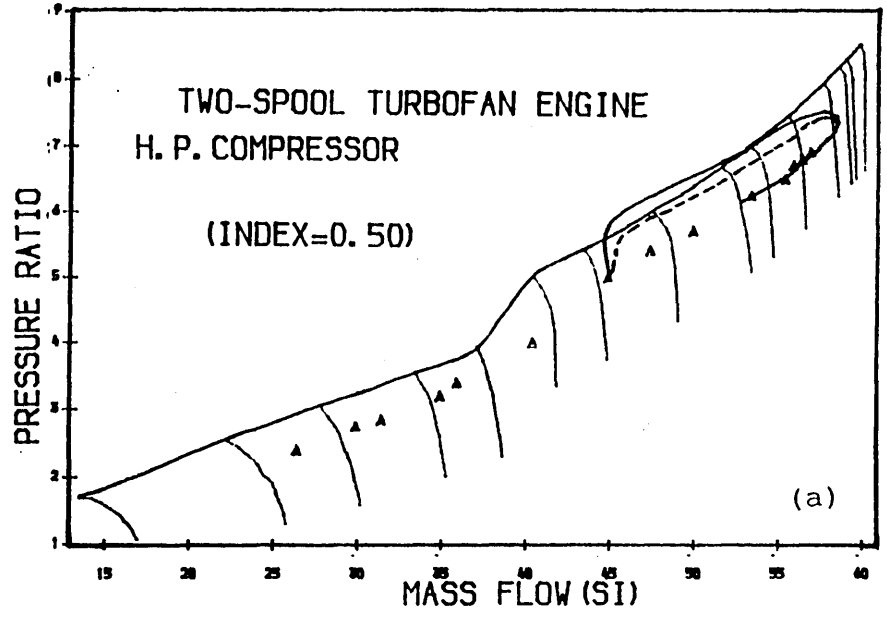

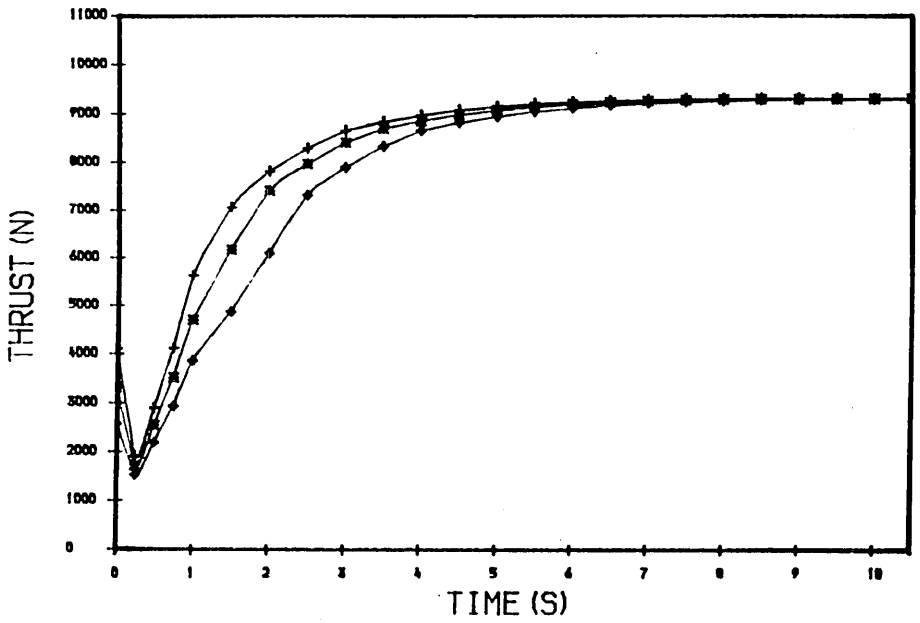

Fig. 143

PREDICTED HOT ACC. AT 41,000 FT
FUEL SCHED. H.P.T. DISC (HUB) TP. COMP.

◆ FUEL COMPENSATED (INDEX=1.00)

* FUEL COMPENSATED (INDEX=0.50)

\+ WITHOUT COMPENSATION

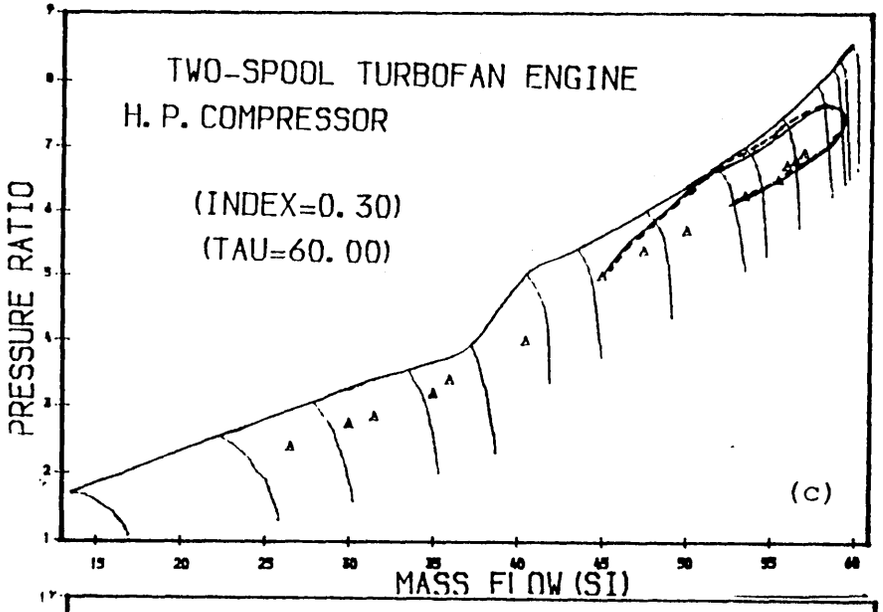

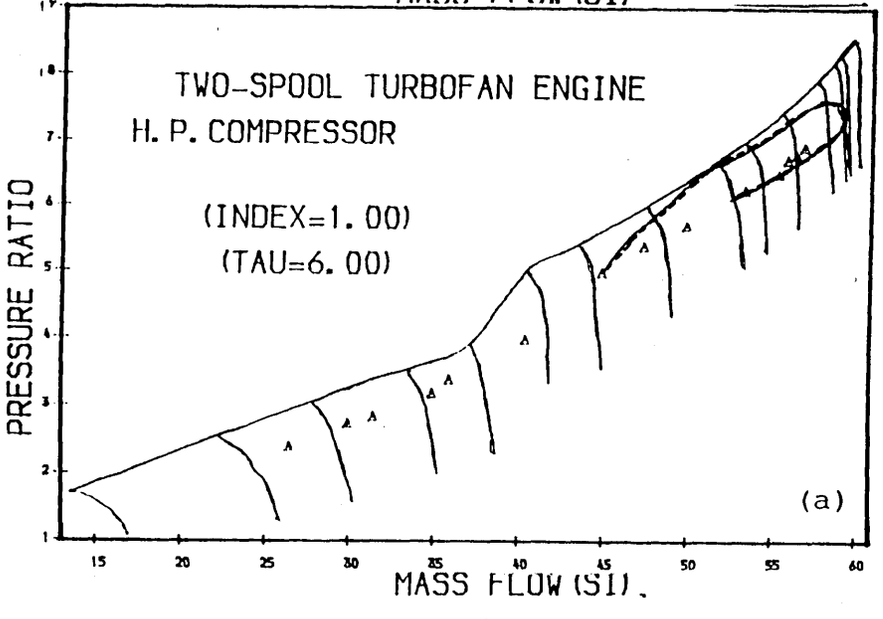

Fig. 144

PREDICTED PATHS OF THE H. P. COMP.
DURING COLD ACCEL. AT 41,000 FT
FUEL SCHEDULE COMPENSATED WITH
A FUNCT. OF H. P. SHAFT DELAYED SPEED

- - - — WITH FUEL SCHEDULE COMPENSATED
——— HEAT TRAN. WITHOUT COMPENSATION
▲ STEADY-RUNNING

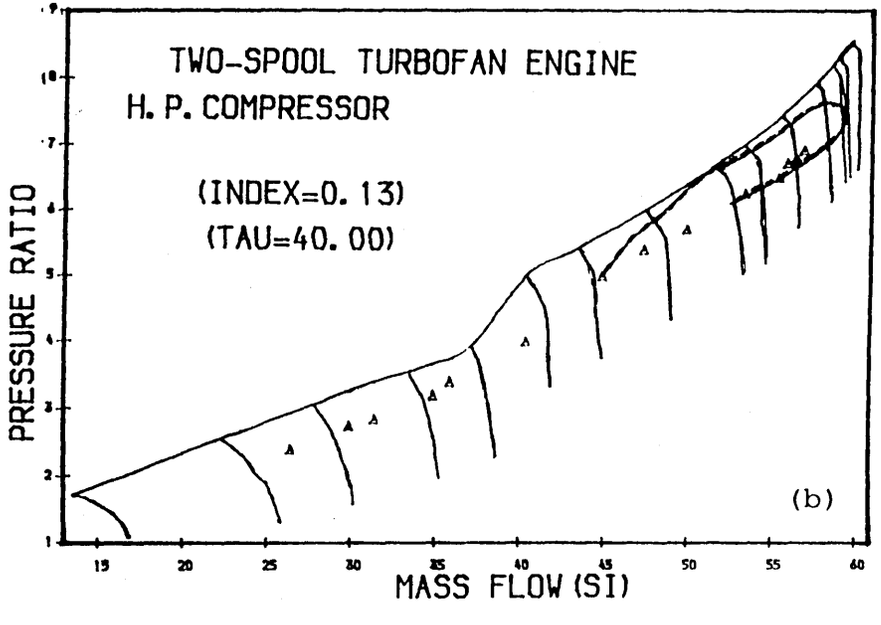

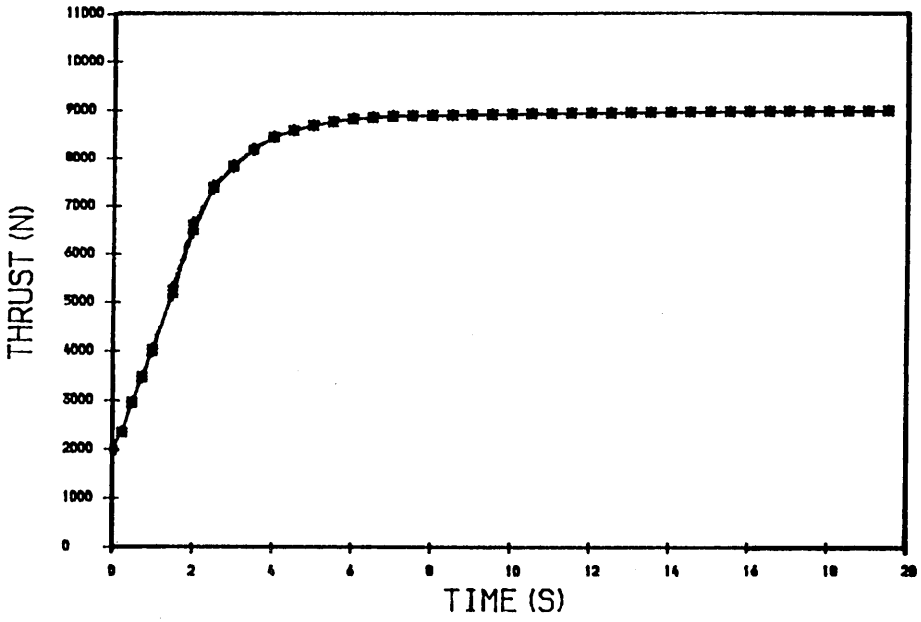

Fig. 145

PREDICTED COLD ACC. AT 41,000 FT
FUEL SCHED. H. P. SHAFT DELAYED SPEED

◆ FUEL COMPENSATED (INDEX=0.30) ; $\mathcal{Z} = 60.00$
▲ FUEL COMPENSATED (INDEX=0.13) ; $\mathcal{Z} = 40.00$
✱ WITH FUEL COMPENS. (INDEX=1.00) ; $\mathcal{Z} = 6.00$
+ WITHOUT COMPENSATION

Fig. 146

PREDICTED PATHS OF THE H. P. COMP. DURING HOT ACCEL. AT 41,000FT FUEL SCHEDULE COMPENSATED WITH A FUNCT. OF H. P. SHAFT DELAYED SPEED

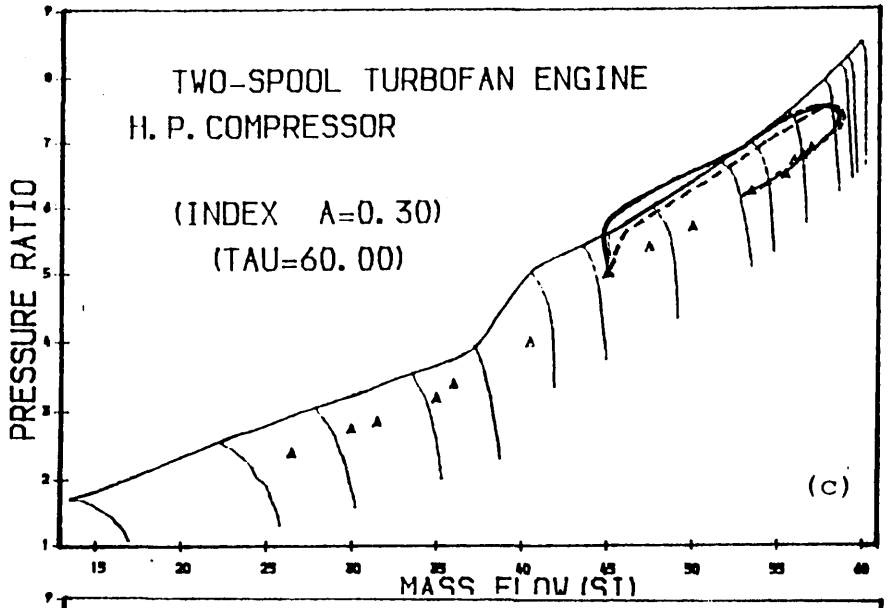

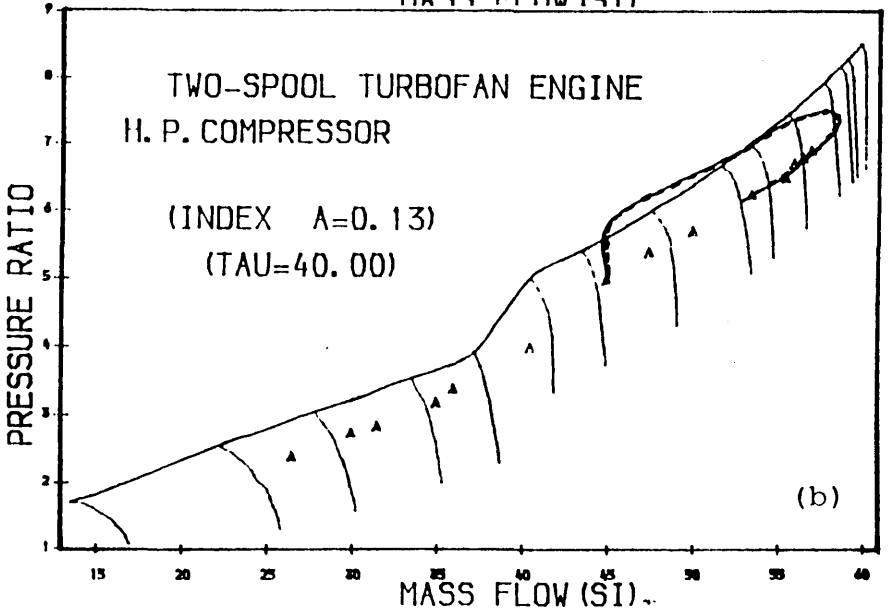

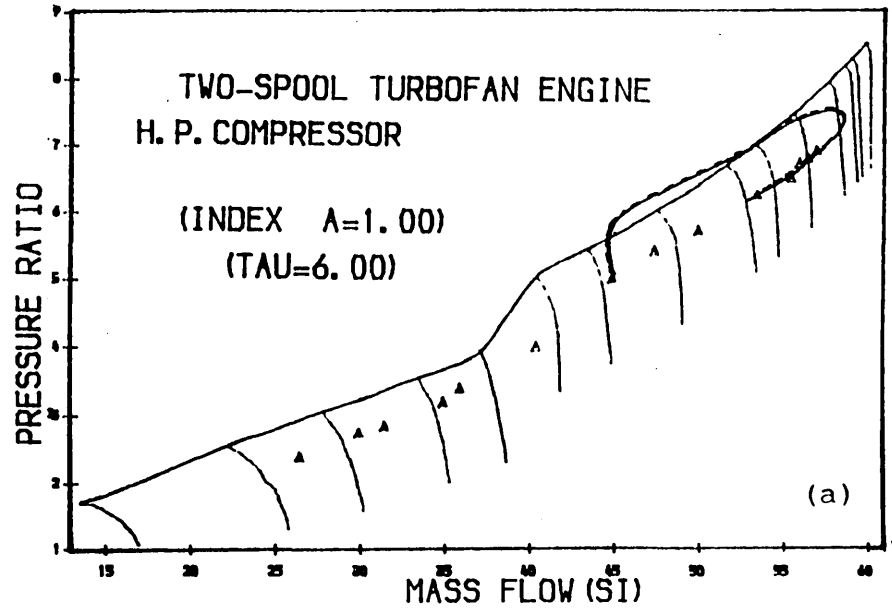

WITH FUEL SCHEDULE COMPENSATED

HEAT TRAN. WITHOUT COMPENSATION

▲ STEADY-RUNNING

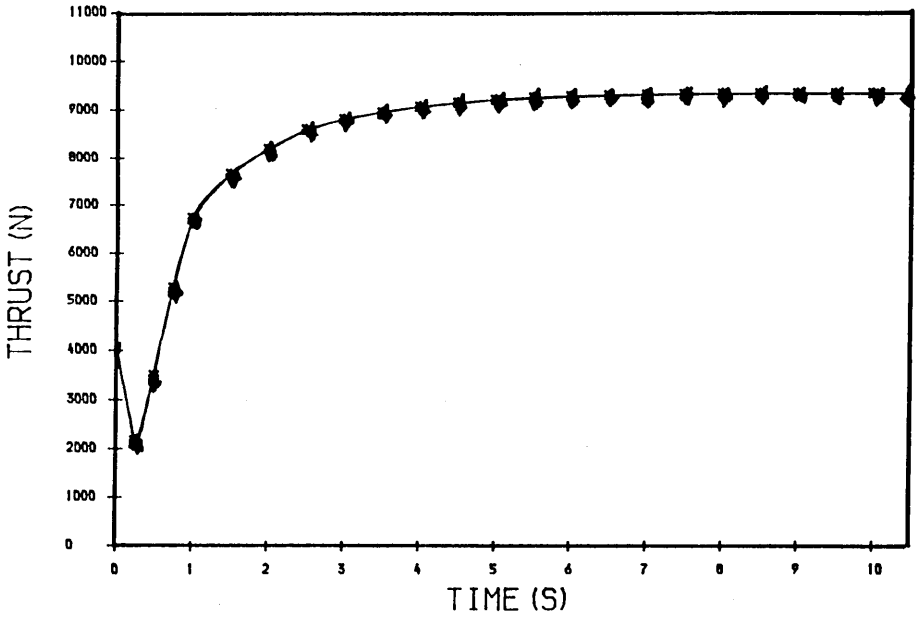

Fig. 147

PREDICTED HOT ACC. AT 41,000 FT
FUEL SCHED. H.P. SHAFT DELAYED SPEED

◆ FUEL COMPENSATED (INDEX=0.30); $\tau = 60.00$
▲ FUEL COMPENSATED (INDEX=0.13); $\tau = 40.00$
✱ FUEL COMPENSATED (INDEX=1.00); $\tau = 6.00$
\+ WITHOUT COMPENSATION

Fig. 148 TRANSIENT ACC. AT 41,000 FT
H. P. SHAFT DELAYED SPEED COMP.

——— INDEX = 1.00 ; τ = 6.00

*** INDEX = 0.13 ; τ = 40.00

– – – – – INDEX = 0.30 ; τ = 60.00

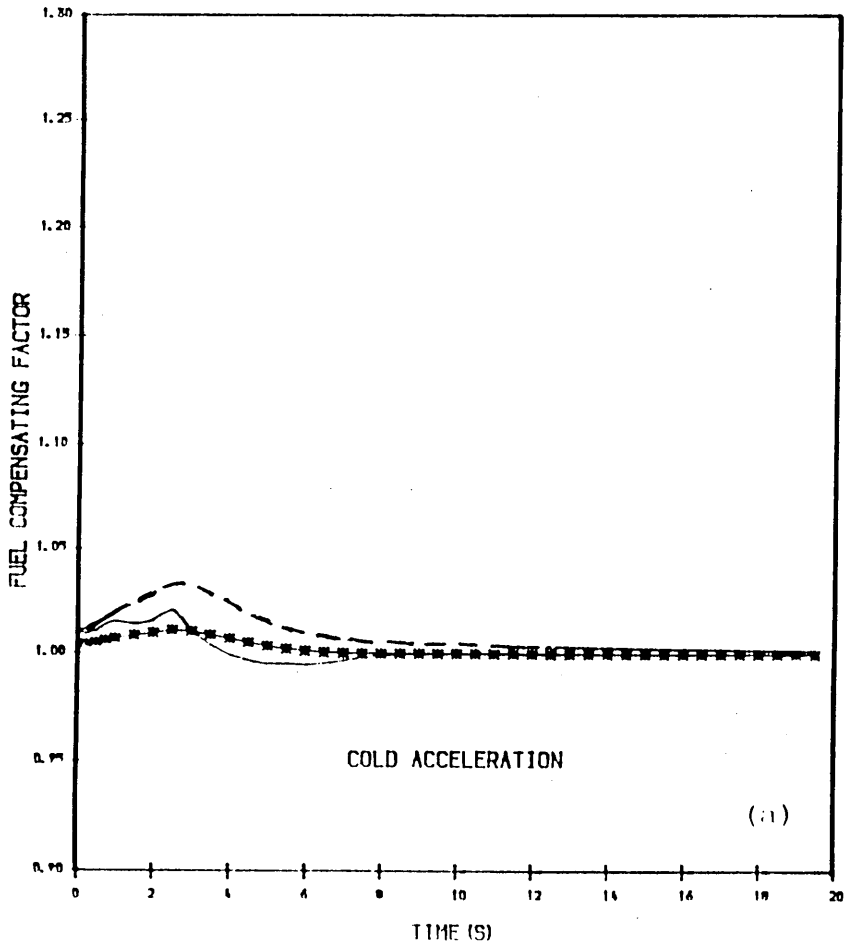

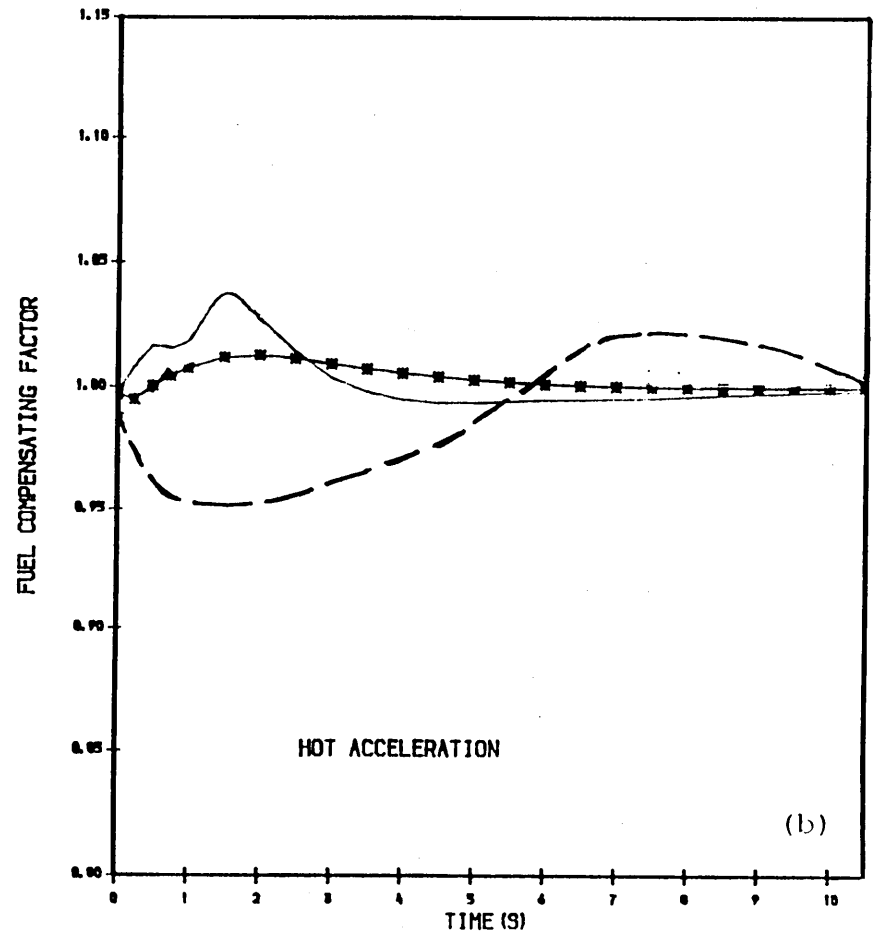

Fig. 149

PREDICTED PATHS OF THE H.P.COMP.
DURING ACCEL. AT 41,000FT
FUEL SCHEDULE COMPENSATED WITH
A FUNCT. OF H.P.SHAFT DELAYED SPEED

------ WITH FUEL SCHEDULE COMPENSATED
——— HEAT TRAN. WITHOUT COMPENSATION
▲ STEADY-RUNNING

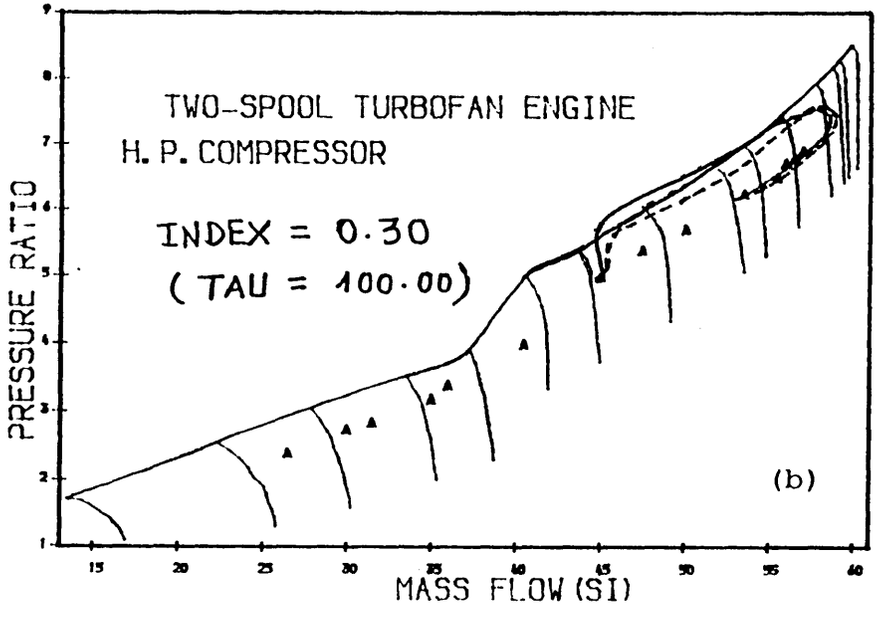

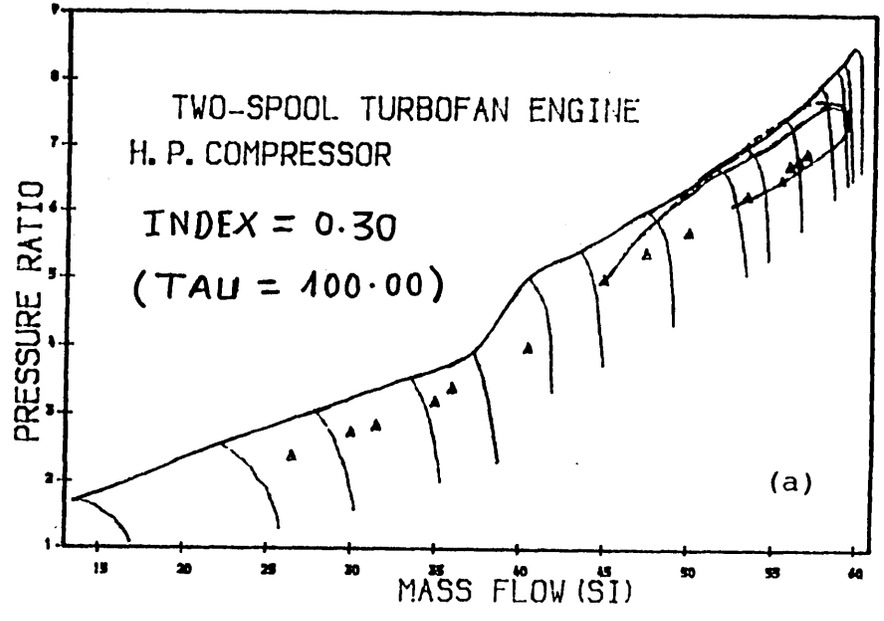

(a) COLD ACCELERATION

(b) HOT ACCELERATION

Fig.150 SUMMARY OF FUEL SCHEDULE COMPENSATION SCHEME

Method			Temperature Response of a characteristic component																Delayed HP shaft speed		
charact.			BLADE						DISC (H.P.T)										Time Constant τ		
Compones			H.P.C			H.P.T			Hub			Diaphragm			platform			Disc Average T_2			6.00	40.00	60.00
INDEX			0.5	1.0	2.0	0.1	0.3	0.5	0.20	0.25	0.30	0.20	0.25	0.30	0.10	0.15	0.20	0.15	0.25	0.35	1.00	0.13	0.30
Sea-Level ; Ma = 0.2	ACCELERATION	Cold	//	+	−	+	//	−	+	//	−	+	//	−	−	−	+	//	+	−	+	//	+
		Hot	//	−	−	+	−	−	//	+	+	//	+	+	−	−	−	−	//	+	−	//	+
	INDEX								0.30	0.50	1.00										1.00	0.13	0.30
	τ																				6.00	40.00	100.00
Altitude 40,000 ft ; Ma = 0.8	ACCELERATION	Cold							//	+	−										−	−	+
		Hot							//	+	+										−	−	+

+ very good prediction
// accepted prediction
− unsatisfactory predict.

APPENDIX: 1

RAMPED FUEL FLOW SCHEDULE

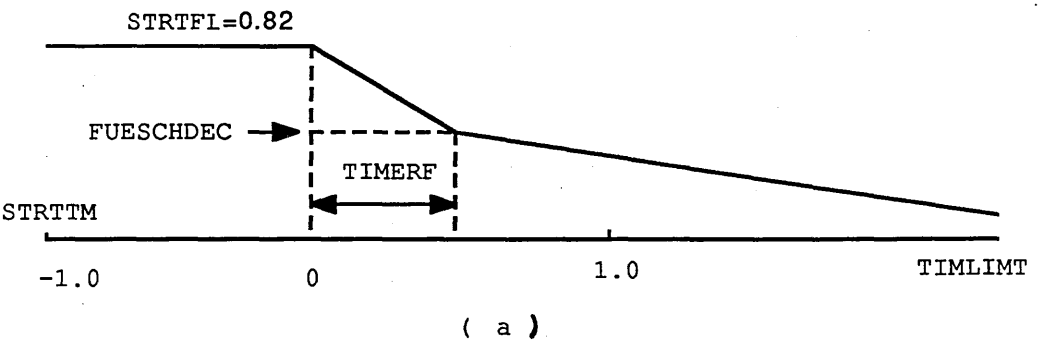

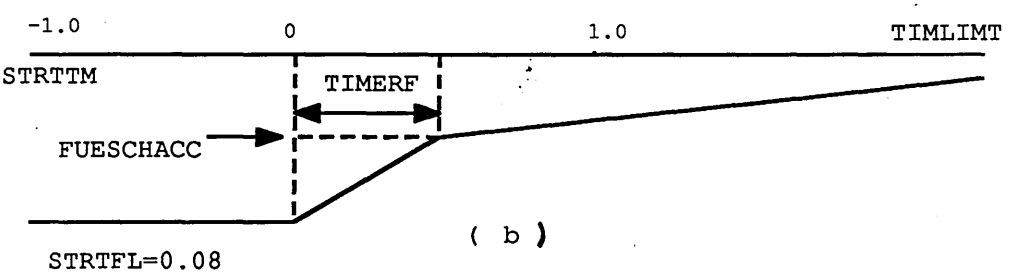

RAMPED FUEL SHEDULE DURING TRANSIENT OPERATION.

(a) DECELERATION

(b) ACCELERATION

APPENDIX : 2

BLADE COOLING

Ainley was able to set down a simple equation, defining the heat transfer process in the cooled turbine blades (see figure below) with the assumption of uniform chordwise temperature :

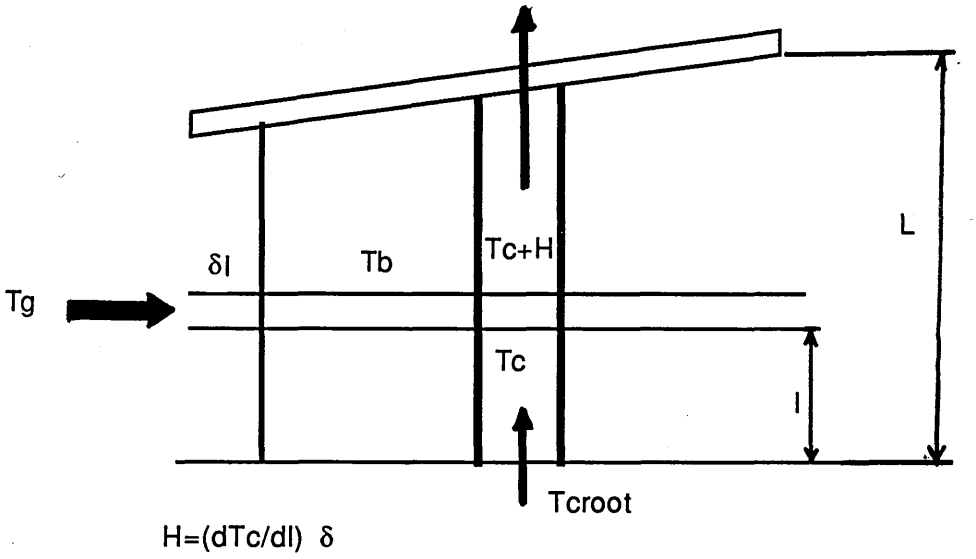

$$h_g\ A_g\ (T_g - T_b)\,\delta\ell = h_c\ A_c\ (T_b - T_c)\,\delta\ell = m\ C_p\ \frac{dT_c}{dl}\ \delta\ell$$

the solution to the above equation, becomes :

$$\frac{T_g - T_b}{T_g - T_c} = \left[\frac{m}{1+m}\right]^{-\frac{L}{n}\left(\frac{1}{1+m}\right)\frac{l}{L}} = e$$

where :

$$m = \frac{h_c\ A_g}{h_g\ A_g} \qquad \text{and} \qquad n = \frac{m\ C_p}{h_g\ A_g}$$

e, being the cooling effectiveness of the system.

APPENDIX: 3

CALCULATION OF THE TIME CONSTANT

T_g and T_m the gas stream temperature and metal temperature, respectively. Initially during transient acceleration, T_g increases instantanously whereas T_m takes longer to reach the same value (see figure below).

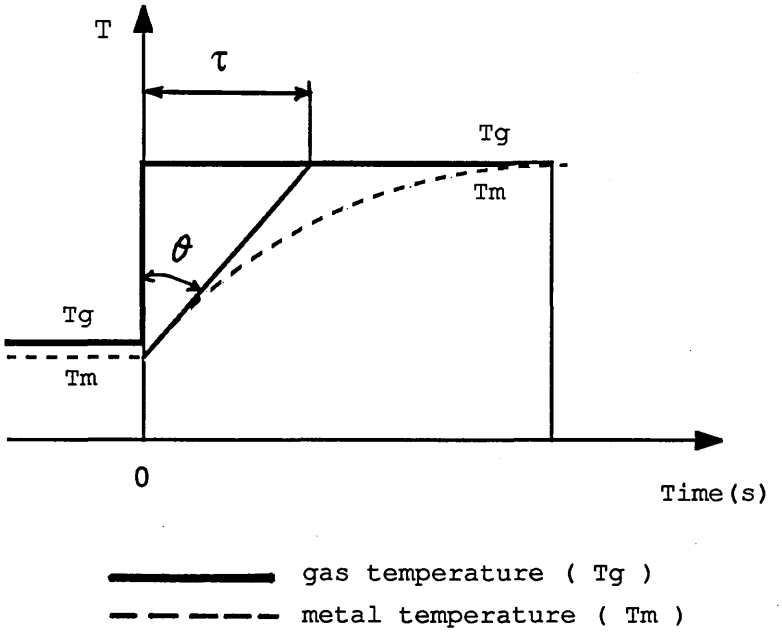

Initially rate of heat transfer from gas to metal is given by:

$$q = h\ A\ (T_g - T_m)$$

q is also given by :

$$q = m\ C_p\ dT \quad , so$$

$$\frac{dT}{dt} = \frac{q}{m\ c_p} = \frac{h\ A\ (T_g - T_m)}{m\ c_p} \quad , \text{ this gives}$$

$$\int_1^2 \frac{dT}{dt} = \int_1^2 \frac{h\ A\ (T_g - T_m)}{m\ c_p}\ dt$$

with $\alpha = T_g - T_m$ we will have

$$\frac{dT}{dt} = -\ \frac{d\alpha}{dt} \quad \text{and therefore}$$

$$\frac{d\alpha}{\alpha} = -\ \frac{h\ A}{m\ c_p} \int_0^t dt \quad , \text{ the solution is}$$

$$\alpha = \alpha_o\, e^{-\frac{h\ A}{m\ c_p}\ t}$$

$$\tau = \frac{m\ c_p}{h\ A} \quad \text{being the time constant}$$

of the thermal response of the material

the solution becomes: $\alpha = \alpha_o\, e^{-\frac{t}{\tau}}$

APPENDIX. 4

CALCULATION OF MEAN TEMPERATURE

In figure below we consider a component in gas turbine engine which is subjected to the temperature T_u in the upper side and T_l in the lower side.

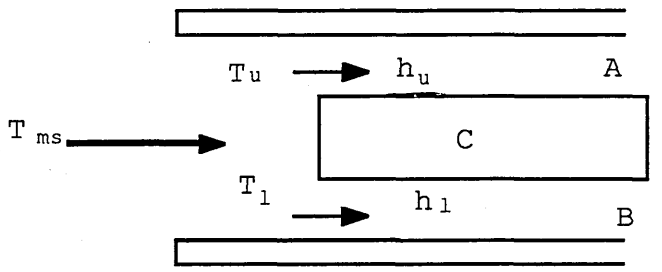

If h_u and h_l are the respective heat transfer coefficients, responsible for the heat exchange between the gas flowing in zone 'A' and the component, zone 'B' and the component (see figure below), the mean stabilised temperature T_{ms} is given by:

$$T_{ms} = T_l + (T_u - T_l)\frac{\frac{1}{h_l}}{\frac{1}{h_l} + \frac{1}{h_u}} \quad \text{and therefore,}$$

$$T_{ms} = \frac{T_l\, h_l + T_u\, h_u}{h_l + h_u}$$

T_{ms} is the temperature which drives the change of temperature of the component (c).